Quantifying the impact of historical and future climate change on windstorm insured loss in Great Britain

Richard Hewston

This thesis is submitted in fulfilment of the requirements for the degree of Doctor of Philosophy at the University of East Anglia.

School of Environmental Sciences

June 2008

Abstract

Windspeed receives relatively little attention in the literature compared with other meteorological variables, despite affecting many industries. European extratropical cyclones create 70-75% of all European insured losses, with an annual average of £1.5-2bn. This project quantifies the impact of historic and future climate change on wind-related insured loss in the UK, using an observational windspeed dataset established here and RCM model data.

A continuous 26-year (1980-2005) record of daily mean 10-metre windspeeds and daily maximum gust speeds (DMGS) at 43 UK Met Office stations is established. Statistically significant decreases in damaging windspeeds, of up to 20%, are found at stations in southern England during that period. Supplemented by dynamically downscaled reanalysis data, statistically significant increases of up to 8% are seen at locations in northern England and in Scotland in the period 1959-2001.

An operational windstorm loss model for Great Britain is developed, incorporating socio-economic data to account for the exposure and vulnerability of domestic properties to the windstorm hazard. Damaging windspeeds are found to be those DMGSs exceeding the local 98th percentile. The model captures the variability in losses reasonably well, although losses are markedly underestimated.

Impacts of individual storm events dating back to 1959 are quantified using Loss Potentials, which are indicative of insured losses. Annual Loss Potentials reveal no statistically significant temporal trends in the period 1959-2005, although a slight increase is suggested between 1959-1979.

Three RCM simulations reveal increases of 15-34% in future (2071-2100) Loss Potentials relative to baseline values. Without adaptation of domestic properties to the future wind regime, these estimates rise to 38-533%. Greatest Loss Potential increases are projected in South East England with adaptation, and in North West England without adaptation. Increases in frequency and intensity of damaging windspeeds in winter, simulated by this three member ensemble, drive the increases in Loss Potentials.

Acknowledgements

This project was carried out under funding from the Worshipful Company of Insurers, at the University of East Anglia, under the supervision of Drs Stephen Dorling and David Viner.

For the provision of observational wind data thanks are due to the UK Met Office and British Atmospheric Data Centre, in particular Belinda Robinson for her patience and dedication. The UK Met Office also kindly made the PRECIS Regional Climate Model and the PRECIS-Re dataset available for use, with David Hein providing excellent and timely technical assistance with the running of PRECIS. Further technical assistance was supplied by Julie Harold and Matt Livermore, without whom my computer would have exited the building via the window on several occasions.

Thanks must go to Neil Carrington and the Ecclesiastical Insurance Group, who kindly shared loss data and advice, aiding in the development and validation of the windstorm loss model.

The utmost gratitude goes to Steve, my primary supervisor, for his constant support throughout the project. His belief in my abilities and my work was unwavering, despite my own doubts at times. I greatly appreciate his advice and his ability to understand when I needed time to get to grips with things myself. Thanks must also be given for his catches out in the deep off my rank bad bowling.

My fellow PhD students and office mates must be credited for their constant support and help, and for their advice and suggestions proffered in the pub. Thanks must go to friends and family for their, at times, helpful and well thought out comments, and also for their encouragement. And of course I'll be forever in debt to Amber for her inspiration, patience and help throughout.

Contents

List of Figures

List of Tables

Abbreviations and Acronyms

- ABI – **A**ssociation of **B**ritish **I**nsurers
- AWS – **A**utomatic **W**eather **S**tation
- BADC – **B**ritish **A**tmospheric **D**ata **C**entre
- CDL – **C**limate **D**ata **L**ogger
- CHRM - **C**limate **H**igh-**R**esolution **M**odel; a RCM derived from the operational weather forecasting models of the Swiss and German meteorological services, described in Vidale *et al.* (2003)
- CLM **- C**limate **L**okal**m**odell; a RCM based on the German Weather Service weather forecast model **L**okal**m**odell, described in Steppeler *et al.* (2003)
- DALE - **D**igital **A**nemograph **L**ogging **E**quipment
- DMGS – **D**aily **M**aximum **G**ust **S**peed
- ECHAM4 - **E**uropean **C**entre **HAM**burg **4**; an atmosphere only GCM described in Roeckner *et al.* (1996)
- ECHAM5 - **E**uropean **C**entre **HAM**burg **5**; an atmosphere only GCM described in Roeckner *et al.* (2003)
- ECMWF - **E**uropean **C**entre for **M**edium-range **W**eather **F**orecasts
- EIG – **E**cclesiastical **I**nsurance **G**roup
- ERA40 - **E**CMWF 45-year **re**a**n**alysis of the global atmosphere and surface conditions 1957–2002
- ESAWS - **E**nhanced **S**ynoptic **A**utomatic **W**eather **S**tation
- GCM – **G**eneral **C**irculation **M**odel
- GIS – **G**eographic **I**nformation **S**ystem
- HadAM3H -Third **Had**ley centre **A**tmosphere **M**odel version **H**; an atmosphere only GCM described in Pope *et al.* (2000)
- HadAM3P -Third **Had**ley centre **A**tmosphere **M**odel version **P**; an updated version of HadAM3H, described in Gordon *et al.* (2000) and Pope *et al.* (2000)
- HadCM2 - Second **Had**ley Centre **C**oupled **M**odel; a coupled ocean-atmosphere GCM described in Johns *et al.* (1997)
- HadRM3H - Third **Had**ley Centre **R**egional **M**odel version **H**; a RCM developed from HadAM3H, described in Jones *et al.* (1995)

- HadRM3P – Third **Had**ley Centre **R**egional **M**odel version **P**; an updated version of HadRM3H, described in Jones *et al.* (2004)
- HIRHAM4 - Danish **Hi**gh **R**esolution Limited Area Model **Ham**burg version 4, described in Christensen *et al.* (1998).
- hPa – **h**ecto **Pa**scals
- IDW - **I**nverse **D**istance **W**eighted
- IPCC – **I**ntergovernmental **P**anel on **C**limate **C**hange
- IPCC SRES – IPCC **S**pecial **R**eport on **E**missions **S**cenarios
- MIDAS - **M**et Office **I**ntegrated **D**ata **A**rchive **S**ystem
- MPI-OM1 – First **M**ax **P**lanck **I**nstitute **O**cean **M**odel described in Marsland *et al.* (2003)
- MSLP – **M**ean **S**ea **L**evel **P**ressure
- Munich Re – Munich Reinsurance Company
- NCEP – **N**ational **C**enter for **E**nvironmental **P**rediction
- NCAR – **N**ational **C**enter for **A**tmospheric **R**esearch
- NERC – **N**atural **E**nvironment **R**esearch **C**ouncil
- OS - **O**rdnance **S**urvey
- OPYC3 - **O**cean on iso**PYC**nal coordinates, described in Oberhuber (1993)
- PML - **P**robable **M**aximum **L**oss
- PRECIS - **P**roviding **RE**gional **C**limates for **I**mpact **S**tudies; a RCM based on HadRM3P
- RCAO - Swedish **R**ossby **C**entre **A**tmosphere–**O**cean high resolution regional model, described in Räisänen *et al.* (2004)
- RCM – **R**egional **C**limate **M**odel
- RPI - **R**etail **P**rices **I**ndex
- RPIX - **R**etail **P**rices **I**ndex e**X**cluding Mortgage Interest Payments; a tool used to adjust losses to a constant value, and described in Appendix B, and in Office of National Statistics (2007)
- SAMOS - **S**emi **A**utomatic **M**eteorological **O**bserving **S**ystem
- SOA – **S**uper **O**utput **A**rea; UK boundaries for socio-economic statistics aggregation. Described at www.statistics.gov.uk/geography/soa.asp
- Swiss Re – Swiss Reinsurance Company

- UK – United Kingdom of Great Britain and Northern Ireland
- UKMO – United Kingdom Met Office (formerly an abbreviation of Meteorological Office, but now an official name itself)
- US – United States

Chapter 1: Weather and Insurance

Insurance is a method of transferring or distributing risk and, in one form or another, can be traced back several millennia. Chinese merchants in 2000BC would distribute their cargo over many sea-going vessels in order to minimise losses should one of them sink. Marine insurance boasts the first ever formal insurance contract, dating back to 1370 in Genoa (Swiss Re, 2002). The rapid growth of the international shipping trade in the 1600s led to the development and equally rapid growth of marine insurance. Subsequently Lloyd's of London was formed, and from its coffee shop origin it has become the world's leading market for marine insurance.

Today the insurance industry[1] is a $3 trillion[2] industry, covering a multitude of risks as varied as weather interruption of weddings to injuries of professional athletes. One of the cornerstones of the insurance industry is managing the risk associated with natural hazards, such as earthquakes and flooding. Insuring against adverse effects of weather is a core business. Increasingly weather related events are dominating not only the news, but also losses to global non-life insurers.

1.1 Weather Related Damage

Since 1970, of the most expensive 40 insured loss events, 34 were weather related with 29 due to windstorm (Zanetti, 2008). The top 15 loss events are presented in Table 1.1.

[1] All references to the insurance industry also include the reinsurance industry.
[2] All $ values refer to the US dollar at the January 2008 value, unless stated.

Insured Loss ($m indexed to 2007)	Date	Event	Country / Region
68515	25/08/05	Hurricane Katrina	US, Gulf of Mexico
23654	23/08/92	Hurricane Andrew	US, Bahamas
21999	11/09/01	World Trade Centre, Pentagon Terrorist attacks	US
19593	17/1/94	Northridge Earthquake	US
14115	02/09/04	Hurricane Ivan	US, Caribbean
13339	19/10/05	Hurricane Wilma	US, Mexico, Jamaica
10704	20/09/05	Hurricane Rita	US, Cuba
8840	11/08/04	Hurricane Charley	US, Cuba, Jamaica
8599	27/09/91	Typhoon Mireille	Japan
7650	15/09/89	Hurricane Hugo	US, Puerto Rico
7413	25/01/1990	Winter Storm Daria	Northern Europe
7223	25/12/1999	Winter Storm Lothar	Northern Europe
6097	18/01/2007	Windstorm Kyrill	Northern Europe
5659	15/10/87	Storms and flooding	Northern Europe
5650	26/08/04	Hurricane Francis	US, Bahamas

Table 1.1 - The 15 most costly insurance losses 1970-2007. Adapted from Zanetti (2008).

Worldwide weather related catastrophic events, such as flooding, windstorms and heat waves, cost insurers an annual average of $10bn (Zanetti, 2008). If non-catastrophic events are included, this figure doubles. In the UK alone insured weather related losses (excluding subsidence), with increasing frequency, exceed £1bn a year (ABI, 2007a). An examination of the trends in insured losses related to weather events is presented in section 1.2. Globally, of the 294 great natural catastrophes[3] which occurred between 1950 and 2004, 48% were windstorm related, 34% flood related and 18% related to extremes of temperature (Munich Re, 2005). However, approximately 70% of the losses from these events result from windstorm damage, associated with

[3] The definition of "Great Natural Catastrophe" used by Munich Re (2007) is in line with United Nations, who consider a natural catastrophe great if "the affected region's ability to help itself is clearly overstretched and supraregional or international assistance is required. As a rule, this is the case when there are thousands of fatalities, when hundreds of thousands of people are left homeless, or when overall losses – depending on the economic circumstances of the country concerned – and/or insured losses are of exceptional proportions."

tropical cyclones, tornadoes and extratropical cyclones. Often less spectacular than their tropical sisters, European extratropical cyclones, with a longer lifespan and a larger geographic footprint, have on occasion produced catastrophic losses comparable to hurricane losses in North America. This is borne out by the experience of European windstorms Daria, Lothar and Vivian along with the storm of 16th October 1987 (often referred to as 87J in the insurance industry), which all rank in the top 15 global insured loss events in Table 1.1. Malmquist (1999) states that losses from extratropical cyclones in Europe in 1990-98 were equivalent to losses in North America from hurricanes (both averaging roughly £1bn a year in that period).

Climate related perils in the UK

Although windstorms are the dominant peril driving UK climate related losses, it is important to have an appreciation of the other major perils, namely flooding and subsidence. Although the insurance industry does not consider subsidence as a "weather" peril, it must be considered in discussions of climate related perils. In the UK, windstorm damage on average accounts for just over half of weather related domestic property insured losses each year, with flooding and pipe damage contributing the majority of the remainder (ABI, 2007a). Commercial and domestic subsidence losses combined are generally slightly lower than windstorm losses. Further discussion of the historic trends in these losses may be found in section 1.2.2.

Flooding

A common misconception is that flooding is the most costly weather peril UK insurers face; most likely due to the media attention flooding receives. However, flooding is a traumatic experience, and due to the proximity of urban areas to rivers and the coast, is a risk to 2 million homes in the UK (ABI, 2007b). Currently, coastal flooding losses are minimal due to effective defences, most notably the Thames barrier. However, inland flooding has an extensive history in the UK, highlighted by the events of the summer of 2007, where heavy rainfall over a four week period saw claims exceed £3bn (ABI, 2007c).

Extensive work has been undertaken by the Environment Agency, and insurers alike, in assessing flood risk. In March 2004 Norwich Union unveiled new technology allowing the assessment of the flood risk of individual houses, rather than traditional approaches of assessing the flood risk at a postcode-wide scale. Media hype surrounding "sky rocketing premiums" and "uninsurable homes", although greatly exaggerated, certainly caught the attention of the public.

The risk of flooding is the most understood and well modelled weather related risk, and is increasingly becoming a political issue. A recent Association of British Insurers (ABI) report (ABI, 2005b) discusses the flood risk posed to 200,000 extra homes the government is planning to build in the South East by 2016. It is estimated that an extreme flood in this area would lead to damages in excess of £12-16bn, with £4-5bn coming from the new developments. The ABI is encouraging the government to increase communication between developers and the insurance industry at an early stage in order to minimise flood risk.

Subsidence

Subsidence (downward motion) and heave (upward motion) describe the movement of the ground, often resulting in structural damage to properties or their foundations. Collective losses from these two processes are generally referred to as subsidence losses. Annual insured losses due to subsidence for both domestic and commercial properties combined are approximately £300m (ABI, 2007a). Causes of subsidence and heave include glacial rebound, extraction of groundwater and mining operations. In the UK, subsidence (heave) is often the result of a decrease (increase) in soil volume due to drying (rehydration) of clay soils. This process is governed by the amount of water present in the ground, a function of several climate parameters, including precipitation, temperature, and humidity. Unlike flooding and windstorm damage, subsidence is not considered a weather peril as no one weather event can trigger a subsidence event. It is the cumulative effect of weather over several months (and potentially seasons) that leads to subsidence damage. For this reason it is classified as a climate related peril. Although the ideal conditions for subsidence to occur are largely unknown, a

common belief is that two dry summers, with an intervening dry winter, often leads to subsidence events.

Pipe Damage

Losses due to burst pipes, often as result of freezing and thawing during winter months, make up approximately 10%[4] of the weather related insured domestic property loss each year (ABI, 2007a).

Windstorm

Wind-related insured losses are classified as "storm" losses by the insurance industry, which includes the negligible direct effect of rain and hail, but not flooding. Hence, "storm" losses, generally used by the insurance industry, are referred to as "windstorm" losses in this project. Windstorm losses from domestic properties in the UK amount to over £340m a year, based on 1998-2005 data (ABI, 2007a). On average 200,000 properties (equivalent to just under 1% of the UK building stock) suffer wind-related damage each year (Sanders and Phillipson, 2003), with approximately half of home owners expected to file at least one claim related to windstorm damage in their lifetime. Deaths and injuries from windstorms are low (on average 6 deaths and 144 minor injuries per year) and mostly associated with road traffic accidents and structural failure (Baxter *et al.*, 2001). However, significant events, such as the October 1987 storm (described in section 1.1.1) result in a high number of fatalities. The fact that trees were in leaf during the October 1987 storm contributed to its destructiveness, a feature that will be revisited on several occasions in this project.

Windstorm damage is the result of wind loads exceeding the resistance of the structure, affecting parts of the building such as roofs, envelopes and openings. Sacre (2002) studied wind damage in France following windstorm Lothar in 1999, finding most severe structural damage occurred near the sea and in open country, as a result of smoother terrain and reduced surface friction. Meanwhile structures in urban areas suffered mainly from damage to openings. Roofs are especially prone to suffering damage due to wind.

[4] A change in data collection methods, discussed in section 1.2.2 means this figure is calculated on 2004-2007 figures only.

Spence *et al.* (1998) report nearly 80% of wind damage is associated with the roof of a building. Blackmore and Delpech (2002) found this figure rose to 90% when considering damage during the October 1987 and January 1990 storms. The roof is a particularly susceptible part of any structure since windspeeds increase with height, and roofs of other buildings often generate turbulence due to their sharp, jutting edges.

The windstorm risk to the UK, and indeed Europe as a whole, is poorly understood largely due to the historical fluctuation of windstorm activity. Prior to the last few years, it is generally accepted that the windstorm risk was largely underestimated by the insurance industry (Bresch *et al.*, 2000). However, the loss potential is very high, as demonstrated by multi-billion pound losses associated with windstorms Lothar, Martin, Kyrill and 87J. The following section explores historic storm events to highlight some of the underlying factors which result in European windstorms becoming large loss events.

1.1.1 Examples of recent windstorm events

One of the core principles of insurance is the limited risk of large, or catastrophic, losses. This section describes a selection of historic windstorm events that have not only had a major impact on the population of the affected region, but also impacted heavily on European reinsurers and insurers. For the most part the descriptions of the resultant damage and losses of these windstorms are confined to the British Isles, however it should be noted that the nature of extratropical cyclones mean their geographic footprints often, if not always, result in damage and losses across several European countries.

The '87 "Hurricane"

Also known as the Great Storm of 1987, and 87J in the insurance industry, the storm struck the UK in the early hours of 16th October 1987. The storm was labelled a "hurricane" by the media following the infamous words of Michael

Fish, who stated “a hurricane is not on the way” during a forecast for the BBC (BBC, 2007)[5].

Formation and Track

The origins of the system can be traced back to the Bay of Biscay where a cyclone began forming in the early hours of 15th October. A marked contrast across the polar front was present at the time, generating a strong thermal gradient. A complete description of the development of the storm is detailed by Burt and Mansfield (1988). During 15th October the cyclone deepened and moved northwards, reaching the English channel at midnight, with a central pressure of 953hPa (Burt and Mansfield, 1988). The system made landfall in Cornwall before tracking northeast towards Devon and then over the Midlands, going out to sea via the Wash. The depression tracked quickly across the UK while filling slowly, with the strongest gusts, of up to 50 ms^{-1}, recorded along the south-eastern edge of the storm, severely affecting Essex and Kent (UKMO, 1988). The track of the storm centre is shown in Figure 1.1.

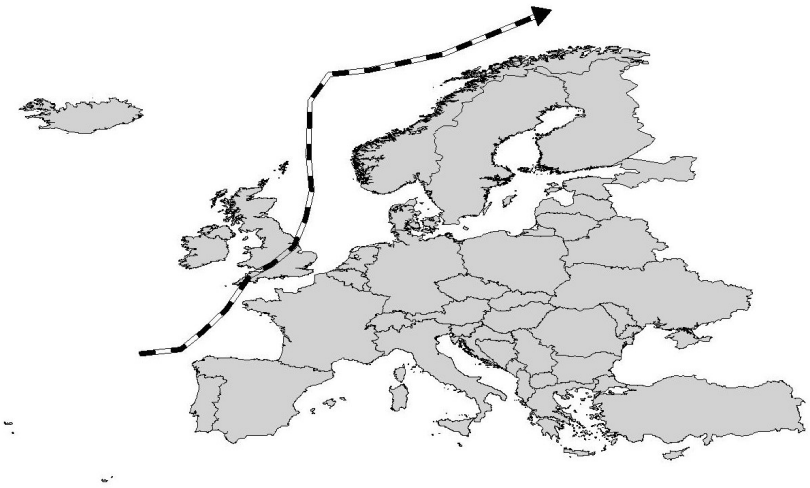

Figure 1.1 - Track of the October 1987 storm. Source: Hanson *et al.* (2004).

Records were not only set by high windspeeds, but the rises in pressure seen with the passage of the warm front were exceptional. Several stations in southern parts of England saw pressure rise over 8 hPa in an hour, with the

[5] In fact Michael Fish was referring to Florida, and did warn the UK to 'batten down the hatches there's some really stormy weather on the way'.

most rapid recorded at Hurn, in Hampshire, with a one hour rise of 12 hPa (UKMO, 1988).

Damage and Losses

The unusual southern track of the storm across England, coupled with the fact that the trees were still in leaf, resulted in unprecedented damage. The strongest gust measured in the UK was at Shoreham, on the Sussex coast, which recorded a gust speed of 52 ms^{-1} at 0310 GMT (UKMO, 2007a). Further inland, gusts exceeding 36 ms^{-1} were recorded, as shown by the 70 knot contour in Figure 1.2. Burt and Mansfield (1988) report the storm's prominent wind direction was from the south (originating from 170-190^{o}), markedly different from the westerly direction (230-280^{o}) normally associated with the highest windspeeds at most stations. Windspeeds from this southerly direction and at this time of year (when trees are in leaf) are very uncommon. Hanson (2001) observes that comparable gust speeds at that time of year were only recorded once at Boscombe Down and twice at Dover, in the last 50 years.

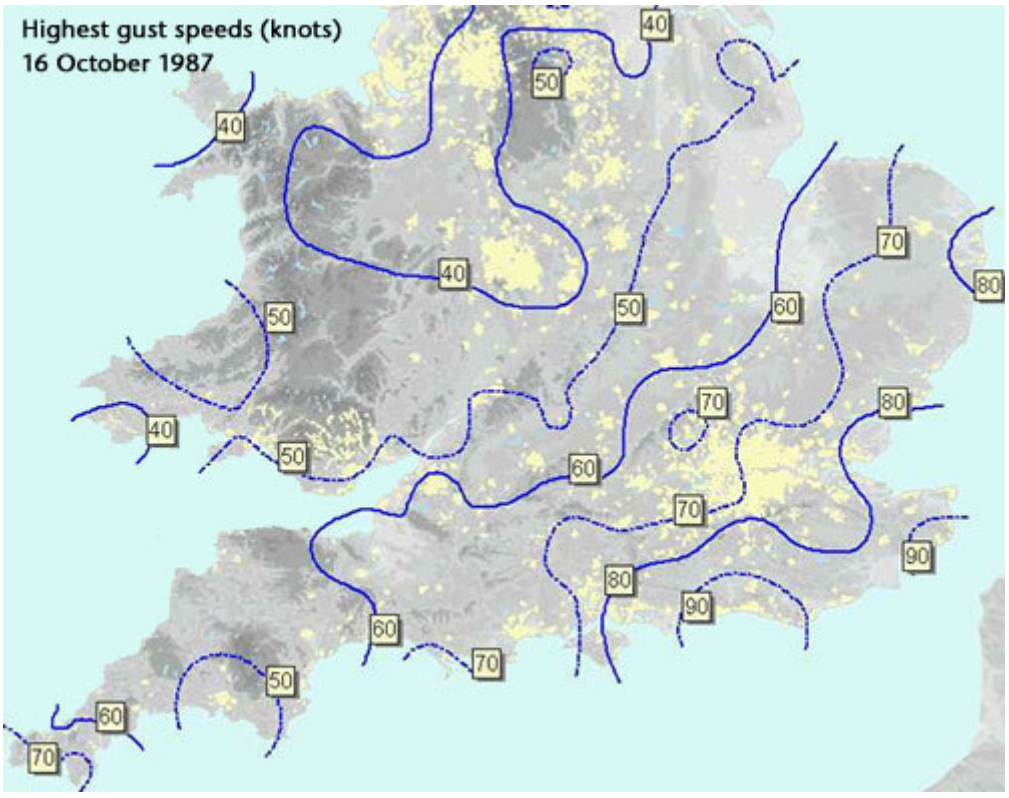

Figure 1.2 - Highest gust speeds (in knots, equivalent to 0.515 ms^{-1}) associated with the October 1987 storm. Source: UKMO (2007a)

Munich Re (1999) report the storm cost insurers just under £1.85bn (equivalent £3.6bn in 2007), with total economic losses in the region of £2.2bn (equivalent to £4.7bn in 2007). Over 25 million people were affected by the storm, though fortunately only 21 deaths resulted from it (Baxter *et al.*, 2001). The fact that the storm struck in the early hours of the morning meant the number of casualties were kept to a minimum as few people were on the roads or outside of their homes. However, hundreds of thousands of people were left without power for several days.

Some 15 million trees were felled, blocking transport routes and leaving widespread structural damage to buildings across England and Wales (Dlugolecki *et al.*, 2001). The combination of the trees being in leaf, coupled with a high soil moisture content brought about by wet antecedent conditions, meant trees were highly susceptible to being uprooted. Compounding this was the fact that southeast England had not suffered a severe windstorm for several decades, enabling many ageing trees to survive in that period, while weakening and becoming highly susceptible to wind damage. Levels of damage, not just to trees but also to structures, are likely to be higher when the impacted region has not experienced a windstorm for several years (Blackmore, 1994a).

Windstorm Daria (January 1990)

The winter of 1989-1990 was one of the stormiest and most damaging winters on record, exemplified by Windstorm Daria (commonly referred to as the Burns' Day storm) on 25th January. A second storm, Windstorm Vivian, buffeted the UK between 26th and 28th February 1990. UK weather related property losses that year reached their highest mark on record (1987-2007) at over £3.9bn (2007 value), mainly driven by losses from this stormy period.

Formation and Track

Daria began as a wave on a cold front off the eastern United States coast on 23rd January 1990. It deepened as two baroclinic zones merged and became embedded in an upper trough of a powerful jet stream moving eastward (Hanson *et al.*, 2004). The system underwent rapid strengthening in the early

hours of 25th January, with the central pressure dropping to 968hPa (Figure 1.3A).

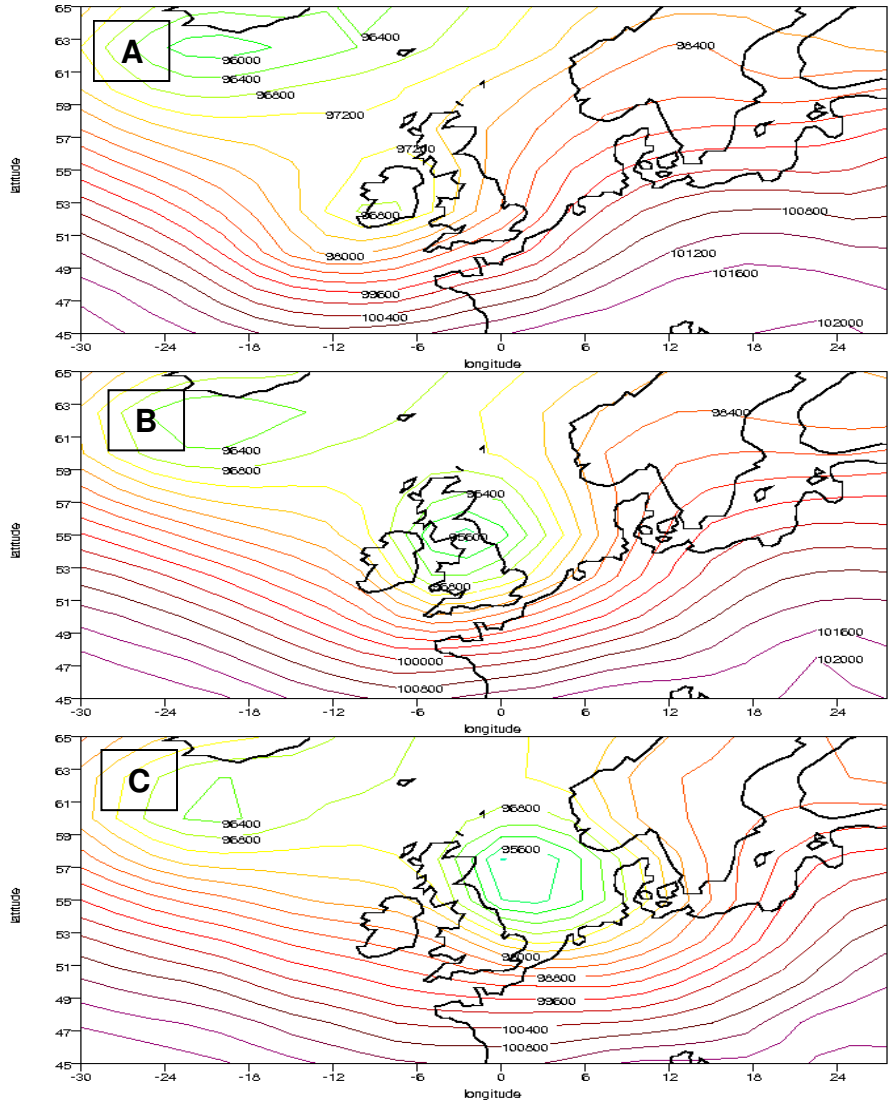

Figure 1.3 - Mean sea level pressure patterns for Windstorm Daria from ECMWF ERA40 reanalysis data, at A) 0600GMT, B) 1200GMT and C) 1800GMT 25th January 1990. Contours are shown in Pascals.

Damage and Losses

The western and southwestern flanks of the cyclone brought the most severe winds. Gusts exceeding 46ms^{-1} were recorded over a large area of southern England and Wales, with the highest gust speed of 48 ms^{-1} measured at Aberporth (McCallum, 1990).

Insured losses for Daria in the UK amounted to £1.9bn (equivalent to £3.2bn in 2007 values), while insured losses in Europe as a whole totalled £3.1bn

(£5.4bn in 2007 values[6]) (Munich Re, 2002b). Spence *et al.* (1998) estimated these losses in the UK were equivalent to more than 0.1% of the total insured amount. Damage from Windstorm Vivian on 25th February 25th 1990, which followed a similar track to Daria, resulted in insured losses of £0.5bn (£0.8bn in 2007 values) in the UK, and £1.1bn (£1.8bn in 2007 values) for Europe overall.

Daria was more damaging than the October 1987 windstorm as it had a much wider geographic footprint. Forty seven people lost their lives, and half a million homes were left without power (Baxter *et al.*, 2001). The death toll was higher than the October 1987 storm due to the fact that it struck during the day, with peak intensities occurring between 0900-1500GMT across the UK. The UK Meteorological Office (UKMO, 2007b) reported that three million trees were felled during the storm, significantly lower number than during the October 1987 storm. The fact that there were no leaves on the trees may have contributed to the lower tree damage than October 1987. Another possible contributing factor may have been the exceptionally high damage to trees in 1987. This may have had the effect of removing any weak trees, leaving relatively few trees which were susceptible to wind damage.

Windstorm Erwin (January 2005)

High winds and torrential rain associated with Windstorm Erwin lashed Northern Europe between 7-9th January 2005, killing 17 people and causing widespread property damage.

Formation and storm track

Just west of Ireland at 1800GMT on the 7th January, a perturbation in the polar front led to the formation of windstorm Erwin. Strong upper-level winds, associated with the jet stream, were located aloft of the surface storm, drawing air from below, leading to upper air divergence and enhancing the pressure reduction. Rapid intensification over the next twelve hours led to a decline in the central pressure of 25 hPa to 970 hPa, and by the morning of the 8th January (0600GMT) the centre of the storm was located just east of the

[6] This figure corresponds with that in Table 1.1 ($7.4bn), given the £/$ rate at the time of the event was $1.5.

UK. At this stage the majority of extratropical cyclones begin to weaken as they track over northern Europe due to the effects of surface friction and unsupportive upper air conditions. However, a jet streak was still positioned directly over the centre of the system and led to further intensification. Erwin deepened and tracked to the north of Denmark over Norway, reaching its minimum pressure of 960 hPa on the afternoon of the 8th January, just northeast of Oslo, Norway. Peak gusts of 40 ms^{-1} were recorded at coastal weather stations in Denmark, and Hano, an island off the coast of Sweden, experienced hurricane strength winds with gusts of up to 42ms^{-1} (Benfield, 2005).

As Erwin continued to move eastward it weakened, filling slowing but still bringing high winds and rainfall to Germany, Latvia, Estonia and Lithuania. Figure 1.4 shows the track of windstorm Erwin and the affected areas.

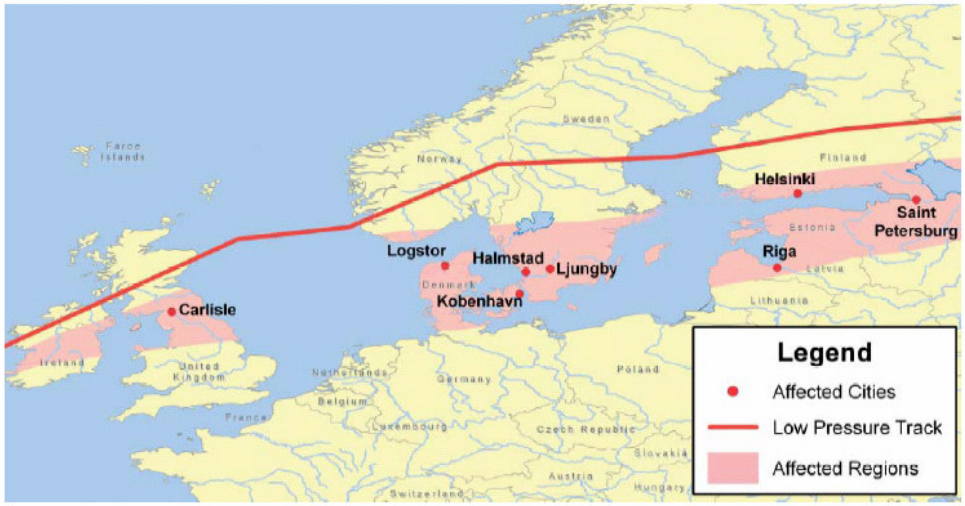

Figure 1.4 - Track of windstorm Erwin Source: Guy Carpenter (2005a)

Damage associated with Erwin

Figure 1.5 shows an analysis chart at 0000GMT on 9th January 2005 with Erwin having crossed the British Isles and now centred over the Baltic Sea. The steep pressure gradient between north and south Sweden, illustrated by the tight isobars, resulted in high windspeeds. The pressure gradient is clearly steeper over northern England and Scotland, compared with southern England, indicating higher windspeeds in these regions.

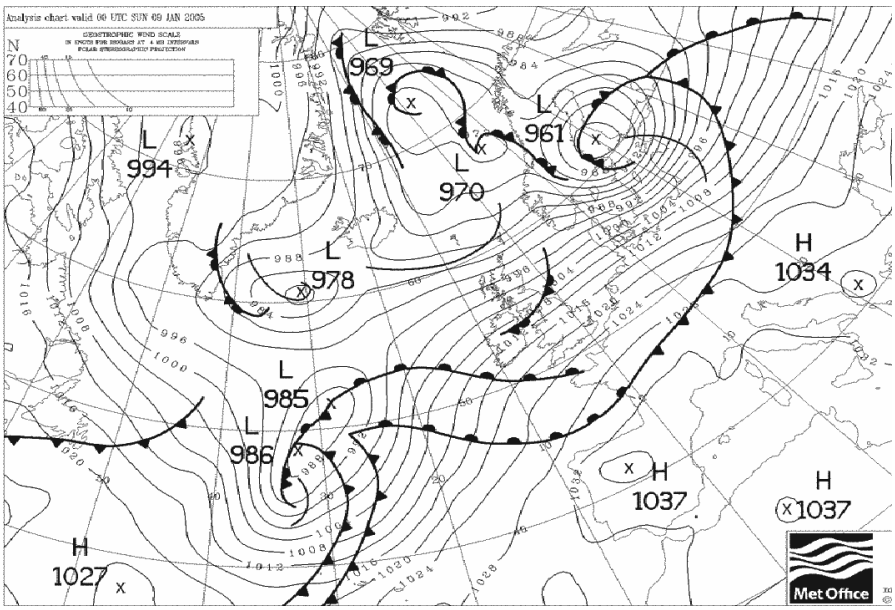

Figure 1.5 - Analysis chart at 0000GMT on the 9th January 2005. Source: www.wetterzentrale.de

Erwin moved across Northern Ireland and Scotland, bringing severe gales on its southern flank to the rest of British Isles. A gust of 46 ms^{-1} was recorded at St. Bees Head (Cumbria) (Eden, 2005) while Durham experienced gusts over 38 ms^{-1}, and Ronaldsway, on the Isle of Man, recorded a 40 ms^{-1} gust, emphasising that it was northern England which suffered the worst conditions. The fact that central and southern England were largely spared from damaging winds kept insured losses relatively low, when compared with the October 1987 storm and windstorm Daria. Had Erwin tracked slightly further south, bringing its path over highly populated areas like the Midlands and the South East, insured losses would have been significantly higher.

Industry wide, the figure for total losses relating to Windstorm Erwin is roughly £1bn (Zanetti, 2006). UK losses in the UK are estimated at £250m (Guy Carpenter, 2005b), with approximately two thirds of this resulting from windstorm loss and remainder from flood losses. Three people died in the UK, while 70,000 homes lost power following heavy rain and powerful winds. A month's rainfall fell in parts of the Lake District in just 3 days, causing several rivers to burst their banks. Extensive flooding in Carlisle saw 30,000 homes lose their power and 3,000 people evacuated as flood waters reached 1.8m before subsiding on 9th January (Guy Carpenter, 2005b).

Windstorm Kyrill (January 2007)

Northern Europe experienced a powerful extratropical cyclone in the form of Windstorm Kyrill, which left a large trail of damage in its wake on 18th January 2007. The British Isles, northern France, the Netherlands, Germany, Austria, Poland and the Czech Republic all reported substantial damage and loss of life.

Formation and Track

The origins of Kyrill crossed the east coast of North America at midday on 16th January, and, propelled by an exceptionally fast jet stream, reached the UK in just two days. As the system moved over the Atlantic it developed rapidly, and as the storm approached the British Isles on the 18th January its central pressure dropped to 965hPa (Guy Carpenter, 2007).

Figure 1.6 shows Kyrill west of Ireland as it moved rapidly towards the British Isles. Coupled with developing high pressure areas over southern Europe this enabled the formation of large pressure gradients, which led to the high windspeeds across much of the British Isles and northern Europe. Unlike most systems, as Kyrill passed over the British Isles and the North Sea it underwent further deepening, enabling damaging winds to be sustained as it moved into mainland Europe.

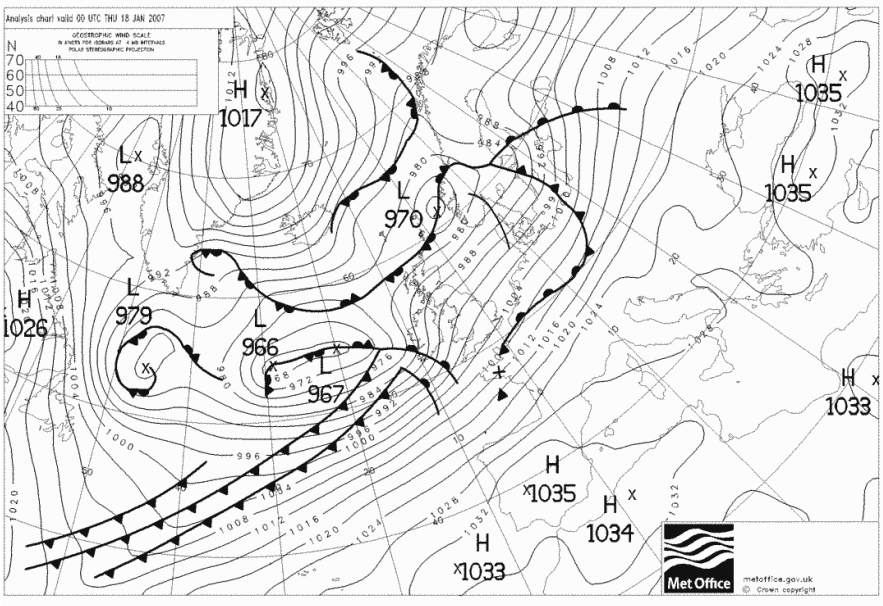

Figure 1.6 – Sea Level Pressure chart at 0000GMT on the 18th January 2007. Source: www.wetterzentrale.de

Damage Associated with Kyrill

Kyrill was not an unusual windstorm in the sense of high windspeeds; however, it was somewhat unusual in that damaging windspeeds persisted for more than 24 hours, partly as a result of the reintensification as Kyrill crossed the UK. Kyrill did not have the intensity of the October 1987 storm, but did have similar footprint to Daria, although slightly lower windspeeds, as shown in Figure 1.7. The highest gust speed observed was 44 ms^{-1} at Needles Lighthouse, while speeds exceeding 31 ms^{-1} were recorded throughout central parts of England and Wales, with gusts in coastal areas exceeding 36 ms^{-1} (Benfield, 2007). These were some of the highest windspeeds to hit the UK since Daria.

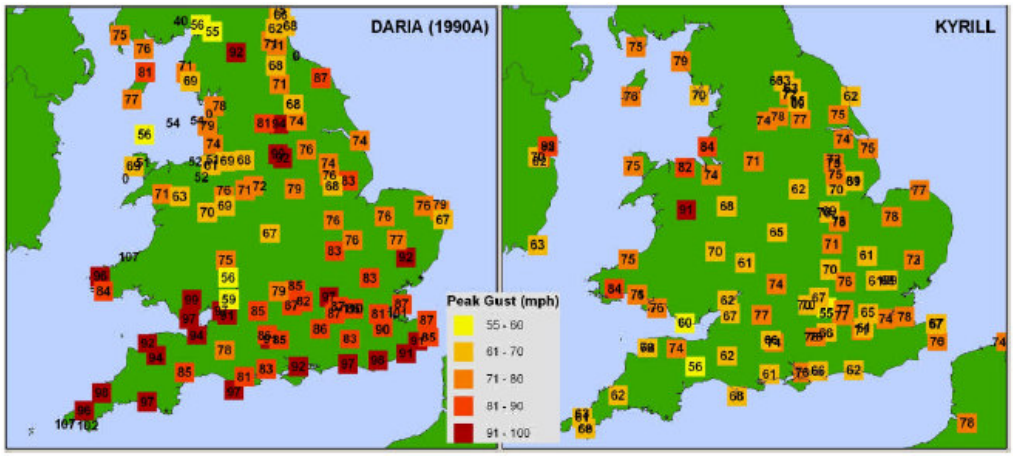

Figure 1.7 - Comparison of maximum gust speeds (in mph, equivalent to 0.45 ms^{-1}) observed in windstorms Daria and Kyrill. Source: Benfield (2007).

The ABI (2007a) place estimates of the insured loss in the UK at £600m. European wide losses are estimated at £3.1bn, with over half that stemming from losses in Germany (Zanetti, 2008). Loss information from this storm was difficult to obtain initially since relatively low levels of damage were caused over a very wide area, resulting in many small claims.

The UK suffered widespread structural damage to buildings, felling of trees and power lines. Flights were suspended at all major airports and rail networks were badly disrupted. Nine people lost their lives, while several hundred thousand homes were left without power. Storm damage was not restricted to the land, with the container ship Napoli suffering damage in the English Channel, before deliberately grounding off the Devon coast to prevent

it breaking up in deep water, with estimated hull damage and cargo losses of £50m (Alovisi *et al.*, 2007).

1.2 Historic Trends in Climate Related Natural Catastrophes

This section describes some of the trends seen in both economic and insured losses resulting from natural catastrophes, with a focus on climate related events.

To a large extent published data on global annual losses encompass all natural catastrophes, including geological (earthquake, tsunami and volcanic events). Analysis of trends in this category of events is beyond the scope of this project; however, data are presented which includes loss figures for all natural catastrophes. Where this is the case it is important to note that although geological events make up 30% of all natural catastrophic events resulting in over $1bn losses between 1970 and 2002, they only produce 18% of the total insured losses (Munich Re, 2002a). This figure of 18% is dominated by losses following the Northridge earthquake in 1994, which resulted in insured losses exceeding £10bn (well over half the total amount of insured losses from geological events since 1970). Geological events tend to have a low economic impact despite their abundance and high fatality numbers (Munich Re (2002a) estimate 48% of natural catastrophe fatalities result from geological events). This is demonstrated by the Kashmir earthquake in 2005 (nearly 90000 deaths, £3bn economic losses, but minimal insured losses), and the Indian Ocean tsunami in 2004 (over 250000 deaths, direct economic losses of approximately £6.5bn, yet insured losses did not exceed £1bn) (Munich Re, 2005; Munich Re, 2006). Therefore the inclusion of geological related insured loss in natural catastrophe loss figures can largely be overlooked when considering trends in these data.

1.2.1 Worldwide Trends

Worldwide, the number and costs of catastrophic weather events have increased dramatically in recent years. Figure 1.8 shows the upward trend of economic and insured losses associated with all natural catastrophes since 1970, of which over 80% are associated with weather events. Insured losses have risen from a negligible level in the 1950s to an annual average value exceeding $15bn (based on the last decade of losses) (Munich Re, 2007).

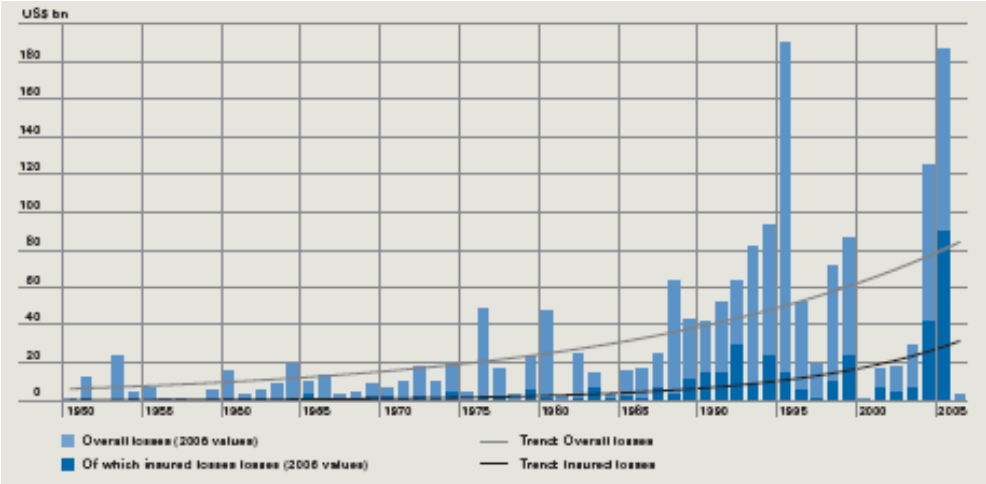

Figure 1.8 - Worldwide annual economic and insured losses from catastrophic events (2006 US$ billion). Source: Munich Re (2007).

The most dominant type of natural catastrophe, in terms of the number of events, economic and insured losses is windstorm. Windstorm losses make up over 70% of all insured losses, while on average 40% of natural catastrophes are windstorms (Munich Re, 2002a). The high number of windstorms per year, relative to other natural catastrophes, is shown in Figure 1.9.

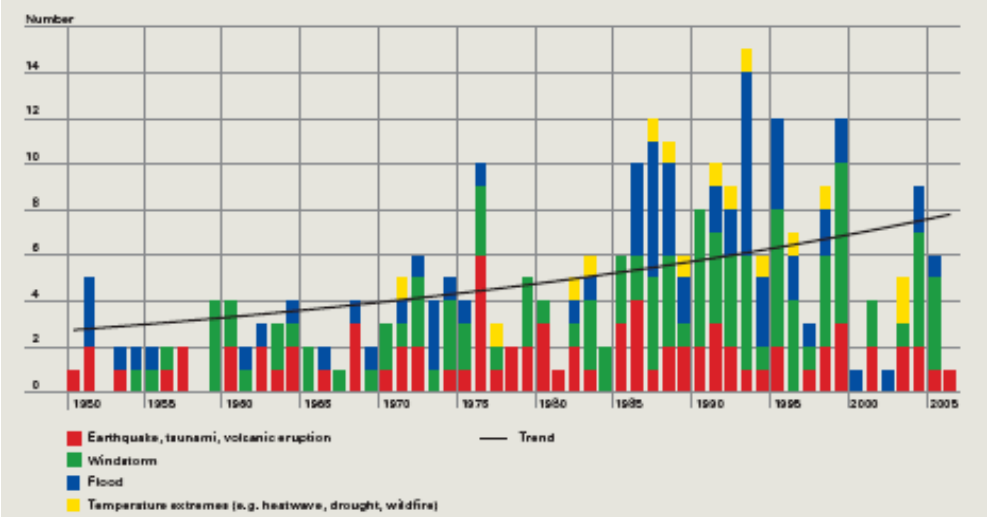

Figure 1.9 - Number of Great Natural Catastrophes each year. Source: Munich Re (2007).

The number of Great Natural Catastrophes has risen from an annual average of 2 in the 1950s and 2.7 in the 1960s to 5.1 in the last 10-year period (1996-2006). The annual average number of geological events (red bars in Figure 1.9) have risen from 0.7 in the 1950s, and 1.1 in the 1960s to 1.4 in the last decade, indicating the overall increase is driven by increases in weather related catastrophes.

The upward trend exhibited in Figure 1.8 can be largely explained by economic and demographic changes, and is discussed in detail in section 1.2.3. A contributing factor to this trend may be the increased frequency and severity of extreme events associated with climate change (IPCC, 2007), demonstrated by the upward trend in Figure 1.9. The potential role of climate change in increasing catastrophes and losses is a contentious topic. Leading reinsurers Munich Re (2007) and Swiss Re (Brauner, 2002; Zanetti, 2007) contend that the climate change is contributing to loss increases, while there is a certain amount of scepticism in both the political and insurance arenas. The issue of climate change and insurance is further reviewed in section 1.5.

1.2.2 UK Trends

Identifying significant trends in the loss figures for the UK is difficult since data for climate related losses are only available back to 1987 (1988 for

subsidence claims). These data, collated by the Association of British Insurers (ABI) from over 85% of the UK's insurers, are shown in Figure 1.10. The graph is dominated by large loss events, such as the October 1987 storm, windstorm Daria in 1990 and the autumn floods of 2000.

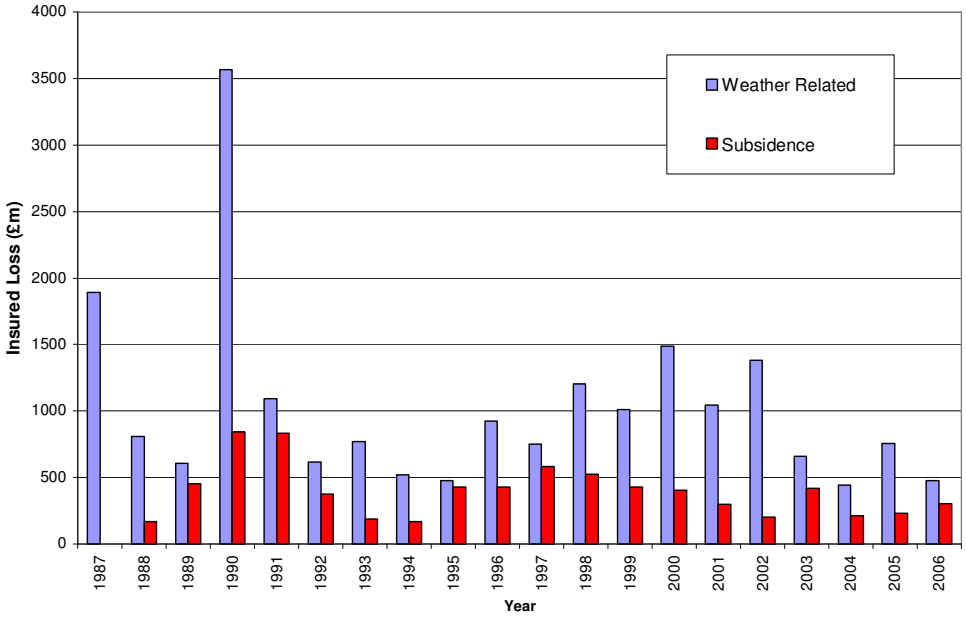

Figure 1.10 - Climate related insured property losses in the UK in 1987-2006 (adjusted to 2007 £ values). No value for subsidence in 1987 is available. Source: ABI Statistics.

Domestic property losses make up just under 75% of these losses, with commercial property losses making up the remainder. Weather related business interruption losses are not included in this analysis, but amount to an annual average of £25m (equivalent to 2.5% of total losses).

Since the final quarter of 1997 the ABI have collected information on the nature of the weather related domestic property losses, falling into three categories; storm (i.e. windstorm), flooding and pipe damage. Since 1997 half of all losses have been due to storm. There is some difficulty in assessing the contribution of flood and pipe damage due to a change in ABI's data collection methods in 2004 to incorporate a more reliable breakdown of "escape of water". This was brought about by the observation of high levels of weather related burst pipe losses in summer months that were not considered credible. Since that point the data show that the relative contributions of flood and burst pipes losses to weather related annual loss, have changed from 16% to 26%, and 36% to 10% respectively. Due to the prevalence of windstorm events over

flood events between 2004 and 2006, the figure for flooding appears artificially low. However, it is clear from Figure 1.11 that since the adjustment in data collecting methods, flooding and storm damage produce the most significant insured domestic property losses.

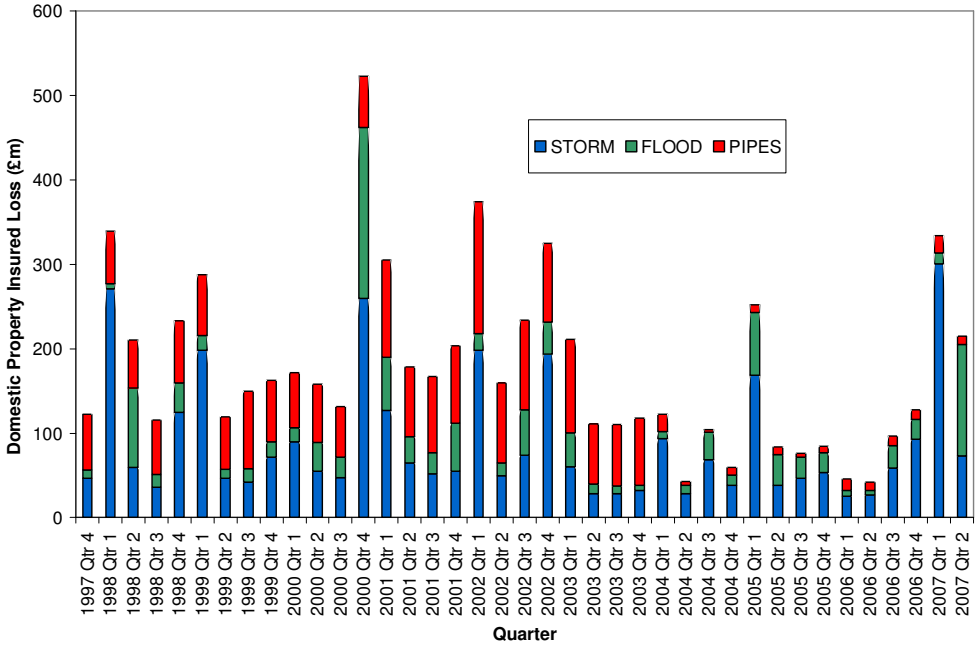

Figure 1.11 - Weather related insured domestic property losses in the UK in 1997-2006 (adjusted to 2007 £ values). Source: ABI statistics.

The Building Research Establishment (BRE) has collated details of building damage due to wind since 1962, through examinations of newspaper reports (e.g Blackmore and Tsokri, 2004; Tsokri and Blackmore, 2003). Annually, the number of damage locations is recorded, although no information regarding the financial impact is included. Figure 1.12 presents the data for 1962-2002.

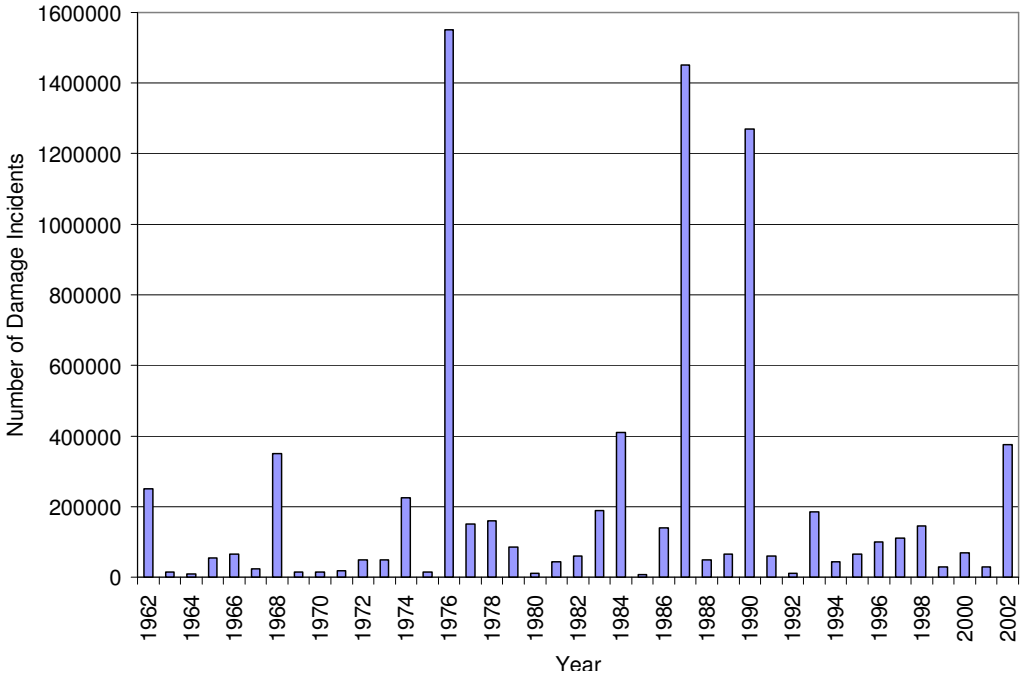

Figure 1.12 - Number of wind damage incidents 1962-2002. Source: Blackmore and Tsokri (2004).

Interpreting these data can be problematic since newspaper reports of damage can be heavily dependent on what other news is available at the time and the degree of public interest. The difficulty in assessing long term trends in damage numbers is also compounded by the increase in media coverage in recent decades. Large events, such as the October 1987 and 1990 Burn's Day storms are clearly evident in these data, and correspond with peaks in insured domestic property losses in Figure 1.10. Additionally, the damage associated with "Capella" in January 1976 is reflected here, which impacted a wide area including central and northern England. However, claims are estimated to be three to four times lower (even after allowing for inflation) for this event compared with the October 1987 storm. Higher insured losses were recorded in the 1987 storm largely due to the greater impact in southeast England, where property values are higher (RMS, 2007).

A "storm catalogue" developed by Palutikof and Skellern (1991) for the insurance industry ranks 47 severe storms affecting the UK between 1920 and 1990, based on maximum recorded windspeed, storm duration and other variables not described. The relative severity of each storm was assessed using the local one-in-fifty-year gust speed. Unfortunately, the Palutikof and Skellern (1991) report is commercially sensitive, and although the storm catalogue is briefly described in Palutikof *et al.* (1997), the full details of

methodology utilised and the potential financial impact of these storms is unavailable. However, the Burns Day storm ranks first, with Capella second and the October 1987 storm ranking fourth. Due to the limited nature of the ABI loss records prior to 1990 it is difficult to make an assessment of the accuracy of the storm catalogue in identifying high impact (in terms of insured loss) windstorm events.

It has been demonstrated here that a very short (less than 10 years) and inhomogeneous record exists regarding the impacts of different weather events on insured domestic property losses in the UK. Alternate sources of information, e.g. media sources (Blackmore and Tsokri, 2004), are available which document wind damage in the UK. However, interpreting data from such sources can be problematic, and they carry little information regarding economic or insured losses. For these reasons no attempt is made here to establish a trend in weather-related UK insured losses.

1.2.3 Socio-economic shifts and increasing losses

In addition to changes in the climate system, several other factors play a role in producing the upward trends in economic and insured losses described in section 1.2.1. Shifts in population number and density, changing economics, and varying insurance coverage and penetration influence the economic and societal impact of weather events. In the last 50 years not only has world population increased dramatically, but the number of people living in areas at risk of severe weather events has also increased (IPCC, 2007). For instance the population in coastal counties of Florida increased from less than 500,000 in 1900 to over 10 million in 1990 (Pielke Jr. and Landsea, 1998). In Australia 25% of the population growth between 1991 and 1996 occurred within 3km of the coast (Hawker, 2007). There has also been an increase in wealth, coupled with a rapid increase in insured assets, again not just in total, but in at risk areas (Zanetti *et al.*, 2005). More than $7trillion of insured property lies along the Gulf and Atlantic coasts in the United States, comprising 16% of the total insured property in that country (Mills, 2005). In conjunction with these factors, changes associated with insurance have taken place through the years.

Munich Re (2002b) suggest changes in insurance density and average sum insured per policy between 1990 and 1999 increased the exposed property value by a factor of 1.8-2. Changes in coverage, penetration, height of deductibles and the way in which claims are handled only add to blur the trend line. For instance, certain countries in Europe have mandatory domestic property flood insurance, while others do not (Menzinger and Brauner, 2002). Thus, interpreting European wide flood losses would be difficult. Disentangling societal and economic shifts from any trends in insured loss data is very difficult, with no standard methodology.

Several studies have tackled this issue, primarily focussed on one region or type of natural catastrophe. In an analysis of all weather related catastrophic events in the US (defined as exceeding $100m insured property losses) Changnon and Changnon (1998) normalised losses from over 200 events. Inflation, growth in wealth and changes in the value, location and density of property at risk were taken into consideration. Normalised data revealed no temporal trend, with the top 10 loss events showing an even distribution. In a review of material to date, Changnon *et al.* (2000) concluded that upward trends in losses from all weather extremes in the US are driven by economic and societal changes.

Pielke Jr. and Landsea (1998) considered hurricane losses in the US in the period 1950-1995. After normalising the insured loss data for inflation over that period, an upward trend in losses was still evident. However, by simulating losses based on 1995 population and wealth characteristics, this upward trend was removed revealing a multidecadal variation in losses with peaks in the 1940s-60s and 1990s. Pielke Jr. *et al.* (2008) updated this study, including an analysis of losses up to 2005, again finding no upward trend in normalised losses, but noting that the period 1996-2005 suffered the second greatest normalised loss in the last 11 decades, following 1926-35. However, Emanuel (2005) found that over the last 30 years there has been an increase in the destructiveness of hurricanes due to an increase in storm lifetimes and intensity. This, the author contends, coupled with changes in socio-economics, is driving the upward trend in hurricane losses in the US.

Changnon (2007) analysed winter storm damage in the US, normalising data using three different adjustments. The first altered property values, and repair costs, to 2003 US dollar values, while the second accounted for changes in the property market of each affected area. A third adjustment was made to correct figures for relative changes in the proportion of properties that were insured against weather perils. Analysis of 202 winter storms, each causing in excess of $1million in insured property losses, showed that the average number of storms per 5-year period had declined since 1949. However, the normalised loss values, over the same period, showed an upward trend. This study indicates that increases in winter storm size and intensity, are contributing to an upward curve in insured losses.

Little work has been done in this area (quantifying socio-economic impacts on insured loss trends) on weather events outside of the US however. The Insurance Australia Group acknowledges the effect of changing demographics on loss increases in Australia, but no attempt is made at quantifying these effects (Coleman, 2002). In a discussion on extreme temperatures in the Swiss Alps, Beniston and Stephenson (2004), state that increases in insured losses from extreme weather events are impacted by increases in population density, but do not quantify this effect. Bouwer and Vellinga (2002) highlight the role of increasing urbanisation on global increases in losses from precipitation related events, but again with no quantification.

Despite the uncertainty involved in normalising losses, the role of socio-economics in rising insured losses is increasingly considered in the literature. However, several human factors, which could have played a role in actually masking losses, have not been dealt with satisfactorily. Kunkel *et al.* (1999) point out that despite the upward trend in losses, the number of deaths from weather events in the US, has shown little change over time. Improved building codes and construction techniques, increased and improved defence systems, early warning systems and improved forecasts mean populations are generally more prepared for extreme weather events (Valverde Jr. and Andrews, 2006; Mills, 2005). These features not only directly protect properties, but give the inhabitants enough warning to add further protection (e.g. sandbagging before a river bursts its bank). All the losses discussed in

this section refer to direct losses from weather events. Secondary losses such as those resulting from power outages and damage to transport and communications infrastructure, are not considered. Furthermore, tertiary impacts, such as effects on the tourist industry, or regeneration projects are not considered. If these secondary and tertiary losses were factored into the loss data, the upward trend would be even more exaggerated (Mills, 2005).
Following an international workshop involving 32 leading climate and disaster researchers, including members from the insurance and reinsurance industry, consensus statements were reported by Hoppe and Pielke Jr. (2006), including;

- "*Analyses of long-term records of disaster losses indicate that societal change and economic development are the principal factors responsible for the documented increasing losses to date*"
- "*There is evidence that changing patterns of extreme events are drivers for recent increases in global losses*"

It is clear, from the material cited in this section, and these two statements that there is much work to be done in this area. Quantification of the impact of changing socio-economic factors on increasing economic and insured losses is essential in order to assess the potential impact of changing frequency and intensity of weather events. In the future, constantly fluid populations and economies will be subjected to climate related natural catastrophes, likely with increasingly expensive consequences, both financially and in terms of human life. Any changes in extreme weather events brought about by a shift in climate will impact directly on economic and insured losses. A discussion of the issues surrounding climate change and the insurance industry is presented in section 1.5.

1.3 Estimating Insured Loss with Catastrophe Modelling

The magnitude of losses associated with weather related natural catastrophes, described in the previous two sections, can carry serious economic consequences for the region and people affected, the political body responsible for that region as well as the insurance industry. All three parties

have a vested interest in managing the risk posed by severe weather events, and mitigating against them. One of the keys of risk management is the identification and analysis of the risk. Catastrophe modelling is a tool that provides a thorough analysis of the risk, in this case a thorough understanding of the potential impact of natural catastrophes on a certain location. This section introduces the role of catastrophe modelling in the insurance industry, and describes some studies which endeavour to model losses from natural catastrophes.

1.3.1 The role of catastrophe modelling in the insurance industry

Catastrophe modelling was not widely utilised until nine insurers became insolvent following Hurricane Andrew in 1992, which resulted in then record losses in the US (Grossi and Kunreuther, 2006). Currently, catastrophe models are in widespread use with several independent modelling firms serving the insurance industry. Leading companies, such as EQECAT, Applied Insurance Research (AIR) and Risk Management Solutions (RMS), have developed models covering most climate related perils worldwide.

Generally, a catastrophe model is comprised of four modules; hazard, exposure, vulnerability and loss. The hazard module contains information on the nature of the weather event, incorporating such things as storm track, intensity and duration. Within the exposure module details of the type of properties at risk are stored, including building specifications and age. The third module, vulnerability, is key to producing a realistic catastrophe model. Hazard and exposure are combined to produce a vulnerability curve, which describes the expected damage for a given magnitude or intensity of hazard. A fourth component, loss, is usually employed by the insurers, and incorporates the vulnerability curve and policy conditions, to produce estimates of insured loss.

If the catastrophe model is repeatedly run using different information in the hazard module (e.g. varying storm intensity), output can be used to form an exceedance probability curve (Grossi *et al.*, 2005). This curve, with loss on the

horizontal axis and the probability of the event occurring on the vertical axis, is utilised by insurers for managing their property portfolio. It can be used to form the basis for writing more policies in a certain location, based on a predetermined, finite amount of risk the insurer is willing to accept. For example, should an insurer specify an acceptable risk level as a 0.4% exceedance probability (i.e. a return period of 250 years for that particular weather related event), a probability exceedance curve, shown in Figure 1.13, can be used to estimate the loss at this probability value. This value is termed Probable Maximum Loss (PML) (Grossi *et al.*, 2005), and in this example that value would stand at $21million.

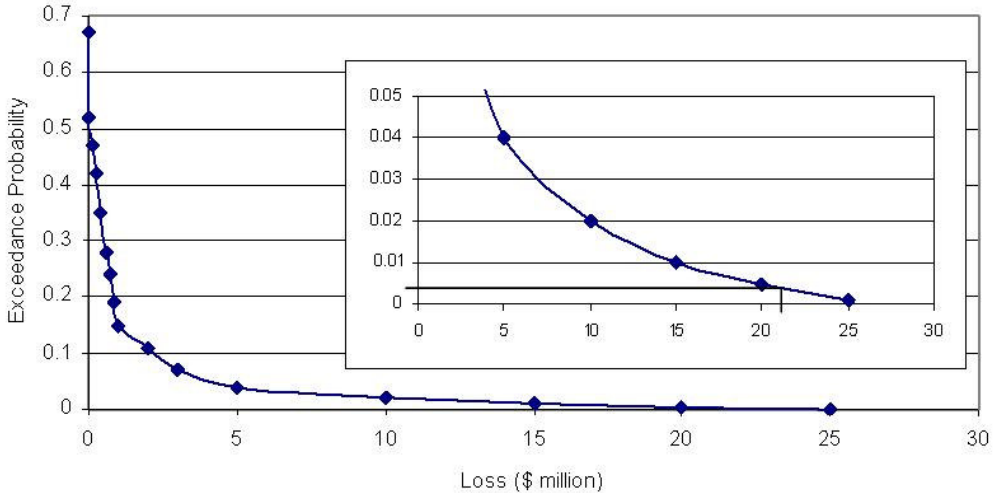

Figure 1.13 - Example of a probability exceedance curve. Source: Grossi *et al.* (2005).

Writing more policies would increase the exposure, resulting in the exceedance probability curve shifting to the right, i.e. for the same 0.4% risk level, the PML would be higher. However, the insurer could then decide to raise the deductible levels in the policies (changing information in the loss module), to shift the curve back to the left.

Confidence in the probability exceedance curve is increased the more the catastrophe model is run, using different information in the hazard module. To produce an exceedance probability curve for a European windstorm, one could run the catastrophe model with hazard information from all documented historical windstorms in Europe. However, since there have been a relatively small number of European windstorms documented in detail, a stochastic set of events is often generated, based on these documented events. This

method is utilised by Swiss Re, in their European Windstorm model, using a Monte Carlo simulation to develop a stochastic event set (Schwierz *et al.*, in submission). These are then used in the hazard module of the catastrophe model to extend the tails of the probability exceedance curve (i.e. allowing the estimation of the loss of a 1 in a 500 year storm, despite only having meteorological records of storms going back 200 years). AIR developed an alternative to this method in 2000, using Numerical Weather Prediction (NWP) to generate an event set for European extratropical cyclones (Dailey and Keller, 2006). The initial conditions of historical extratropical cyclones are perturbed slightly in the Fifth-Generation NCAR / Penn State Mesoscale Model (MM5). The model is then run, allowing these perturbations to propagate through time, producing a simulation of a new extratropical cyclone. This process can be repeated many thousands of times to develop an extensive, dynamically consistent, event set.

Catastrophe models are designed to estimate direct losses as well as indirect losses such as business interruption and relocation, but often do not capture subsequent losses, such as impacts resulting from offsite power outages, or mould (Grossi and Kunreuther, 2006). However, within the latest version of the RMS (2006a) European Windstorm model lies an additional loss amplification module, which includes some of these secondary losses. The module incorporates such impacts as demand surge, claims adjustment and inflation as well as the economic impact of reconstruction.

1.3.2 Modelling European windstorm risk

Data used in catastrophe models developed in the private sector, and indeed the model structures, are commercially sensitive and therefore there is little or no information on them in the public domain. Given the “black box” nature of the catastrophe models used in the insurance industry, there is very little chance of external validation or evaluation (Mills *et al.*, 2002). However, several studies exist in the academic literature which seek to model the European windstorm peril.

A windstorm damage index, based on windspeed and storm track, along with a measure of the vulnerability of properties at risk, is suggested by Blackmore (1994b) for the UK. Initially an assessment of the vulnerability of properties was made by analysing historical storms and damage reports in the media. This allowed the author to produce a vulnerability index which describes the number of locations of damage in 100km grid squares, based on the peak windspeed recorded in those grid squares. In order to calculate the level of damage for a given storm, the peak windspeeds are normalised to the maximum design windspeed, in each grid box, and combined with the vulnerability index. This can then be combined with the information regarding the average cost per damage location to produce an estimate of the losses produced by any given storm. Although results showed that this relationship was not valid for all storms, it does provide a method for looking at probable maximum loss for a windstorm event for the whole of the UK.

Rootzen and Tajvidi (1997) used statistical extreme value theory to investigate the relationship between storms and insured losses in southern Sweden between 1982 and 1993. Windspeed measurements from 78 storms were considered, and an attempt was made to correlate these with the resulting insured losses. The square of the maximum windspeed recorded at each station for each storm was taken, since this is proportional to wind pressure, which is related to damage. However, no correlation was found between these squared windspeeds and insured losses. The relationship between windspeed and damage has been shown, with regularity, to be a non-linear one. Heneka and Ruck (2004) cite two Munich Re studies which suggest that raising windspeeds to the power of 2.7 or to a power between 4 to 5 prove more accurate predictors of damage. A cubic relationship is utilised by Klawa and Ulbrich (2003); a logical one given that the advection of kinetic energy is dependent on the cube of the windspeed. Furthermore, the power dissipated by a tropical cyclone is shown by Emanuel (2005) to be related to the cube of the windspeed.

In an update to their previous study Rootzen and Tajvidi (2001) considered the same period and region, with the same storms and losses, but this time employed pressure readings to calculate geostrophic windspeeds, which were

then compared to insured losses. Again, little correlation was found. The results suggest that estimating damage from surface winds using geostrophic windspeeds may not be the most reliable method. With a varying landscape, the relationship between geostrophic windspeed and surface windspeeds may fluctuate across the study region. These studies do not include any consideration of vulnerability or exposure, so an inclusion of some vulnerability factor applied to different areas of the study region may have improved the correlation. Blackmore (1994a) reports that when even relatively low windspeeds are reached the most vulnerable properties (those which are poorly maintained, constructed or designed) will have already suffered damage, despite not necessarily reaching their design speed. Any further damage to adjacent buildings would require the windspeed to exceed the design speed. Baxter *et al.* (2001) highlight the importance of factoring in a vulnerability function. They found the primary cause of death from structural failure in a windstorm is related to chimney collapse, which in turn is related to the type and maintenance of the building.

Incorporating vulnerability into a loss model is clearly important. Klawa and Ulbrich (2003) normalised gust speeds in Germany to the local 98th percentile value to account for a "wind climate". The rationale being that building resistance cannot be considered homogenous over the entire area of study. Northern Germany is exposed to higher windspeeds than the south (Heneka and Ruck, 2004), and Klawa and Ulbrich (2003) found the same windspeed caused more damage in the south than the north. A similar pattern was found in the north and south of the UK (Blackmore, 1994a), where windspeeds of 29 ms^{-1} in the south, 33 ms^{-1} in the north, result in similar damage. In an analysis of the number of incidents of wind related damage per 10000 households, Spence *et al.* (1998) found that to produce a similar level of damage in the southwest of England windspeeds needed to be 6 ms^{-1} higher than those in the southeast. In comparison, windspeeds need to be 5 ms^{-1} higher in the north and 13 ms^{-1} higher in Scotland, compared with southeast England. Dorland *et al.* (1999) state that varying building standards in the Netherlands might cancel out any regional differences in vulnerability to windstorms. It was noted by Blackmore (1994b) that the locations in the UK which experience the most severe windstorms, are not those which record the most damage. So,

the assumption that building resistance is somehow adapted to wind climate seems valid. Spence *et al.* (1998) suggest that the vulnerability curve for any type of building could be a two-step polynomial, indicating some threshold value of windspeed below which no loss will be observed. The use of a high local windspeed percentile value as a threshold for damage in loss models, means only the extreme windspeeds in each location are considered to result in damage. Using additional socio-economic information may result in a more accurate estimation of the vulnerability of a particular region to the windstorm peril.

The potential inclusion of information regarding property type, or value (i.e. exposure information) in loss models could perhaps result in more accurate predictions of storm losses. In a study of storm losses in the Netherlands, Dorland *et al.* (1999) discovered that average income per household is not a good indicator of sum insured, and subsequently not useful in estimating insured windstorm losses. Furthermore, they found that losses were not related to storm duration either. Based on five storm events the authors developed a relationship between the number of properties and businesses in an area, the meteorological variables of the windstorm, and the resulting insured loss. Gust speeds, and not mean windspeeds, were shown to produce better estimates of storm losses, a finding in line with observations by Baxter *et al.* (2001). This seems a valid assumption given that gust speeds are considered by engineers when designing buildings (Spence *et al.*, 1998).

The use of maximum gust speeds as a parameter in predicting storm losses was continued by Klawa and Ulbrich (2003). They created a windstorm loss model using empirical functions and adjusted loss data provided by the German Insurance Association. Gust speeds from 24 stations across Germany were coupled with population information, to create a storm index (or storm damage function). This was then validated against actual storm loss data for the period 1970-1997, to create a loss model. Despite being a very simple model it reproduced the inter-annual variability of storm-related losses with a correlation coefficient $r = 0.96$. It even managed to simulate to impacts of individual storm events.

The use of gust speeds in estimating storm losses is not universally accepted, however. Combining loss information and windspeed data from the October 1987 storm and windstorm Daria in the UK, Hanson *et al.* (2004) found that maximum hourly mean windspeed windspeeds, and not gust speeds, were a more accurate predictor of insured loss. In this study Hanson *et al.* (2004) weighted the meteorological data by DAMSEL scores (Detailed Aspect Method of Scoring Excluding Location). DAMSEL combines information on elevation, aspect, soil and topex value (a measure of topographic exposure, representing the degree to which a location is sheltered). This had the affect of increasing windspeeds at more exposed locations, while leaving windspeeds at the least exposed sites unchanged. It also allowed the inclusion of surface roughness and altitude in the model. Damage was shown to be inversely related to the DAMSEL score. This implies that more sheltered locations suffer greater losses, and damage is not necessarily greatest where windspeeds are at their maximum, in line with Blackmore (1994b). This suggests that properties in built up areas are more vulnerable to windstorm damage than those in open countryside. The final model Hanson *et al.* (2004) developed showed losses could be realistically simulated, using maximum hourly mean windspeeds, distance from storm centre and DAMSEL scores. Given that the model construction methodology addresses issues of multicollinearity of independent variables, the inclusion of both distance form storm centre and maximum windspeed is interesting. One would assume the high correlation between these variables would result in the exclusion of one of them. This suggests that the distance from storm centre variable affects losses in non windspeed-related manner. One may speculate that the way in which claims are handled following a storm event could result in the distance from storm centre variable being an important variable. Following a large storm event in a particular area it is more likely that claims from this area do not undergo as stringent verification as claims from other regions during quieter periods, as insurers and loss adjustors personnel resources are stretched. Additionally, fraudulent claims are more likely to be filed, and paid, for policies held for properties near a storm centre.

Dorland *et al.* (1999) suggest that incorporation of more meteorological parameters, such as precipitation information, may increase accuracy of

predictions of storm losses. Rootzen and Tajvidi (2001) have a similar sentiment suggesting that their study could have benefited from treating summer and winter storms separately. They point to ground conditions and presence of leaves on trees as factors in the amount of damage delivered by a storm. This would seem a logical suggestion following the discussion of damage in the UK resulting from the October 1987 storm, when the trees were in foliage, and Windstorm Daria, when they were not (see section 1.1.1). In terms of direct damage, following personal communication between Klawa and Ulbrich (2003) and several primary insurers and reinsurers, they considered hail and rain damage negligible in Germany. Similarly in the UK direct damage from rain is not considered a significant contributor to insured losses (personal communication with Neil Carrington, Ecclesiastical Insurance Group).

Modelling the European windstorm peril is both of commercial and academic interest. In order to estimate insured loss it has been shown here that the key is to understand the relationship between the meteorological variables and the structures or regions at risk. The following section describes some of the characteristics of the UK climate that result in windstorm being the primary cause of domestic property insured loss.

1.4 The UK Wind Regime

The contribution of windstorm losses to overall insured loss in the UK is very significant, with some major windstorm loss events described in section 1.1.1. However, it is important to note that smaller, less severe wind damage events also occur across the UK throughout the year. The prevalence of wind damage can be attributed to the UK wind regime. This section aims to describe the nature of the UK wind regime as well as some of the synoptic scale features that can result in large loss events. Section 1.4.1 then discusses some the potential impacts climate change may have on the UK wind regime, and subsequently insured losses.

The primary constraint on the average wind field in the UK is the track of low pressure systems (including extratropical cyclones) in the mature or decaying stage of their lifecycle (Palutikof *et al.*, 1997). Baroclinic zones along the polar front, and stimulation from higher levels, cause cyclones to form, which then track across the North Atlantic and usually follow a path between Scotland and Iceland. A full discussion of the impact of extratropical cyclones on the UK wind regime follows later in this section. Windspeeds tend to be highest in the northwest of the UK due to its proximity to the track of the low pressure systems, with the southeast seeing the lowest windspeeds. Generally the highest winds and predominant wind directions lie in the southwest quadrant of the compass (Palutikof *et al.*, 1997).

Topography is a secondary constraint on the wind field in the UK. The highest windspeeds are measured along the west coast of Ireland and Scotland due to lower drag coefficients over the sea. Drag coefficients over land are higher and subsequently the wind speeds decrease further inland. The effect of reduced friction on windspeeds over the sea is no longer present further than a few hundred metres inland. Orographic effects lead to windspeeds increasing with altitude. These factors combine to produce the mean wind field for the UK, depicted in Figure 1.14. However, it should be noted that various permutations of weather patterns and geography result in day-to-day deviations. In fact the major windstorm in October 1987, which resulted in the extensive insured loss described in section 1.1.1, was due to its exceptional southerly track.

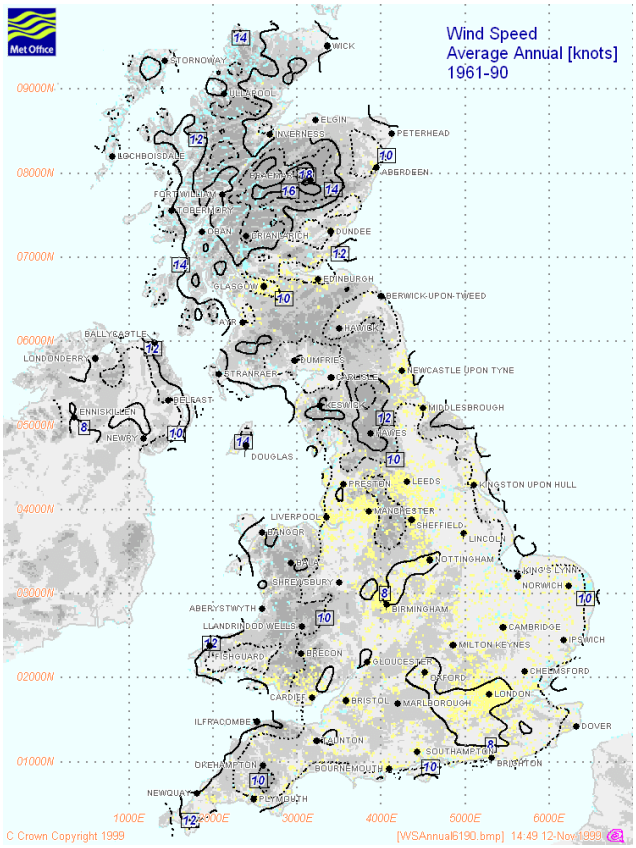

Figure 1.14 - Annual average windspeed (in knots, equivalent to 0.515 ms^{-1}) 1961 – 1990. Source: UK Met Office - www.met-office.gov.uk/climate/uk/averages/

Defining regions of the UK based temperature and precipitation is very common; Barrow and Hulme (1997) and Wheeler and Mayes (1997) cite several works which identified regional climates of the British Isles based on these meteorological variables. However, it seems a classification method based on wind characteristics is largely overlooked. Miller *et al.* (1987) do define different regions of the UK based on their wind exposure, for use by the forestry industry. The zones they developed closely follow the contours in Figure 1.14.

The highest mean windspeeds and most exposed zones are in the southwest of Cornwall and along the west coast of Scotland. North Scotland's west coast is similarly exposed to westerlies, although the highest mainland mean windspeeds occur over the peaks of the Grampian Mountains. In contrast the region with the lowest wind exposure and mean windspeeds is shown to be southeast England. The low values in southern parts of the UK highlight the

exceptional nature of the windspeeds recorded during the October 1987 storm.

In an analysis of potential wind energy generation by the UK, Sinden (2007) considered hourly mean windspeeds in excess of 25 ms^{-1} (cut off speeds for turbines). He found 96% of hours, in a 34-year record of 66 stations, recorded speeds below that threshold. The most extreme event (in terms of area affected by winds over 25 ms^{-1}) saw 43% of the UK affected simultaneously. Figure 1.15 shows that windspeeds exceeding 25 ms^{-1} affect over a third of the UK simultaneously roughly once every three years.

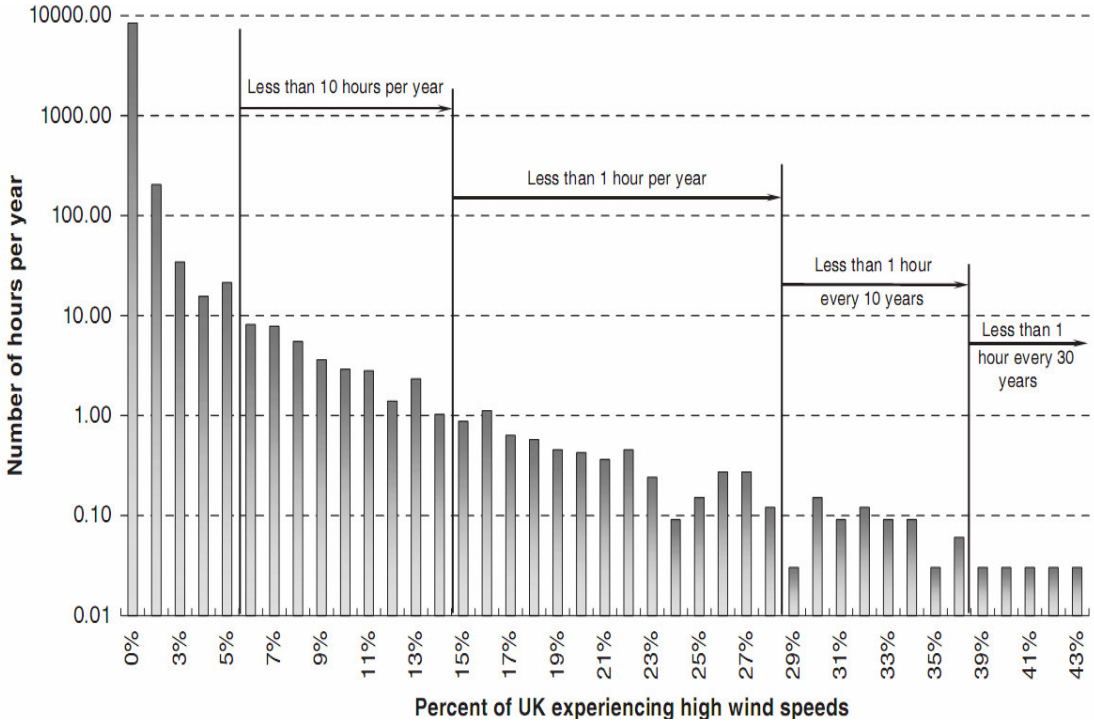

Figure 1.15 - Frequency and extent of UK land area affected by high windspeed events. Source: Sinden (2007).

Windstorms also show different temporal and spatial patterns over the UK, illustrated in Figure 1.16.

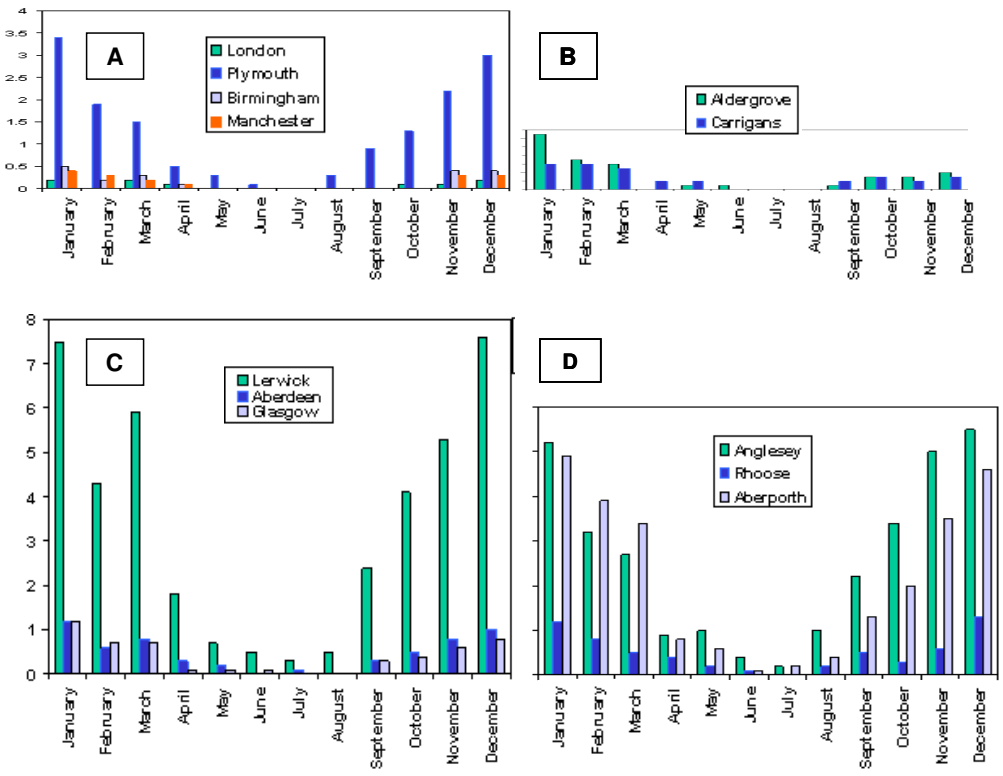

Figure 1.16 - Average number of days of gales (windspeeds exceeding 17.2ms^{-1}, or Beaufort scale 8) per year in different regions of the UK (based on the period 1961-1990). Panel A refers to England, B to Northern Ireland, C to Scotland and D to Wales. Source: UKMO (2007c)

The location receiving the highest number of gales per year, on average, is Lerwick in Scotland, while the least are recorded in Manchester. Interpreting these graphs is somewhat difficult. It can be argued that, based on Figure 1.16, Wales sees more gales per year than Scotland, as two stations show winter peaks over 5 gales per year in Wales, but only one in Scotland. Similarly, data from Plymouth could skew an overall England average, implying that it receives more gales a year than Northern Ireland. The limited number of stations and lack of spatial coverage means that conclusions of this nature may be somewhat misleading. However, these plots serve as an indication of the relative storminess of different UK regions. The fact that coastal stations (Plymouth, Lerwick, Anglesey and Aberporth) record more gales per year than the remaining stations in their respective countries put together, reflects the patterns shown in Figure 1.14.

The wind characteristics of the UK are described above in terms of mean windspeeds. Sinden (2007) presents an assessment of high windspeeds, with the UKMO (2007c) data describing the spatial characteristics of gale days

(also based on mean windspeeds). However, the literature describing the UK climate contains very little information regarding gustiness. The importance of gust speeds in assessing the potential impact of a windstorm has been shown in section 1.3.2. The lack of literature covering gust speeds may be explained by the lack of availability of homogenous gust measurements across the UK (Sinden, 2007).

Extratropical Cyclones

Extratropical cyclones are low pressure systems, and as already described, play a dominant role in governing the wind climate of the UK. While it is not the intention here to provide a full description of the formation and development of extratropical cyclones, as this topic is well covered in the literature (McIlveen, 1992; Ahrens, 2002; Barry and Chorley, 1998), it is important to understand some of the processes that are involved in the generation of damaging European windstorms. Development of cyclones in the mid and high latitudes leads to their nomenclature as extratropical. Cyclones help redistribute energy within the climate system, generally from the equator to polar regions. In the case of the extratropical cyclones that affect the UK, their development usually results from a disturbance on a frontal boundary in a region exhibiting a steep horizontal temperature gradient (known as a baroclinic zone) (Barry and Chorley, 1998). Upper air divergence, associated with an upper level jet (such as the Polar jet stream), is a trigger for this disturbance. Hence the position of the Polar Front in the northern Hemisphere, usually located between 40-60^{o}N, largely determines the track of extratropical cyclones. In summer the Polar jet is located further north, resulting in a relatively low number of extratropical cyclones impacting the UK. In winter however, the Polar jet moves southward, leading to greater extratropical cyclone activity over the UK (Ahrens, 2002). This greatly explains Blackmore (1994a) finding that 77% of the 47 most severe UK windstorms between 1962 and 1993 were in December, January and February, while none occurred in the summer months between May and August. A similar pattern is shown in the average number of gale days per year, shown in Figure 1.16. All four regions of the UK have minimum counts for gale days in the summer months, while the greatest number of gales are

recorded in December and January. Further evidence of this trend is presented by Sinden (2007), who found wind power availability in winter (December, January and February) in the UK was almost double that in summer (June, July and August). The intensity of the polar jet varies seasonally due variations in the temperature and pressure gradient across the polar front. The greatest windspeeds tend to occur in winter when the temperature gradient it at its greatest.

It must be noted, however, that not all extratropical cyclones develop into damaging storms. In order for this to occur, the system must undergo rapid deepening, forced from above and by associated thermodynamic and dynamic processes. Ulbrich *et al.* (2001) describe the development of three damaging European windstorms in December 1999. The synoptic patterns on each occasion show a band of extremely high baroclinicity in the proximity of the cyclone track. Latent heat release, from precipitation, also aids intensification of extratropical cyclones as it causes low level flow to accelerate towards the centre of the low pressure system (Danard *et al.*, 2004). The presence of an air mass with a high equivalent potential temperature, lying to the south of the extratropical cyclone track in December 1999 was identified by Ulbrich *et al.* (2001). This may have led to further intensification of the system due to latent heat release. A number of damaging European extratropical cyclones undergo "explosive" deepening. This almost exclusively maritime phenomenon refers to the rapid intensification of a cyclone, driven by a combination of; strong upper-level forcing, intrusion stratospheric high potential vorticity air, latent heat release, surface energy fluxes from the ocean and enhanced local baroclinicity from differential surface heating (Wang and Rogers, 2001). In the eastern North Atlantic extreme explosive cyclogenesis often occurs when a parent cyclone, lying northeast of an incipient low, advects high potential vorticity air southwards at upper levels, while enhancing lower baroclincity at lower levels.

The Sting Jet

Although high windspeeds are associated with the cold fronts of extratropical cyclones, an extreme class of explosively deepening extratropical cyclones, with particularly damaging windspeeds, has been identified by Browning

(2004). Notably, Windstorm Erwin and 16th October 1987 exhibited these features.

An illustration of a fully developed extratropical cyclone is shown in Figure 1.17. The warm conveyor belt (W1) extends along the primary cold front (CF1), before rising above the warm front. Warm air from the secondary warm conveyor belt doubles back, crossing the dry slot region in lower levels, before rising up above the bent back warm front (WF2). This air flow then fans out forming the upper cloud head. Below this lies the cold conveyor belt, which at the southern tip, begins to hook around (cyclonic circulation) forming a secondary cold front (CF2). Once this formation is in existence damaging winds are likely to occur due to an intrusion of dry air, descending from upper levels (bringing momentum down through the atmosphere), and overrunning the secondary cold front within the dry slot region. This process enhances windspeeds at the surface, with maximum windspeeds located in the dry slot. Grønås (1995) suggested strong winds were developed as a result of secondary, mesoscale cyclogenesis in the bent-back warm front (WF2). Due its shape, and damaging windspeeds, this feature became know as “the poisonous tail” (Grønås, 1995).

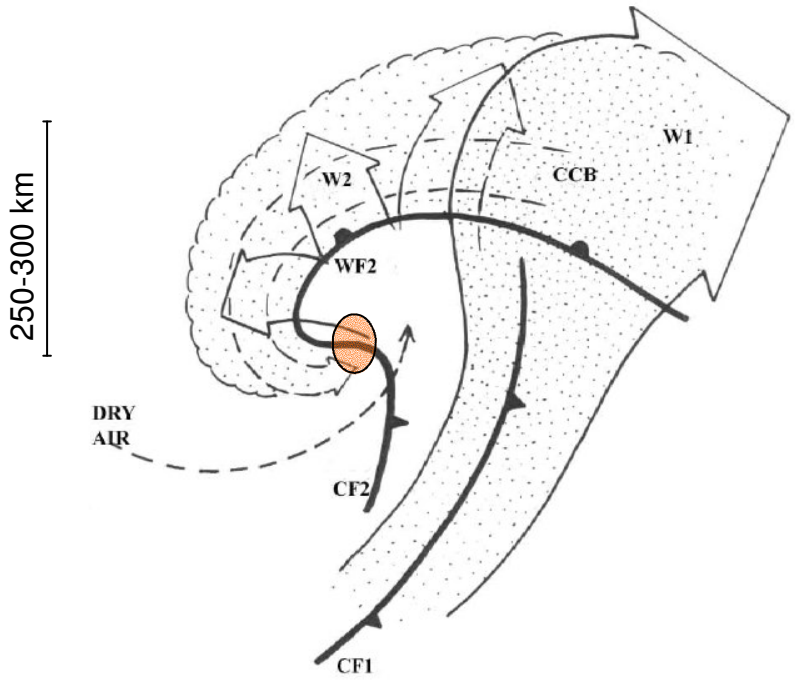

Figure 1.17 - Conceptual model of the principal airflows in an extratropical cyclone. CF1 (CF2) refer to the primary (secondary) cold front and similarly WF2 refer to the secondary warm front. W1 (W2) represent the primary (secondary) warm conveyor belt, and similarly CCB refers to the cold conveyor belt. The orange zone represents the area of windspeed maxima. Source: Browning (2004).

Based on observational data Browning (2004) suggests that strong evaporation at the tip of the cloud head further enhances the dry slot windspeeds, dubbing this the “sting in the tail” or the Sting Jet. He suggests the latent heat release from the evaporation of cloud droplets and rainfall within this region of slantwise descent results in even higher gust speeds measured at the surface. In addition, conditional symmetric instability in, and upwind of, the dry slot region could produce mesoscale slantwise circulations, contributing to the enhancement of surface gust speeds.

Both Windstorm Erwin (January 2005) and the October 1987 storm (described in section 1.1.1) showed evidence of a Sting Jet. Figure 1.18 is a thermal satellite picture taken at 1147GMT on the 8th January 2005. The cloudless region, highlighted with the red arrow, indicates the dry slot - a tongue of very dry air being dragged down from above, bringing the strong winds above the depression to the surface. The Sting Jet, located at the evaporative tip at the southern point of the cloud head, lies just below the head of the red arrow. The most damaging winds were associated with this feature as it passed over the UK and Scandinavia.

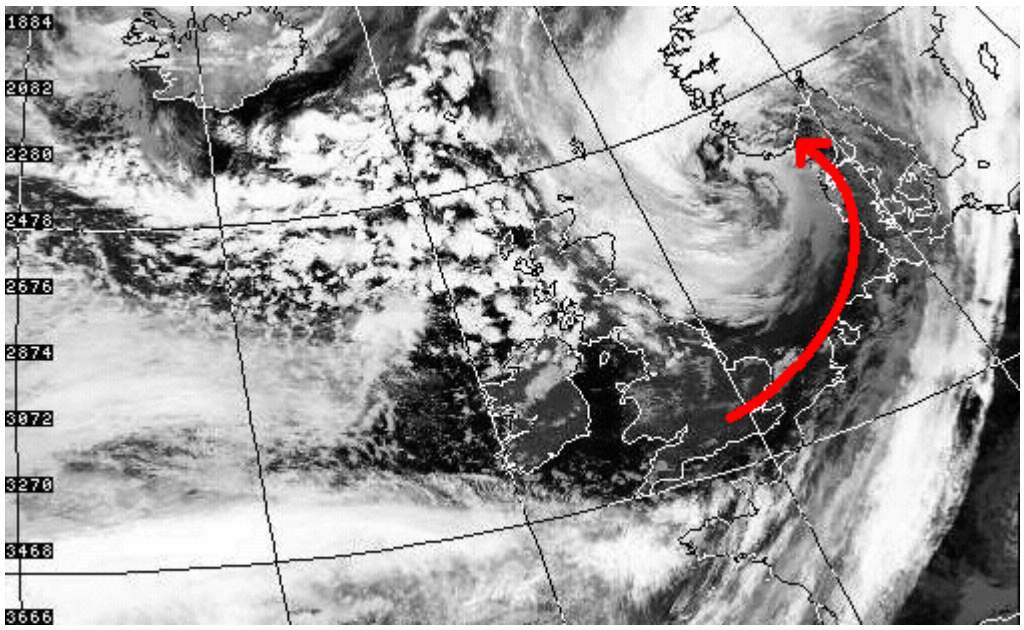

Figure 1.18 - Thermal satellite picture at 1147GMT, 8th January 2005. The red arrow indicates the ‘dry slot’. Source: Dundee Satellite Receiving Station (http://www.sat.dundee.ac.uk/)

1.4.1 Future climate change and the UK wind regime

Consensus in the scientific world is that climate change is a reality for this and future generations (IPCC, 2007). Climate in the UK has seen a change over the last 50 years to one which is both, on average, warmer and wetter. It is thought that this trend is set to continue, with models suggesting summer temperature increases of up to 3°C by the 2050s in southern England, coupled with increases in winter rainfall by up to 15% (Hulme *et al.*, 2002). Given that the UK wind regime is largely governed by extratropical cyclones, any changes in the frequency, intensity, or track of these systems will have a direct impact on the UK. This section describes some of the studies assessing the potential impact of climate change on the features of the European wind regime.

Lozano *et al.* (2004) describe two basic concepts relating the potential change in frequency and intensity of extratropical cyclones to climate change. In an enhanced greenhouse gas atmosphere, one scenario is that the upper troposphere becomes heated by long-wave terrestrial radiation, resulting in an intensification of vertical and latitudinal transport of heat. As already stated, extratropical cyclones act to redistribute energy from lower latitudes to the poles, so this scenario suggests they will become more intense. An alternative scenario is that polar surfaces will warm more than those in lower latitudes, reducing the lower troposphere temperature gradient, and thus reducing the intensity of extratropical cyclones.

In a 2060-89 time slice experiment perform by Lozano *et al.* (2004) using the Global Circulation Model (GCM) ECHAM4[7], fewer storms are simulated to impact the UK. However, it is suggested that the intensity of the remaining storms will increase. Similar results were presented by Lambert (1995), who found a decrease of about 4% in the number of winter extratropical cyclones in a doubled carbon dioxide atmosphere, in both the Northern and Southern Hemisphere. He also saw a shift towards more intense systems, suggesting the increased moisture in the atmosphere as a driver. Carnell and Senior

[7] **E**uropean **C**entre **HAM**burg 4 – An atmosphere only GCM, developed by the Max Planck Institute described in Roeckner *et al.* (1996)

(1998) point to the decrease in baroclinicity (i.e. reduced temperature gradient between the poles and higher latitudes) to explain their findings of a reduction in extratropical cyclones in the North Atlantic and North Pacific in future climate simulations. They used the Hadley Centre coupled ocean-atmosphere model, HadCM2[8], to run simulations of the Northern Hemisphere climate in 2006-36 and 2070-2100, finding that in the later period storm tracks in the North Atlantic had shortened leading to a reduction in the number of extratropical cyclones moving over Europe. Although a reduction in overall frequency was observed, they also found an increase in more intense low pressure systems.

Knippertz *et al.* (2000) used the ECHAM4/OPYC3[9] GCM to study the effects of climate change on Northern Hemisphere winter extratropical cyclone formation. Aside from a tendency for more intense cyclones they found a shift to the northeast in the position of cyclone cores, over the eastern North Atlantic and Europe. The intensity of the cyclone track in these locations showed increases up to 15%. These changes were quantified in terms of mean and extreme (upper 1%) windspeeds. Increases of 0.6 ms^{-1} were shown in the mean windspeeds across Northern Europe, including the UK, representing an increase of 8%, with extreme windspeed increases showing a similar magnitude of change.

The northwards shift in cyclone activity resulting from future climate change, described by Knippertz *et al.* (2000), can be attributed to alterations to the extratropical cyclone track. Yin (2005) highlights future climate simulations pointing towards a fairly conclusive result; that climate change will create a poleward shift in the cyclone tracks in the Northern Hemisphere mid-latitudes. Simulations from a 15 GCM ensemble show warming in the tropical upper troposphere and increased tropopause height, producing an upward and poleward expansion of the midlatitude baroclinic zone, resulting in a poleward shift in cyclone track.

[8] The second **Had**ley Centre **C**oupled **M**odel – a coupled ocean-atmosphere GCM described in Johns *et al.* (1997)

[9] A coupled atmosphere-ocean GCM, combining ECHAM4 and OPYC3 (**O**cean on iso**PYC**nal coordinates, described in Oberhuber (1993))

Given that simulations of future climate involving GCMs, such as those detailed above, are run at very coarse temporal and spatial resolutions it is sometimes the case that smaller, rapidly developing, extratropical cyclones are not simulated well. Therefore, some caution should be applied when interpreting results from these studies. However, downscaling methods can be applied that produce simulations of future climates with a much higher spatial and temporal resolution. A full discussion of these methods occurs in section 2.2.1. Statistical downscaling is utilized by Pryor *et al.* (2006b) and Pryor *et al.* (2005b) in an analysis of future windspeeds over Scandinavia. Both studies simulate lower mean windspeeds and lower extreme windspeeds (90% percentile value of mean windspeeds) in that region by the end of the 21st century. Dynamical downscaling, which involves forcing Regional Climate Models (RCMs) with GCM output, is an alternative method. Leckebusch and Ulbrich (2004) employed such a method, using HadRM3H[10] to produce climate simulations over Europe. In an analysis of extreme windspeeds (95th percentile of mean windspeeds) they found the simulated 2070-2100 climate (under an A2 emissions scenario) exhibited a dipole structure, with decreases up to 6% (equivalent to 1ms^{-1}) north of 57^{o}N and increases up to 7% (0.7ms^{-1}) to the south. These greatest increases were located over southern parts of the UK. Leckebusch and Ulbrich (2004) related these changes to an increase of extreme cyclone track density over western Europe between 55-60^{o}N. They also report that simulations of future climate under a B2 emissions scenario produced a similar pattern of results, but with lower magnitudes of changes.

Dramatic increases in computational speed have led to increased utilisation of RCMs in simulating future climates. Woth *et al.* (2006) analysed output from four RCMs to compare the simulated wind climate over the North Sea in 2070-2100 to the current climate (considered as the climate simulated by the models for the 1961-1990 baseline). Extreme windspeeds (considered as the 99th percentile value of windspeeds), relative to the baseline run, were shown to have increased by up to 1.4 ms^{-1} over the area of study. However, it should be noted that these increases are over the sea only, where, due to the lower

[10] Third **Had**ley Centre **R**egional climate **M**odel developed from HadAM3H, described in Jones *et al.* (1995). HadAM3H (Third **Had**ley centre **A**tmosphere **M**odel version **H**) is an atmosphere only GCM described in Pope *et al.* (2000).

drag coefficients, absolute changes in windspeed are expected to be higher than those on land.

Leckebusch *et al.* (2006) also employed multiple RCMs, as well as multiple GCMs in their analysis of the impact of climate change on winter (October to March) windspeeds over Europe. Future simulations (2071-2100) revealed a reduced track density of extratropical cyclones over Europe, however if only the most extreme systems (upper 5th percentile) are considered an increase is shown over western and central Europe. This suggests an overall reduction in winter extratropical cyclones impacting Europe, but also a shift towards more intense systems. Winter windspeed output from the RCM future simulations was compared to a 1961-1990 baseline run. The 90th, 95th and 99th percentile values of maximum daily windspeed from the baseline run were taken, and used as threshold values on which to assess the simulated future windspeeds. The number of days these thresholds were exceeded in both the baseline and future simulations was calculated. This allowed the assessment of future changes in the frequency of extreme winter windspeeds, which, depending on the model considered, show increases up to 300%. The more extreme windspeeds (i.e. the 99th percentile threshold) showed the greatest increase in frequency. In addition to the frequency of extreme winter windspeeds, changes in their intensity were also analysed. Based on the 99th percentile values, the changes in intensity of extreme winter windspeeds were shown to vary between -16 to +16% compared to the baseline climate simulation. It is important to note here, that this study is for the entire European region, and different RCM and GCM combinations produce varying regional changes, such that it is difficult to ascertain a conclusive climate change signal in future UK winter windspeeds. For instance two model chains produce decreases in extreme windspeed intensity of up to 4% over the southern UK, while two others show increases up to 8%. Despite these differences Leckebusch *et al.* (2006) summarise that for Europe as a whole future simulations exhibit a tendency towards higher and more frequent extreme windspeeds in winter months.

In one of a limited number of studies on the potential effect of climate change on windspeeds specifically in the British Isles, Hanson *et al.* (2004) generated

a simulation of climate for periods 1961-1990 (baseline) and 2071-2100 using HadRM3H. Daily mean and maximum windspeed data were analysed to identify any changes in the UK wind regime. With a similar methodology utilised by Leckebusch *et al.* (2006), Hanson *et al.* (2004) found that in the future climate simulation (under A2 emissions scenario) the number of days per year with maximum daily windspeeds higher than the baseline 95th percentile value was reduced across the whole of the UK (by up to a maximum of 5-6 days over southern Ireland, Wales, central England and East Anglia). A similar pattern, but with slightly smaller decreases was observed for the future simulation run under the B2 emissions scenario. Overall, under an A2 emissions scenario, Hanson *et al.* (2004) conclude that the frequency and intensity of extreme windspeeds in future climate simulations is reduced over southern Ireland, Wales, central England and East Anglia, while the remainder of the British Isles will see no significant changes. Simulations under the B2 scenarios show a similar pattern but slightly smaller reductions in intensities and frequencies, and indeed some increases in a few regions.

From the discussion of climate change studies above, it is clear that great progress has been made in understanding some of the ways in which the future European wind regime may be different from that of today. Earlier studies were limited to non-transient greenhouse gas emissions (e.g. Lambert, 1995), while some, due to limited computational resources, were confined to simulation periods of only 5 years (e.g. Beersma *et al.*, 1997). Even at their highest temporal and spatial resolution GCMs do not fully capture the formation of some smaller extratropical cyclones, and increasingly RCMs are being utilised (Leckebusch *et al.*, 2006). Consensus in the literature seems to be that a poleward shift in extratropical cyclone tracks in the Northern Hemisphere is likely under a changing climate (Yin, 2005; Knippertz *et al.*, 2000). In conjunction, an increase is seen in the track density of the most extreme cyclones over Western Europe (Leckebusch and Ulbrich, 2004; Hanson *et al.*, 2004; Lozano *et al.*, 2004). These findings suggest that, overall, fewer storms are simulated to impact Europe, but there will be a shift towards more intense systems. However, in terms of windspeeds, a climate change signal over the UK is difficult to detect given the various results produced by different GCM-RCM model chains (Hanson *et al.*, 2004; Leckebusch *et al.*,

2006). Regional patterns of change vary between RCM simulations depending on the driving GCM as well as the emissions scenario.

1.5 Future Climate Change and Insurance

The previous section described some of the potential alterations in the wind regime of the British Isles resulting form climate change. Any shifts in the frequency and intensity of extreme events, associated with climate change, will have a direct effect on general insurance, with the greatest impact being on property insurance (Dlugolecki, 2004). The losses from climate related events described in section 1.2, means the insurance industry is clearly sensitive to any climate shifts. Owing to this fact, within the finance sector, insurers have been prominent in addressing the climate change issue. This section describes the increasing awareness of insurers to the potential impacts of climate change and how catastrophe models can be adapted to assess potential future losses due to European windstorms.

Generally, insurers make underwriting decisions for risks of economic losses based on information from historic events. Should the pattern of these events be altered, such as a shift in climate, then the basis of these decisions is changed. There has been an awareness of the climate change issue within the insurance industry for many years. Leading reinsurance companies Swiss Re (Brauner, 1994) and Munich Re (1999) have long been involved with research on the potential impact of climate change on the industry. The European industry was the first, and is still the most active, in addressing climate change issues (Mills and Lecomte, 2006), ranging from the direct impact on insured losses, to in-house carbon disclosure projects. Increasingly, the possible effects of climate change on the industry are garnering interest worldwide (Coleman, 2002). However, the short-term nature of insurance means that the topic of potential climate change impacts on the insurance industry is met with some scepticism within certain sections of the industry (Salt, 2000). Following the record losses of the hurricane seasons of 2004 and 2005, a large part of that scepticism, most notably in the United States, has been eroded (Stephenson, 2007).

In the UK, the ABI is particularly active in promoting awareness of the potential impacts of climate change on the insurance industry, commissioning the 2004 report "A Changing Climate for Insurance" (Dlugolecki, 2004). Lloyd's (2006), one of the world's leading insurance markets, has also recently launched a climate change program, committing resources to the investigation of the impact of climate change on business and the insurance industry, in the UK and abroad.

Munich Re (2007) conclude "in view of continued global warming, we anticipate a long-term increase in severe, weather-related natural catastrophes". They also anticipate an intensification of European winter storms in the coming century. The ABI state that changes in windstorms and coastal flooding resulting from climate change pose the greatest risk to the UK insurance industry, with the potential for European wind-related losses to double by 2050 (Dlugolecki, 2004). Berz (2005) and Valverde Jr. and Andrews (2006) call for the insurance industry to fully assess its exposure to climate change impacts before they begin to be manifest. Meanwhile Coleman (2002) warns the insurance industry that it could face bankruptcy unless it addresses the climate change issue immediately. The following section discusses how such an assessment may be carried out through use of catastrophe models.

1.5.1 Incorporating a shifting climate into loss models

The insurance industry finds itself in a unique position with regard to climate change. On the one hand the potential affect of a shifting climate could result in significant financial losses. On the other hand the nature of insurers as risk assessors means they are ideally place to evaluate these impacts. Pre-existing tools, such as catastrophe models, can be adapted to estimate losses in future climates. The following discussion describes such estimates, both by the insurance industry and in the academic literature.

The importance of quantifying the risks posed by climate change to direct insured losses are well illustrated in Figure 1.19. The graph shows a disproportionate increase in loss ratio (insured loss relative to premiums paid)

with increasing windspeeds. For instance a 40% increase in windspeeds (from 100 to 140 km/h) produces a 100% increase in the loss ratio.

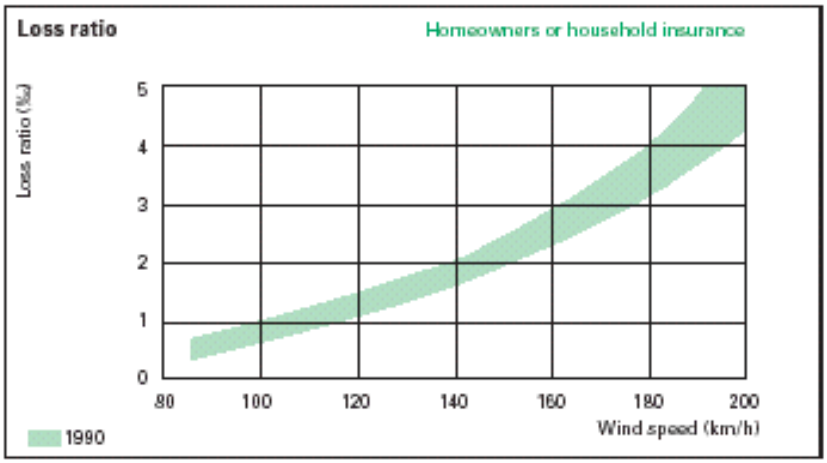

Figure 1.19 - Household insurance loss ratios in Great Britain, at various windspeeds record in the 1990 January and February storms. Source: Munich Re (2002b)

Similar plots are presented by Spence *et al.* (1998) for the October 1987 storm in the UK, and by Hawker (2007), who found a 25% increase in peak gust speeds can result in a 650% increase in damage. This illustrates the danger to the insurance industry; a small shift in climate (such as a slight increase in peak gust speed in storms) could have a dramatic impact on insured losses.

Recent hurricane losses in North America have prompted catastrophe modelling firms to reassess the "climatologies" used in their models (McGhee *et al.*, 2007). In other words the storm set used in the hazard module of the catastrophe model, have been upgraded to reflect a period of high activity. RMS (2006b) increased the landfall frequency of hurricanes in their model following a consultation with four leading hurricane climatologists, who predicted increases of about 20% in category 1-2 hurricane landfall, and 30% in category 3-5, over the next five years relative to 1990-2005 baseline. This had the result of increasing average annual losses within the model by 40% along the Gulf coast, Florida and Southeast, and by 25-30% in the Mid-Atlantic and Northeast coastal regions relative to those derived using the long-term (1900-2005) historical average hurricane frequencies. RMS, along with other companies, now issue two estimates of loss; one based on the long

historical record and one based on this short period of high activity (McGhee *et al.*, 2007).

1.5.2 Estimating future losses due to European windstorms

As with the data within, and structure of, catastrophe models, information regarding the estimations of future insured losses by catastrophe modelling companies is largely unavailable to the public. Several studies in the academic literature do exist however. Dorland *et al.* (2000) consider the effect on windstorm losses of a 2%-6% increase in gust speeds (conceivable increases, they argue, for climate in 2025 and 2075 respectively). Applying these increases to model results for the October 1987 storm and Windstorm Daria (January 1990), revealed increases of 20-110%, 14-68% and 9-41% in insured losses from domestic properties, commercial properties and commercial contents respectively. Taking into account future changes in demographic and economic growth, Dorland *et al.* (2000) estimate increases over 100% in insured damage to domestic and commercial properties.

A unique study saw the combination of RCM output with Swiss Re's operational insurance loss model (Schwierz *et al.*, in submission). However, the loss model was greatly simplified whereby only one average vulnerability curve was applied to all types of risk, i.e. one windspeed resulted in the same insured loss regardless of the location (or property type). Two RCMs (namely CHRM[11] and CLM[12]) were used to generate baseline climate simulations (1961-1990) using reanalysis data, and also simulations of future climate (2071-2100) driven by two different GCMs (HadAM3 and ECHAM5[13]). Windspeed information from these simulations was converted into potential storm days, which could then be used to generate a probabilistic set of storm events via Monte-Carlo simulation which could be used in the loss model. Results from this study show increases in the Annual Expected Loss (AEL) for

[11] **C**limate **H**igh-**R**esolution **M**odel; a RCM derived from the operational weather forecasting models of the Swiss and German meteorological services, described in Vidale *et al.* (2003)
[12] **C**limate **L**okal**m**odell; a RCM based on the German Weather Service weather forecast model **L**okal**m**odell, described in Steppeler *et al.* (2003)
[13] **E**uropean **C**entre **HAM**burg 5; an atmosphere only GCM described in Roeckner *et al.* (2003)

Europe of 44%, including an increase of 35% for the UK. However, due to the wide range of future wind climate simulations generated the uncertainty surrounding the UK figure makes it insignificant. Figure 1.20 illustrates changes in AEL for other European countries.

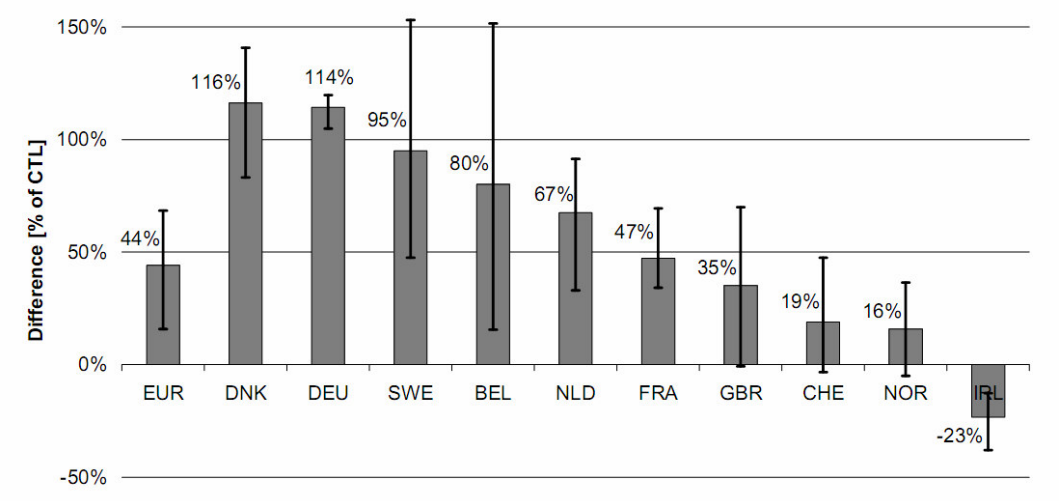

Figure 1.20 - Changes in Annual Expected Loss from windstorms under climate change found by Schwierz *et al.* (in submission).

With a focus on the UK and Germany Leckebusch *et al.* (2007) took windspeed information from four GCMs (HadCM3, HadAM3P[14], ECHAM4 and ECHAM5) to assess changes in insured losses in a simulated 2070-2099 climate. Using a similar threshold for damage (98th percentile of windspeeds) to Klawa and Ulbrich (2003), reanalysis data (ERA40) were used to derive a relationship between the wind data and annual insured losses in the UK and Germany. Having found that wind data from simulations of a baseline climate produced similar loss values to reanalysis data, the same relationship was used on wind data from future climate simulations to estimate future losses. Adaptation to climate change was considered by taking the 98th percentile threshold in the future simulation as well as the baseline. This means that regardless of future changes in windspeeds it is still only the top 2% of winds that will result in damage. This is illustrated in Figure 1.21, where the current threshold for damage is the 98th percentile value of windspeeds (exceedance probability = 0.02, windspeed = 27ms^{-1}). Without adaptation the future threshold for damage remains at 27ms^{-1}, while with adaptation this figure rises to 41ms^{-1} (the future 98th percentile value). In the example provided below,

[14] HadAM3P -Third **Had**ley Centre **A**tmosphere **M**odel version **P**; an updated version of HadAM3H, described in Gordon *et al.* (2000) and Pope *et al.* (2000)

without adaptation properties would be significantly more likely to suffer wind related damage.

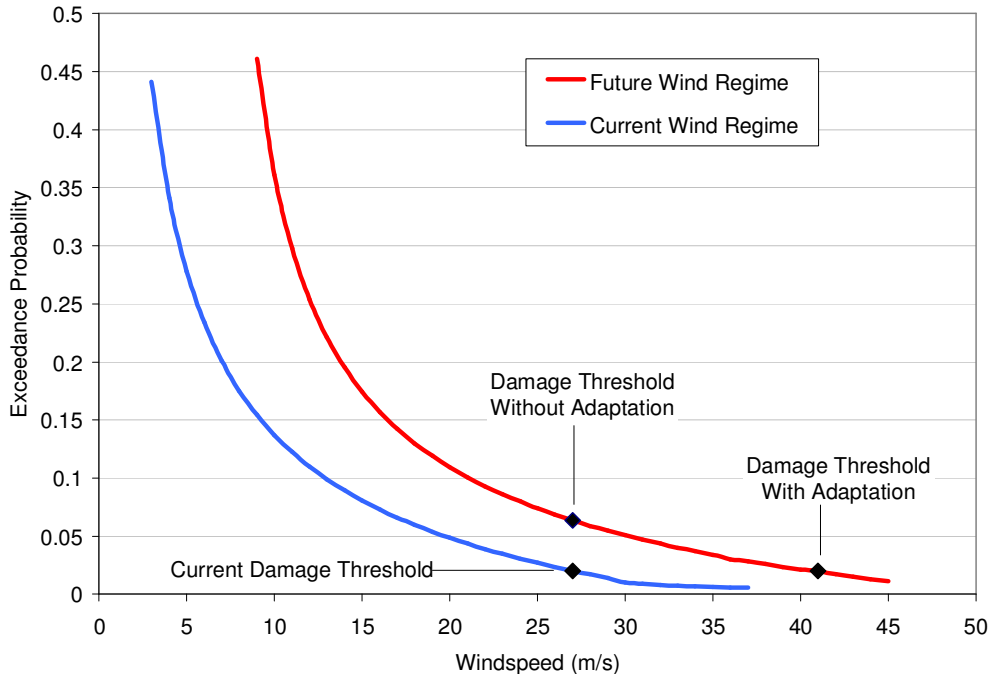

Figure 1.21 – Future damage thresholds with and without adaptation of properties to the future wind regime.

When considering the ensemble mean of four GCMs, Leckebusch *et al.* (2007) found relative increases in loss ratios of 37% and 21% for the UK and Germany respectively, without adaptation. With adaptation these figures dropped to just 4% for the UK, while Germany actually showed a reduction in losses of 8%. Three of the four GCMs showed similar results to each other; however HadAM3P showed markedly less pronounced positive changes and more pronounced negative changes in loss ratios.

Pinto *et al.* (2007) utilised the same methodology as Leckebusch *et al.* (2007) but used only one GCM (ECHAM5/MPI-OM1[15]) to produce an ensemble of 2060-2100 climate simulations over Europe (3 simulations under emissions scenario A1B, and three under A2). In this study the relationship between the wind data and annual insured loss was derived from German loss information only. The relationship was subsequently applied to the UK, France, Portugal/Spain and Norway/Sweden as these regions were deemed to share a similar economic development. Contrary to results presented in Leckebusch

[15] A couple atmosphere-ocean model, combining ECHAM5 and MPI-OM1 (**M**ax **P**lanck **I**nstitute **O**cean **M**odel described in Marsland *et al.*, 2003)

et al. (2007) future losses in Germany were simulated to increase with, and without, adaptation under both A1B and A2 scenarios. Future UK losses were simulated to increase by 8% (43%) under the A1B scenario with (without) adaptation, while under the A2 scenario simulated changes are -4% (+24%). Perhaps more worryingly for the insurance industry is the simulated reduction in return periods, indicated by the increase in inter-annual variation in simulated losses. It must be noted, however, that both Pinto *et al.* (2007) and Leckebusch *et al.* (2007) do not consider socio-economic changes, such as population shifts, in their studies.

It has been shown here that a limited number of methodologies exist to estimate future losses of European windstorms, including the utilisation of both GCM and RCM information. However, it appears that, despite the vulnerability of the UK to the windstorm peril in the future (ABI, 2005c), there is insufficient data to provide confident estimations of potential future losses in this country.

1.6 Research Aims

There are three main objectives to this research; an assessment of the historic and future variability of the UK wind regime, construction of a windstorm model to calculate insured losses from windstorms, and the application of that model to estimate potential future losses under a changing climate.

(i) Assessing the historical and future UK wind regime

It has been identified in the literature discussed in section 1.3.2 that storm damage is often related to the peak gust speed, rather than the mean windspeed. The mean wind regime of the UK is reasonably well understood, as described in section 1.4. However, a gap in the literature regarding gust speeds has been identified. Applications for mean windspeed data include wind energy projects (Sinden, 2007; Pryor *et al.*, 2005a), for which long, continuous datasets of observed mean hourly windspeeds have been established. However, no such dataset for gust speeds exists. To address this the first aim of this project is to investigate the UK Met Office wind data

archives, and establish a long, continuous, homogenous gust speed dataset. Using this dataset, a thorough analysis of the inter- and intra-annual variability of the surface windspeed variables that relate to damage will be undertaken in Chapter 3. Although this project is focussed on wind damage and insured losses, this gust speed and mean windspeed datasets will be valuable in other applications. A knowledge of the local characteristics of gust and mean windspeeds is directly relevant to those involved in the design of structures (Spence *et al.*, 1998), sailing activities (Spark and Connor, 2004; Strefford, 2002; Wieringa, 1980) and wind energy (Pryor *et al.*, 2005a).

In order to supplement the observational data, reanalysis data will be used. Reanalysis data incorporate observations, and, using a fixed analysis method and model, produces a range of meteorological variables on a 6-hourly basis for a period in excess of 40 years. A wealth of information regarding mean windspeeds is stored in reanalysis data, and has been explored by Pryor *et al.* (2006a), Smits *et al.* (2005) and Hanson *et al.* (2004), amongst others. These investigations have been made using coarse resolution data (grids of 150 km and greater). Given the relatively small surface area, and complex coastline of the UK, dynamically downscaled reanalysis data will be utilised in this study. High temporal and spatial resolution RCM data, driven by reanalysis data, will provide information on the UK wind regime back to 1959. In order to assess whether the RCM data is realistic, they will be compared to the observations in section 3.3, for the period of when the datasets overlap (1980-2001). Subsequently, the reanalysis driven RCM data will be used to provide information on the spatial and temporal trends of damaging windspeeds for the period predating the observational record (1959-1979). Hence, with the observation and reanalysis driven RCM datasets an assessment of the inter- and intra-annual variations of damaging windspeeds can be made for the period 1959-2005.

The literature discussed in section 1.4.1 regarding the potential impact of climate change on windspeeds tends to focus on Europe as a whole. Several studies utilise GCMs to assess future changes to the frequency and intensity of extratropical cyclones over Europe, including Lozano *et al.* (2004), Knippertz *et al.* (2000) and Yin (2005) amongst others. The coarse spatial

resolution of GCMs means inferences regarding changes to future windspeeds are difficult to draw, especially on a regional scale. Dynamically (e.g. Hanson *et al.*, 2004; Rockel and Woth, 2007) and statistically (e.g. Pryor *et al.*, 2005b; Pryor *et al.,* 2006b) downscaled data for future windspeeds have been produced, with the dynamical downscaling process considered to be more reliable for maximum windspeeds due to their heavy dependence on terrain (Pryor *et al.*, 2005c; Schwierz *et al.*, in submission). As this project is focussed on the UK, rather than the whole of Europe, it is possible to run a RCM at a higher temporal and spatial resolution than previous studies. The RCM will be run at a spatial resolution of 0.22 degrees (~25km) and on a 2.5-minute timestep for the future periods 2021-2050 and 2071-2100. In order to produce an estimate of the uncertainty in the simulations two different driving GCMs will be utilised, namely ECHAM4 and HadAM3P, and two different emissions scenarios employed (A2 and B2). Further discussion of these future simulations occurs in section 2.2.3. These simulations of future climates will provide information on the impact of climate change on surface windspeeds over the UK, and are presented in Chapter 6. As a detailed study of the observed wind climate will have been undertaken, any future changes in windspeeds can be assessed relative to present day values.

(ii) Construction of a windstorm model

Weather related domestic property insured losses in the UK amount to roughly £1bn a year on average. Over half of these losses result from windstorms. While the flooding peril, the source of the second highest annual losses, is well understood by the insurance industry, estimations of windstorm risk tend to be less accurate. Catastrophe models, discussed in section 1.3.1, used in industry are not in the public domain and therefore a rigorous validation of them is not possible.

Literature regarding the estimation of the European windstorm risk is discussed in section 1.3.2. Dorland *et al.* (2000), Hanson *et al.* (2004) and Klawa and Ulbrich (2003) present models aimed at quantifying windstorm risk. However, these studies are somewhat limited; the first two consider only a limited number of storms, while the third is restricted to Germany and annual losses. Therefore, the second aim of this research is to use the unique

observational wind dataset collated in the first part of the project to derive a deterministic relationship between windstorm losses and meteorological variables. From this an operational loss model will be developed in Chapter 4, capable of simulating insured loss values produced by a given storm. This model, developed from a limited temporal record of losses, may then be applied to the long record of meteorological information to produce a full evaluation of windstorm risk. Chapter 5 presents an assessment of the historic impact of windstorms on insured losses in Great Britain, utilising both observed and model data. An assessment of the impact of individual storm events dating back to 1959 will be made using the windstorm loss model in conjunction with observational and RCM data.

This project will not only benefit from the new gust speed dataset described above, but will have access to 15 years of individual insurance claims from Ecclesiastical Insurance Group, as well as quarterly industry data. It is clear from the literature described in section 1.3.2 that some form of vulnerability function must be included in this relationship in order to accurately estimate insured losses. To this end, the role of various socio-economic factors in contributing to windstorm losses will be explored. Census information and data from a private demographic information specialist (Experian), including population, household counts, property types and average house prices will be utilised.

(iii) Quantifying the impact of the historical and future UK wind regime on insured windstorm losses

The observational and model windspeed datasets developed through the initial part of the first research aim are utilised in Chapter 5, along with the windstorm loss model, to produce loss estimates for historical windstorms. The use of dynamically downscaled reanalysis data and observational data will allow individual windstorms dating back to 1959 to be identified and their impacts quantified. Long term spatial and temporal variations in windstorm losses will be analysed.

Combining the information on future climate generated by achieving the second part of first research aim, with the windstorm loss model developed in

the second, will allow the fulfilment of the third aim; an assessment of future insured losses resulting from windstorms in Great Britain. Results regarding changes in the future UK wind regime are presented in Chapter 6, along with an assessment of the impact of these changes on future windstorm losses.

Leckebusch *et al.* (2007) and Pinto *et al.* (2007) estimate future loss potential in Europe using GCM data. The limitations of this coarse resolution data, for the Great Britain especially, have already been discussed. However, these studies do indicate that estimation of future losses is plausible. Through the use of RCM data a more reliable estimate of Great Britain windstorm risk can be attained. Although Schwierz *et al.* (in submission) use RCM data, the Swiss Re loss model utilised in the study is not discussed due to its commercial sensitivity. The transparent nature of the windstorm loss model constructed in Chapter 4 will allow results to be replicated with other RCM output, or enable the methodology to be applied to other parts of Europe.

As discussed in section 1.2.3 temporal variations in insured losses are affected by demographic and economic shifts. Separating the impact of a changing climate from socio-economic factors in historic trends of losses is becoming an increasingly explored area (e.g. Changnon, 2003; Changnon, 2007; Pielke Jr. *et al.*, 2008). While a similar investigation for Great Britain windstorm losses is beyond the scope of this project, some elements of socio-economic shifts and changes in insurance coverage and density will be considered when estimating historic losses.

1.7 Summary

Chapter 1 introduces the concept of insurance and how it is applied to weather-related risks. It is unclear whether the upward trend in annual worldwide weather-related insured losses, demonstrated in section 1.2, can be attributed solely to changes in climate. Several studies, highlighted in section 1.2.3, identify a variety of socio-economic shifts that contribute to this upward trend. In the UK industry-wide annual insured loss records only exist back to 1987, preventing any long term trends from being identified. The

primary source of weather-related insured loss in the UK stems from wind damage, with annual windstorm losses contributing over 50% of the total weather-related domestic property losses (equivalent to £340m per year).

The focus of this project is on the impact of extratropical cyclones on the UK. Four damaging windstorms from the last two decades are discussed in terms of their meteorological characteristics and their economic impact in section 1.1.1. While the windspeeds recorded during these individual storms are widely documented, the literature generally overlooks the UK wind regime, particularly with regard to damaging windspeeds. The initial aim of this project is to utilise observational and reanalysis data to provide an assessment of the UK wind regime, with a specific focus on damaging windspeeds. Section 1.4 highlights some of the literature portraying the current wind regime, as well as a number of studies utilising climate simulations to describe future wind regimes. It is clear from the discussion in section 1.4.2 that there is no consensus with regard to simulations of the future UK wind regime, partially due to the variety of models, and different spatial and temporal resolutions, utilised.

Quantifying insured losses from weather-related hazards can be achieved using catastrophe models, as described in section 1.3. There is currently a dearth of publicly available information on such models due to their commercial nature. A limited number of studies, discussed in section 1.3.2, have attempted to estimate European windstorm risk. These studies have suffered from a lack of high resolution, long term insured loss and meteorological data. Even fewer studies, detailed in section 1.5.2, have assessed the impact of climate change on future windstorm insured losses in Europe. This project aims to fill a gap in the literature by providing an estimation of the future windstorm losses in Great Britain, using high temporal and spatial resolution insured loss and RCM data.

The methods and data utilised to achieve the research aims in section 1.6 are presented and discussed in Chapter 2, with results presented in Chapters 3-6. A summary of findings and conclusions are provided in Chapter 7.

Chapter 2: Data, Methodology and Tools

The data and methodology used to achieve the project aims outlined in section 1.6 are described in this chapter. In order to assess the historic and future variability of the UK wind regime a combination of observational data and model data are used, including ECMWF (European Centre for Medium-range Weather Forecasts) reanalysis data and RCM (Regional Climate Model) output. These datasets are discussed below in conjunction with a description of PRECIS (Providing REgional Climates for Impact Studies), the RCM used in this study. Methods utilised to develop an operational windstorm loss model are described in section 2.3. Section 2.4 provides details of how climate simulations from PRECIS are coupled with the windstorm loss model to quantify the impact of the historic and future UK wind regime on windstorm losses.

2.1 Quantifying historical variability in the UK wind regime

As highlighted in section 1.4, consideration of damaging windspeeds in the literature describing the UK wind regime is largely overlooked. To fill this gap the assessment of historic wind variability in this project has a focus on daily maximum gust speeds, but also considers mean daily windspeeds. Hourly windspeed observations, recorded between 1970 and 2005, are investigated, with the data collection and quality control methods discussed in section 2.1.1. Model data from two sources, ECMWF reanalysis (ERA40) and PRECIS, are not only used for comparison to the observations, but also to extend the period of study back to 1959. The ECMWF reanalysis model and the data utilised in this study are discussed in section 2.1.2. A full description of PRECIS is found in section 2.2.2. The observed and model data describing the UK wind regime are analysed in Chapter 3, including the identification and quantification of any spatial and temporal variations.

2.1.1 Observational data

There is an eternal desire for long, high resolution, continuous datasets of observations in the atmospheric science world. It has been noted that wind is one of the meteorological variables with the least dense observational network (New *et al.*, 1999). It is the aim of this project to identify a network of UK Met Office observing stations with a continuous, homogenous, long term record of mean windspeeds and gust speeds at a high temporal resolution. The following paragraphs describe how wind is measured at these stations along with how a network of stations was established for use in this project. Issues regarding quality control, sources of error and limitations of the dataset, are also discussed.

UK Met Office Data

The source of observational data used in this study is the UK Met Office, whose data are stored at the British Atmospheric Data Centre (BADC); the Natural Environment Research Council's (NERC) designated data centre for the Atmospheric Sciences. Surface (10-metre) wind information was extracted from two UK Met Office datasets; the Met Office Land Surface Data (UKMO, 2006a) and MIDAS[1] Land Surface Observations Station data (UKMO, 2006b).

Met Office Land Surface dataset

This dataset contains daily land surface measurements for the period 1900-1999 from the Met Office station network. From January 1985 onwards, hourly measurements are stored in the archive. A variety of variables are recorded, including wind parameters, air temperature, soil temperature, sunshine duration and radiation, and rainfall. This dataset was superseded by the MIDAS Land Surface Stations data.

MIDAS Land Surface Observations Station dataset

Measurements from UK Met Office stations on a daily and hourly basis, of the same meteorological variables described above, are stored in the MIDAS database. Records extend back to 1958 from the present. In this study the majority of the data were extracted from the MIDAS Land Surface

[1] **M**et Office **I**ntegrated **D**ata **A**rchive **S**ystem

Observations dataset, although during the data extraction process there was a transition from one dataset to the other as the Met Office Land Surface dataset was phased out.

Formats of Archived Data

Wind observations from UK Met Office stations are collated in conjunction with a variety of other variable, and archived. Within these archives a variety of wind information exists, recorded and stored in various formats. These reports carry a "Message Type" which describes which variables are stored within them. Table 2.1 details the message types which contain wind information, the duration over which measurements are made and their accuracy.

Message Type	Period of Observation	Accuracy of Observation				
		Mean wind		Maximum Gust		Time of max gust
		direction (deg)	Speed (knots)	direction (deg)	Speed (knots)	
HWND6910	HH-60 to HH-00	10	1	10	1	In tenths of hour
3208b	0900 (instant reading)	10	1	-	-	-
HCM	HH-70 to HH-10	10	1	10	1	minute
METAR	HH-20 to HH-10	10	1	-	1	-
SYNOP	HH-20 to HH-10	10	1	-	1*	-
ESAWWIND	HH-70 to HH-10	10	1	10	1	minute
HWNDAUTO	HH-70 to HH-10	10	1	10	1	minute
DLY3208	24 hour run of wind from an Ordinary Climatological Station					
AWSHRLY	HH-70 to HH-10	10	1	10	1	minute

Table 2.1 – Accuracy and timing of surface windspeed data from various Message Types stored by the BADC. HH refers to the observation time (for instance HH-60 to HH-00 refers to the 60 minutes preceding the observation time). * Measured over the period HH-70 to HH-10.

Due to a combination of requiring gust speeds and data availability, only a selection of these message types were utilised in this study. Data contained in the following message types were extracted;

- HWND6910 - Mean hourly wind and gust from analysis of anemograph record reported on Form 6910.
- HWNDAUTO - Mean hourly wind and gust from Digital Anemograph Logging Equipment (DALE).
- ESAWWIND - Mean hourly wind and gust from Automatic Weather Station (AWS).
- SYNOP – Mean hourly wind from 10-minute observation, along with a maximum gust speed recorded over a 60-minute period.
- HCM – Hourly Climate Messages produced from automated systems such as ESAWS (Enhanced Synoptic Automatic Weather Station), SAMOS (Semi Automatic Meteorological Observing System) and CDL (Climate Data Loggers)

Full details of all the meteorological variables contained in these datasets are available in the *Met Office Surface Data Users Guide* (UKMO, 2007d). The guide contains detailed information regarding known errors and measurement techniques for all variables. Information specifically regarding windspeed data, along with its relevance in this study, is summarised below.

Measurements of windspeed from UK Met Office stations are recorded in knots (1 knot is equivalent to $0.515 ms^{-1}$) to the nearest knot, and their direction (from which the wind is blowing) in degrees, to the nearest 10 degrees. Requirements set out by the Met Office call for mean windspeed to be measured within 1 knot or 10%, and gust speeds to within 10%, and direction to within 5 degrees. Windspeed observations are recorded at a 10-metre height, except in certain circumstances described later.

The message types listed above comprise a combination of automatic and manual observations. Manual analysis of anemographs (Message Type HWND6910) was carried out by an observer. Each hour the mean wind speed and direction, along with the maximum gust speed recorded in that hour, is logged. The direction of the maximum gust speed is not reported for each

hour, but is reported for the maximum gust speed recorded in each 24 hour period (0000-2359) (i.e. the daily maximum gust speed). Windspeeds with a value of 1 knot are not reported, and a value of 0 knots is only reported when the wind shows no, or slight, variation over the whole hour. When the mean windspeed is measured at less than 2 knots and the vane shows gusty and not smooth variations, a mean windspeed is reported as 2 knots and a gust speed of 0 knots. All gust speeds are reported as measured except in this case. Since this study focuses on high windspeeds, any errors arising from these issues surrounding low windspeeds are insignificant. Much of the data concerning the early period of this study come from these manual analyses of anemographs, generally performed at the end of each month.

Sources of Error

More recently, wind information is recorded and reported in real time via automated systems, such as ESAWS, SAMOS, and CDL (reported in HCM and ESAWWIND Message Types). The importance of having a knowledge of the duration over which windspeed is measured is highlighted by Kestens and Teugels (2002). Maximum gust speeds are normally recorded from 3-second averages of windspeed; however, this is not the case for early SAMOS systems and in all current ESAWS stations. In these cases gust speeds are the measured average windspeed over 1.5 seconds. Gust speed information manually extracted from anemographs, is also considered to be measured on this time period. DALE systems, reporting wind information under the HWNDAUTO message type, were widely installed in 1980-84. DALE records 1 minute wind information which is processed into hourly data. The gust speed reported by these systems is a 3-second average windspeed, however a scaling error existed before the early 1990s (exact date unknown) causing reported mean windspeeds and gust speeds to be 5% too low. This error was not corrected in ESAWS stations as the effect of measuring gust speeds over 1.5 seconds, instead of 3 seconds, cancels out the 5% reduction. DALE systems are largely being phased out in favour of SAMOS sites. Metadata regarding the times over which gust speeds are estimated, at various stations, through the years, is poorly recorded and was not available to support this project. Exhaustive data extraction and screening was carried out, with the aim of establishing a network of stations with a homogenous method of

recording wind gusts. Unfortunately, this was not possible, as the above discussion of the various methods utilised for gust measurement testifies. However, given that the Met Office did not correct the 5% error arising from the DALE in ESAWS stations suggests that only a 5% difference exists between gust speeds measured over 3 seconds and 1.5 seconds. Gust speeds from human analysed anemographs is approximately 1.5 seconds, but will vary slightly from observer to observer. Therefore, the measurement accuracy stipulated by the Met Office (10%) exceeds the differences in gust speeds arising from the different periods over which they are calculated. For this reason, along with the paucity of metadata, no attempt is made to standardise gust speeds.

Spence *et al.* (1998) contend that the use of a 3-second gust speed is best for estimating building damage, as these are the measurements utilised by engineers in building designs. Unfortunately, a mix of gust speeds estimated from 1.5- and 3-second averages of windspeed are used in this study. However, the difference in gust speeds recorded by these two different methods is estimated to only 5%. It is plausible that engineers may have encountered similar difficulties in establishing a homogenous gust speed dataset when considering building specifications. Indeed, given that the building stock of the UK was largely designed and constructed before the introduction of automated systems, the HWND6910 message type would have been the primary source of information. As already stated, this Message Type carries gust speeds derived from anemographs over roughly 1.5 seconds.

Over 99.9% of the data used in this study are sourced from HCM, HWND6910, HWNDAUTO and ESAWWIND message types. Although differences in methods of gust speed measurement exists, as discussed above, to all intents and purposes data from these Message Types can be considered homogenous. The exception to this are data extracted from the SYNOP reports which are used in this study to supplement missing data in the other Message Types. Mean windspeeds in the SYNOP reports are measured over a 10-minute period in the observation hour, and therefore will not be consistent with mean windspeeds measured over the course of a full hour. For this reason mean windspeeds from SYNOP Message Types are not included

in the study. However, the maximum gust speed measured in a 60-minute period is recorded, with that period running from HH-70 to HH-10 (e.g. for an observation time of 1800, the period over which the maximum gust speed will be obtained is 1650-1750). No information on the time the gust was recorded is stored. This is contrary to all other Message Types utilised in this study, which consider the 60-minute period immediately prior to the observation time (in the previous example this period would be 1700-1800). Subsequently, use of gust data from SYNOP reports in conjunction with other Message Types may result in double counting, with the same gust being reported for two different hours (continuing the previous example, the same gust, recorded at 1658 in the 1700 HWNDAUTO message, could also be reported as the maximum gust in the 1800 SYNOP message). Where possible the incorporation of SYNOP data in this study was avoided. Nevertheless, on occasion, it was necessary, although less than 0.1% of the total gust speed data are from the SYNOP Message Type. In these instances double counting has been avoided by a careful consideration of the timing of the gust in previous observation hour (present in other Message Types). If the gust speed reported in the SYNOP message is equal to that reported in the final 10 minutes of the previous observation period (i.e. HH-10 to HH-00), it is omitted from the dataset. This has a relatively insignificant impact on the final results since only 48 observations were rejected for this reason, out of over 9 million hourly observations utilised in this study.

Aside from potential errors present in the data stemming from using a variety of Message Types, other sources of errors may lie in the wind measurements themselves. Traditionally the majority of UK Met Office stations have used the Munro cup anemometer and vane in their wind measurements. This was connected to an anemograph which would then be studied by an observer, who then reported the data. Automatic logging systems, such as DALE, were introduced widely in the 1980s, negating the need for human analysis of the anemograph. The Munro anemometer was maintained throughout. Errors surrounding DALE have already been discussed. However, errors may be introduced into the windspeed measurements through the use of the Munro anemometer. A drawback of the Munro anemometer is that the cup has a large inertia, resulting in a slow response time. Of greater concern, perhaps, is

the 6-knot start up speed required by the Mk2 and Mk4 versions. Since 1998 the Met Office began replacing the Munros with lightweight, highly responsive, anemometers. Again, since this project is primarily concerned with high windspeeds and gust speeds the 6-knot threshold for Munro anemometers is of little concern.

Calibration errors may also exist, with the UKMO (2007d) stating that systematic errors may be present in speeds derived from anemographs (HWND6910 Message Types), with a likely magnitude of error of 5%. No information regarding which stations and time periods this may be applicable to was available. Given that the error of 5% is within the bounds of the maximum measurement error of 10% stipulated by the Met Office, in conjunction with the lack of metadata, no correction is made for this error.

A further source of error may be related to poor exposure. As stated previously, the anemometer should be installed at a 10-metre height and sited in level, open terrain, where the distance between any obstruction and the anemometer is at least 10 times the height of the obstruction. On occasion this is not possible and the anemometer height is raised. All anemometers are assigned an effective height, defined as the height above open, level terrain at which windspeeds would be equal to those actually measured by the anemometer. Where there is a large discrepancy between the effective height and the actual height, corrections are made to the windspeeds, but not the gust speeds, in the SYNOP message. Stations where this occurs are not considered in this study.

Data Extraction and Processing

The previous section described some of the issues regarding data from different Message Types that are of importance when establishing a reliable dataset for use in this study. The extraction and processing of archived BADC records to create the dataset utilised in this study is described here. Initially, an investigation of all Met Office stations with records stored at the BADC was undertaken in order to establish whether wind information was reported and over which periods the station operated. Unfortunately, the limited metadata

available did not always accurately reflect the availability of wind data stored in the archive. The nature of the BADC archive system required that annual data for each different message type from each different station had to be downloaded separately. Often, empty files were downloaded for stations for years which were stated to contain data, but did not. For this reason data from each station for each year and each Message Type had to be analysed separately, as the metadata were inadequate. Large periods of missing data existed in annual files of one Message Type, which had to be replaced with data from another Message Type. Due to some of the issues described in the previous section, and the high volume of data in different Message Types, this was a very time intensive process, taking several months.

Several instances were found where a reading of 99 was reported as the mean windspeed or gust speed. This suggested that a measurement of 99 knots had been made by that station. The value of -999 is used in the datasets stored at the BADC to indicate a missing measurement. It was the opinion of the author that the majority, if not all, of the readings of 99 knots were erroneous. Following correspondence with the BADC, it is thought that data corruption had resulted in the reporting of a 99 value instead of -999. Confirmation of this was obtained via an inspection of the days with 99-knot readings. It was found that the vast amount of these readings occurred in locations, or on days, for which a 99-knot windspeed (mean or gust) would have been highly unlikely (for instance when all other measurements that day were almost an order of magnitude lower). On these occasions the 99 values were removed, and the hourly observation left blank. This turned out to be the case for all the mean windspeeds and gust speeds with a 99-knot reading. It must be noted that mean windspeeds did not approach 99 knots in the final dataset, however gust speeds exceeded this value on several occasions. Indeed, no mention of mean windspeeds of this magnitude is made in the literature considered in section 1.4 (e.g. Palutikof *et al.*, 1997; Wheeler and Mayes, 1997). Meanwhile, gust speeds of this magnitude, although very rare, are documented by UKMO (1988) and UKMO (2007a).

Further quality control was run on the data to ensure that no mean windspeeds exceeded the maximum gust speed, except in the case where the

mean windspeed is recorded as 2 knots and the gust speed zero, as previously described. Therefore, for all cases with a maximum gust speed of zero which did not have a mean windspeed of 2 knots, the gust data were removed. However, this rarely had an impact on the daily maximum gust speed, since it is unusual to have 24 consecutive hours without a recorded gust. On the occasions where it was necessary to remove the gust data, only one or two hourly observations were recorded that day.

Once it was established that the station had a continuous record of mean windspeed and gust speed data, hourly measurements from the various Message Types were amalgamated. The maximum gust speed and mean windspeed were found for each day. Ideally, each day should contain 24 hourly measurements; however, this was not always the case. For days with no measurements reported for either gust speed or mean windspeed, daily maximum gust speed and daily mean windspeed on that date were omitted from the dataset for that station. Such occasions are referred to as "missing days" in this study. The daily mean windspeed may be misrepresented if the number of hourly measurements included in its calculation is too low. In order to ascertain a reliable daily mean windspeed at least 12 measurements are required. If the period has fewer than this number, it is considered as a "missing day". The number of missing days of mean windspeed and daily maximum gust speed at each station are detailed in Table 2.3.

Establishing a Network of Stations

It was hoped that the period of study would be 1976-2005, encompassing thirty years of data (the norm for an assessment of climate). However, the desire to have an extensive, well distributed, network of stations, weighted against data limitation issues, resulted in the shortening of this period to 1980-2005. Where possible the number of missing days in each station's 26-year record has been limited to 365 (equivalent to 3.84%) in line with Moberg and Jones (2004). However, an exception was made for Durham (7.57% of days missing in the maximum daily gust record). The reasoning for this is the sparseness of available data from the northeast of England. Furthermore, the location of a station in this area was seen as necessary for the windstorm loss

model construction, since a high concentration of properties are situated in this region.

The locations of two stations are known to have changed during the period of study; Leeming in 1996 and West Freugh in 1995. The station coordinates for Leeming changed from 54.296°N and 1.531°W to 54.295°N and 1.529°W, while maintaining an elevation of 32 metres above sea level. The magnitude of this shift in location is roughly 200 metres. The coordinates of West Freugh changed from 54.850^0N and 4.945°W to 54.858°N and 4.934°W, roughly equivalent to a move of 1300 metres, again maintaining its elevation of 11 metres above sea level. Before data from these stations could be included in the study it is clearly important to assess the effect of these location changes on windspeed data in the station records. To avoid confusing any long term shift in wind regime at these stations with a change in station location, 5 years of data either side of the move date were analysed. A Student's T-test and F-Distribution test is carried out on the mean windspeeds as well as the gust speeds, to establish whether there is a significant difference in the windspeed characteristics before and after the stations moved. In the case of both stations the change in location was shown to be insignificant at the 99% confidence level. Therefore, the datasets from these stations are considered homogenous, and are included in the study. Following a similar analysis on data from Wick Airport, in northern Scotland, the station was excluded from the study. Despite no available metadata confirming a station move, the windspeed data suggest either a change in station location or a change in observation method has resulted in inhomogeneities in the record. Figure 2.1 demonstrates this, with the annual mean windspeed recorded at Wick Airport dropping nearly 50% between 1993 and 2001. For comparison, annual mean windspeeds from the two stations which did undergo a site change, Leeming and West Freugh, but did not show any inhomogeneities in their datasets, are also included in Figure 2.1.

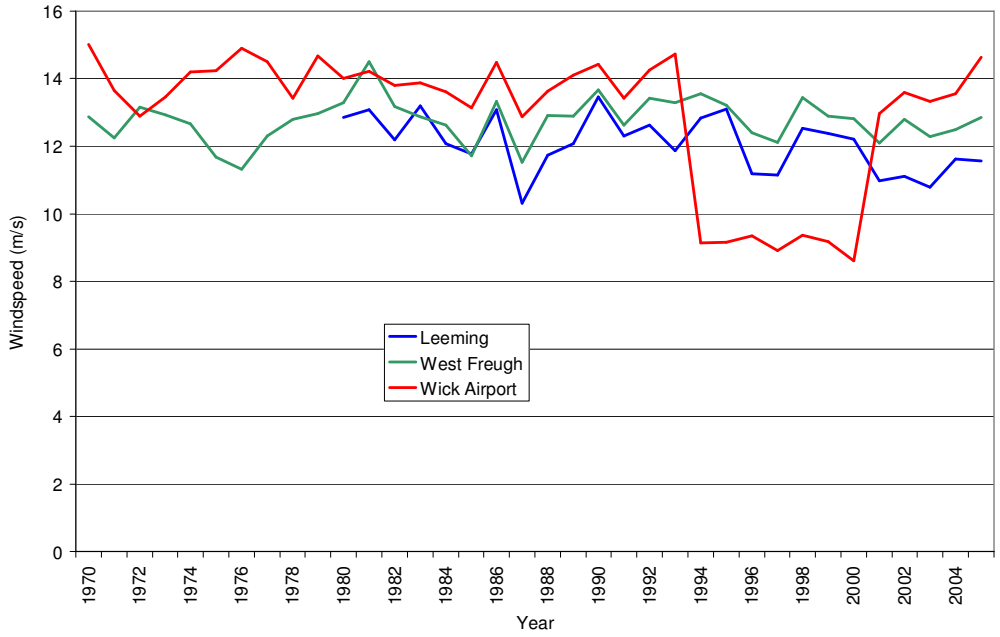

Figure 2.1 - Annual mean windspeed at Leeming (blue), West Freugh (green) and Wick Airport (red) for the period 1970-2005. Windspeeds recorded at Leeming prior to 1980 are unavailable.

The result of extensive data extraction and screening is a network of 43 stations with long, continuous records of hourly mean windspeed and gust speed, representing a relatively good coverage of the UK. Producing this dataset took 3-4 months to complete, due the difficulties involved in data extraction and quality control described above. A map of the locations of the stations incorporated in this study is shown in Figure 2.2. Table 2.2 details the station elevation and period for which a continuous record of wind data has been derived. The number of missing days in the 1980-2005 dataset is also shown in Table 2.3.

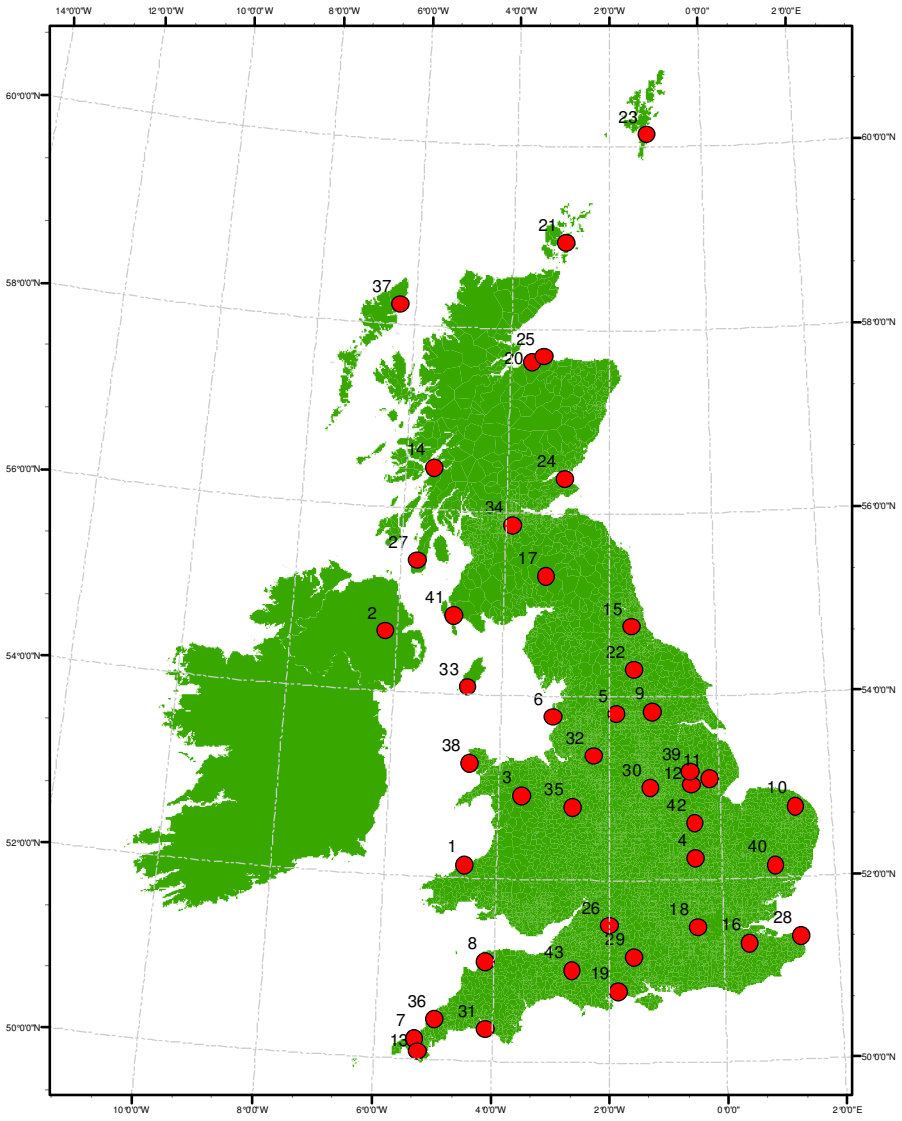

Figure 2.2 - Map of the network of stations adopted for this study. The station numbers correspond with the station names in Table 2.2.

Although the distribution of stations is relatively even across the UK and can be considered representative of the whole region, there are perhaps two locations which are not represented satisfactorily for this study. The west Midlands and South Wales are bereft of stations and are significant population centres. These factors may negatively influence the effectiveness of the windstorm loss model developed in Chapter 4.

No.	Station	Latitude	Longitude	Elevation (m above sea level)	Period station data are available	
					From	To
1	Aberporth	52.138	-4.570	115	Jan 1970	Dec 2005
2	Aldergrove	54.650	-6.217	68	Jan 1970	Dec 2005
3	Bala	52.906	-3.583	163	May 1975	Dec 2005
4	Bedford	52.225	-0.464	85	Jan 1977	Dec 2005
5	Bingley	53.811	-1.866	262	Jan 1972	Dec 2005
6	Blackpool Squires Gate	53.776	-3.038	10	Jan 1970	Dec 2005
7	Camborne	50.218	-5.326	87	Nov 1978	Dec 2005
8	Chivenor	51.088	-4.147	6	Jan 1980	Dec 2005
9	Church Fenton	53.835	-1.197	8	Jan 1980	Dec 2005
10	Coltishall	52.755	1.352	17	Jan 1970	Dec 2005
11	Coningsby	53.093	-0.171	6	Jan 1970	Dec 2005
12	Cranwell	53.031	-0.502	62	Jan 1980	Dec 2005
13	Culdrose	50.085	-5.254	78	Jan 1977	Dec 2005
14	Dunstaffnage	56.450	-5.438	3	Jan 1973	Dec 2005
15	Durham	54.767	-1.584	102	Jan 1980	Dec 2005
16	East Malling	51.286	0.449	33	Jan 1978	Dec 2005
17	Eskdalemuir	55.311	-3.205	242	Jan 1970	Dec 2005
18	Heathrow	51.478	-0.448	25	Jan 1970	Dec 2005
19	Hurn	50.779	-1.834	10	Jan 1980	Dec 2005
20	Kinloss	57.645	-3.561	5	Jan 1970	Dec 2005
21	Kirkwall	58.952	-2.898	26	Jan 1970	Dec 2005
22	Leeming	54.296	-1.531	32	Jan 1980	Dec 2005
23	Lerwick	60.139	-1.184	82	Jan 1970	Dec 2005
24	Leuchars	56.377	-2.861	10	Jan 1970	Dec 2005
25	Lossiemouth	57.712	-3.321	6	Jan 1970	Dec 2005
26	Lyneham	51.502	-1.991	145	Jan 1977	Dec 2005
27	Machrihanish	55.441	-5.695	10	Jan 1970	Dec 2005
28	Manston	51.349	1.353	44	Jan 1970	Dec 2005
29	Middle Wallop	51.148	-1.569	90	April 1974	Dec 2005
30	Nottingham Watnall	53.005	-1.250	117	Jan 1970	Dec 2005
31	Plymouth Mountbatten	50.354	-4.120	50	Jan 1970	Dec 2005
32	Ringway	53.355	-2.279	69	Jan 1970	Dec 2005
33	Ronaldsway	54.085	-4.631	16	Jan 1970	Dec 2005
34	Salsburgh	55.862	-3.871	277	Jan 1980	Dec 2005
35	Shawbury	52.794	-2.662	72	Jan 1980	Dec 2005
36	St Mawgan	50.438	-4.995	103	Jan 1970	Dec 2005
37	Stornoway Airport	58.214	-6.318	15	Jan 1970	Dec 2005
38	Valley	53.251	-4.534	10	Jan 1970	Dec 2005
39	Waddington	53.175	-0.521	68	Jan 1970	Dec 2005
40	Wattisham	52.123	0.959	89	Jan 1970	Dec 2005
41	West Freugh	54.850	-4.945	11	Jan 1970	Dec 2005
42	Wittering	52.610	-0.459	73	Jan 1970	Dec 2005
43	Yeovilton	51.005	-2.640	20	Jan 1977	Dec 2005

Table 2.2 – Details of the network of UK Met Office stations adopted for this study.

No.	Station	Daily Maximum Gust Speeds		Daily Mean Windspeeds	
		No. of missing days	missing %	No. of missing days	missing %
1	Aberporth	13	0.14	11	0.12
2	Aldergrove	39	0.41	2	0.02
3	Bala	269	2.83	132	1.39
4	Bedford	84	0.88	78	0.82
5	Bingley	289	3.04	233	2.45
6	Blackpool Squires Gate	132	1.39	80	0.84
7	Camborne	4	0.04	0	0.00
8	Chivenor	312	3.29	306	3.22
9	Church Fenton	49	0.52	6	0.06
10	Coltishall	18	0.19	0	0.00
11	Coningsby	115	1.21	63	0.66
12	Cranwell	34	0.36	27	0.28
13	Culdrose	343	3.61	335	3.53
14	Dunstaffnage	167	1.76	139	1.46
15	Durham	719	7.57	620	6.53
16	East Malling	220	2.32	88	0.93
17	Eskdalemuir	46	0.48	6	0.06
18	Heathrow	27	0.28	1	0.01
19	Hurn	352	3.71	247	2.60
20	Kinloss	359	3.78	0	0.00
21	Kirkwall	62	0.65	45	0.47
22	Leeming	19	0.20	0	0.00
23	Lerwick	14	0.15	4	0.04
24	Leuchars	41	0.43	13	0.14
25	Lossiemouth	3	0.03	2	0.02
26	Lyneham	185	1.95	183	1.93
27	Machrihanish	19	0.20	14	0.15
28	Manston	48	0.51	41	0.43
29	Middle Wallop	45	0.47	25	0.26
30	Nottingham Watnall	21	0.22	15	0.16
31	Plymouth Mountbatten	126	1.33	110	1.16
32	Ringway	112	1.18	40	0.42
33	Ronaldsway	17	0.18	17	0.18
34	Salsburgh	240	2.53	185	1.95
35	Shawbury	322	3.39	305	3.21
36	St Mawgan	1	0.01	0	0.00
37	Stornoway Airport	27	0.28	21	0.22
38	Valley	38	0.40	30	0.32
39	Waddington	21	0.22	0	0.00
40	Wattisham	1	0.01	1	0.01
41	West Freugh	6	0.06	5	0.05
42	Wittering	47	0.49	10	0.11
43	Yeovilton	106	1.12	52	0.55

Table 2.3 – Number of missing days in the daily maximum gust and daily mean windspeed record of each station in the network.

It should be noted that during the course of this study George (2006) produced a 52-station network of 10-minute (SYNOP) surface windspeeds for the period 1970-1999. Similar issues regarding the reliability of some data were found, and the majority of station locations coincide with those employed here. However, this study benefits from utilising other Message Types, which incorporate a continuous windspeed measurement (over 60 minutes), providing a more accurate representation of the maximum hourly gust speed in particular.

The dataset of daily mean windspeeds and daily maximum gust speeds is analysed and discussed in Chapter 3. Appendix A contains the map presented in Figure 2.2 along side a list of stations, and is regularly referred to in the following chapters.

The range of elevations of the network of stations listed in Table 2.2 is relatively narrow given the range of elevations present in the whole of the UK. As described in section 1.4, locations with higher elevations tend to be subjected to higher windspeeds, and this is borne out by observed windspeed data presented in Chapter 3. In order to account for differences in station elevation in the windstorm loss model the windspeeds are normalised to local percentile values. The windstorm loss model is developed in Chapter 4, which contains further details regarding the normalising of windspeeds.

2.1.2 Model data

Observational data are just one form of information that is available to describe historic variation in the UK wind regime. Regional Climate Model (RCM) output for the period 1959-2001, from PRECIS, is also utilised in this study. The method by which these data are generated is described below. A full description of the PRECIS model and its simulation methods can be found in section 2.2.2. In order to assess the benefits of using dynamically downscaled reanalysis data, this study also incorporates reanalysis data from the ECMWF, which are summarised below.

ECMWF Reanalysis Data (1959-2001)

Both the NCEP/NCAR[2] and the ECMWF have constructed reanalysis datasets, with the objective of providing data from a fixed analysis method, and model, over an extended time period. The ECMWF Reanalysis project ERA15, initially produced data for 1979-1993. This was updated in ERA40 to encompass the period August 1957 to August 2002. The project applies a Variational Data Assimilation technique, used in the ECMWF operational NWP forecast model, to past observations and satellite observations. This produces a global analysis of the atmosphere and land and sea surface conditions every 6 hours.

A thorough description of the input data, the model used and assimilation process is provided by Uppala *et al.* (2005). Input into the ECMWF model includes land-based and ship-based observations, radiosonde data, buoy data, and satellite data, amongst others. The 60-level vertical resolution of the model is an upgrade from the 31 levels in the model used for ERA15. The model used for ERA40 also has a relatively high spectral T159 horizontal resolution (compared with T62 used in the NCEP/NCAR reanalysis and T106 in ERA15). The surface windspeed reanalysis data used in this project are provided on a N80 Reduced Gaussian grid. This grid is comprised of 80 latitudinal grid points in each hemisphere, corresponding to 1.125°, while the number of longitudinal grid points varies from 320 at the equator to 18 near either pole. At the latitude of the UK, the longitudinal grid spacing is approximately 1.875°.

Surface mean windspeed is resolved from the 10-metre U and V wind components provided in the 6 hourly reanalysis for the period 1959-2001. Unfortunately, no estimation of gust speed is available. The daily mean windspeed is calculated from the four 6 hourly windspeed values, and the daily maximum mean windspeed is also found. These variables comprise the reanalysis dataset to be used in this project.

[2] **N**ational **C**enters for **E**nvironmental **P**rediction and **N**ational **C**enter for **A**tmospheric **R**esearch

The ERA40 data used in this project were downloaded from the ECMWF website (http://data.ecmwf.int/data/index.html). The reason ERA40 data were utilised, ahead of NCEP/NCAR reanalysis data, was due to the fact that lateral boundary conditions utilised in PRECIS are derived from the full period of ERA40 data. Lateral boundary conditions derived from NCEP/NCAR reanalysis data are only available for the 1979-2004. In addition, ERA40 is a second generation reanalysis product, and is therefore preferable to NCEP/NCAR reanalysis data (Santer *et al.*, 2004).

RCM data (1959-2001)

The final dataset utilised to assess the historical wind variability in the UK is RCM output from PRECIS. A summary of PRECIS, and the variables produced by the simulations, is presented in the following section. The dynamical downscaling of GCM data for future simulations of climate is relatively common practice. However, the same principals can be applied to dynamically downscale the coarse resolution reanalysis data described above. In order to generate a simulation of climate in 1959-2001 PRECIS was run with lateral boundary conditions from ERA40 data. Hourly data were produced, at a horizontal resolution of 0.22^{o} latitude by 0.22^{o} longitude over the UK (equivalent to approximately 25 km x 25 km). Surface variables utilised in this study included hourly 10-metre maximum and mean windspeeds, and pressure at mean sea level. The advantages of using dynamically downscaled reanalysis data, especially for a UK domain, lie in an improved land-sea mask and orography, and land use representation. The added value PRECIS brings to reanalysis data, in terms of 10-metre windspeeds, is assessed in section 3.3.3. However, a thorough consideration of the benefits of dynamically downscaling reanalysis is beyond the scope of this study. This dataset is kindly provided by the Hadley Centre.

Both sets of model data rely upon the quality and reliability of data assimilation in the ERA40 project. As described above, this process employs historic observational data to constrain models generating information on the background state of the atmosphere. Biases in these analyses can therefore be reduced by incorporating more observational data. Greater reliability of reanalysis data has been demonstrated for the period following the

introduction of meteorological observations from satellites (1979 onwards) (Bengtsson *et al.*, 2004; Simmons *et al.*, 2004). Simmons *et al.* (2004) found the correlation between observed monthly mean surface temperature and both ERA40 and NCEP/NCAR reanalyses, was higher in the period 1979-2001, compared with 1958-2001. Correlations were markedly lower in the earlier period in regions where observations were scarcer, such as Australia and the Southern Hemisphere as a whole. However, correlations of European values, where observations are more abundant for that period, are not diminished to the same degree. Hence, these factors should be borne in mind when considering data for the period 1959-1979 in both the ERA40 and dynamically downscaled reanalysis datasets utilised here.

2.2 Modelling future climates of the UK

The first objective of this project is to assess the historic and future variability of the UK wind regime. Using the data described in section 2.1 the initial part of this aim is achieved. In order to complete the task future simulations of the UK climate must be developed. Given the relatively small geographic area of the UK, future simulations of climate produced from Global Climate Models (GCMs) are often too coarse to provide suitable detail for use in impact studies, including the effects of wind on building structures (Sanders and Phillipson, 2003). For that reason, dynamically downscaled climate information is used in this study. This section details the methodology employed in producing these downscaled simulations. Initially, the process and benefits of dynamical downscaling is presented in section 2.2.1. Following this section 2.2.2 describes the RCM used in this study (PRECIS) to provide future climate simulations. Section 2.2.3 details the boundary conditions and emissions scenarios utilised in the PRECIS experiments. Results form these experiments, and a complete analysis of the future UK wind regime, are presented in Chapter 6.

2.2.1 Downscaling techniques

Output from GCMs is generally produced at a relatively low spatial resolution, typically on a grid spacing of approximately 150-300 km. Impact studies often require information at scales of 50 km or less. Therefore, downscaling techniques have been developed by climate scientists to derive regional, high resolution, climate information from GCMs. Two methods of downscaling are statistical and dynamical.

Statistical downscaling is carried out by deriving an empirical relationship between large scale climate parameters produced by GCMs, and the near surface variable of interest. A relationship is derived from either a long, homogenous, historical observational record alone, or more commonly between observations in conjunction with large scale parameters from GCM output for present day climate. A drawback of statistical downscaling is that, in order to quantify the variable of interest in simulations of future climates, it relies upon the empirical relationship between predictors and predictands to be temporally stable. But due to the complex feedback mechanisms present in the atmosphere this assumption may not always be valid.

Dynamical, or physical downscaling, involves the production of finer resolution climatic variables from GCM data via a numerical model (i.e. a RCM). The domain area of the RCM is usually greatly reduced from that of the driving GCM, however the spatial resolution on which output is produced can be as fine as 1 km (Goyette *et al.*, 2003). By employing a RCM, orography and land cover are considered in greater detail than in GCM simulations and these can be important factors when considering local scale features such as windspeed (Christensen and Christensen, 2007). A further advantage which dynamical downscaling holds over statistical downscaling is that it can be carried out over areas with little or no observational record. Palmer (2005) emphasises this benefit for analysing extreme events, for which observational records are minimal (e.g. damaging wind events). It should be noted however, that this perceived benefit cannot be verified due to these short records. In contrast to empirical relationships, RCMs respond in a physically consistent manner to external conditions not experienced in the training period. Aside from being

computationally more intensive than statistical downscaling, dynamical downscaling is theoretically preferable (Schwierz *et al.*, in submission; Pryor *et al.*, 2005b). For this reason dynamical methods are utilised in this study.

2.2.2 The PRECIS model

Considerations of the drawbacks and benefits of statistical and dynamic downscaling are discussed above, and led to the conclusion that a dynamical method would be more appropriate for providing high resolution information on the future UK wind regime. The main disadvantage of dynamical downscaling is the computation expense. However, the Hadley Centre's PRECIS (**P**roviding **RE**gional **C**limates for **I**mpact **S**tudies) system, configured from the third generation of the Hadley Centre RCM, has been explicitly developed to run on an inexpensive fast PC. The PRECIS model is based on the atmospheric component (HadAM3P) of the Hadley Centre's coupled climate model HadCM3. A thorough description of PRECIS is provided by Jones *et al.* (2004). However, it is important to have an appreciation of the model in order to have confidence in the output data, so a summary is provided here.

PRECIS is a high resolution atmospheric and land surface model which can be applied, over a limited area, to any region of the globe. Dynamic flow, radiative processes, clouds and precipitation, along with the atmospheric sulphur cycle are all described in the model, along with the land surface and deep soil.

Spatial and Temporal Resolution

The atmospheric component of PRECIS is assumed to be in hydrostatic equilibrium, so vertical motions are diagnosed separately from equations of state. The model incorporates 19 vertical layers; from approximately 50 m up to the 0.5 hPa pressure level.

A domain defined on a standard latitude-longitude grid has a convergence of meridians at the poles, resulting in distortion in those regions. This may result in problems when calculating fast-travelling waves (Drost *et al.*, 2007). To

overcome this PRECIS, and other models, solve equations in spherical polar coordinates on a rotated latitude-longitude grid. This has the effect of moving the coordinate pole away from the geographic pole so that the equator passes through the centre of the region of interest. This results in a relatively even grid spacing throughout the domain. In the case of PRECIS the grid spacing options are 0.44^o x 0.44^o or 0.22^o x 0.22^o depending on the user's preferences. In order to maintain numerical stability at these horizontal resolutions a timestep of 5 minutes at 0.44^o x 0.44^o, or 2.5 minutes at 0.22^o x 0.22^o is required. The higher resolution (0.22^o x 0.22^o) is used at all times in this study.

Boundary Conditions

Surface and lateral boundary conditions are required in order for numerical models to solve equations. In PRECIS, surface boundary conditions are prescribed over water only, where a timeseries of surface temperatures and ice extent is required. There is no vertical constraint in the model, with the upper boundary not prescribed. Surface boundary conditions are updated every 24 hours. Dynamical atmospheric information is provided at the horizontal edges of the domain by lateral boundary conditions, including surface pressure, horizontal wind components, temperature and humidity. Lateral boundary conditions are updated every 6 hours, and are derived from coarser resolution output from HadAM3P, ECHAM4 and ERA40. A description of the HadAM3P and ECHAM4 models are provided in section 2.2.3. A full sulphur cycle is represented in PRECIS and this requires a further set of boundary conditions, including sulphur dioxide, sulphate aerosols and associated chemical species.

Gust Parameter

The current version of PRECIS does not contain gust parameterisation. Unfortunately, output data from a RCM with a dynamic gust parameterisation on the required spatial and temporal resolution were unavailable for this study. Hourly maximum windspeed can be used as a proxy of gust speed in accordance with Leckebusch *et al.* (2006). The hourly maximum windspeed is obtained from the maximum timestep mean windspeed in each hour, i.e. in this study the maximum 2.5-minute mean windspeed in each hour.

The incorporation of dynamical gust parameterisation in RCMs is a relatively new technique. The Goyette *et al.* (2003) study of gust speeds in Switzerland and Belgium was one of the first to use a physical gust parameterisation. Using the Canadian RCM (CRCM) at 20, 5 and 1 km resolution for a very limited temporal and spatial domain, they managed to replicate gust speeds in two storms reasonably well. They found the higher the resolution, the better the gust parameterisation performed. Rockel and Woth (2007) analysed windspeed data from 8 RCMs over the European domain, finding that only the two with empirical gust parameterisation (CLM[3] and CHRM[4]) were able to simulate daily maximum windspeeds in excess of 24.5 ms^{-1} in the control period (1961-1990). Due to the sparse nature of long term gust speed records in Europe, a limited number of stations, over a restricted area (2 in Germany, 5 in the Czech Republic) were used in this validation. Even with the gust parameter, simulated data for two locations significantly underestimated the number of storm events (windspeeds of 17.2 ms^{-1} or above). This is due to poorly represented land-sea mask and orography at those locations.

CHRM was also utilised by Leckebusch *et al.* (2006), who compared winter daily maximum windspeeds from the simulations of 1961-90 climate of four RCMs, including PRECIS and CHRM (both at 50 km resolution), to observations from one station, Lille in France. They found that the 3 RCMs without gust parameterisation underestimated the daily maximum windspeeds, while CHRM overestimated them. PRECIS (HadRM3P) provided the most realistic maximum windspeeds of the 3 RCMs without gust parameterisation, as shown in Figure 2.3.

[3] CLM **-** **C**limate **L**okal**m**odell; a RCM based on the German Weather Service weather forecast model **L**okal**m**odell, described in Steppeler *et al.* (2003)

[4] CHRM - **C**limate **H**igh-**R**esolution **M**odel; a RCM derived from the operational weather forecasting models of the Swiss and German meteorological services, described in Vidale *et al.* (2003)

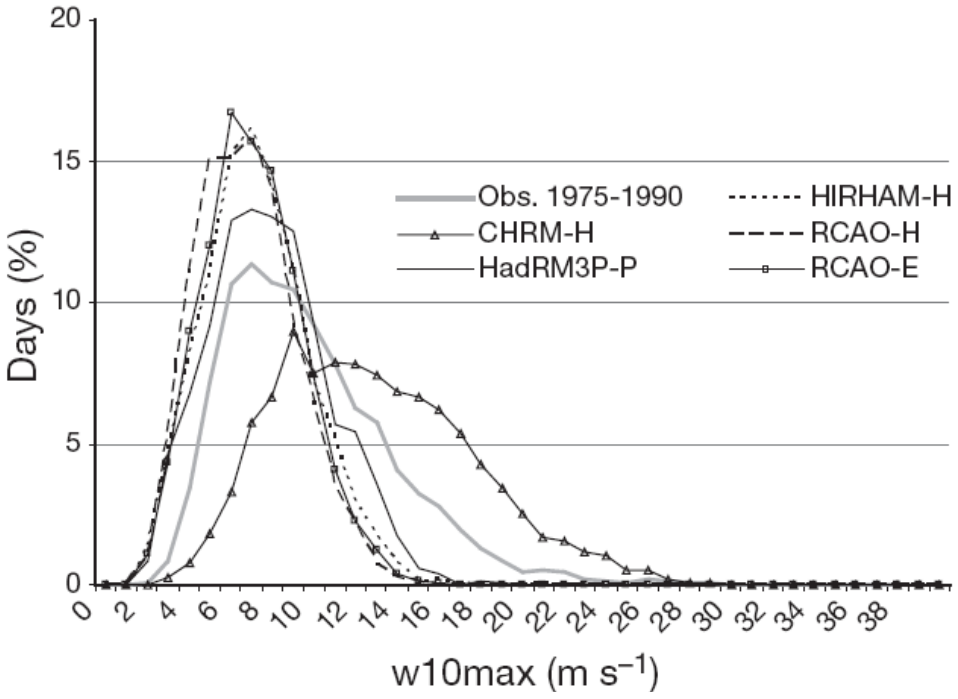

Figure 2.3 - Probability density functions of observed and simulated daily maximum windspeed in winter at Lille (1975-1990) and at nearest RCM grid points. HIRHAM[5] and RCAO[6] refer to Danish and Swedish RCMs respectively. The suffixes –H, -P and –E indicate the driving GCMs HadAM3H, HadAM3P and ECHAM4/OPYC respectively. Source: Leckebusch *et al.* (2006)

In considering just the upper tail of this distribution of daily maximum windspeeds, Leckebusch *et al.* (2006) suggest that the more accurate reproduction of values by the CHRM may have been accidental. For instance, when a 20 ms^{-1} threshold was taken, observational data exceeded this value 34 times in the 16-year record, while CHRM simulated its exceedance on 196 days.

The CHRM and CLM models were used in the Schwierz *et al.* (in submission) study of European storm losses. They found that even using the gust parameterisation the RCMs produced a smoothed distribution of speeds when compared with observational gusts. For this reason a correction factor was applied to the simulated gust speeds before they were incorporated into the loss model.

[5] HIRHAM4 - Danish **Hi**gh **R**esolution Limited Area Model **Ham**burg version 4, described in Christensen *et al.* (1998).

[6] RCAO - Swedish **R**ossby **C**entre **A**tmosphere–**O**cean high resolution regional model, described in Räisänen *et al.* (2004)

In conclusion, few currently operational RCMs employ a gust parameterisation, and in even fewer is it dynamic. A thorough investigation into the perceived benefits of using gust parameterisation has yet to be carried out for Europe, mainly due to the lack of long term observational datasets (Leckebusch *et al.*, 2006). Initial results, however, suggest that in Europe the ability to simulate gust speeds realistically is heavily dependent on accuracy of the representation of invariant variables like the land-sea mask and orography.

In terms of assessing the potential impact of climate change on gust speeds, the assumption that these changes will be highly connected to changes in mean windspeeds seems valid (Dorland *et al.*, 1999; Jungo *et al.*, 2002; Leckebusch *et al.*, 2006). Although data from RCMs with gust parameterisation are available they are not on the temporal or spatial resolution desired in this project, nor was it available at the project's outset. For these reasons the PRECIS model was adopted for use in this project. Limitations regarding gust speed estimations, described above, and are discussed further when the results are analysed in Chapter 3.

2.2.3 Description of experiments

A number of climate simulations are carried out using PRECIS, in addition to the reanalysis driven experiment described in section 2.1.2. This section describes the experiments simulating "current" (1961-90) and future climates, including details on spatial and temporal resolution, emissions scenarios and lateral boundary conditions. A summary of the experiment details is provided in Table 2.4. Each experiment, in real time, took between 4 and 5 months to complete, running in parallel on six 2.4Ghz processors.

Experiment Name	Time Period	SRES Emissions Scenario	Source of Lateral Boundary Conditions
PRECIS-Re*	1959-2001	-	ERA40
PRECIS-EA	1961-1990	A2	ECHAM4
PRECIS-EA-Mid	2021-2050	A2	ECHAM4
PRECIS-EA-Late	2071-2100	A2	ECHAM4
PRECIS-H	1961-1990	-	HadAM3P
PRECIS-HA	2071-2100	A2	HadAM3P
PRECIS-HB	2071-2100	B2	HadAM3P

Table 2.4 - Summary of PRECIS climate simulations used in this study. *Data comprising PRECIS-Re are kindly provided by the Hadley Centre

Temporal and spatial resolution

All experiments are run on a rotated pole latitude-longitude grid, with a 0.22^{o} spacing, equivalent to approximately 25 km. Model iterations are carried out at a 2.5-minute timestep. Hourly output data are stored for a variety of variables, including mean windspeed, maximum windspeed and Mean Sea Level Pressure. With the exception of PRECIS-Re, each model year consists of 360 days, and each variable dataset consists of 259200 records (30 years x 360 days x 24 hours = 259200). The PRECIS-Re dataset consists of 43 years, with 365 (366) days in a (leap) year, resulting in 376944 records.

Temporal and Spatial Extent

The atmospheric component of PRECIS takes just a few model days to reach equilibrium with the lateral boundary conditions. However, several months are required before equilibrium is reached between the temperature and moisture in the deep soil levels. For this reason a 1-year spin-up period is employed, during which no output data are utilised. So to produce a 30-year climate simulation the model runs for 31 model years.

The ECHAM4-driven runs begin at the start of the month of December, while the HadAM3P-driven runs begin at the start of the month of January. So the year runs from December to November in ECHAM4-driven simulations, while HadAM3P-driven simulation years run from January to December. This fact is insignificant since each simulation contains 30 12-month periods, but is included for completeness.

PRECIS-Re was run by the Hadley Centre and carried out over the whole of the NW Europe. A subsection of this data comprising of 116 by 108 grid points, was extracted and analysed. This subsection had northwest, northeast, southwest and southeast corner coordinates of 328.53° Longitude, 61.68° Latitude; 21.20° Longitude, 66.83° Latitude; 345.75° Longitude, 38.70° Latitude and 15.99° Longitude, 41.69° Latitude respectively. The other experiments were run over a more limited area to minimise processor time, centred on the British Isles, comprising of 72 by 80 grid points. This region had northwest, northeast, southwest and southeast corner coordinates of 335.64° Longitude, 61.35° Latitude; 8.79° Longitude, 65.20° Latitude; 346.81° Longitude, 45.24° Latitude and 9.19° Longitude, 47.82° Latitude respectively.

Lateral Boundary Conditions

Aside from the PRECIS-Re run, described in section 2.1.2, lateral boundary conditions are provided by two atmosphere-only GCMs, namely ECHAM4 and HadAM3P. Reanalysis data from ERA40 at 1.25° latitude by 1.875° longitude resolution were used as lateral boundary conditions for PRECIS-Re.

HadAM3P

HadAM3P is the most recent atmosphere-only model developed by the Hadley Centre, forced by surface boundary conditions (sea-surface temperature and sea-ice fraction) from HadCM3 and observations. Gordon *et al.* (2000) and Pope *et al.* (2000) provide an in depth description of HadAM3P. Lateral boundary conditions for PRECIS have been derived from data from two HadAM3P time slices, 1960-1990 and 2070-2100.

ECHAM4

Software has been developed to allow PRECIS to be driven by other modelling centres' GCMs, including Max Planck Institute's ECHAM4. Roeckner *et al.* (1996) describe ECHAM4 in further details. In contrast to HadAM3P, lateral boundary data derived from ECHAM4 is available for the entire 1960-2100 period.

Emissions Scenarios

For simulations of future climates the concentrations of greenhouse gases are prescribed by IPCC SRES (Special Report on Emissions Scenarios) storylines (Nakicenovic *et al.*; 2000). Storyline A2 is used in the ECHAM4 driven experiments, while HadAM3P driven simulations are run under A2 and B2 storylines. These storylines are two of the most commonly used in future climate simulations, and are the only two available for use in PRECIS. The A2 scenario is often thought of as the "business as usual" storyline, with atmospheric concentrations of CO_2 rising to about 850ppm by 2100. The scenario describes a very heterogeneous world, with regionally orientated economic development and continuously increasing population. The B2 scenario describes a world with a greater focus on local, rather than global, solutions to economic, social and environmental stability. The continuously increasing population growth is slower than in the A2 scenario, and atmospheric CO_2 concentrations only reach about 600ppm by 2100.

The SRES scenarios also prescribe the changing emissions of anthropogenic sulphur dioxide, which, along with natural background emissions and other relevant chemicals, are incorporated in the sulphur cycle component of PRECIS.

Uncertainty

There is an increasing availability and utilisation of climate models in simulating the responses of the atmospheric system to various emissions scenarios. As a result it is becoming increasingly necessary to have an appreciation of the uncertainty surrounding the modelling process (e.g. Rowell, 2004; Woth *et al.*, 2006). A number of uncertainties present themselves when using a GCM-RCM model chain: sampling uncertainty, due to a finite number of years; model uncertainty, resulting from the parameterisations and techniques employed in the RCM and GCMs; and radiative forcing uncertainty, associated with the various emissions scenarios (Déqué *et al.*, 2007). A generally accepted method of assessing uncertainty is through the use of ensembles (Christensen and Christensen, 2007).

Although a thorough analysis of uncertainty in future climate simulations is beyond the scope of this project (the ENSEMBLES[7] project is explicitly designed to this), a number of climate simulations were undertaken to sample some of the uncertainty. Incorporating two driving GCMs in this study provides a sampling of the model uncertainty, while the use of the A2 and B2 emissions scenario allows an assessment of the radiative forcing uncertainty. Due to computer resource limitations the sampling uncertainty is difficult to assess since future simulations are limited to 30 years in each experiment. However, the greatest uncertainty tends to surround the choice of driving GCM, followed by the choice of emission scenario (Déqué *et al.*, 2007), so this project samples the major sources of uncertainty.

2.3 Developing a windstorm loss model

The final stage of the project is the development of a tool to estimate insured storm losses based on the wind characteristics of the windstorm. As outlined in Chapter 1, in order to accurately model the impact of weather events on insured losses, an estimation of the vulnerability and exposure of the properties at risk is required, as well as an understanding of the hazard characteristics of the particular weather event. For the UK, the windstorm hazard can be assessed using windspeed and gust speed datasets developed in this project. In order to quantify vulnerability and exposure, various socio-economic datasets are accessed. Windspeed observations, in conjunction with socio-economic variables, are combined to construct the windstorm loss model, which is verified against actual insured loss data. The datasets used in the model development are described below, along with the GIS (Geographic Information System) methods utilised in the development process. The windstorm loss model is developed and its performance assessed in Chapter 4.

[7] Ensembles is a 5 year Integrated Project (2004-09) supported by EC's 6th Framework Programme, providing ensemble-based predictions of climate changes and their impacts (http://ensembles-eu.metoffice.com).

2.3.1 Socio-economic data

The quantification of the exposure and vulnerability of the UK domestic property stock is required in order to produce a realistic windstorm loss model. Previous studies, described in section 1.3.2, identify some socio-economic variables which may help in this quantification, mostly concerned with property (Dorland *et al.*, 2000) and population numbers (Klawa and Ulbrich, 2003).

Socio-economic data have been obtained for this study from the 1971, 1981, 1991 and 2001 Census data, from the Census Dissemination Unit (CDU) via their website Casweb (http://casweb.mimas.ac.uk/). In addition to these data, Experian, a private demographic information specialist company, provide publicly accessible datasets on the CDU website (http://cdu.mimas.ac.uk/experian/index.htm). The information is digitised, and can be visualised using ArcGIS 9.1 (the GIS software used in this projected) using UK boundary information from the UKBorders website (http://borders.edina.ac.uk/html/). Before a discussion of the various attributes of the Experian and Census datasets is provided, it is important to have an understanding of the spatial resolution at which the data are aggregated.

Boundary Data

Socio-economic statistics have been traditionally collected in the census on the spatial scale of electoral wards. Since these wards vary massively in terms of population (from fewer than 100 to more than 30,000) they are not ideal for nationwide comparisons. Additionally, wards are subject to regular boundary changes. As a result a range of areas with consistent size, known as Super Output Areas (SOAs) (described at http://www.statistics.gov.uk/geography/soa.asp), were developed in England and Wales. These are aggregated from Output Areas (OAs) which, for the England and Wales 2001 census, are based on postcodes at the time of the census and fit within boundaries of 2003 statistical wards. This process means that some postcode units are split between OAs. The minimum size for an OA was set at 40 households and 100 residents. Three levels of SOA exist; upper, middle and lower, ranging in population size from a minimum of

25,000[8], 7200 and 1500 respectively. Scotland developed "data zones" (slightly lower populations than the lower SOA) and "intermediate geography" (with population numbers between lower and middle SOA), while the Northern Irish equivalent are also called SOAs (and contain similar population numbers to lower SOAs).

In addition to SOAs and electoral wards, socio-economic data are also available at a level based on postcodes. Unit postcodes can be aggregated into postcode areas, districts, and sectors. Using the example of "AB12 3CD", the postcode area is represented by "AB", the district by "AB12" and the sector "AB12 3". As of February 2007 there are 124 postcode areas, 3,082 districts, 11,717 sectors and over 2.4 million unit postcodes in the UK (including live and terminated postcodes) (ONS Geography, 2007).

Experian Data

Experian have developed a classification system, Mosaic Public Sector, which provides extensive information on the socio-demographics, lifestyles, culture and behaviour of UK citizens. A comprehensive analysis of citizens at postcode and household level provides data on demographics, socio-economics and consumption, financial measures, property characteristics, and property values. These data are available for 2004 and 2005 at the Lower SOA resolution. The number of households of each Mosaic type are calculated in each Lower SOA and reported in this dataset. Mosaic classifies all UK citizens into 61 different lifestyle types (for full details see the online help file at http://cdu.mimas.ac.uk/experian/documentation.htm). Population number and median household income is also included in the dataset, along with projections of population figures for the next ten years.

The description of the Mosaic types appears to be somewhat subjective (ranging from type A01, Symbols of Success - Global Connections, to type K61, Rural Isolation – Upland Hill Farmers), but is grounded in statistical information gathered by Experian over the years. The Experian data-bank includes information from censuses, electoral registers, shareholder and

[8] The upper SOA boundaries have yet to be finalised

directors' lists, house price data from the land registry and local levels of council tax. Supplementing this is Experian's own market research data. As a commercial entity Experian do not make available their complete statistical dataset. While the Mosaic Public Sector dataset is rich in qualitative information, there is little to quantify the exposure and vulnerability of properties to the windstorm hazard.

However, additional Experian data were made available for the year 2000. This dataset includes a variety of statistical information at the postcode sector level, in addition to the Mosaic types. Information regarding household number, population, average sales price of each property type, and standardised average sales price, on a postcode sector level, was extracted and used in the development of the windstorm loss model. Standardised average property prices are based on all property type sales in that postcode sector, but also consider the nationwide demand for certain property types.

Census Data

England and Wales census data, along with Scottish census data are available for 1971, 1981, 1991 and 2001 at various spatial resolutions. Prior to the 2001 census data are available on ward (or postcode sector) scale, with limited variables on OA scale. The 2001 census data output are at SOA level for England and Wales, and OA level in Scotland. Data used in the development of the windstorm model include household and population number, along with property type information.

Construction of the windstorm loss model in Chapter 4 utilises insurance claims data from 1990 to 2005 for calibration and verification. Census data and Experian data in this period are limited to 1991 and 2001, and 2000 respectively. Sources of reliable, publicly available, data for the interim periods are not accessible. It is not within the scope of the project to fully analyse any demographic shifts within the 1990-2005 period, and so these three datasets are considered as representative of the entire period.

Additional difficulties lay in the fact that the three datasets (census 1991 and 2001, and Experian 2000) contained information based on different spatial

levels. Boundaries of OAs (used in census data) do not coincide with the postcode sector boundaries used in Experian data. To complicate matters further, data for Scotland was not always present, and when it was, it was not necessarily on the same spatial level as England and Wales. These issues are partially resolved using GIS techniques described in section 2.3.3.

Other data

Census and Experian data, discussed above, provide information such as property location and value, which help quantify the exposure of UK properties to the windstorm risk. Additional information regarding property type, age and state of maintenance would enable their vulnerability to be assessed. Unfortunately, not all of this information is readily available in the datasets described above, or elsewhere. Spence *et al.* (1998) propose a vulnerability index for the UK building stock, shown in Table 2.5.

	% of stock	pre 1919	1919-45	1945-64	post 64
% of stock		**26.4**	**19.7**	**21.5**	**32.5**
Terraced houses	**28.1**	1.32	1.15	0.79	0.4
Semi-detached houses	**26.7**	1.54	1.32	0.93	0.49
Detached bungalow	**23.5**	2	1.72	1.21	0.65
Converted flats	**6.9**	1.01	1.13	0.83	0.47
Low-rise flats	**12.7**	0.81	0.7	0.48	0.25
High-rise flats	**2**	0.49	0.42	0.29	0.17

Table 2.5 - Proposed composite vulnerability indices for the UK building stock. Source: Spence *et al.* (1998)

These figures are based on data regarding the condition of various aspects of properties, such as the roof, chimney and walls, in various age bands. As discussed in section 1.3, the roof is the most vulnerable part of a property to windstorm damage, and hence properties with a relatively low roof surface area (e.g. flats and terraced houses) have a low vulnerability index. Chapter 4 contains further details of how the vulnerability index is adapted and utilised in the development of windstorm loss model.

2.3.2 Insured loss data

For calibration and verification of the windstorm loss model some form of actual historic measure of wind-related damage is required. An obvious

measure of damage is the financial costs of repair. Such information is not readily available on a nationwide basis for long periods. However, given the extensive uptake of domestic property insurance in the UK, a vast amount of wind-related insured loss information is archived. Much of this data are stored by insurance companies, and is commercially sensitive. One source of publicly available data is via the Association of British Insurers, who collate claims data from the majority of all UK insurers, presenting quarterly statistics. In addition to these ABI data, this project has benefited from the provision of data from Ecclesiastical Insurance Company (EIG). The following paragraphs describe these datasets and how they are attuned in order to develop the windstorm loss model.

ABI data

Insurance claims information is collected from more than 85% of UK insurers, including all the major companies, by the ABI. All the results are amalgamated for anonymity purposes, and released as nationwide quarterly statistics, available through a subscription service from the ABI (2007a). General Business Quarterly Property Claims are available, containing gross losses resulting from theft, fire, business interruption, subsidence and weather. Incurred losses from weather damage are further categorised into domestic and commercial losses, with domestic property losses separated into pipe, storm and flood damage. The records extend back to 1987, when only a solitary annual figure is available for all weather-related losses. Quarterly data for commercial and domestic losses are available from 1991 onwards. Pipe, storm and flood loss data are available on a quarterly basis from 1997. These details are summarised in Table 2.6.

Year	Commercial Claims	Domestic Claims				Total Weather Related Claims
		Pipes	Storm	Flood	Total	
1987					Annual	Annual
1988					Annual	Annual
1989	Annual				Annual	Annual
1990	Annual				Annual	Annual
1991	Quarterly				Quarterly	Quarterly
1992	Quarterly				Quarterly	Quarterly
1993	Quarterly				Quarterly	Quarterly
1994	Quarterly				Quarterly	Quarterly
1995	Quarterly				Quarterly	Quarterly
1996	Quarterly				Quarterly	Quarterly
1997	Quarterly	Quarterly*	Quarterly*	Quarterly*	Quarterly	Quarterly
1998	Quarterly	Quarterly	Quarterly	Quarterly	Quarterly	Quarterly
1999	Quarterly	Quarterly	Quarterly	Quarterly	Quarterly	Quarterly
2000	Quarterly	Quarterly	Quarterly	Quarterly	Quarterly	Quarterly
2001	Quarterly	Quarterly	Quarterly	Quarterly	Quarterly	Quarterly
2002	Quarterly	Quarterly	Quarterly	Quarterly	Quarterly	Quarterly
2003	Quarterly	Quarterly	Quarterly	Quarterly	Quarterly	Quarterly
2004	Quarterly	Quarterly	Quarterly	Quarterly	Quarterly	Quarterly
2005	Quarterly	Quarterly	Quarterly	Quarterly	Quarterly	Quarterly
2006	Quarterly	Quarterly	Quarterly	Quarterly	Quarterly	Quarterly
2007	Quarterly	Quarterly	Quarterly	Quarterly	Quarterly	Quarterly

Table 2.6 – Availability and temporal resolution of industry claims data from the ABI. *Available from the 4th quarter 1997

The value of individual commercial property losses varies considerably, depending on the nature of the business. Compared to commercial property, UK domestic properties are relatively homogenous; the majority of the building stock is comprised of one or two storey buildings, terraced or semi-detached with pitched tiled or slated roofs (Spence *et al.*, 1998). There is also a greater wealth of information available for domestic properties compared with commercial properties. As a result, commercial losses are not utilised in the development of the loss model. For the purposes of this study claims information is only considered until the end of 2005 (corresponding the end of the windspeed observation record).

The original incurred loss data are reported in actual values, i.e. the losses in the 1987 have not been corrected for inflation and are presented in the ABI data in 1987 pound values. All data presented in this study are corrected to 2005 pound values using the all items RPIX (**R**etail **P**rices **I**ndex e**X**cluding mortgage interest payments) table. The all items RPIX, also known as the underlying rate of inflation, is an index measuring the average price of

consumer goods and services. It can therefore be used to adjust loss values to a constant value. More details regarding the RPIX, and a copy of the table, can be found in Appendix B and in Office of National Statistics (2007). In practice, actual loss values were converted to 2005 £ values using the conversion ratios set out in Table 2.7. Where quarterly data are available they have been converted to 2005 values using a 3-month average RPIX measure. For data only available on an annual basis, a 12-month average RPIX measure is utilised.

Year	Adjustment Ratio				
	1st Quarter	2nd Quarter	3rd Quarter	4th Quarter	Annual
1987					1.87
1988					1.80
1989					1.73
1990					1.63
1991	1.54	1.51	1.48	1.46	1.51
1992	1.44	1.42	1.40	1.39	1.41
1993	1.38	1.36	1.35	1.34	1.35
1994	1.34	1.33	1.32	1.31	1.31
1995	1.30	1.29	1.29	1.28	1.28
1996	1.27	1.26	1.25	1.24	1.24
1997	1.23	1.22	1.21	1.21	1.21
1998	1.20	1.19	1.18	1.17	1.18
1999	1.17	1.16	1.15	1.15	1.15
2000	1.14	1.13	1.13	1.12	1.12
2001	1.12	1.11	1.11	1.10	1.10
2002	1.09	1.09	1.08	1.08	1.07
2003	1.07	1.06	1.05	1.05	1.05
2004	1.04	1.03	1.03	1.02	1.02
2005	1.02	1.01	1.01	1.00	1.00

Table 2.7 - Adjustment ratio to convert loss values into 2005 £ values, derived from the RPIX table in Appendix B.

Ecclesiastical Insurance Group (EIG) data

A variety of insurers were contacted with the hope of collaboration on this project. Due to the commercial sensitivity of claims data, the response was very limited. However, EIG were an exception, kindly providing access to their windstorm-related claims database, extending back to 1980. Loss information has been adjusted to 2005 pound values using the ratios set out in Table 2.7.

Before the raw claims data could be analysed they underwent quality control to resolve a number of issues. Due to a migration of systems at the EIG, not

all storm claims were present in the database. As result, anomalously low losses were present in periods known to have seen high impact windstorms (e.g. October 1987). For this reason claims data for the 1980-89 period have been disregarded.

The development of a windstorm loss model requires that all forms of data must contain spatial information. Therefore, the dataset is further refined with the removal of claims which do not have a valid (either active or terminated) postcode. Claims with partial postcodes are considered invalid, unless they contain postcode sector details. A number of reasons exist causing claims to have invalid postcodes, such as an inputting or system error. Additionally, large numbers of often substantial claims have a postcode classification of "various". Following correspondence with EIG, it was found that these claims relate to policies covering a multitude of locations, and are almost entirely comprised of commercial property claims. As stated previously, the variable nature of commercial claims make them unsuitable for use in the development of the loss model. However, commercial and domestic property claims are present in the EIG database, and for commercial sensitivity reasons, are not segregated. As discussed in section 1.2.2, domestic losses make up about three quarters of the total weather related losses in the UK. Since the EIG claims database can be seen as representative of industry-wide losses, the assumption that about 25% of losses in the EIG database are commercial property seems valid. With the removal of claims with "various" in the postcode column, a 17% reduction in the losses recorded in the EIG database is seen. An additional 7% reduction in the total loss is seen with the removal of invalid postcodes. The remaining claims are assumed to be made up of 90-95% domestic property claims. Ideally, only domestic property claims would be used in the development of the loss model, however, as described this is not possible. Nevertheless, the benefit of the high spatial and temporal resolution of the EIG data, compared with the ABI data, far outweighs discrepancies involved in the inclusion of a small, though unknown, quantity of commercial property claims. Therefore, in the following chapters the EIG data presented are referred to as "domestic property" losses, but is assumed that a small fraction of commercial losses are included.

Once the claims data have been refined it is aggregated at the Postcode Sector level to maintain anonymity of policy holders. It must be noted that the claims included in this dataset are settled, some following adjustment. Any open claims are not included.

2.3.3 GIS Techniques used in model construction

A Geographic Information System (GIS) is an increasingly utilised tool which can store, analyse and manage data with a spatial reference. The ability to link data from different types of datasets, based on their spatial similarities, means GIS can be used for several different purposes. Although GIS is frequently used in the environmental sciences for such things as Environmental Impact Assessment, it is also employed in resource management, sales, marketing and logistics (Kennedy, 2006). A full description of GIS and its capabilities is presented by Kennedy (2006). The project aim of developing a windstorm loss model can be achieved through combining socio-economic data, windspeed information and insured loss values with a GIS. With recent advancements in computer processing speed, increasingly powerful GIS software is available. The software package used in this project is ArcGIS 9.1, described in Environmental Systems Research Institute (2005). The following sections describe how the datasets are geographically referenced (georeferencing) and how the various tools in the ArcGIS software enable the development of an operational windstorm loss model.

Georeferencing

Georeferencing refers to the process of establishing a relationship between a piece of datum and its coordinates on a map, i.e. defining its spatial location. It was necessary to carry out georeferencing for the EIG claims dataset. This was undertaken by utilising the postcode information in the data along with postcode Ordnance Survey (OS) coordinates from UKborders (http://edina.ac.uk/ukborders/). Coordinates for postcodes are at 1-metre resolution on the British National Grid system. A small percentage of the claims had terminated postcodes, but could still be georeferenced as the

UKborders information contained coordinates for all active and terminated UK postcodes. The ArcGIS "join" tool was used to extract the postcode coordinates matching the postcodes in the claims database. As there are over 2.4 million (active and terminated) UK postcodes this process was very time intensive. Once the individual claims are georeferenced they are aggregated into postcode sectors based on boundary data from the Experian 2000 dataset. The aggregation of claims to these spatial levels provides anonymity to individual policy holders. It also allows the inclusion of data with partial postcodes, but containing postcode sector information, to be included.

The network of wind observation stations, described in section 2.1.1, carried with them latitudinal and longitudinal information, so are easily georeferenced. A feature of GIS is that coordinate systems, or map projections, are relatively easily interchanged. So the meteorological data, with latitude and longitude coordinates, are spatially comparable to the claims data which are projected on the British National Grid.

The socio-economic information from census data and Experian come with their own set of boundary data, which can be projected in ArcGIS. For continuity, census data from 1991 and 2001 were transformed to the same spatial level as Experian 2000 data (i.e. postcode sector level). Thus, all data used in the development of the windstorm are on a postcode sector basis, with the boundaries shown in Figure 2.4.

Figure 2.4 - Map of UK postcode sectors

Windspeed Interpolation Methods

The windstorm loss model utilises interpolated wind speeds from the network of observational stations described above, in accordance with Dorland *et al.* (2000), Hanson *et al.* (2004) and Klawa and Ulbrich (2003). Interpolation is a method of fitting a surface to a sample of known data points, allowing the prediction of values at unknown geographic locations. ArcGIS uses an Inverse Distance Weighted (IDW) interpolation method to produce a 3km grid of 250 by 443 cells across the UK domain. In this method, the closer the cell is to a

sample point, the more influence (or weighting) that point has on the estimated value of that cell. A sensitivity analysis regarding the effect of the uneven station coverage depicted in Figure 2.2 on the interpolation process can be found in Appendix C.

Rather than interpolating actual measured windspeeds from the network of stations, the values are normalised to local thresholds first. Using a similar method, Klawa and Ulbrich (2003) showed that by normalising windspeed to the local 98th percentile incorporates a "wind climate" in the loss model, i.e. a measure of local vulnerability. This method assumes that, at any location, only the top 2% of windspeeds cause damage. Following the interpolation of normalised windspeeds the interpolated surface does not reflect orography or surface roughness, but actual windspeeds could be calculated anywhere in the domain, based on a knowledge of the local 98th percentile windspeed value. Klawa and Ulbrich (2003) showed that this method could produce realistic storm loss estimates for Germany. It is hoped that by utilising a much greater density of observation stations in this project (the average area represented by one station is 5000km^2 in this project, compared with a figure of 15,000km^2 in Klawa and Ulbrich (2003)), Klawa and Ulbrich (2003)'s result will not only translate to the UK, but can be improved upon. An analysis supporting the appropriateness of the 98th percentile as a threshold is presented in section 4.1.3. This method negates the need for a Digital Elevation Model which would increase processing time still further.

In this project daily windspeeds and gust speeds are normalised to local percentile thresholds, and then interpolated. From the interpolated surface, a mean and maximum value of the normalised windspeed and gust speed is assigned to each postcode sector, based on the predicted values for each cell within the postcode sector boundary, using the "zonal statistics" tool in ArcGIS. This process is computer intensive, with each year of observational data of one variable taking 11 hours to generate normalised daily values at the postcode sector level. This project benefits from a higher spatial (postcode sector) resolution and longer record (26 years), compared with Dorland *et al.* (2000) (restricted to a limited number of storms at a 2-digit postcode level),

Hanson *et al.* (2004) (limited to 2 storms at the postcode district level), and Klawa and Ulbrich (2003) (no regional breakdown of claims).

2.3.4 Multiple regression analysis

Through georeferencing of claims and interpolation of windspeeds, a set of socio-economic, windspeed and loss data, at postcode sector level is generated for each day. These datasets are utilised in a multiple regression analysis to produce the windstorm loss model in Chapter 4. The principles behind regression analysis are well covered by Tabachnick and Fidell (2001). A regression analysis establishes a statistical relationship between a dependent variable (DV) (or response) and several independent variables (IV) (or predictors).

In this project the aim is to estimate storm losses (the DV), from an array of socio-economic and meteorological data (the IVs). For the purposes of this study standard multiple regression is the preferred method with which to construct the windstorm loss model. Sequential and statistical methods may lead to erroneous weighting (or even inclusion / exclusion) of certain variables resulting from the researcher's choice of when (or whether at all) to input each variable.

A number of issues arise during a multiple regression analysis regarding the suitability of the independent variables, including outliers, multicollinearity, and normality, linearity and homoscedasticity of residuals (Tabachnick and Fidell, 2001). The resolutions of these issues are described in the regression analysis in Chapter 4.

Once the final regression equation is established it can be assessed in a number of ways. The F-test is used to ensure that the IVs are correlated to the DV, i.e. the correlation coefficient (R) is not zero. The correlation of each IV to the DV is assessed by finding the (R) value for each when holding all other IVs constant. The variance explained by all the IVs in combination is assessed using adjusted R^2 ($\check{R}^2$). The R^2 value is often overestimated when dealing with

multiple IVs, since each additional variable in the equation can only add to the value. By using the $\check{R}^2$ value this is not the case and it provides a better measure of goodness of fit of the regression equation. An assessment of the statistical significance of the regression coefficients is carried out using a T-test. This ascertains whether the relationship between the DV and each IV is statistically significant. If they are not, then a regression coefficient is not required.

2.4 Quantifying historical and future windstorm losses

The relationship between socio-economic data, windspeed data and insured loss established through the development of a windstorm loss model in Chapter 4 will be utilised in conjunction with the observed and PRECIS-Re windspeed datasets, to quantify historic (1959-2001) windstorm losses. Results of this assessment are presented in Chapter 5. Future climate simulations (2021-2050 and 2071-2100) will provide the windspeed data required to quantify the effect of the future wind regime on windstorm losses, with results presented in Chapter 6.

In the development of the windstorm loss model, normalised observed windspeeds are interpolated from the 43 network stations to produce an estimate of the daily windspeed and gust speed variables for each postcode district. Simulations of climate developed by PRECIS produce windspeeds on a 25 km grid over the UK. For the purposes of consistency the simulated normalised windspeed from the grid cell corresponding to each station is taken, and an interpolation carried out on these 43 values to produce an interpolated layer. A simulated windspeed is then extracted from this interpolated layer for each postcode sector. An alternative to this method would be to extract simulated windspeeds for each postcode sector directly. However, since the windstorm loss model was developed using interpolated windspeeds, in order to produce reliable results windspeeds from PRECIS simulations must be processed in a consistent fashion.

As described in section 2.1.2 an assessment of the UK wind regime for the period 1980-2005 will be made using observed data. In addition, the PRECIS-Re dataset will allow the assessment of the UK wind regime back to 1959. Using both sets of data, the impact of individual windstorm events will be quantified in Chapter 5. The availability of windspeed data dating back to 1959 allows highly damaging storms to be identified that may have been previously overlooked. The long, continuous record of windspeeds, from both the observed and PRECIS-Re datasets, will allow spatial and temporal patterns of windstorm losses to be identified.

In order to estimate the future impact of climate change on insured losses, windspeed data from the future UK climate simulations will be extracted. Changes in the UK wind regime, relative to "current" climate, are assessed in Chapter 6. The impact of the future wind regime on windstorms loss will be quantified, and changes to the spatial and intra- and inter-annual variations analysed.

As highlighted on several occasions in Chapter 1, changes in the windspeed characteristics of future climates will not be the only variable contributing to variations in future losses. Socio-economic shifts will also play a role in changing patterns of windstorm loss. A thorough assessment of these changes is beyond the scope of this project, however clearly some consideration is necessary. Studies estimating future windstorm loss potentials by Leckebusch *et al.* (2007) and Pinto *et al.* (2007) have incorporated "adaptation" to future climates through the use of normalised windspeeds to percentile values. In future climates, if the assumption is made that the vulnerability of properties is unchanged (i.e. the same top percentage of windspeeds is causing damage) then the property stock could be said to have undergone "adaptation" to the new wind regime. However, in future climates where properties exhibit the same vulnerability they do in the current climate, i.e. without adaptation, the threshold for damage remains constant. In other words, without adaptation, the absolute value of the percentile threshold from the current climate is used as the threshold value in the future. Using these two methods (with adaptation and without adaptation), two estimations of future losses are obtained; one in a world where the risk of damage to

buildings is identical to current levels (with adaptation), and one in a world where the risk of damage is altered based purely on a shift in the wind regime (without adaptation). Locations which see the greatest increase/reduction in the future risk of damage (i.e. change in windspeeds) will not necessarily be the locations which see the greatest increase/reduction in future estimated losses. Therefore, these results could potentially be used as a tool for minimising windstorm losses. By identifying locations which may see an increase in risk of damage, particularly susceptible buildings in that location can be renovated or building codes in that location could be upgraded.

2.5 Summary

The various methodologies and datasets utilised in this project, to complete the research aims described in section 1.6, are described in this chapter.

In order to quantify the historic UK wind regime a combination of observed and model windspeed data are analysed. Extensive data extraction and processing is undertaken to produce a continuous record of observed 10-metre windspeeds from 43 UK Met Office stations for the period 1980-2005, comprising of daily mean windspeeds and daily maximum gust speeds. Difficulties in establishing this dataset, along with details regarding the process employed to ensure data quality, are described in section 2.1.1. To compliment the observed data, and to enable the period of analysis to be extended back to 1959, raw and dynamically downscaled reanalysis data (ERA40 and PRECIS-Re datasets respectively), described in section 2.1.2, are also incorporated in this study. A quantitative analysis of these datasets is undertaken in Chapter 3.

An analysis of the future wind regime of the UK is made possible by the generation of 6 climate simulations, detailed in section 2.2.3. These experiments are carried out using the PRECIS system, configured from the third generation Hadley Centre RCM, described in section 2.2.2. Climate simulations for the UK domain for the periods 2021-2050 and 2071-2100 are generated, and the output analysed in Chapter 6.

Section 2.3 describes the methodology employed in the development of an operational windstorm loss model, capable of producing domestic property insured loss estimates based on windspeed information and various socio-economic data. The socio-economic data and insured loss data utilised in this process are introduced in sections 2.3.1 and 2.3.2 respectively, while the ArcGIS software and data manipulation tools contained within, are detailed in section 2.3.3. The resultant operational windstorm loss model, developed and verified in Chapter 4, is subsequently modified to allow historic (1959-2005) and future (2021-2050 and 2071-2100) windstorm losses to be quantified in Chapters 5 and 6 respectively.

Chapter 3: The Historical Wind Regime of the UK

The first research aim of this project is an assessment of the historic and future UK wind regime. This chapter addresses the first part of this aim, utilising the observation and model data described in section 2.1, to quantify spatial and temporal variations in windspeeds dating back to 1959. The second part of this aim, an analysis of the future wind regime, is presented in Chapter 6.

Using observational data collected from the network of UK Met Office stations described in section 2.1.1 the characteristics of the historic UK wind regime (1980-2005) are analysed in section 3.1. Particular attention is paid to potentially damaging windspeeds. Section 3.2 presents model data from the ERA40 reanalysis and reanalysis-driven RCM experiment (i.e. PRECIS-Re) for the period 1959-2001. The data provide the basis for an analysis of the UK wind regime for a period for which observational data are unavailable (1959-1979). The combination of observational records and model data allow temporal and spatial trends of potentially damaging windspeeds to be identified for the period 1959-2005. The observational dataset forms the basis for the development of a windstorm loss model (research aim (ii)), described in Chapter 4.

In order to have confidence in the model data for the period preceding the observations utilised here, wind variables from ERA40 and PRECIS-Re datasets are compared with observational data in section 3.3. The third research aim is to quantify the historical and future impact of windstorms on insured losses. Chapter 5 describes how the wind datasets established here provide a unique source on which to estimate the effects of historical windstorms. Future climate simulations generated by PRECIS permit an assessment of the impact of the future wind regime on insured losses in Chapter 6. Therefore, the dynamically downscaled reanalysis data (PRECIS-Re) are compared to the original data (ERA40), to quantify the added value provided by the PRECIS model. This analysis is carried out in section 3.3.

A summary of the results presented in this chapter, along with a discussion of their relevance and importance in terms of achieving the research aims and filling gaps in the literature, occurs in section 3.4.

3.1 Analysis of UK wind regime using observational data

Achieving the research aim of an assessment of UK wind regime begins with an analysis of observational data. Mean daily windspeeds and Daily Maximum Gust Speeds (DMGS) are calculated for the period 1980-2005 for 43 stations across the UK. The locations of these stations are mapped in Appendix A, with a description of the data collection provided in section 2.1.1. All windspeeds and gust speeds presented in this chapter are reported in metres per second (ms^{-1}), converted from the original observations record in knots (1 knot = 0.515 ms^{-1}). An analysis of daily mean windspeeds is presented in section 3.1.1, with DMGS assessed in section 3.1.2.

3.1.1 Daily Mean Windspeed

Descriptive Statistics

An analysis of the inter- and intra-annual variation in daily mean windspeeds is presented later in this section, along with an assessment of the spatial variations exhibited in this dataset. Here, descriptive statistics of daily mean windspeed recorded at the 43 stations in the period 1980-2005 are presented in Figure 3.1 and Table 3.1.

No.	Elevation (m above sea level)	max	mean	Std[1]	Percentile Values						
					5th	10th	25th	75th	90th	95th	98th
1	115	20.7	6.8	3.3	2.1	2.7	4.2	9.1	11.4	12.7	14.3
2	68	16.2	4.6	2.1	1.6	2.0	3.0	6.0	7.5	8.5	9.6
3	163	16.6	3.7	2.3	1.0	1.3	1.9	4.9	6.9	8.2	9.7
4	85	15.1	4.7	2.1	1.8	2.3	3.2	5.9	7.6	8.6	9.8
5	262	16.4	4.7	2.3	1.6	2.0	2.9	6.0	7.9	9.2	10.5
6	10	17.9	5.5	2.6	2.0	2.5	3.5	7.1	9.1	10.4	11.8
7	87	17.0	5.7	2.6	2.0	2.5	3.6	7.3	9.3	10.5	11.9
8	6	16.3	5.3	2.6	2.1	2.4	3.3	6.8	9.0	10.2	12.0
9	8	16.3	4.0	2.1	1.4	1.7	2.4	5.2	6.8	8.0	9.5
10	17	14.9	4.4	2.2	1.6	2.0	2.8	5.6	7.4	8.5	9.7
11	6	14.8	4.4	2.0	1.7	2.0	2.9	5.6	7.3	8.2	9.4
12	62	17.5	5.1	2.4	1.9	2.3	3.3	6.6	8.5	9.7	10.8
13	78	19.8	6.1	2.7	2.4	2.9	4.1	7.7	9.9	11.3	12.8
14	3	16.0	4.3	2.2	1.6	1.9	2.6	5.6	7.2	8.4	10.0
15	102	13.9	3.1	2.1	0.7	0.9	1.4	4.2	6.0	7.2	8.5
16	33	11.2	2.5	1.7	0.4	0.6	1.2	3.5	4.9	5.8	6.7
17	242	16.1	3.7	2.1	1.2	1.5	2.2	4.9	6.7	7.8	9.0
18	25	12.8	3.4	1.6	1.2	1.5	2.1	4.3	5.6	6.4	7.4
19	10	14.6	4.0	2.0	1.5	1.8	2.5	5.2	6.7	7.8	8.8
20	5	17.6	4.7	2.2	1.8	2.2	2.9	6.0	7.7	8.9	10.2
21	26	21.8	7.0	3.0	2.8	3.5	4.8	8.9	11.1	12.5	14.2
22	32	15.5	4.2	2.2	1.3	1.7	2.6	5.4	7.1	8.2	9.6
23	82	22.7	7.5	3.4	2.8	3.5	4.9	9.6	12.3	13.9	15.7
24	10	17.0	4.9	2.4	1.8	2.2	3.0	6.2	8.2	9.6	11.0
25	6	18.1	5.2	2.4	2.0	2.4	3.4	6.6	8.4	9.6	11.1
26	145	14.1	4.4	1.9	1.8	2.2	3.1	5.5	7.0	8.0	9.1
27	10	19.4	6.3	3.0	2.2	2.7	4.0	8.1	10.4	11.8	13.5
28	44	15.8	5.0	2.2	2.1	2.5	3.3	6.2	8.0	9.1	10.3
29	90	15.1	4.1	2.0	1.4	1.8	2.6	5.3	6.8	7.9	9.0
30	117	12.7	3.8	1.7	1.5	1.8	2.5	4.8	6.1	7.0	7.9
31	50	18.6	5.4	2.8	1.8	2.2	3.2	7.0	9.3	10.7	12.3
32	69	14.1	4.1	1.9	1.5	1.9	2.6	5.3	6.8	7.7	8.6
33	16	18.8	6.4	3.0	2.3	2.8	4.1	8.3	10.6	12.0	13.4
34	277	19.8	6.6	3.0	2.5	3.1	4.3	8.4	10.7	12.2	13.9
35	72	13.3	4.1	2.0	1.4	1.8	2.6	5.2	6.8	7.8	9.0
36	103	17.8	5.9	2.7	2.2	2.7	3.8	7.5	9.7	11.0	12.3
37	15	19.6	5.8	2.9	1.9	2.4	3.6	7.5	9.8	11.3	12.9
38	10	19.4	6.3	3.3	1.8	2.4	3.6	8.5	11.0	12.5	14.1
39	68	16.1	4.7	2.1	1.9	2.3	3.1	5.9	7.5	8.6	9.6
40	89	14.6	4.8	2.0	2.2	2.6	3.3	5.9	7.6	8.7	10.0
41	11	17.1	5.2	2.6	1.6	2.1	3.2	6.8	8.8	10.0	11.4
42	73	15.3	4.8	2.2	1.8	2.3	3.1	6.1	7.8	8.9	10.1
43	20	16.2	3.9	2.1	1.0	1.4	2.3	5.2	6.8	7.8	9.0

Table 3.1 - General statistics of all daily mean windspeeds recorded in the period 1980-2005 at 43 stations across the UK. All figures are in ms^{-1}. ([1]standard deviation is abbreviated). See Appendix A for location of stations.

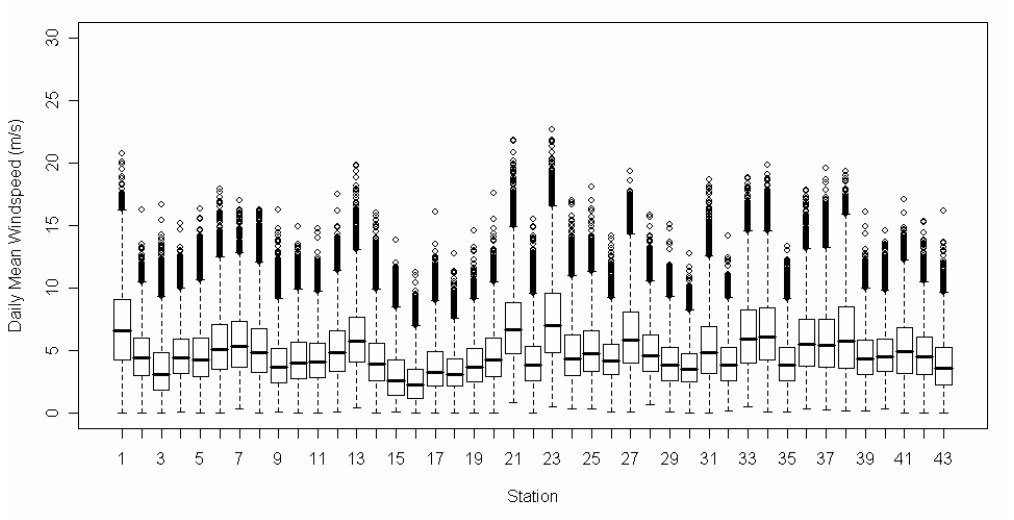

Figure 3.1 - Boxplot of daily mean windspeed recorded at 43 stations across the UK for the period 1980-2005.

Figure 3.1 shows a boxplot of daily mean windspeed for each station in the observation network. The boxplot shows the minimum and maximum values at the ends of the whiskers, with the mean, 25th and 75th percentile values marked by the middle, lower and upper part of the box respectively.

Daily mean windspeeds recorded in the 1980-2005 period reached a maximum of 22.7 ms^{-1} at Lerwick (*station 23*) on 12th March 1996. The second highest station value (21.8 ms^{-1}) was measured at Kirkwall (*21*) on 19th September 1990, while Aberporth (*1*) was the only other station to record a daily mean windspeed over 20 ms^{-1}, with a value of 20.7 ms^{-1} on 16th September 2001. East Malling (*16*) exhibits the lowest maximum daily mean windspeed of 11.2 ms^{-1}. The second and third lowest maximum daily mean windspeed values are recorded at Nottingham Watnall (*30*) and Heathrow (*18*), with values of 12.7 ms^{-1} and 12.8 ms^{-1} respectively.

The average daily mean windspeed for each station is shown in Figure 3.2 (Appendix A details the station numbers and their location). The highest average daily mean windspeed is 7.5 ms^{-1}, recorded at Lerwick (*23*). The second and third highest average daily mean windspeeds are recorded at Kirkwall (*21*) and Aberporth (*1*) (values of 7.0 ms^{-1} and 6.8 ms^{-1} respectively). The lowest mean of daily mean windspeed (2.5 ms^{-1}) is seen at East Malling (*16*). Durham (*15*) and Heathrow (*18*) exhibit the second and third lowest

average daily mean windspeeds, with values of 3.1 ms^{-1} and 3.4 ms^{-1} respectively.

Spatial Variations

Figure 3.2 shows the spatial variations in the average daily mean windspeed recorded at each station between 1980 and 2005, across the UK.

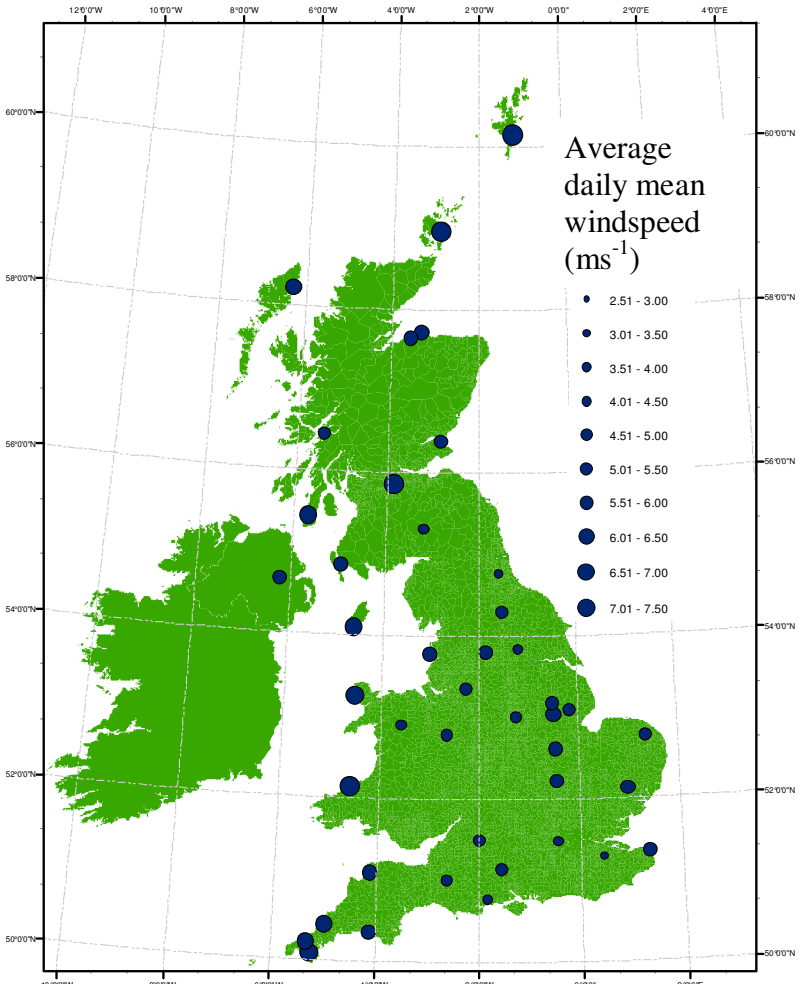

Figure 3.2 - Average daily mean windspeed recorded at 43 stations across the UK in the period 1980-2005.

The windspeeds depicted in Figure 3.2 demonstrate the impact of the proximity of stations to the coast, in particular the west coast. Higher mean windspeeds are recorded at stations located on the south west England peninsular and the Welsh and Scottish coasts, compared to those recorded further inland. Inland, windspeeds are generally lower in the south east region of the UK, increasing with latitude. However, the prominence of coastal stations in Scotland (there are only two inland stations in this country) acts to

mask latitudinal variations in mean windspeeds. These average values of daily mean windspeed and their spatial variations are in line with those described by Wheeler and Mayes (1997) and Palutikof et al. (1997), discussed in section 1.4. This offers some validation to the quality of the dataset, and the network of stations, utilised here. Furthermore, this suggests that gust speed information provided by the observation network can be considered reliable.

Temporal Variations

Inter- and intra-annual variations in daily mean windspeeds recorded by the observation network over the course of the study period are quantified here. The anomaly of the annual mean of the daily mean windspeeds is calculated for each station, relative to the mean of the entire period, with results plotted in Figure 3.3. The rather crowded plot is designed to illustrate the similar patterns followed by the majority of stations throughout the study period, with the clarity of individual station records acknowledged to be quite poor.

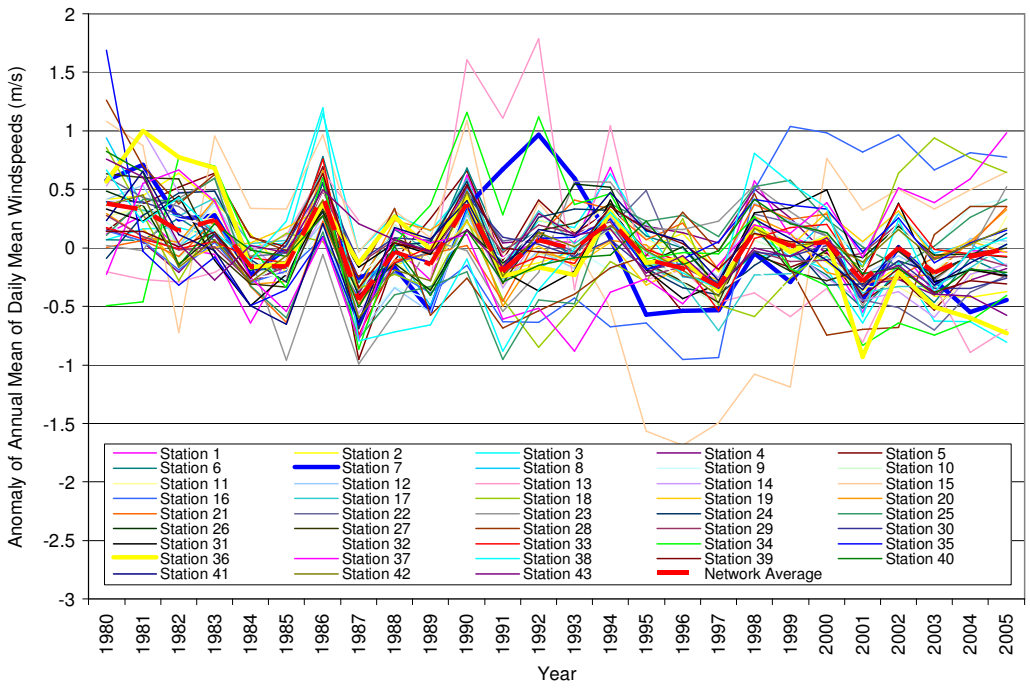

Figure 3.3 – Anomaly of the annual average of daily mean windspeeds recorded at 43 stations across the UK for the period 1980-2005[1]. The network average is shown as a red dashed line.

Generally, stations exhibit similar temporal variations to the Network Average (dashed red line in Figure 3.3). Clearly, some exceptions exist, most notably

[1] Data from Culdrose (13) for 1988 is not included in the temporal analysis as only data for January is available in that year, and hence is not representative of the whole year.

Durham (*15*) between 1995 and 1999, and East Malling (*16*) in 1998, questioning the quality control of data described in section 2.1.1. The daily values of mean windspeeds recorded at Durham over a five-year period (1995-1999) were not found to be significantly different from the rest of the record. However, this plot suggests windspeeds recorded at this station during this period should be treated with care. Similarly, the annual mean values at East Malling displays a sudden jump in 1998, suggesting a discontinuity in the record. This feature is not seen in the DMGS data however. Culdrose (*13*) records markedly high annual mean values in 1990 and 1992, but again daily values in these years were not significantly different from the rest of the record.

The Network Average annual mean of daily mean windspeed in 1986 (1987) is roughly 0.5 ms^{-1} higher (lower) than the long term average. All stations record below average annual means in 1987, while all except Lerwick (*23*) record above average annual means values in 1986. It is interesting to note that a major windstorm, on 16th October 1987, which resulted in extensive damage and insured loss, occurred during a year with below average mean windspeed. This issue is revisited in section 3.1.2.

Overall, a slight downward trend (0.5 ms^{-1}) in annual mean values is exhibited by the Network Average. The temporal trends discussed in this chapter were tested for significance using a two-sided t-test at the 95% confidence level, following Kruger and Shongwe (2004). At the 95% confidence level, 14 (1) stations showed significant decreases (increase) in daily mean windspeeds over the duration of the study. Significant decreases were largely seen in stations in southern and northern regions of England.

Seasonal variations in the daily mean windspeeds are detailed in Table 3.2. As expected, the highest mean windspeeds are recorded in winter (December to February) (Network Average is 5.7 ms^{-1}), while the lowest are seen in summer (June to August) (Network Average is 4.1 ms^{-1}). Autumn (September to November) mean windspeeds tend to be slightly lower than those in spring (March to May) (Network Average of 5.0 ms^{-1} compared with 4.9 ms^{-1}). The 14 stations which exhibit higher seasonal means of daily mean windspeeds in

autumn than in spring are all located in coastal regions, except Durham (*15*). In fact, Camborne (*7*) and Culdrose (*13*) (in Cornwall) are the only west coast stations to record higher seasonal means in spring than in autumn.

	Seasonal mean of Mean Daily Windspeed (ms^{-1})			
Station	**MAM**	**JJA**	**SON**	**DJF**
1	6.5	5.4	7.2	8.3
2	4.7	4.1	4.6	5.2
3	3.7	3.1	3.5	4.4
4	4.8	4.0	4.7	5.4
5	4.6	4.0	4.5	5.5
6	5.3	5.0	5.6	6.2
7	5.8	4.6	5.7	6.6
8	5.3	4.5	5.3	6.2
9	4.2	3.4	3.9	4.6
10	4.5	3.7	4.3	5.1
11	4.6	3.8	4.3	4.9
12	5.2	4.3	5.1	5.9
13	6.2	5.1	6.2	7.1
14	4.3	3.5	4.4	5.1
15	3.0	2.5	3.0	3.8
16	2.7	2.0	2.3	3.1
17	3.9	3.3	3.6	4.2
18	3.5	3.2	3.2	3.7
19	4.1	3.6	3.8	4.5
20	4.8	4.1	4.7	5.1
21	7.1	5.7	7.3	8.2
22	4.4	3.6	4.0	4.7
23	7.4	5.9	7.8	8.9
24	5.0	4.2	4.8	5.5
25	5.3	4.4	5.2	5.7
26	4.6	3.9	4.3	4.9
27	6.1	4.9	6.5	7.5
28	5.1	4.4	4.9	5.6
29	4.3	3.5	3.9	4.7
30	4.0	3.2	3.6	4.4
31	5.3	4.5	5.4	6.3
32	4.3	3.6	4.0	4.6
33	6.0	4.9	6.7	7.9
34	6.7	5.7	6.5	7.5
35	4.3	3.7	3.8	4.5
36	5.8	4.9	6.0	6.9
37	5.8	4.8	5.9	6.9
38	6.0	5.2	6.6	7.4
39	4.8	3.9	4.6	5.3
40	5.0	4.2	4.8	5.5
41	5.2	4.3	5.3	6.1
42	4.9	4.2	4.7	5.5
43	4.1	3.4	3.7	4.5

Table 3.2 – Seasonal mean values of daily mean windspeeds recorded at 43 stations across the UK for the period 1980-2005. Red (green) figures indicate seasons which show a significant (at 95% confidence level) decrease (increase) in values over the duration of the study.

Further analysis of the seasonal means reveal a similar temporal trend to that exhibited by the annual means; mean daily windspeeds show a slight decrease over the period of study in all seasons. This trend is most evident in autumn (September to November) when 13 (1) stations show significant decreases (increase) in mean values, and least evident in winter when two (one) stations show significant decreases (increases). The significant decreasing trends exhibited by stations in winter and autumn tend to be of the magnitude of 0.5 ms^{-1}.

This daily mean windspeeds dataset adds to, and extends, the body of work concerning mean windspeeds in the UK (e.g. Wheeler and Mayes, 1997; Sinden, 2007). The dataset is also utilised in the development of a windstorm loss model in Chapter 4. In addition, the temporal and spatial variations described here put into context those found in the DMGS dataset in the following section.

3.1.2 Daily Maximum Gust Speed

The main focus of this project is on damaging windspeeds, and although mean windspeeds can play a role in structural damage through loading, it is usually wind gusts which are the most destructive. Chapter 4 describes the development of a windstorm model, and shows that wind damage is highly correlated to the 98th percentile value of the daily maximum gust speed (DMGS). For this reason the local 98th percentile of DMGS is considered a threshold for damage, with windspeeds exceeding this threshold considered "damaging" throughout this project. In this section the DMGS data from the 43-station network, described in section 2.1.1, are analysed for the period 1980-2005. Initially, descriptive statistics are presented, followed by an analysis of spatial and temporal variations.

Descriptive Statistics

Table 3.3 presents the descriptive statistics of the observed DMGS data. Some key features of this table are illustrated in Figure 3.4 with further discussion below.

No.	Elevation (m above sea level)	max	mean	Std[1]	Percentile Values							Mean Direction
					5th	10th	25th	75th	90th	95th	98th	
1	115	47.9	15.2	6.3	6.2	7.7	10.3	19.1	23.7	26.3	29.9	212
2	68	38.1	11.9	4.8	5.2	6.2	8.8	14.9	18.5	20.6	23.7	207
3	163	37.1	11.8	5.4	5.2	6.2	8.2	14.4	19.1	21.6	24.7	200
4	85	37.1	11.4	4.5	5.2	6.2	8.2	13.9	17.5	19.6	22.7	199
5	262	40.2	12.4	5.5	5.7	6.7	8.8	15.5	19.6	22.1	25.2	203
6	10	42.7	12.6	5.4	5.7	6.7	8.8	15.5	19.6	22.7	26.3	210
7	87	43.3	14.3	5.7	6.7	7.7	9.8	18.0	21.6	24.7	28.3	205
8	6	41.7	12.9	5.5	6.2	7.2	8.8	16.0	20.1	22.7	25.8	210
9	8	38.6	11.5	4.9	5.2	6.2	8.2	13.9	18.0	20.6	24.2	210
10	17	37.6	11.8	4.7	5.7	6.7	8.2	14.4	18.0	20.6	23.2	195
11	6	39.1	11.7	4.6	5.7	6.7	8.8	13.9	17.5	19.6	22.7	198
12	62	40.2	12.3	4.8	6.2	7.2	8.8	14.9	19.1	21.1	24.2	206
13	78	45.8	14.9	6.3	7.2	8.2	10.3	18.5	23.2	25.8	28.8	200
14	3	41.2	12.5	5.6	5.2	6.2	8.8	15.5	19.6	22.7	26.3	197
15	102	41.2	12.0	6.4	4.1	5.7	7.7	15.5	19.6	23.2	26.3	206
16	33	40.2	10.4	4.7	4.6	5.7	7.2	12.9	16.5	19.1	21.6	198
17	242	37.1	12.6	5.3	5.7	6.7	8.8	15.5	20.1	22.1	25.2	193
18	25	39.1	10.9	4.0	5.2	6.2	8.2	12.9	16.0	18.0	21.1	195
19	10	37.1	11.6	5.2	5.7	6.7	8.2	13.9	18.0	20.1	22.7	196
20	5	37.6	12.7	5.6	5.7	6.7	8.8	16.0	19.6	22.1	24.7	202
21	26	50.0	15.5	6.2	7.2	8.2	10.8	19.1	23.7	26.3	30.4	202
22	32	40.7	12.1	5.0	5.7	6.7	8.8	14.9	19.1	21.1	24.7	207
23	82	48.9	16.4	6.4	7.7	8.8	11.8	20.6	25.2	27.8	31.6	197
24	10	37.6	12.6	5.2	5.7	6.7	8.8	15.5	19.6	22.7	25.2	191
25	6	40.2	13.3	5.2	6.2	7.2	9.3	16.5	20.1	23.2	25.8	205
26	145	38.1	11.8	4.7	5.7	6.7	8.2	14.4	17.5	20.1	22.7	192
27	10	42.2	14.8	5.9	6.7	7.7	10.3	18.5	22.7	25.8	29.4	211
28	44	44.3	12.1	4.7	6.2	6.7	8.8	14.9	18.5	20.6	23.7	193
29	90	40.2	11.5	4.5	5.7	6.7	8.2	13.9	17.5	20.1	23.2	196
30	117	35.5	11.4	4.4	5.7	6.4	8.2	13.9	17.5	19.6	22.1	201
31	50	44.3	13.8	5.8	6.7	7.7	9.8	17.0	21.6	24.2	27.3	205
32	69	40.7	11.5	4.5	5.7	6.7	8.2	13.9	17.5	19.6	22.1	201
33	16	42.7	14.3	5.5	6.7	7.7	10.3	17.5	21.6	24.2	26.8	205
34	277	48.9	14.3	6.5	5.7	7.2	9.8	18.0	22.7	25.8	28.8	191
35	72	35.0	11.6	4.9	5.7	6.7	8.2	13.9	17.5	20.1	22.7	217
36	103	43.8	13.5	5.3	6.7	7.2	9.3	17.0	21.1	23.2	26.8	210
37	15	47.4	14.6	6.1	6.2	7.7	10.3	18.5	23.2	25.8	28.8	189
38	10	40.7	13.8	5.9	5.7	6.7	9.3	17.5	22.1	24.7	27.3	200
39	68	40.2	11.9	4.5	6.2	6.7	8.8	14.4	18.0	20.1	22.7	196
40	89	41.2	11.7	4.4	6.2	6.7	8.8	13.9	17.5	20.1	23.2	202
41	11	38.6	12.9	5.1	6.2	7.2	9.3	16.0	19.6	22.1	25.2	211
42	73	42.2	11.9	4.7	5.7	6.7	8.8	14.4	18.0	20.6	23.7	203
43	20	35.0	11.7	4.8	5.7	6.2	8.2	14.4	18.0	20.6	23.7	205

Table 3.3 - General statistics of all DMGS recorded in the period 1980-2005 at 43 stations across the UK. All figures are in ms^{-1}, except for Mean Direction (degrees). ([1]standard deviation is abbreviated).

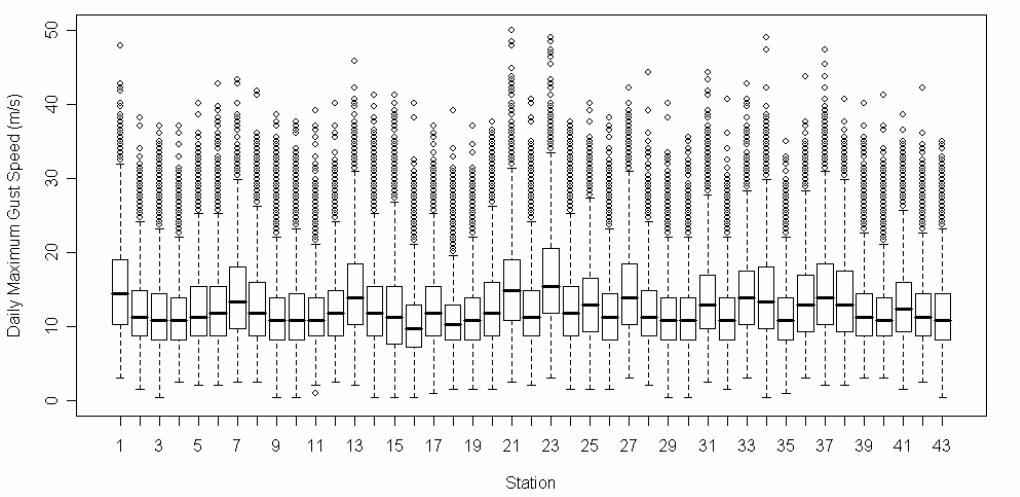

Figure 3.4 - Boxplot of Daily Maximum Gust Speeds recorded at 43 stations across the UK for the period 1980-2005

The highest recorded gust speed in the 1980-2005 period in the network of 43 stations was the 50 ms^{-1} gust recorded at Kirkwall (*21*) on the 29th January 2000. During the course of the study Aberporth (*1*), Lerwick (*23*), Salsburgh (*34*) and Stornoway Airport (*37*) all recorded gusts exceeding 45 ms^{-1}. In terms of minimum DMGSs recorded in the study period, it is assumed the variation seen between stations reflects the instrumentation utilised for observations. Seven stations recorded minimum DMGSs of 3.1 ms^{-1}, which is equivalent to the 6-knot start up speed of the Munro anemometer described in section 2.1.1.

The highest mean DMGS is reported by Lerwick (*23*), with a value of 16.4 ms^{-1}. Only two other stations, Aberporth (*1*) and Kirkwall (*21*), have mean DMGSs exceeding 15 ms^{-1}, reporting values of 15.2 ms^{-1} and 15.5 ms^{-1} respectively. The lowest mean DMGS of 10.4 ms^{-1} is seen at East Malling (*16*), with the second lowest value (10.9 ms^{-1}) reported by Heathrow (*18*). The mean DMGS values for each station are plotted in Figure 3.5.

Looking at 98th percentile values (the threshold for potentially damaging windspeeds) reveals Lerwick (*23*) has the highest at 31.6 ms^{-1}, while Heathrow (*18*) has the lowest at 21.1 ms^{-1}. Kirkwall (*21*) and Aberporth (*1*) report the second and third highest 98th percentile values of 30.4 ms^{-1} and 29.9 ms^{-1} respectively. East Malling (*16*) reports the second lowest 98th percentile value at 21.6 ms^{-1}. The 98th percentile value of DMGS of each station is plotted in Figure 3.6.

The mean direction from which the DMGS originated was calculated for each station, and is shown to be consistently in the south-west sector of the compass. Mean directions varied just 27°, from 189° to 216°.

Spatial Variations

Figure 3.5 shows the spatial variations in the mean of the DMGS recorded at each station between 1980 and 2005, across the UK.

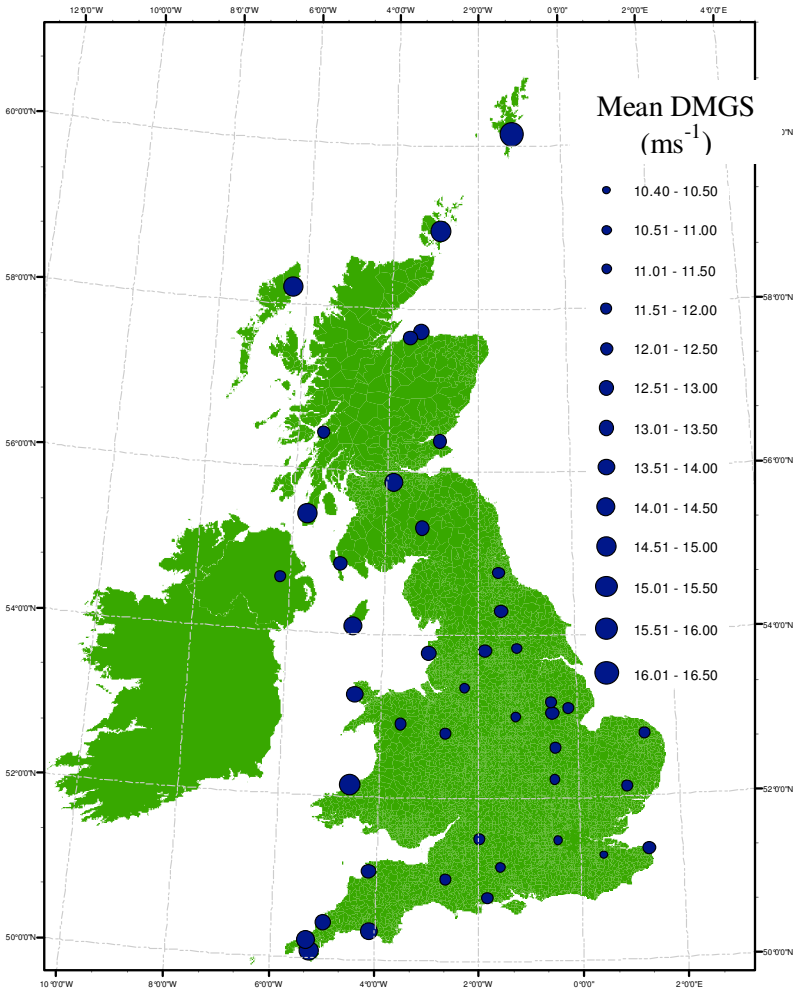

Figure 3.5 - Mean DMGS recorded at 43 stations across the UK for the period 1980-2005.

Geographic variations of mean DGMS are similar to those exhibited by the average of the daily mean windspeeds. Coastal stations record higher mean DMGS than those further inland. This effect is particularly prominent in England and Wales, where a distinct pattern of higher DMGS on the west coast compared with the east coast is evident. These results are expected since the reduced friction over the sea results in increased windspeeds on the

coast relative to those further inland. West coast stations likely record higher DMGS and daily mean windspeeds due to the greater fetch proffered by the Atlantic ocean. As with the mean of the daily mean windspeeds, if the coastal stations are removed, an increase in mean DMGSs is seen with latitude. Again this is as expected; with stations further north tending to be exposed to a greater number of extratropical cyclones, as described in section 1.4.

In terms of damaging winds, Figure 3.6 shows the 98th percentile value of DMGS recorded at each station for the period 1980-2005.

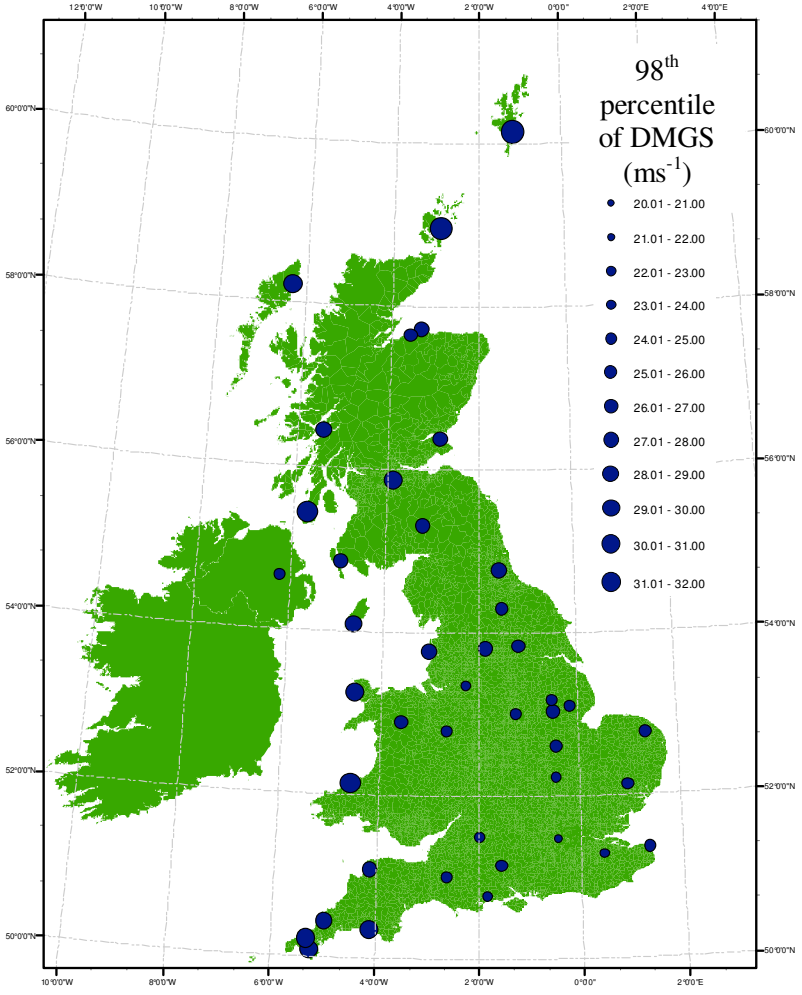

Figure 3.6 - 98th percentile values of DMGS recorded at 43 stations across the UK for the period 1980-2005.

The spatial variation of the 98th percentile value of DMGS is very similar to that shown by the mean DMGS (correlation of the 43 mean values with 98th percentile values produced an R^2 value of 0.92). Meanwhile, the correlation between the 43 stations values of the 98th percentile of DMGS with daily mean

windspeed is reasonably strong (R^2 = 0.69). Again, the coastal effect is evident, with higher values recorded on the west coast, compared with the east. The pattern of increasing values with latitude is more apparent in the 98th percentile values, than in the mean values.

Temporal Variations

The inter-annual variation exhibited by DMGS is shown in Figure 3.7. Once more the figure is designed to illustrate the general trends exhibited by all stations rather than depict individual stations.

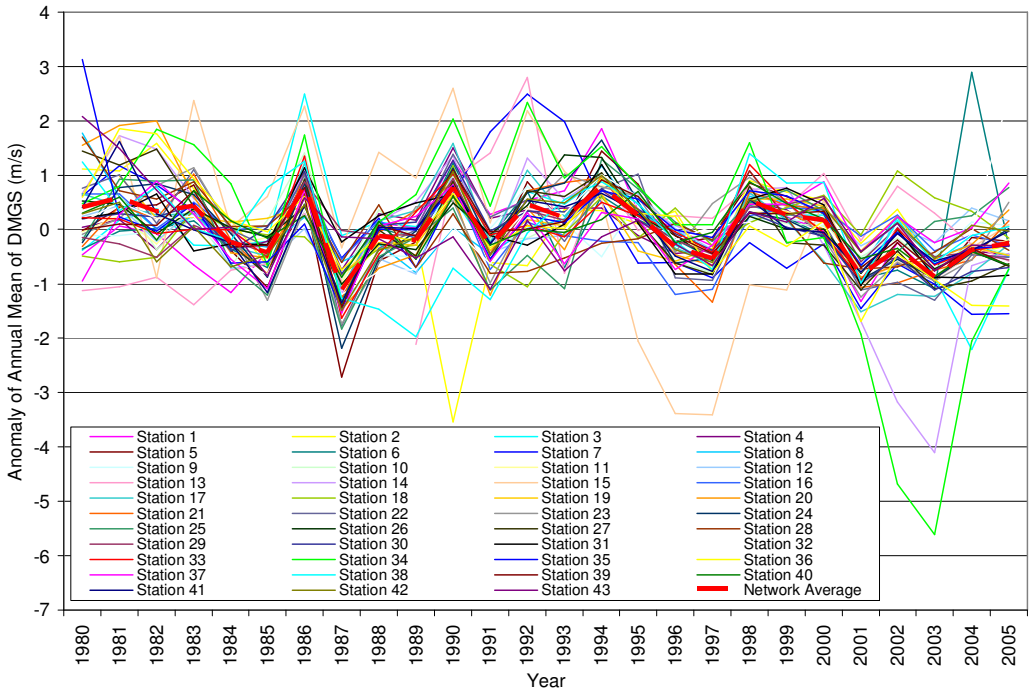

Figure 3.7 – Anomaly of the annual mean of DMGS recorded at 43 stations across the UK for the period 1980-2005. The Network Average is show as a red dashed line.

The markedly below average values of the annual average of daily mean windspeeds recorded at Durham (*15*) between 1995 and 1999 described in section 3.1.1 is mirrored by the annual mean DMGS values shown in Figure 3.7. Even with the removal of this station from the data, the Network Average is still below average in this period. Particular low values for annual mean DMGS are recorded at Dunstaffnage (*14*) and Salsburgh (*34*) in 2002 and 2003. The majority of other stations also show a drop in annual mean values in 2003, but none to the extent of Dunstaffnage and Salsburgh. Also, nearly all other stations exhibit a peak in annual mean DMGS in 2002.

The Network Average annual mean DMGS is highest in 1986 and lowest in 1987, in line with daily mean windspeed values. Overall, a slight downward trend in the values of the annual mean of DMGS is suggested by the data over the course of the study. The Network Average exhibits a 0.5 ms^{-1} decrease in annual means over the duration of the study. Downward trends are seen at 35 stations (12 significant), while a slight upward trend is seen at the remaining 8 stations (2 significant). There appears to be no spatial pattern in these trends with significant increases seen at stations in Cornwall, south east, central and north east England, as well as Scotland. The two significant decreases in annual mean values occur at Culdrose (*13*) (also in Cornwall) and Heathrow (*18*).

The seasonal mean values of DMGS at each station are highest in winter and lowest in summer. Values of DMGS in spring tend to be slightly higher than those in autumn, with 23 stations recording higher spring mean values of DMGS than autumn. The stations where the opposite is true are the same as those exhibiting higher mean windspeeds in autumn than spring, described in section 3.1.1, with the addition of 6 stations (4 of which are coastal, including Camborne and Culdrose). All stations in England, with the exception of those located in the south west peninsula, exhibit higher spring than autumn values. In addition, Eskdalemuir (*17*), Leuchars (*24*) and Aldergrove (*2*) also show this feature.

Eleven stations display significant decreases in the autumn mean value of DMGS over the duration of the study. These stations are largely located in Scotland, with two in Cornwall and three in central and northern England. Significant decreases are found at 8 (7) stations in summer (spring), with winter showing the weakest downward trend in mean values of DMGS, with only 3 stations showing significant decreases and one showing a significant increase. The stations showing decreases in spring, summer and winter mean values generally correspond with those showing the decreasing trends in autumn described above. Between 1980 and 2005, autumn values decrease by 1 ms^{-1}, while reductions of roughly 0.5 ms^{-1} are seen in other seasons.

The variation in the annual 98^{th} percentile values of DMGS is shown below.

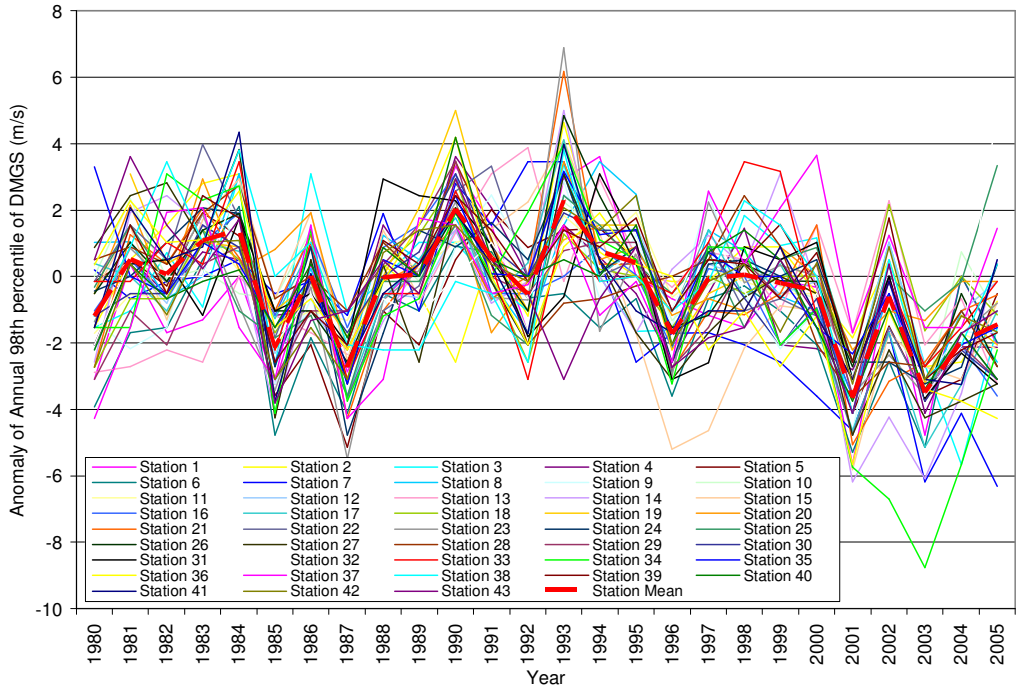

Figure 3.8 – Anomaly of the annual 98th percentile values of DMGS recorded at 43 stations across the UK in the period 1980-2005. The Network Average is shown as a red dashed line.

The below average annual mean DMGS values recorded at Dunstaffnage (14) and Salsburgh (34) in 2002 and 2003, and Durham in 1995-99 are also seen in the annual 98th percentile values of DMGS. The Network Average anomaly is at its highest in the study period in 1993, while in 2001 it is at its lowest mark. Fluctuations shown in the annual mean values of daily mean windspeed and DMGS are reflected in Figure 3.8, but generally with a greater magnitude. The year with the lowest daily mean windspeeds and mean DMGS values (1987), also exhibits below average 98th percentile values of DMGS (Network Average is 2.7ms^{-1} below average). As stated in section 3.1.1, and described in section 1.1.1, a very large windstorm occurred in October 1987, with the UK suffering exceptional economic and insured losses. Results suggest all windspeed values considered here were markedly below average in that year. This may have contributed to the high damage experienced during the storm, with structures and trees not preconditioned to high windspeeds.

A 2 ms^{-1} downward trend is shown by the Network Average between 1980 and 2005. Decreasing trends are exhibited by 38 stations, of which 12 show significant decreases. Six of these 12 stations are located in southern England, with five in northern England and southern Scotland, and one in

central England. The greatest decreases in these stations are shown in southern England at Camborne (*7*) (5.5 ms^{-1} decrease), St Mawgan (*36*) (2.5 ms^{-1}), East Malling (*16*) (3.5 ms^{-1}) and Manston (*28*) (5 ms^{-1}).

Intra-annual variations of the 98th percentile value of DMGS (shown in Table 3.4) reveal seasonal values are highest in winter and lowest in summer. Autumn exhibits higher 98^{th} percentile values of DMGS than spring, with 25 stations recording higher values in autumn than spring, and only 8 stations recording higher values in spring than autumn (at 10 stations the value was identical for spring and autumn). The spatial variation of stations with higher autumn values than spring is similar to that shown for mean DMGS values, described previously.

	Seasonal 98th percentile value of DMGS (ms^{-1})			
Station	**MAM**	**JJA**	**SON**	**DJF**
1	27.8	22.7	28.7	33.5
2	23.2	18.5	23.2	26.8
3	23.3	18.5	23.7	27.8
4	21.6	17.5	21.6	25.2
5	24.2	19.1	23.7	28.4
6	25.5	19.6	25.2	28.3
7	26.8	21.1	27.3	30.9
8	23.7	19.1	25.2	29.4
9	22.7	18.0	22.7	28.1
10	22.7	18.0	22.2	26.3
11	22.2	18.3	22.2	25.2
12	23.2	19.1	23.2	26.8
13	27.8	22.7	28.3	31.9
14	24.2	17.7	24.7	29.9
15	25.2	20.6	25.2	30.7
16	20.8	17.0	20.6	24.2
17	23.7	20.1	24.7	27.8
18	20.1	16.5	20.5	23.7
19	21.6	18.0	22.2	25.8
20	23.7	19.6	24.2	28.3
21	28.3	21.7	29.9	35.0
22	23.7	19.1	23.7	29.4
23	29.4	22.7	31.4	35.0
24	24.7	19.6	25.2	28.3
25	24.7	20.1	25.8	29.4
26	21.6	17.5	21.9	25.8
27	26.8	20.6	28.3	32.5
28	23.2	18.5	23.7	26.8
29	21.6	17.2	21.6	26.3
30	21.6	18.0	21.1	24.7
31	25.2	21.1	26.8	30.9
32	21.1	17.6	21.6	25.4
33	24.7	20.1	26.3	29.9
34	26.8	22.2	27.8	32.5
35	21.6	18.0	21.7	26.3
36	25.2	20.1	25.8	29.9
37	26.3	20.6	28.8	32.1
38	24.8	21.1	27.8	30.5
39	22.2	18.0	21.6	26.8
40	22.2	18.5	22.2	25.8
41	22.8	19.1	25.2	28.3
42	22.7	18.5	22.7	26.8
43	22.7	18.0	23.2	26.3

Table 3.4 – Seasonal 98th percentile value of DMGS recorded at 43 stations across the UK for the period 1980-2005. Red (green) figures indicate seasons which show a significant decrease (increase) in values over the duration of the study.

Downward trends over the course of the study are suggested by the seasonal values of the 98th percentile of DMGS in all seasons. Autumn shows the strongest trend with 15 stations showing significant decreases, and the Network Average decreasing 2.5 ms^{-1} of the course of the study. The 15 stations are largely located in central and northern England and southern Scotland. The Network Average winter value indicates a 1.5 ms^{-1} decrease over course of the study, with the spring value dropping 2 ms^{-1} and the summer value 1 ms^{-1}. Unlike mean windspeeds and also seasonal mean values of DMGS, no stations show any significant increases in the seasonal 98th percentile of DMGS.

The decrease in 98th percentile values on both an annual and seasonal basis suggests that over the course of the study the frequency of damaging windspeeds has decreased. In conjunction, slight decreases in the mean values of DMGS and daily mean windspeeds are found. Furthermore, the annual standard deviation of DMGS shows significant decreases at 16 stations with only 6 suggesting slight upward trends. The Network Average exhibits a significant decrease from 5.2 ms^{-1} to over 4.8 ms^{-1}. This indicates that the frequency of extreme DMGS is decreasing over the course of the study. The impact this has on insured losses is assessed in Chapter 5.

The inter-annual trends in daily mean windspeeds and DMGSs identified in Figure 3.3, Figure 3.7 and Figure 3.8 are largely driven by winter values. A major mode of atmospheric variability in the Northern Hemisphere is the North Atlantic Oscillation (NAO), with winter values exhibiting strong inter-decadal variability. The strength of the NAO can be assessed using an index based on the difference between the normalised sea level pressure between Gibraltar and Southwest Iceland (Jones *et al.*, 1997). Updated values are presented by Osborn (2006) and available from http://www.cru.uea.ac.uk/~timo/projpages/nao_update.htm. The time series of December-March NAO index is plotted (red line) alongside the anomaly of the mean (blue) and 98th percentile (green) of DMGS for those months in Figure 3.9, for the period 1980-2005.

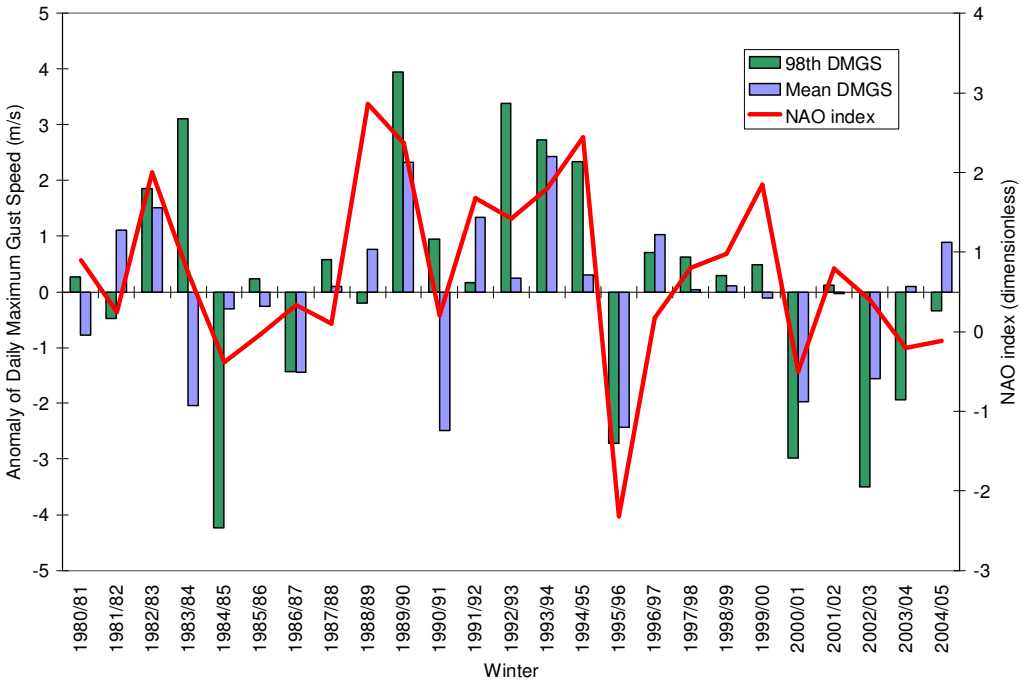

Figure 3.9 – December-March anomalies of mean (blue bars) and 98th percentile (green bars) values of DMGS, and NAO index (red line).

Generally, a more positive NAO index coincides with higher values of mean and 98th DMGSs, shown in Figure 3.9. This seems logical given that in this phase the prevailing westerly winds are stronger. In addition, a strong NAO (more positive NAO index) results in a stronger storm track, with a northeast orientation, directing depressions into northwest Europe. Reasonably strong correlations exist between December-March NAO index and mean DMGS (R^2 = 0.36) and 98th percentile DMGS (R^2 = 0.42). The downward trend seen in the winter NAO index since the mid 1990s is likely responsible for the downward trend in daily mean windspeeds and DMGS described in this section. A further comparison of model windspeeds to variations in the NAO is presented in section 3.2.

Timing of DMGS

The spatial and temporal variations of DMGS are described above. However, another factor affecting the impact of windstorms on the UK is the timing of their occurrence. As described in section 1.1.1 damaging windspeeds occurring during periods when the majority of the population is at home will have less of an impact than those occurring during periods when they are not. During periods of damaging windspeeds personal injury and transport disruption are more prevalent when the public are outside or travelling. Hence,

high windspeeds occurring during the night will tend to have less impact on the day-to-day lives of the population than those occurring during the day. However, it should be noted that this refers directly to the personal impact of damaging windspeeds and not to the resultant structural damage. There is no indication that degree of structural damage is dependent on the timing of the damaging winds. The time of the day DMGSs are recorded across the network of observing stations between 1980 and 2005 is illustrated in Figure 3.10.

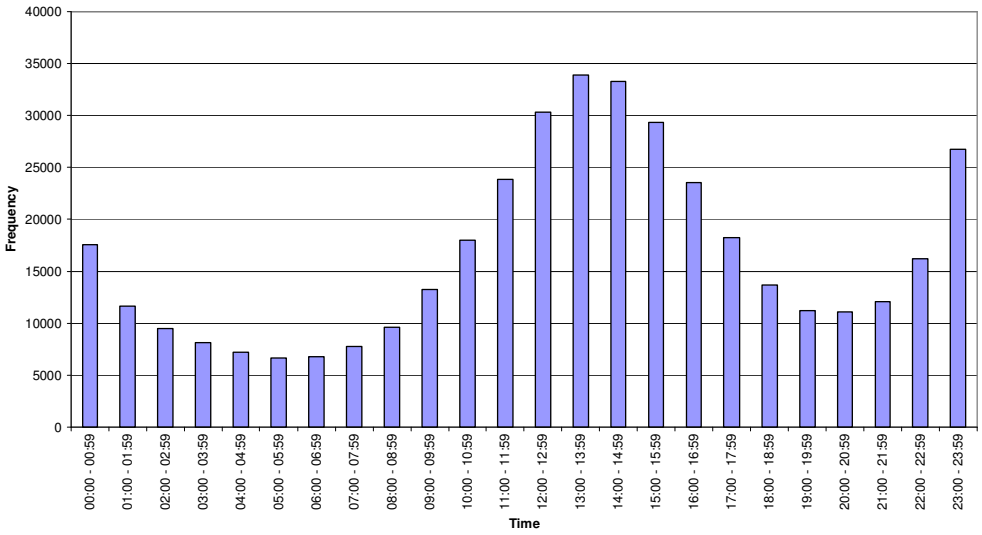

Figure 3.10 - Timing of DMGS recorded at 43 stations across the UK for the period 1980-2005.

Two peaks are shown in the timing of the DMGS; one during the afternoon at 1300-1500, and another during the night at 23:00-01:00. If this analysis is limited to damaging winds, (those exceeding the 98th percentile value of the DMGS), a similar pattern is revealed (Figure 3.11).

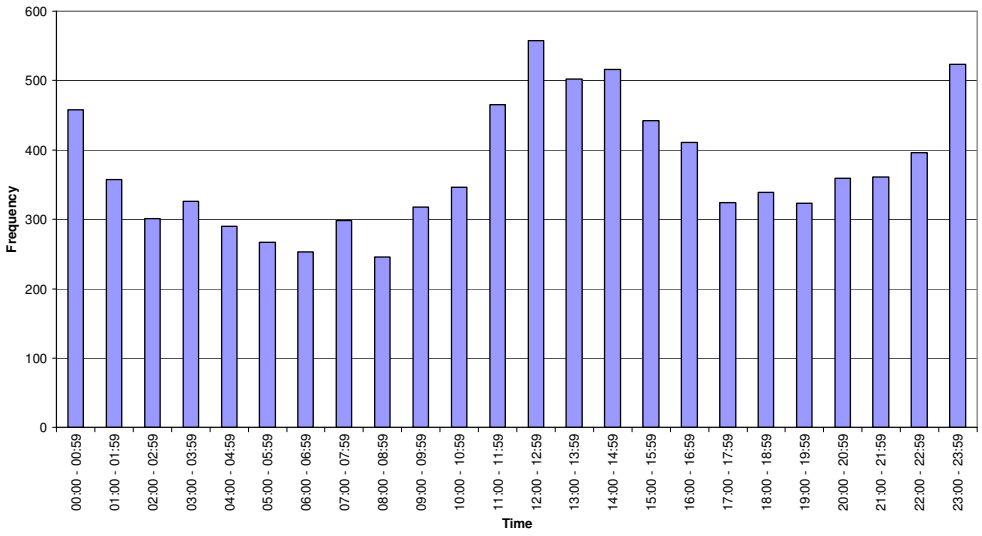

Figure 3.11 - Timing of the upper 2% of DMGS recorded at 43 stations across the UK for the period 1980-2005.

This diurnal pattern is still evident when the analyses are limited to DMGSs exceeding thresholds of 20, 25 and 30 ms^{-1}. The occurrence of the maximum gust speed in the afternoon results from a greater likelihood of atmospheric instability. A positively driven lapse rate (temperature falling with height due to surface heating) facilitates mixing and downdrafts from the synoptically driven winds at a higher level. Thermally driven vertical mixing leads to the transfer of energy to the surface manifesting in the form of gusts. Since this process is dependent on solar radiation it follows that the afternoon peak in the timing of DMGS should vary seasonally. This is evident from Figure 3.12.

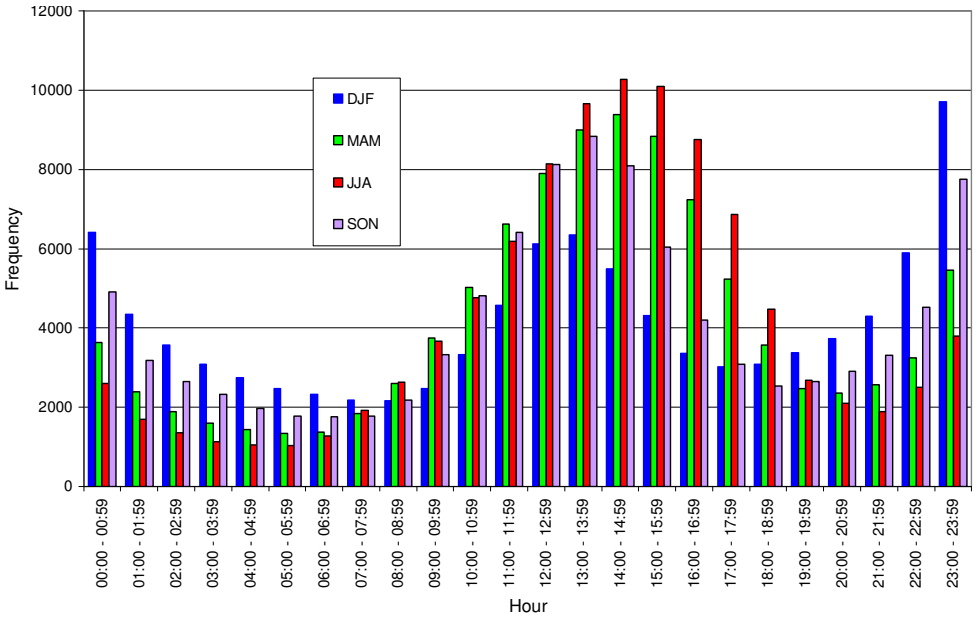

Figure 3.12 - Timing of the DMGS recorded at 43 stations across the UK for the period 1980-2005 in each season.

During the winter months the afternoon peak in timing of DGMSs occurs slightly earlier than in summer. Figure 3.12 also shows that in winter months the majority DMGSs are recorded during the period 23:00-01:00. This nocturnal peak is less evident in summer months, when DMGSs recorded in the afternoon are more prevalent. DMGS occurring in afternoon peaks are likely more common in summer months due to the increased solar radiation compared with other seasons.

The nocturnal peak is likely to be a result of surface cooling. A temperature inversion, created by night-time cooling at the surface, compresses and lowers the layer containing the wind maxima driven by synoptic conditions. This subsequently leads to gusty surface conditions. The presence of a low level jet may also be responsible for producing this night-time peak in the timing of DMGSs. The factors involved in the formation of the nocturnal jet are not fully understood; Conangla and Cuxart (2006) provide an overview of some potential mechanisms. The central theory outlined by Blackadar (1957) suggests that in the early evening cooling results in the rapid conversion of the boundary layer from a convective to stable state. During the transition the lower layers undergo turbulent mixing, while a stress-free layer exists above the nocturnal surface inversion. This shear-free layer is free of any frictional constraints and a supergeostrophic flow results from undamped inertial oscillation. This feature is also impacted by local conditions such as terrain and land-sea effects.

The presence of a nocturnal peak in timing of DMGS is a rather surprising result, and not one previously reported in the literature. Significantly, in terms of wind-related damage, this peak also exists when only damaging windspeeds are considered. In order to try to ascertain the atmospheric mechanisms occurring to produce this peak an investigation was carried out using wind profiler data. Seven wind profilers, at sites across the UK are operated by the Met Office, although Wattisham (station 40) is the only one corresponding to a station used in this study. Data containing high temporal resolution (every 30 minutes) information on windspeeds through the atmosphere (from 152 m to 8000 m), were extracted from the BADC archives. Unfortunately, the dataset from the Wattisham wind profiler only overlaps with

the observed 10-metre windspeed dataset for the period 2001-2005. All the occasions when the DMGS occurs between 2300 and 0100 in the Wattisham 10-metre windspeed dataset were identified. A screening process was undertaken to remove dates when the DMGS was likely driven by frontal progression. This left only 9 dates, for which the wind profiler data were analysed. Unfortunately, the wind profiler data are somewhat inconsistent, with large quantities missing, including 7 of the days of interest. Data from the remaining two days were analysed, but suffered from several missing readings, rendering results inconclusive. Furthermore, the lowest level windspeeds are recorded at 152 m, which makes a thorough assessment of processes driving the 10-metre difficult. For this reason a further investigation using the Wattisham wind profiler data was not undertaken.

Histograms of the timing of the DMGS recorded at each station are compared to the overall pattern in Figure 3.11. Coastal stations tend to produce a more smoothed graph, with a reduction in the afternoon peak, and the nocturnal peak becoming more dominant. Epitomising this is Aberporth (*1*), which recorded over 1000 instances of the DMGS measured in the 23:00-23:59 period, while just over 400 were recorded in the afternoon peak at 12:00-12:59. Inland stations tend to produce patterns with a more exaggerated peak in the afternoon, and reduced nocturnal peaks. Afternoon peaks are likely the result of surface heating and subsequent instability in surface layers through convection. This process will be dampened at coastal stations, and hence the afternoon peaks in DMGS are reduced. The graphs also suggest that the afternoon peak is later with increasing latitude; the afternoon peak at Middle Wallop (*29*), Nottingham Watnall (*30*) and Salsburgh (*34*) is at 13:00-59, 14:00-14:59 and 15:00-15:59 respectively. However, some caution must be applied when interpreting this pattern given the prevalence of coastal stations in the higher latitudes.

3.2 Modelling the historical UK wind regime

The characteristics of the UK wind regime, derived from an observation network, are described above for the period 1980-2005. In this section,

reanalysis data (ERA40) and dynamically downscaled reanalysis data (PRECIS-Re), for the period 1959-2001, are examined. This allows the assessment of the UK wind regime prior to the period of observation. This dataset is utilised to identify historic storms occurring as far back as 1959, with their impact, in terms of insured losses, calculated in Chapter 5.

The ERA40 and PRECIS-Re data are subsequently compared with the observational data to ensure their reliability. It is important to ascertain that PRECIS is capable of producing realistic windspeeds as it used to simulate the future UK wind regime in Chapter 6. The ERA40 and PRECIS-Re datasets are described in section 2.1.2. The comparison of gridded climate model data to station observations carries with it its own limitations discussed by Moberg and Jones (2004) and Osborn and Hulme (1997) amongst others. In order to directly compare gridded data with station observations, data are extracted from the grid box centres with the nearest coordinates to the observation station. If that grid box is over the model sea then the station is "moved" to the nearest land grid box (but one which was not more that two moves north-south or east-west). These datasets are presented and discussed in terms of stations (directly comparable to the observation stations), although clearly the values represent that of a whole grid-cell.

Section 3.2.1 analyses the ERA40 data, quantifying spatial and temporal variations in windspeed, while section 3.2.2 presents results from the PRECIS-Re experiment. The comparison between model data and observations for the period 1980-2001 is undertaken in section 3.3. By comparing the performance of PRECIS-Re and ERA40 data in replicating the 1980-2001 wind regime described the observations, an assessment of the added value of the PRECIS model is then made.

3.2.1 ECMWF Reanalysis data

The ERA40 reanalysis data used in this study are described in section 2.1.2. As previously stated, the ERA40 data contain no gust speed variable. To allow direct comparison with the observational dataset, the mean and maximum

value of the 6-hour values are found for each day and considered the daily mean windspeed and DMGS respectively. Descriptive statistics are presented for the period 1959-2001, including an analysis of trends for the period 1980-2001. This provides the basis for the comparison with observed data in section 3.3.

Daily Mean Windspeed

The characteristics of the daily mean windspeed data for the period 1959-2001 are shown in Figure 3.13. Daily mean windspeeds are highest at Lerwick (*23*) and Kirkwall (*21*), while the lowest mean values are seen at Leuchars (*24*), Bingley (*5*) and Shawbury (*35*).

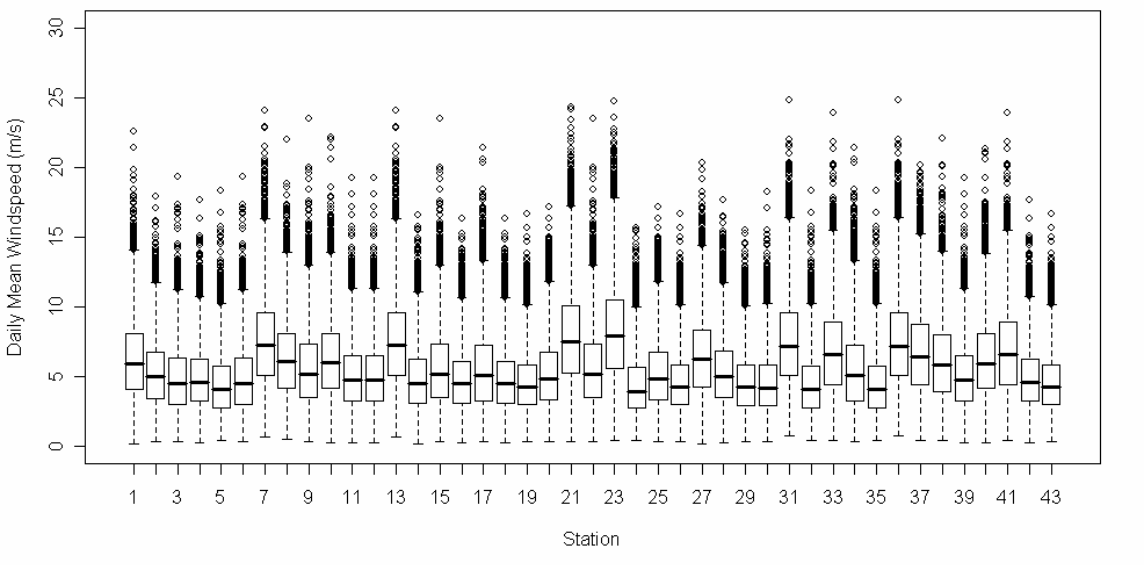

Figure 3.13 - Boxplot of ERA40 Daily Mean Windspeed at 43 stations across the UK for the period 1959-2001.

A slight upward trend in annual average daily mean windspeed for the period 1959-2001, is evident in Figure 3.14. The Network Average shows an increase of approximately 0.3 ms^{-1} during this period, with 34 stations showing increasing annual mean values, of which 8 are significant (two in Cornwall, two in northern England, two in southern Scotland and two in northern Scotland). No significant downward trends are seen at any station.

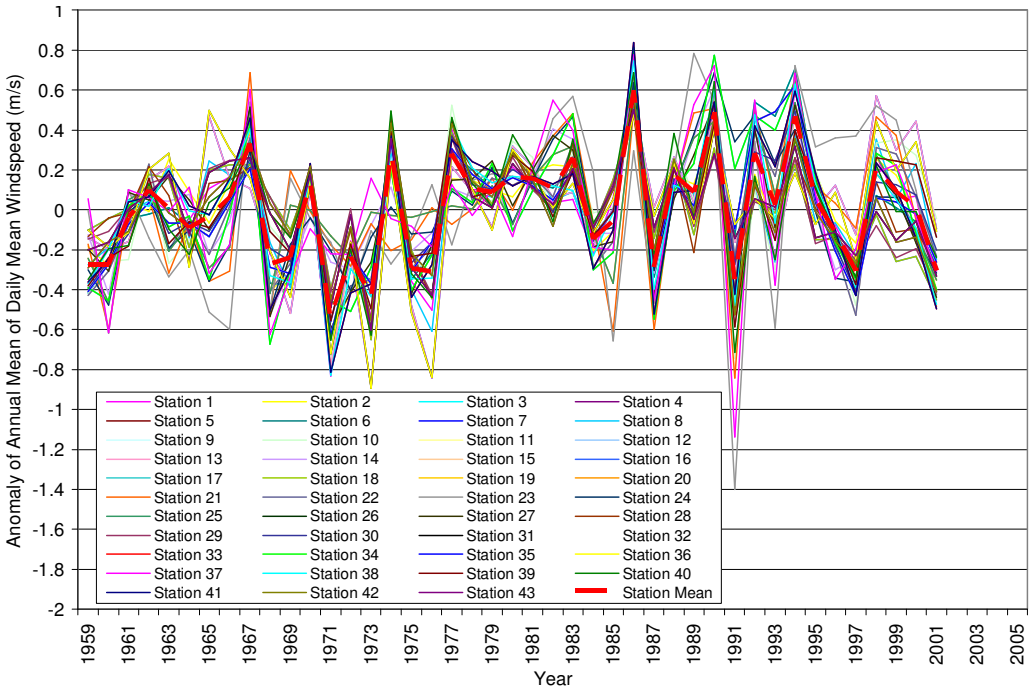

Figure 3.14 – Anomaly of the annual average of ERA40 daily mean windspeeds at 43 stations across the UK for the period 1959-2001. The Network Average is shown as a red dashed line.

The highest annual average daily mean windspeed values are in 1986 and 1990, while the lowest values are in 1971 and 1973.

A seasonal analysis reveals winter as the season with the highest daily mean windspeed values. Seasonal mean values are 2 ms^{-1} higher in winter than summer (the season with the lowest value). Spring values are marginally (0.4 ms^{-1}) lower than autumn, which, in turn, are 0.8 ms^{-1} lower than winter. During the period 1959-2001 an upward trend is seen in average winter and autumn daily mean windspeeds. Winter values increase (significantly) at all (24) stations with the Network Average indicating an increase of nearly 1 ms^{-1} over the study period. Stations displaying significant increases in this season are all located in central and northern England and in Scotland. The upward trend is less defined in autumn, with only 2 stations exhibiting significant upward trends. Summer values indicate a slight decrease (less than 0.2 ms^{-1}) with 36 (5) stations showing (significant) downward trends.

DMGS

A boxplot of the DMGS data from the ERA40 dataset for 1959-2001 is shown in Figure 3.15.

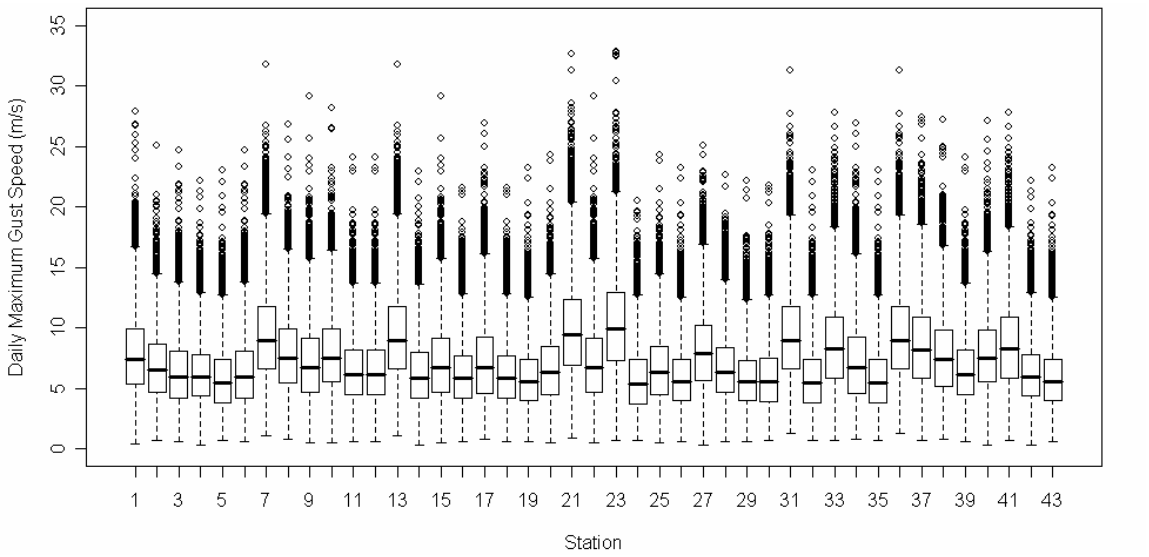

Figure 3.15 - Boxplot of ERA40 DMGS at 43 stations across the UK for the period 1959-2001.

The highest annual mean and 98th percentile values are seen at Lerwick (*23*) and Kirkwall (*21*). The lowest mean values are seen at Leuchars (*24*), Shawbury (*32*) and Bingley (*5*), while the lowest 98th percentile values are for Middle Wallop (*29*), Shawbury and Bingley.

Annual mean values of DMGS, shown in Figure 3.16, suggest an upward trend during the period 1959-2001. The Network Average shows a significant upward trend of 0.4 ms^{-1}. Forty stations display increasing annual mean values, with 23 showing significant increases. The majority of these stations are located in central and northern England and western Scotland.

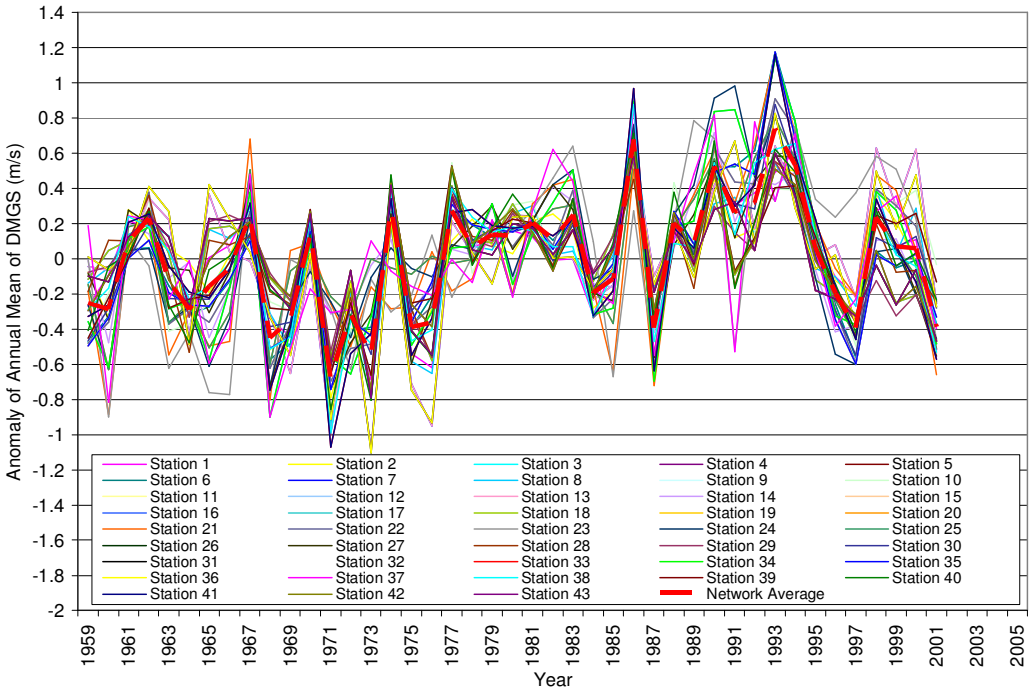

Figure 3.16 – Anomaly of the annual mean of ERA40 DMGS at 43 stations across the UK for the period 1959-2001. The Network Average is shown as a red dashed line.

Seasonal mean values of DMGS reveal a significant upward trend of the Network Average in winter of just over 1 ms^{-1}. All stations exhibit increasing values in this season, with the 24 showing significant increases, corresponding to those showing significant increases in the annual values. Autumn values also suggest an upward trend, with 37 stations showing increasing values, although only one is significant. Mean spring and summer values indicate no temporal trends.

The annual 98th percentile values plotted in Figure 3.17 exhibit two prominent peaks in 1991 and 1993, when the Network Average exceeds the long term value by over 4 ms^{-1} on both occasions. This feature is also seen in annual 98th percentile values for daily mean windspeed, with the peaks exceeding the long term value by over 2 ms^{-1}.

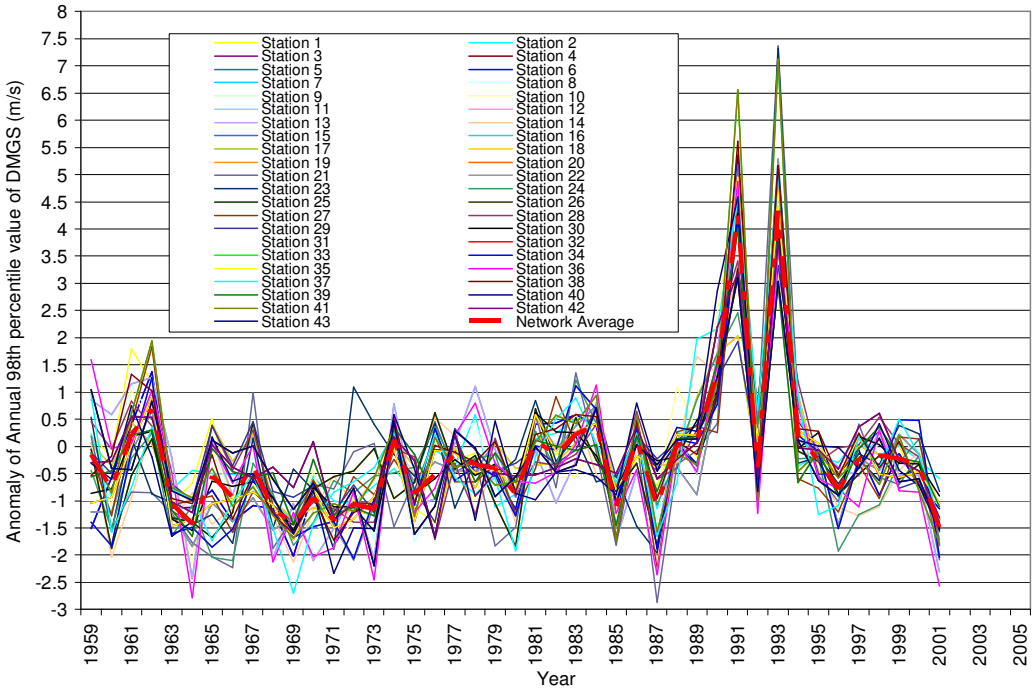

Figure 3.17 – Anomaly of the annual 98th percentile value of ERA40 DMGS at 43 stations across the UK for the period 1959-2001. The Network Average is shown as a red dashed line.

A rising trend in annual 98th percentile values is shown by all stations, with 17 exhibiting significant trends. These stations are similar to those exhibiting significant increases in mean DMGS values, located in central and northern England and mainland Scotland. The Network Average increases by 1.5 ms^{-1} from 1959 to 2001.

Seasonal values of the 98th percentile of DMGS are highest in winter and lowest in summer, with an average difference of just under 5 ms^{-1}. Autumn values are almost 2 ms^{-1} lower than those in winter, while spring values are just under 3 ms^{-1} lower than winter. Temporal analysis reveals an increase in the winter and spring 98th percentile values of 2 ms^{-1} and 1 ms^{-1} respectively. All stations show upward trends in both seasons, though only two are significant in spring, while 19 are in winter (largely corresponding to those stations showing an upward trend in annual values). Summer and autumn values suggest no significant changes at any station.

A closer analysis of DMGS data in 1991 and 1993 is undertaken to establish causes of the sharp peaks in the 98th percentile value identified in Figure 3.17. Winter values exceed the long term value by 4.5 ms^{-1} and 6.2 ms^{-1} in 1991

and 1993 respectively, and are the principal drivers producing the 1991 and 1993 peaks. The autumn value in 1991 exceeded the long term value by 3.5ms^{-1}, also contributing to the magnitude of the annual peak. Further discussion of these peaks occurs in section 3.3.3.

Trends in ERA40 data 1980-2001

In order that ERA40 data can be compared to observations in section 3.3, trends in the data for the period 1980-2001 are analysed here.

Daily Mean Windspeed

A downward trend between 1980 and 2001 is suggested in annual average daily mean windspeeds, with 40 stations showing a reduction in values in this period, including 8 displaying significant decreases. These stations are all located in the south and east regions of England. The Network Average indicates a decrease in annual mean values of 0.3 ms^{-1} during this period.

Seasonal averages of daily mean windspeed suggest downward trends in all seasons, with the greatest decrease of 0.5 ms^{-1} occurring in autumn. Seasonal mean values in autumn show a reduction at 39 stations (10 significant). These stations are located in southern England and central Scotland. Forty stations exhibit downward trends in summer values, though only 2 are significant. Spring (winter) values decrease in 31 (26) stations during the 1980-2001 period, though none are significant trends.

DMGS

Annual mean values of DMGS indicate a slight reduction (less than 0.2 ms^{-1}) between 1980 and 2001, with 34 stations showing decreasing values, including significant downward trends at 6 stations (all in the central part of southern England). Annual values of the 98th percentile of DMGS indicate a very slight decrease during the same period. Although 28 stations suggest a slight downward trend, none are significant. The period is yet again dominated by two peaks in 1991 and 1993 where annual values of the 98th percentile exceeded the long term values by almost 4 ms^{-1} on both occasions.

Seasonal mean and 98th percentile values of DMGS indicate a decrease in autumn values of just over 0.5 ms^{-1} over the period 1980-2001. Mean values at 39 (10) stations show (significant) decreases in that period, while 98th percentile values at 41 (1) stations showed (significant) decreases. The 10 stations exhibiting significant increases are located in southern England and all coastal stations in mainland Scotland. An upward trend (Network Average increases less than 0.2 ms^{-1}) in both winter mean and 98th percentile values is suggested by 28 and 34 stations respectively, though none are significant. Values of the 98th percentile of DMGS in spring (summer) at 33 (28) stations suggest downward trends, with 4 (0) showing significant trends.

3.2.2 PRECIS-Re

The UK wind regime modelled by ERA40 data has been analysed in section 3.2.1. This dataset was used as lateral boundary conditions in PRECIS to produce the PRECIS-Re dataset. This section describes the spatial and temporal variations shown by PRECIS-Re wind data, providing an assessment of the UK wind regime in the period preceding the observational dataset (back to 1959). An analysis of trends in 1980-2001 provides the basis for PRECIS-Re to be compared with observations in order to ascertain the reliability of the RCM data.

Output data from PRECIS utilised in this study include hourly mean 10-metre windspeeds and hourly maximum 10-metre windspeeds. These variables are the mean, and maximum 10-metre windspeeds, of the 24 2.5-minute timesteps in each model hour. For comparison to the observational data the daily mean is found, and daily maximum “gust” value is considered as the maximum 2.5-minute value recorded in that model day. Although 2.5 minutes is clearly much longer than the duration of a gust, as described in section 2.2.2, the maximum mean windspeed in each timestep may be considered a reasonably reliable proxy for gust speeds (Dorland *et al.*, 1999; Jungo *et al.*, 2002; Leckebusch *et al.*, 2006).

Daily Mean Windspeed

Descriptive statistics of the daily mean windspeeds extracted from the PRECIS-Re dataset are shown in Table 3.5 and Figure 3.18.

No.	max	mean	Std[1]	Percentile Values						
				5th	10th	25th	75th	90th	95th	98th
1	16.84	5.78	2.47	2.16	2.68	3.89	7.44	9.15	10.20	11.34
2	16.55	5.25	2.20	2.08	2.57	3.58	6.66	8.28	9.24	10.32
3	12.94	4.76	1.92	1.94	2.37	3.30	6.02	7.39	8.18	9.07
4	14.84	5.24	2.19	2.10	2.59	3.59	6.64	8.25	9.23	10.39
5	13.93	4.87	2.05	1.90	2.38	3.33	6.18	7.64	8.59	9.69
6	19.81	6.39	2.78	2.57	3.06	4.26	8.14	10.23	11.49	13.05
7	16.32	5.79	2.41	2.37	2.88	3.97	7.29	9.07	10.19	11.56
8	15.08	5.02	2.08	2.07	2.48	3.43	6.34	7.87	8.80	9.98
9	15.14	5.29	2.25	2.12	2.60	3.57	6.69	8.37	9.41	10.60
10	15.69	5.56	2.30	2.30	2.77	3.82	7.01	8.75	9.79	10.99
11	15.48	5.58	2.35	2.26	2.75	3.80	7.07	8.83	9.87	11.08
12	14.66	5.35	2.25	2.14	2.64	3.64	6.79	8.46	9.45	10.64
13	16.32	5.79	2.41	2.37	2.88	3.97	7.29	9.07	10.19	11.56
14	13.62	4.98	2.02	2.24	2.58	3.42	6.23	7.80	8.76	9.83
15	17.60	5.79	2.50	2.32	2.77	3.84	7.39	9.26	10.42	11.59
16	15.35	5.11	2.13	2.09	2.53	3.49	6.47	8.03	9.01	10.17
17	11.87	4.39	1.82	1.73	2.13	3.01	5.58	6.89	7.70	8.55
18	14.88	5.07	2.12	2.04	2.49	3.47	6.40	7.97	9.01	10.12
19	14.98	4.91	2.08	1.99	2.41	3.34	6.20	7.76	8.75	9.94
20	15.59	5.66	2.33	2.35	2.80	3.86	7.18	8.88	9.93	11.04
21	23.20	7.56	3.18	2.95	3.63	5.13	9.62	11.87	13.29	14.83
22	13.66	4.97	2.09	1.99	2.43	3.39	6.29	7.84	8.79	9.87
23	23.15	7.87	3.24	3.14	3.87	5.41	9.96	12.32	13.67	15.27
24	17.88	6.18	2.82	2.44	2.89	3.93	8.01	10.17	11.47	12.74
25	16.30	5.67	2.39	2.30	2.78	3.84	7.19	8.94	10.01	11.26
26	14.59	4.93	2.05	2.00	2.42	3.38	6.24	7.73	8.67	9.73
27	14.59	4.94	2.13	1.84	2.30	3.34	6.32	7.80	8.78	9.84
28	18.48	6.35	2.76	2.45	2.99	4.19	8.18	10.19	11.39	12.62
29	14.36	4.91	2.05	2.02	2.44	3.36	6.19	7.72	8.69	9.79
30	13.95	5.08	2.12	2.06	2.51	3.47	6.43	8.02	8.93	10.02
31	14.35	5.30	2.04	2.46	2.86	3.75	6.56	8.11	9.06	10.26
32	13.87	4.80	1.91	2.13	2.51	3.35	5.99	7.38	8.28	9.40
33	19.14	6.31	2.72	2.41	3.00	4.26	8.07	10.07	11.24	12.57
34	14.26	4.77	2.16	1.81	2.21	3.10	6.13	7.75	8.81	9.92
35	13.84	4.72	1.97	1.85	2.30	3.24	5.98	7.41	8.27	9.29
36	15.87	5.50	2.25	2.30	2.78	3.80	6.91	8.56	9.61	10.87
37	17.64	6.53	2.82	2.37	3.02	4.42	8.34	10.43	11.71	12.96
38	15.99	5.27	2.25	2.18	2.60	3.54	6.68	8.41	9.44	10.62
39	15.14	5.39	2.27	2.17	2.66	3.67	6.83	8.53	9.52	10.72
40	15.58	5.37	2.23	2.24	2.69	3.69	6.78	8.43	9.52	10.68
41	19.93	7.07	3.01	2.74	3.37	4.79	9.07	11.17	12.50	14.04
42	14.76	5.27	2.20	2.11	2.60	3.61	6.68	8.31	9.28	10.44
43	14.03	4.83	1.96	2.04	2.46	3.35	6.06	7.50	8.44	9.48

Table 3.5 - General statistics of all daily mean windspeeds from PRECIS-Re at 43 stations across the UK for the period 1959-2001. All figures are in ms^{-1}. ([1]standard deviation is abbreviated).

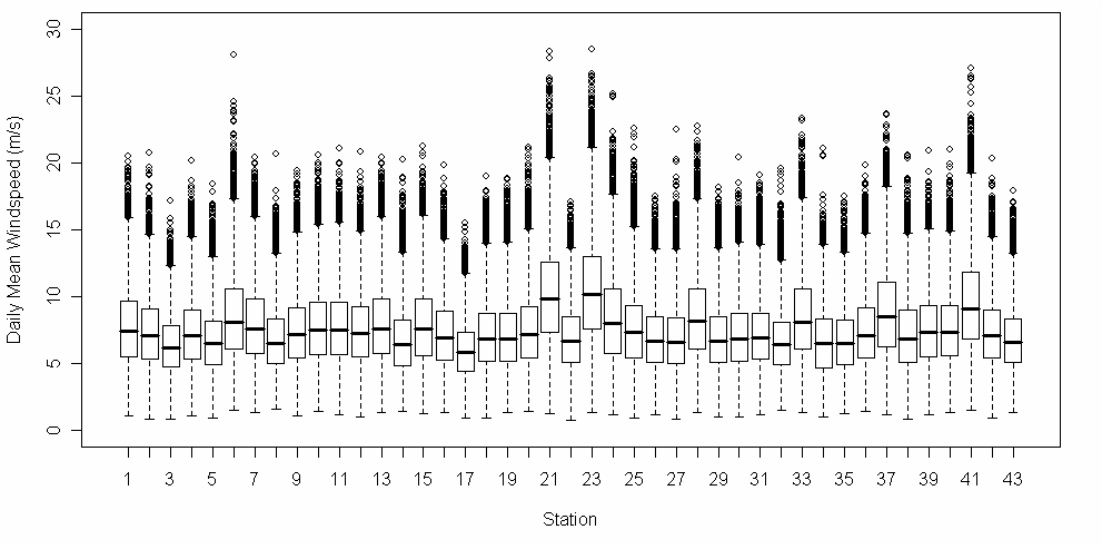

Figure 3.18 - Boxplot of PRECIS-Re Daily Mean Windspeed at 43 stations across the UK for the period 1959-2001.

Average daily mean windspeeds are highest at Lerwick (*23*), Kirkwall (*21*) and West Freugh (*41*), and lowest at Bala (*3*), Eskdalemuir (*17*) and Shawbury (*35*).

Over the period 1959-2001 a slight upward trend is evident in the data (Figure 3.19), with an approximate increase in the Network Average annual mean of $0.2ms^{-1}$. All stations show an upward trend, with 13 exhibiting significant increases between 1959 and 2001. These stations are all located in Scotland except for Durham (*15*), Camborne (*7*) and Coltishall (*10*), illustrating that the significant increases are largely confined to northern parts of the UK.

Annual average daily mean windspeed values (shown in Figure 3.19) are at a maximum in 1990, with a secondary peak in 1986, the same years as ERA40 data. Minimum values of annual average of daily mean windspeed are shown in 1971 and 1977. Although ERA40 daily mean windspeeds are at their lowest in 1971, similar to those in PRECIS-Re, 1977 actually exhibits above average values in PRECIS-Re but below average in ERA40.

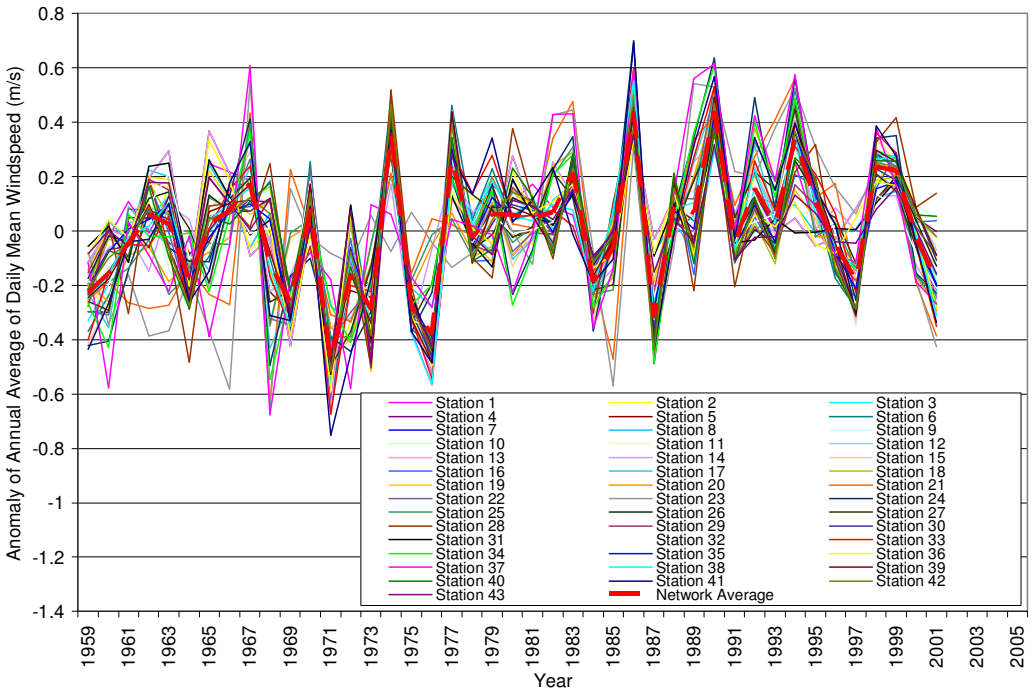

Figure 3.19 – Anomaly of the annual average of PRECIS-Re daily mean windspeeds at 43 stations across the UK for the period 1959-2001. The Network Average is shown as a red dashed line.

A seasonal analysis reveals that winter is again the season with the highest average daily mean windspeeds, and summer the lowest. Autumn mean values of daily mean windspeed are slightly lower than those of spring (22 stations have a higher seasonal mean in autumn than spring). For the period 1959-2001, the data suggest increasing daily mean windspeeds in all seasons except summer, with winter showing the greatest increase (just under 0.5 ms^{-1}), followed by autumn. All stations in winter and autumn show an upward trend in seasonal means with 16 and 2 stations showing significant increases, respectively. These stations are located in Scotland and northern England. Summer mean values show a decreasing trend (0.2 ms^{-1} overall) at 31 stations, none of which are significant.

DMGS

Descriptive statistics of the DMGS extracted from the PRECIS-Re dataset are shown in Table 3.6 and Figure 3.20.

No.	max	mean	Std[1]	Percentile Values						
				5th	10th	25th	75th	90th	95th	98th
1	20.51	7.74	2.96	3.44	4.07	5.50	9.66	11.77	13.11	14.60
2	20.73	7.37	2.71	3.30	4.02	5.39	9.11	11.05	12.21	13.49
3	17.20	6.37	2.19	3.08	3.65	4.77	7.81	9.30	10.22	11.25
4	20.20	7.32	2.69	3.33	4.02	5.34	9.00	10.96	12.16	13.60
5	18.43	6.70	2.40	3.09	3.76	4.96	8.20	9.90	11.00	12.17
6	28.07	8.61	3.22	4.32	4.94	6.12	10.60	13.07	14.51	16.33
7	20.38	7.97	3.00	3.65	4.32	5.75	9.84	12.05	13.52	15.09
8	20.69	6.83	2.48	3.39	3.86	4.99	8.31	10.23	11.50	12.84
9	19.37	7.46	2.77	3.33	4.05	5.41	9.20	11.18	12.42	13.83
10	20.59	7.80	2.83	3.63	4.33	5.71	9.61	11.65	12.87	14.41
11	21.08	7.79	2.86	3.54	4.29	5.67	9.62	11.63	12.99	14.42
12	20.81	7.50	2.75	3.41	4.12	5.48	9.25	11.20	12.46	13.85
13	20.38	7.97	3.00	3.65	4.32	5.75	9.84	12.05	13.52	15.09
14	20.24	6.77	2.43	3.52	3.95	4.89	8.27	10.16	11.30	12.67
15	21.27	7.89	2.95	3.66	4.29	5.62	9.83	11.94	13.27	14.71
16	19.79	7.22	2.64	3.30	3.98	5.30	8.90	10.78	12.01	13.37
17	15.49	5.98	2.12	2.79	3.36	4.40	7.35	8.83	9.75	10.75
18	18.98	7.10	2.64	3.21	3.88	5.20	8.72	10.64	11.94	13.30
19	18.80	7.12	2.65	3.27	3.92	5.19	8.75	10.63	12.01	13.51
20	21.13	7.54	2.75	3.73	4.27	5.42	9.28	11.28	12.52	13.93
21	28.35	10.14	3.79	4.51	5.47	7.35	12.58	15.24	16.83	18.76
22	17.07	6.91	2.49	3.16	3.83	5.08	8.52	10.27	11.38	12.56
23	28.52	10.47	3.86	4.74	5.67	7.58	13.01	15.63	17.31	19.24
24	25.19	8.41	3.32	3.86	4.43	5.79	10.56	13.07	14.45	16.08
25	22.55	7.61	2.84	3.62	4.19	5.45	9.37	11.46	12.69	14.27
26	17.50	6.91	2.54	3.15	3.80	5.08	8.49	10.32	11.58	12.90
27	22.50	6.86	2.57	3.04	3.70	5.00	8.45	10.26	11.48	12.78
28	22.71	8.56	3.26	3.86	4.52	6.13	10.61	13.04	14.49	16.19
29	18.19	6.94	2.56	3.23	3.85	5.09	8.51	10.34	11.67	13.07
30	20.44	7.12	2.60	3.27	3.92	5.21	8.77	10.59	11.83	13.15
31	19.09	7.25	2.57	3.77	4.24	5.34	8.76	10.72	12.17	13.71
32	19.54	6.67	2.30	3.48	3.91	4.94	8.08	9.73	10.85	12.13
33	23.31	8.51	3.29	3.74	4.42	6.08	10.61	13.00	14.51	16.09
34	21.10	6.71	2.63	2.85	3.46	4.71	8.39	10.28	11.40	12.72
35	17.50	6.70	2.44	3.03	3.70	4.92	8.27	9.97	11.06	12.30
36	19.83	7.46	2.75	3.57	4.15	5.41	9.14	11.22	12.61	14.08
37	23.61	8.85	3.47	3.83	4.56	6.27	11.08	13.67	15.07	16.83
38	20.60	7.24	2.78	3.44	3.89	5.10	8.97	11.02	12.31	13.82
39	20.95	7.57	2.78	3.42	4.17	5.53	9.34	11.30	12.58	13.99
40	20.96	7.58	2.75	3.49	4.21	5.57	9.31	11.30	12.52	14.08
41	27.08	9.50	3.58	4.38	5.17	6.81	11.81	14.40	16.04	17.82
42	20.35	7.36	2.69	3.34	4.05	5.40	9.05	10.99	12.21	13.62
43	17.89	6.86	2.48	3.23	3.84	5.09	8.37	10.17	11.40	12.87

Table 3.6 - General statistics of all DMGS from PRECIS-Re at 43 stations across the UK for the period 1959-2005. All figures are in ms^{-1}. ([1]standard deviation is abbreviated).

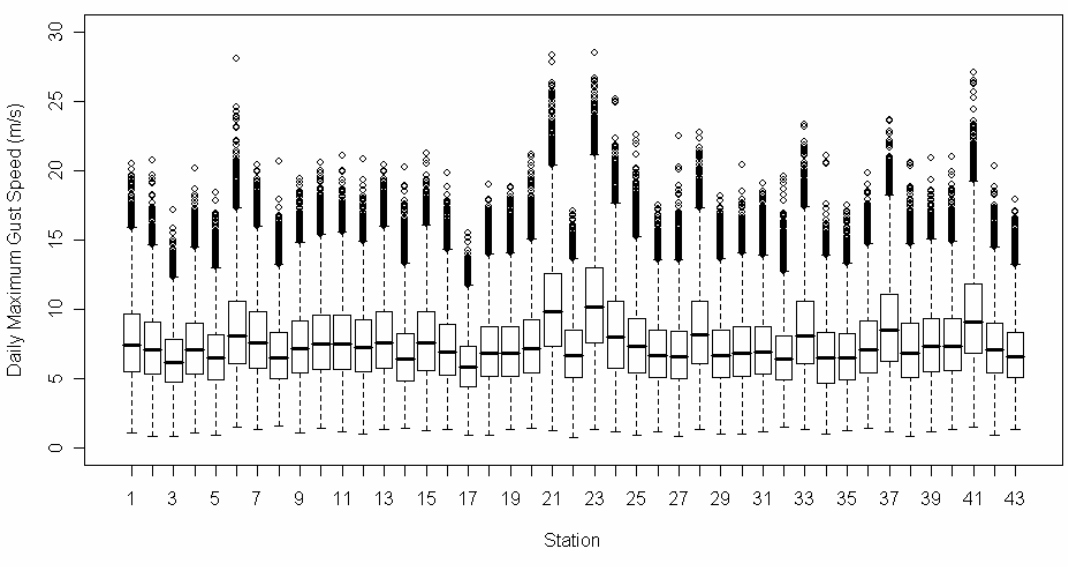

Figure 3.20 - Boxplot of PRECIS-Re DMGS at 43 stations across the UK for the period 1959-2001.

The highest mean and 98th percentile values of DMGS are seen at the same stations which saw high daily mean windspeed values, namely Lerwick (*23*), Kirkwall (*21*) and West Freugh (*41*). Stations showing the lowest values of mean and 98th percentile of DMGS are Bala (*3*), Eskdalemuir (*17*) and Ringway (*32*).

Figure 3.21 suggests an rising trend in the annual mean of DMGS between 1959 and 2001, with the Network Average exhibiting a significant increase of 0.4 ms^{-1}. An upward trend is also seen in the annual 98th percentile value of DMGS, with the Network Average increasing by 0.75ms^{-1}. All stations show an upward trend in the annual mean and 98th percentile values of DMGS. The 15 stations exhibiting significant increases in annual values are the same as those showing significant increases in annual average daily mean windspeeds, with the exception of Culdrose (*7*). Of the 9 stations exhibiting significant increases in the 98th percentile value of DMGS, 6 are located in Scotland, with Ronaldsway (*2*), Valley (*38*) and Manston (*28*) the remaining three.

Annual means of DMGS are at a maximum in 1986 and 1990 and at a minimum in 1971 and 1987, while annual 98th percentile values are highest in 1990 and lowest in 1971.

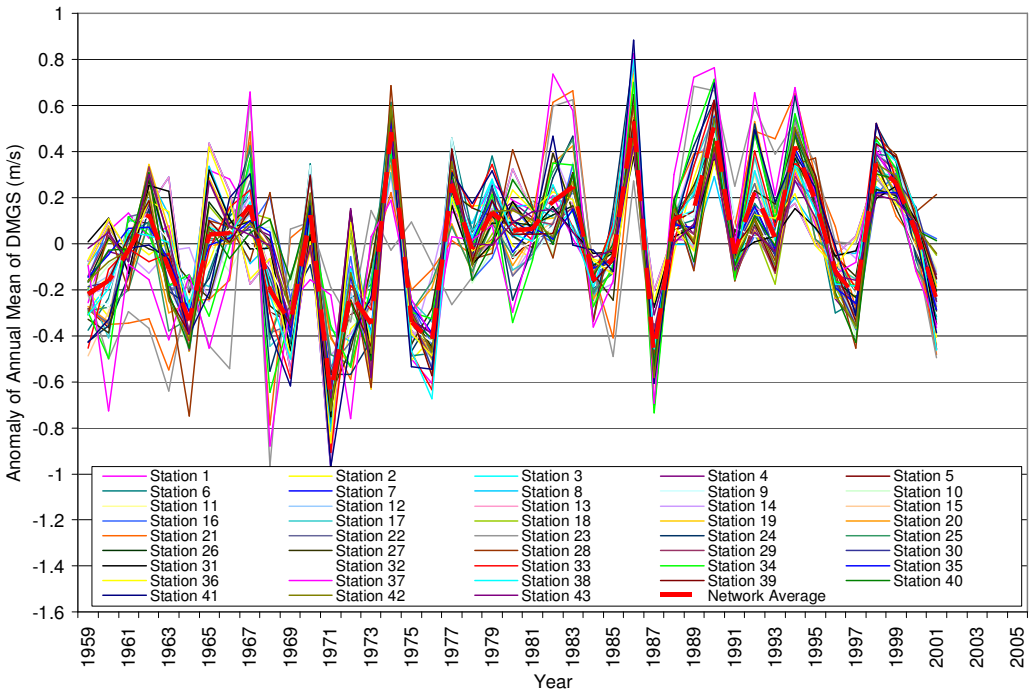

Figure 3.21 – Anomaly of the annual mean of PRECIS-Re DMGS at 43 stations across the UK for the period 1959-2001. The Network Average is shown as a red dashed line.

Seasonal mean and 98th percentile values of DMGS are highest in winter and lowest in summer. Mean seasonal values are higher in autumn than spring at 24 stations, the majority of which are coastal. Seasonal values of 98th percentile of DMGS are higher in autumn than spring at 42 stations, with Kirkwall (*21*) the only exception.

Temporal trends in seasonal means suggest increasing winter, autumn and spring mean values over the period 1959-2001, with the greatest increase in winter (Network Average increases by 1 ms^{-1}). All stations show an upward trend in winter and autumn mean values of DMGS, while 35 stations show an upward trend in spring, and 25 stations show a downward trend in summer. However, with the exception of 12 stations (all in northern England and Scotland) in winter, none of these trends are significant. The reduction in summer values is less than 0.2 ms^{-1}. In terms of the seasonal 98th percentile values of DMGS, all stations exhibit increases in winter and spring, with significant upward trends at 7 stations (again in northern England and Scotland) and 1 station, respectively. The Network Average shows an increase of 1 ms^{-1} in winter and just over 0.5 ms^{-1} in spring. Autumn and summer values of 98th percentile exhibit a downward trend in 41 stations, with

one station and 4 stations showing significant decreases, respectively. Reductions of just under 0.5 ms^{-1} are seen in the Network Average for these seasons from 1959 to 2001.

The inter-annual trends in PRECIS-Re DMGS are now compared to the NAO variation, with December-March values shown in a similar fashion to Figure 3.9.

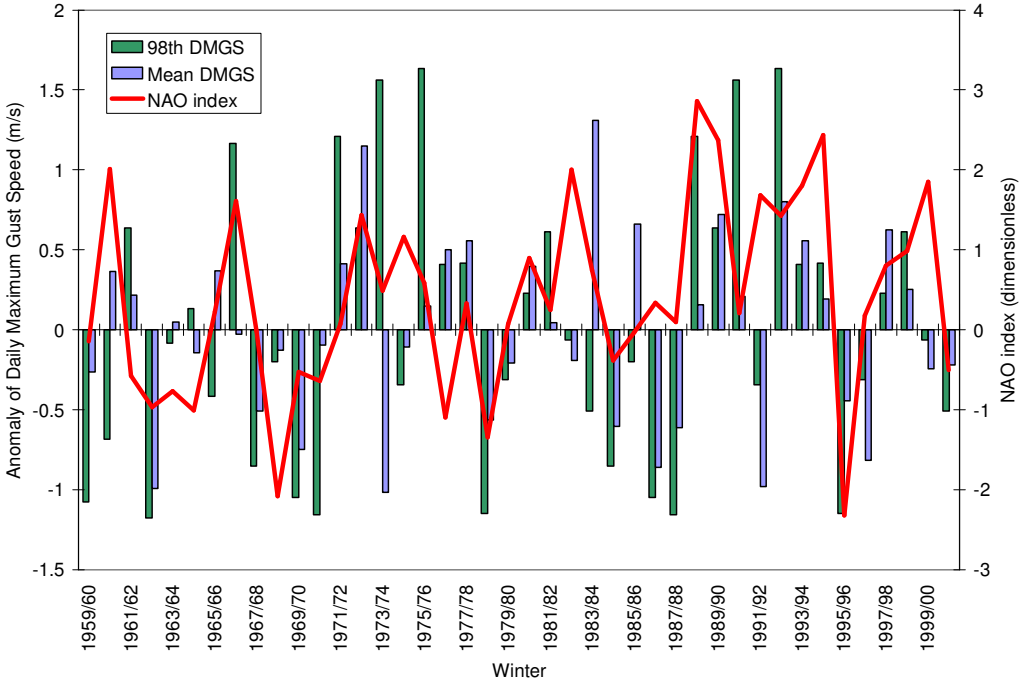

Figure 3.22 – December-March anomalies of mean (blue bars) and 98th percentile (green bars) values of DMGS, and NAO index (red line).

Figure 3.22 again demonstrates that a more positive December-March NAO index corresponds to more positive DMGS anomalies. The upward trend in the NAO index between the late 1960s and early 1990s is likely driving the slight overall (1959-2001) trend in daily mean windspeed and DMGSs described in the this section. In addition to the NAO index, previous work by Alexandersson *et al.* (2000) and Matulla *et al.* (2007) suggest an increase in geostrophic windspeeds from the early 1960s to mid 1990s. Utilising a pressure triangles method (calculating geostrophic windspeeds form surface pressure measurements) both studies found increases in the standardised 95th and 99th percentiles of geostrophic windspeed over northwest Europe.

Trends in PRECIS-Re data 1980-2001

In order that comparisons between observations and model data can be made in section 3.3, variations in the model data are examined for the period for which observations are available (i.e. 1980-2001).

Daily Mean Windspeed

Annual average daily mean windspeeds show a slight upward trend at 18 stations, and a slight downward trend at 25 stations, during the period 1980-2001 in the PRECIS-Re data. An overall decrease of less than 0.1 ms^{-1} is suggested by the Network Average, although none of the stations exhibit significant trends.

Seasonal averages of daily mean windspeed suggest a decreasing trend over the period 1980-2001, in summer and autumn, with the greatest reduction in autumn (Network Average decreases by 0.5 ms^{-1}). Autumn (summer) mean values show downward trends at 42 (41) stations, of which 3 (0) show significant downward trends. Upward trends, of lesser magnitude, are shown by 42 (33) stations in winter (spring), though none are significant.

DMGS

Overall, slight downward trends are suggested in the annual mean values of PRECIS-Re DMGS, with 30 stations showing downward trends, though none are significant over the period 1980-2001. The Network Average decreases less than 0.1ms^{-1} in this period. A slight increase in annual 98th percentile values is suggested with 21 stations showing an increase, and 22 a decrease, though again, none are significant. Again, the overall increase in this period is negligible (Network Average increases less than 0.1ms^{-1}).

Seasonal mean values of DMGS follow similar temporal patterns to those of daily mean windspeeds, with a downward trend exhibited in summer and autumn. The Network Average exhibits the greatest decrease in autumn (0.5 ms^{-1}). All stations show a downward trend in autumn, with 5 (all in northern Scotland) displaying significant downward trends, while 42 stations show a downward trend in summer values, but none are significant. Spring and winter show upward trends at 29 and 43 stations respectively, though none are

significant. The Network Average increases by 0.5 ms^{-1} in winter, although no stations exhibit significant trends. Seasonal 98th percentile values in summer and autumn show (significant) downward trends in 39 (2) and 41 (4) stations respectively. Network Average decreases of 0.5 ms^{-1} and 0.75 ms^{-1} are evident in summer and autumn values respectively. A slight (less than 0.1 ms^{-1}) downward trend is also suggested by the spring values, with 24 (3) stations showing a (significant) decrease. Meanwhile, an upward trend (Network Average increases 0.5 ms^{-1}) is seen in winter 98th percentile values, with every station exhibiting an upward trend, although none are significant.

3.3 Comparison of modelled data to observations

The aim of this section is to compare the observation dataset with reanalysis data (ERA40) and reanalysis driven RCM data (PRECIS-Re) described in sections 3.2.1 and 3.2.2 respectively. The reliability of model data over the period 1980-2001 provides an estimate of the confidence in the model data preceding the observations (1959-1979). In addition, it is important to establish confidence in the ability of PRECIS to accurately simulate windspeed, as future simulations are used in Chapter 6 to investigate the impact of the future UK wind regime on insured losses. Section 3.3.1 compares PRECIS-Re windspeed data to the observations, while section 3.3.2 considers the ERA40 data. This concludes with an assessment of the added value provided by PRECIS when considering reanalysis data in section 3.3.3.

3.3.1 PRECIS-Re

Daily mean windspeeds and DMGSs from the observation dataset and PRECIS-Re dataset for the period 1980-2001 are compared. The degree to which model data capture the variability in the observed data (i.e. correlation) is assessed using R^2 values. The R^2 values for DMGS are plotted in Figure 3.23. The highest value (0.74) is seen at Aberporth (*1*), while the lowest (0.45) is seen at Valley (*38*). No immediate spatial trend is evident for the whole of

the UK, however low values tend to be seen along the east coast of northern England and mainland Scotland. Also, values in East Anglia and the south east of England tend to be lower than those in western regions of the UK. A similar plot for R^2 values for daily mean windspeeds (not shown), produces a similar spatial pattern, though values tend to be slightly (5-10%) higher.

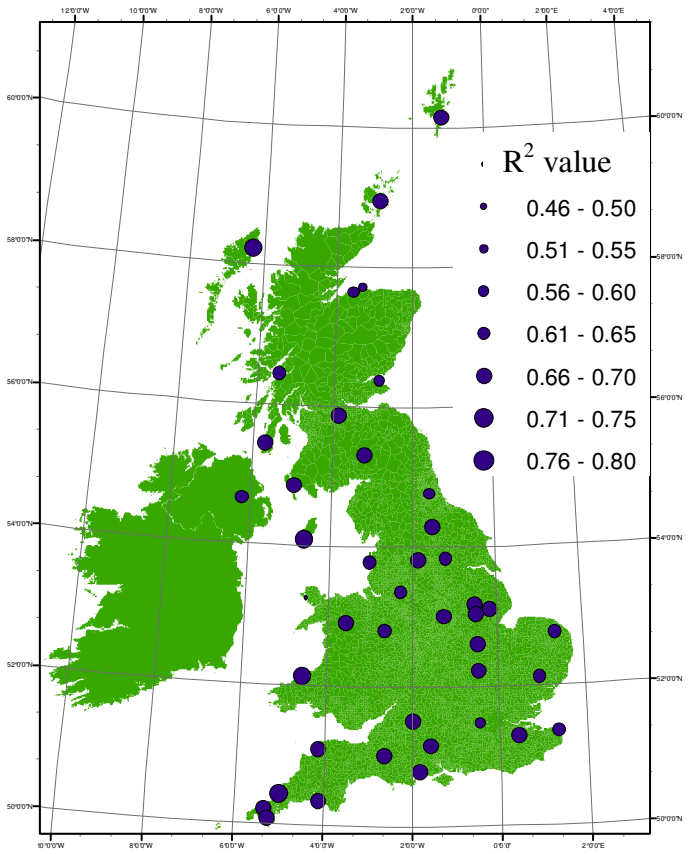

Figure 3.23 - R^2 values indicating the strength of the correlation between PRECIS-Re DMGS data and observations. Values calculated from all days in the period 1980-2001.

The reliability of PRECIS-Re data to capture variability at the monthly level is shown in Figure 3.24, indicating the slightly higher values of R^2 measured when daily mean windspeeds are considered, compared to DMGS. Seasonal values of R^2 are 40% and 30% higher in winter than in summer for DMGS and mean daily windspeeds respectively. The ability of PRECIS-Re to simulate DMGSs accurately in winter is especially important given this project is focussed on high impact windstorms, which predominantly occur in winter.

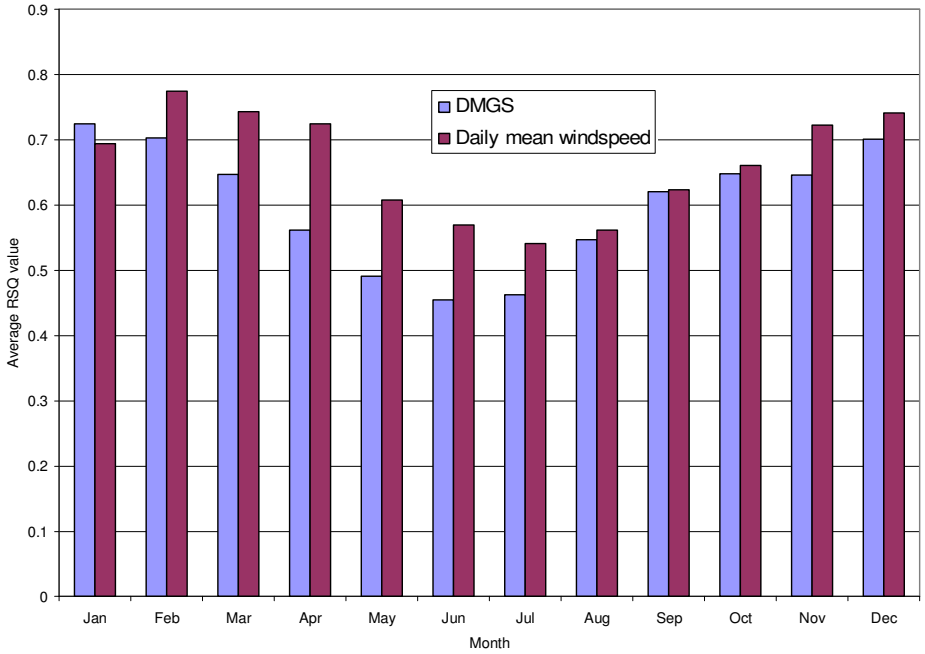

Figure 3.24 - R^2 values indicating the intra-annual variation in strength of the correlation between PRECIS-Re DMGS (blue) and daily mean windspeed (purple) data and observations. Values are the mean of all station R^2 values, which are calculated from all days in the period 1980-2001.

Since this project is concerned with damaging windspeeds the PRECIS-Re DMGSs exceeding the observed 98th percentile value are compared with observations at each station. The strength of this correlation is illustrated by R^2 values plotted in Figure 3.25. Values of R^2 are noticeably lower than those above. These low values are partially a result of the limited number of DMGSs considered (the top 2% of cases is equivalent to approximately 161 days in 22 years). Results from a seasonal and monthly analysis are not meaningful due to the uneven distribution of DMGSs exceeding the 98th percentile value throughout the year.

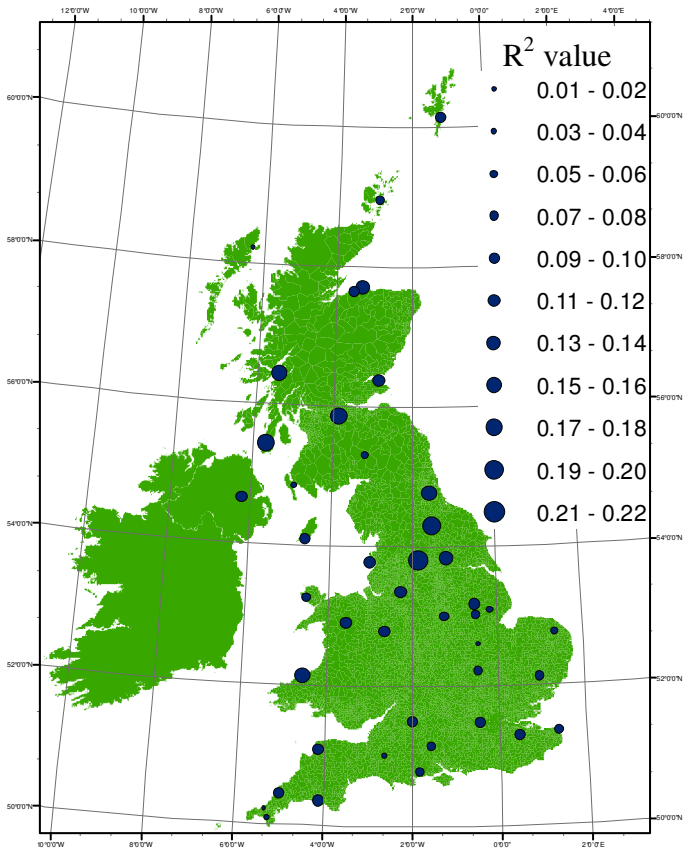

Figure 3.25 - R^2 values indicating the strength of the correlation between the top 2% of PRECIS-Re DMGS data and observations. Values calculated from days on which the PRECIS-Re DMGS exceeds the 98th percentile, in the period 1980-2001.

While the R^2 values provide information on the variability captured by model data, it is also important to consider absolute values. An analysis of the absolute errors between model and observed windspeeds is presented in section 3.3.3.

3.3.2 ERA40

The DMGS data from ERA40 for the period 1980-2001 are correlated against observations at each station, and the R^2 values for the period displayed in Figure 3.26. The spatial variation is similar to that exhibited by the PRECIS-Re data in Figure 3.23. Values for daily mean windspeeds are not shown, but again display a similar pattern to the PRECIS-Re data. In both cases, however, R^2 values are slightly lower.

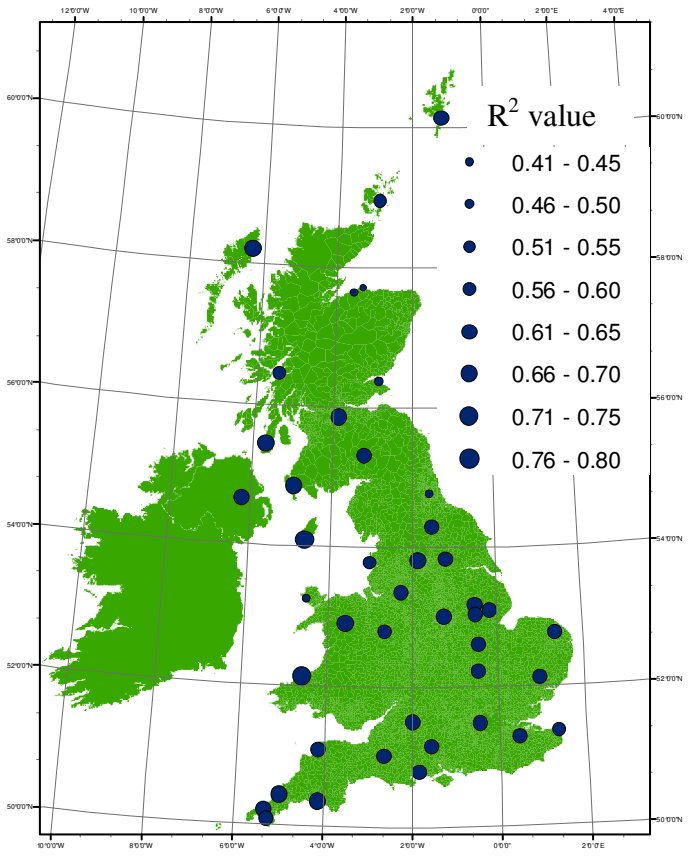

Figure 3.26 – R^2 values indicating the strength of the correlation between ERA40 DMGS data and observations. Values calculated from all days in the period 1980-2001.

Values of R^2 are typically 0.05 lower than those achieved with PRECIS-Re data for both DMGS and daily mean windspeed. Monthly values of R^2 for daily mean windspeeds are greater in every month than DMGS values. The highest values of R^2 are achieved in winter, with a seasonal R^2 value of just under 0.7 for both DMGS and daily mean windspeeds, with the lowest in summer (just under 0.5).

The top 2% of DMGSs, when correlated with observations, result in slightly lower R^2 values than those found for PRECIS-Re, typically by 25%, and exhibit a similar spatial pattern to that shown in Figure 3.26. Absolute errors between ERA40 data and observations are explored in section 3.3.3. A further comparison between the performance of PRECIS-Re and ERA40 in replicating observed windspeeds is described in the next section.

3.3.3 PRECIS Added Value

The ability of ERA40 and PRECIS-Re datasets to reliably simulate mean daily windspeeds and DMGS recorded in the observed dataset is discussed above. Given that PRECIS-Re is driven by ERA40 data, there is no surprise that the spatial variations of R^2 values are similar for both the model datasets. This section quantifies the added value of using dynamically downscaled reanalysis data (i.e. PRECIS-Re), over coarser resolution reanalysis data (ERA40).

As stated in section 3.3.2 a stronger correlation (higher R^2 value) is found between PRECIS-Re DMGS and observations, compared to ERA40 and observations, at 38 stations (shown in blue in Figure 3.27). The reverse occurs at the remaining 5 stations (shown in red).

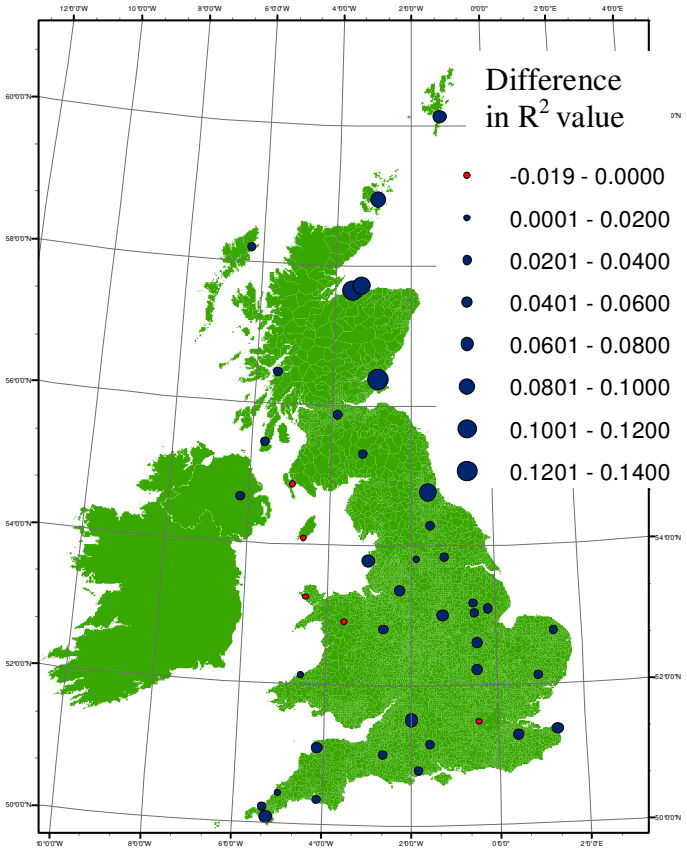

Figure 3.27 - Difference in R^2 values between PRECIS-Re data and observations, and ERA40 data and observations for DMGS data (ie. Figure 3.23 minus Figure 3.26). Blue dots indicate stations where PRECIS-Re outperforms ERA40, while red dots indicate the reverse.

Figure 3.27 suggests that ERA40 data outperform PRECIS-Re in grid cells on the south west coast of Scotland, Isle of Man and northern regions of Wales. There appears to be no clear spatial pattern of locations exhibiting a stronger correlation between PRECIS-Re and observations, although there is a tendency for the variability exhibited by west coast stations in Scotland to be captured more accurately. Mean daily windspeed data from ERA40 and PRECIS-Re compared to observations exhibit a similar pattern, although only 3 stations (Camborne (*7*), St Mawgan (*36*) and Valley (*38*)) produce higher R^2 values with ERA40 data than PRECIS-Re.

The ability of model data to accurately simulate damaging windspeeds (i.e. the upper 2% of DMGS) is difficult to assess given the limited record length. The annual mean deviation of all stations from the local long term 98th percentile value is shown in Figure 3.28.

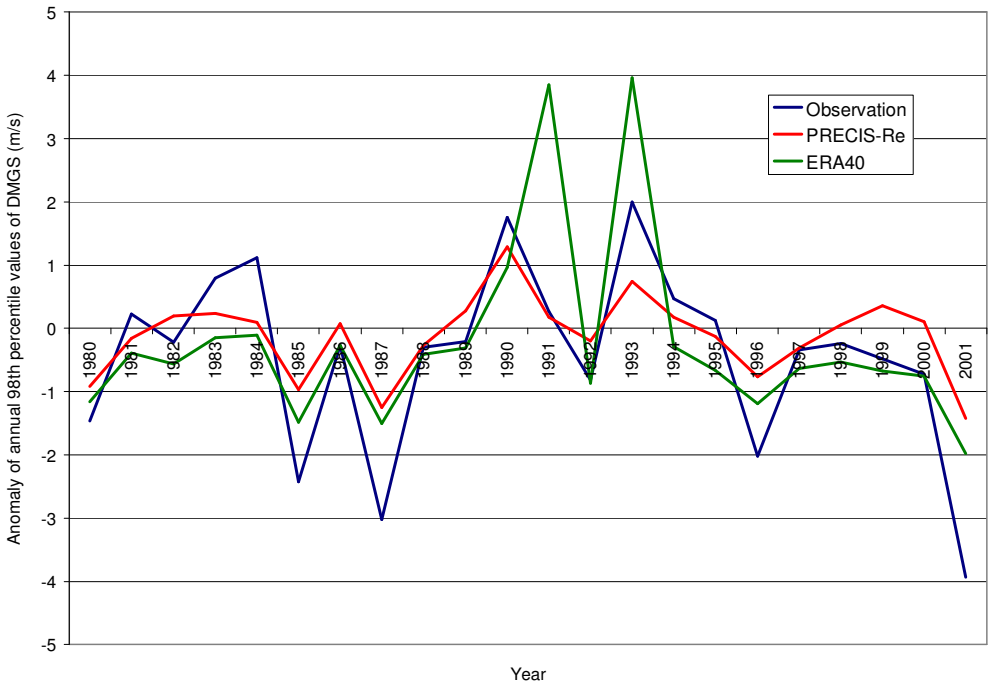

Figure 3.28 – Anomaly of the annual 98th percentile values of DMGS at 43 stations across the UK, for observation (blue), PRECIS-Re (red) and ERA40 (green) data.

The variation shown by the observations in Figure 3.28 is not fully captured by the model data. PRECIS-Re data tend to show less variation than ERA40, and overall shows a closer correlation to observation data. ERA40 data are dominated by two above normal peaks in 1991 and 1993. Although peaks are

seen in the observation data in these years, the 1991 peak is markedly lower than in the reanalysis data. In fact, observation data show a comparable peak to 1993 in 1990, which is captured by PRECIS-Re. While the annual 98th percentile values of ERA40 DMGS produce a significant peak in 1991, the mean values and annual daily mean windspeeds, while slightly above average, are not as prominent. Closer inspection of the 1991 ERA40 DMGS data reveal no obvious erroneous values, while no documentation of such a peak could be found in the literature (eg. Uppala *et al.*, 2005). The fact that the PRECIS-Re data generally follow the fluctuations in the ERA40 data, except in 1991, suggests there may be a discrepancy between the data utilised to produce the ERA40 dataset here, and the reanalysis data used as lateral boundary conditions in PRECIS-Re in that year.

There is a tendency for ERA40 to perform more accurately in years where the 98th percentile values are below the long term average. When only these years are considered, R^2 values for ERA40 data increases by an average of 0.04 at each station, and drops by a similar amount for PRECIS-Re data. However, the reverse is true for above average years. The focus of this project on windstorm damage, means that it is more important to accurately capture the variability of high damaging windspeeds (i.e. above average years) than low damaging windspeeds.

Although a number of stations exhibit relatively high R^2 values when model data are compared with observations, it is important to have an appreciation of how accurately absolute windspeeds are simulated. The Network Average annual mean and 98th percentile values of daily mean windspeed and DMGS are plotted in Figure 3.29. Mean daily windspeeds produced by ERA40 and PRECIS-Re tend to be slightly higher than those observed, while DMGS are substantially lower than those observed.

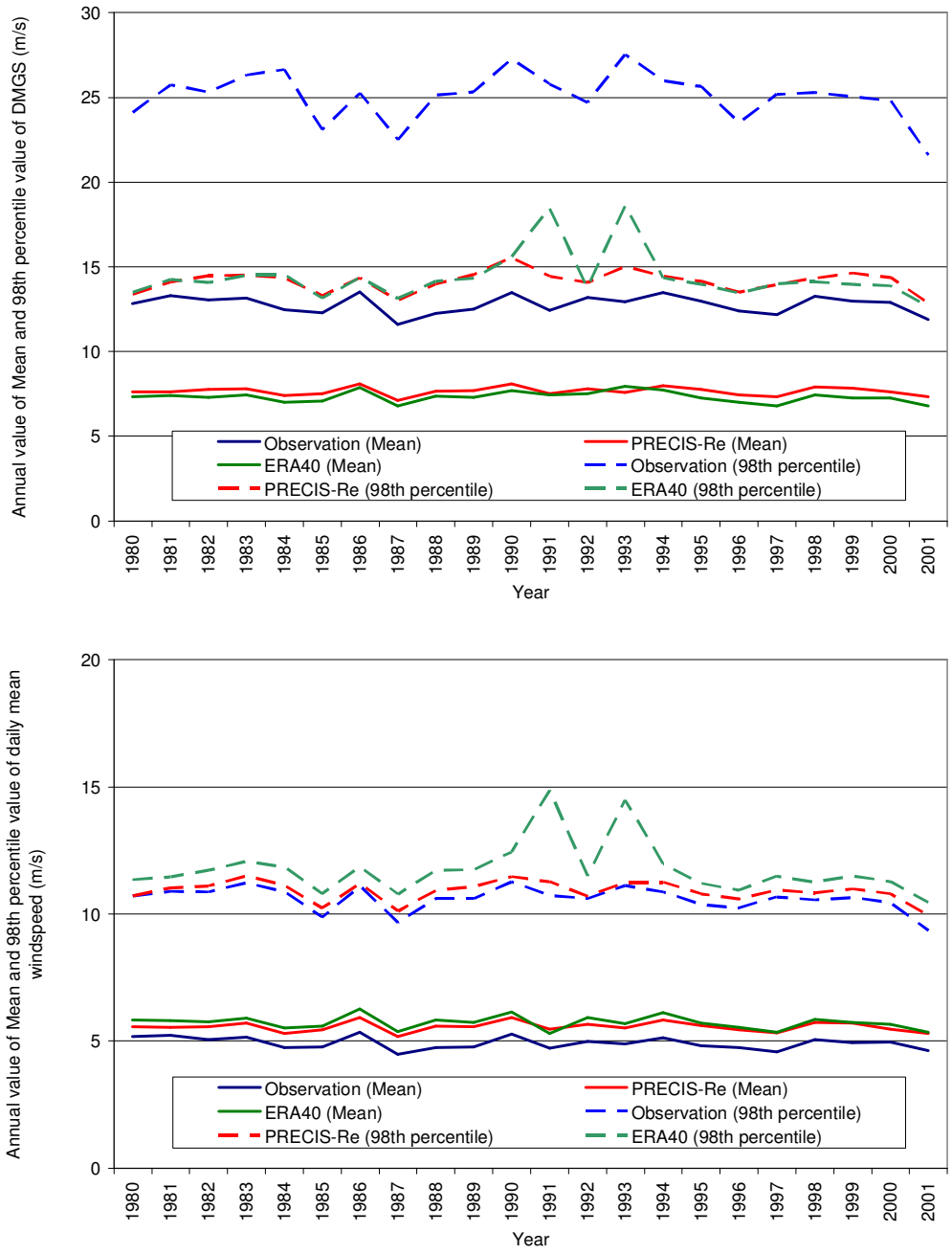

Figure 3.29 - Mean value of annual mean (solid) and 98th percentile value (dashed) of DMGS (above) and daily mean windspeed (below) at 43 stations across the UK.

Absolute errors between PRECIS-Re and observations are smaller than between ERA40 and observations for both daily mean windspeed and DMGS. A greater difference between PRECIS-Re and ERA40 values is seen in the DMGSs, compared to daily mean windspeeds, and in particular in the 98th percentile value of DMGS (dashed lines in bottom plot of Figure 3.29). This is likely partly a manifestation of the temporal resolution of the model data, described in section 2.1.2. ERA40 windspeeds are 10-minute values, every 6 hours, while the PRECIS-Re data are continuous 2.5-minute values.

Therefore, ERA40 will likely not capture the highest DMGS as well at PRECIS-Re.

The two peaks in 1991 and 1993 in ERA40 windspeeds, originally identified in section 3.2.1, are not shown in the PRECIS-Re data or by observations. Although a slight peak is shown in the 98th percentile values of observed DMGS and daily mean windspeed, its magnitude is significantly lower than that suggested by ERA40 data. Other than these two years the temporal trends exhibited by model data closely follow those shown in observed data. The spatial variation of these absolute errors is now considered.

The ratio of PRECIS-Re daily mean windspeeds to observed values at each station for the period 1980-2001 ranges from 0.72 to 2.17, with an average of 1.13. This ratio confirms the results shown in the lower panel of Figure 3.29; the average daily mean windspeeds are overestimated by just over 10%. This ratio shows slight (5%) intra-annual variation, with the lowest value in spring (1.10) and highest in autumn (1.16). Inter-annual variations vary less than 10%. The ratio of ERA40 data to observed values shows a slightly narrower range between stations of 0.85 to 1.56, with an average of 1.16. Intra-annual variation is also less with spring values (1.10) the lowest and autumn (1.15) the highest.

Overall, the ratio of PRECIS-Re DMGS to observed data is 0.60, with individual station values varying from 0.46 to 0.75. These values confirm the pattern shown in the upper panel of Figure 3.29; mean DMGS values are underestimated by approximately 40%. At each station this value does not vary annually to a large degree (not more than 10%). Intra-annual variations of the ratio are also minimal; overall a 2% difference exists between the minimum in spring (0.59) and the maximum in autumn (0.61). A similar study of ERA40 DMGS data produces a slightly lower overall ratio (0.56), but with less variation between stations (0.47 to 0.69). The intra-annual variation mirrors that of PRECIS-Re data.

A slightly lower ratio is produced when the top 2% of DMGSs are considered, with an overall PRECIS-Re to observed ratio of 0.55. ERA40 data exhibit a

similar ratio to that of all DMGSs, with a value of 0.57. From station to station these ratios vary from 0.43 to 0.70 (0.49 to 0.68), for PRECIS-Re (ERA40) data. The ratio of the upper 2% of observed DMGS to model data at each station is shown in Figure 3.30.

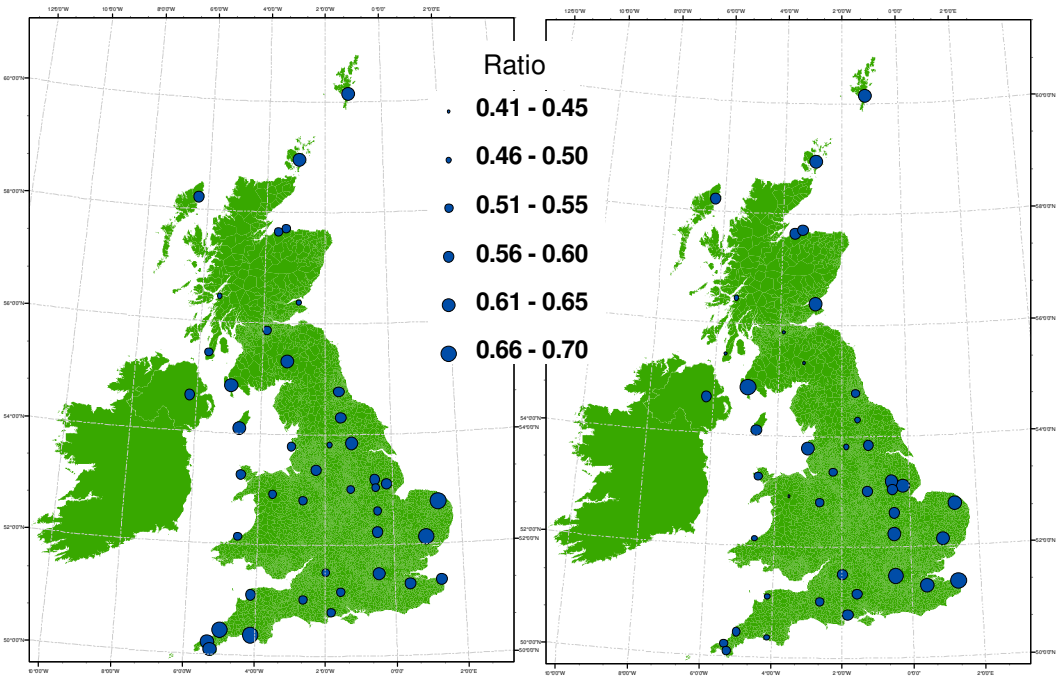

Figure 3.30 - Ratio of ERA40 (left) and PRECIS-Re (right) to observed DMGSs exceeding the 98th percentile values in the period 1980-2001.

Stations exhibiting lower ratios of the upper 2% of PRECIS-Re to observed DMGS values tend to be those at high elevation (e.g. Eskdalemuir (*17*) (262 metres above sea level), Bala (*3*) (163 m a.s.l.), Bingley (*5*) (262 m a.s.l.) and Salsburgh (*34*) (277 m a.s.l.), and those on the west coast. A similar pattern is seen for the ratios of daily mean windspeeds and the full record of DMGS. This suggests that the orography mask used in the PRECIS model does not accurately reflect the altitude at these stations. Model elevations for Bala, Bingley and Salsburgh are 240 m, 385 m, 121 m and 112 m a.s.l. respectively; markedly different from their actual elevations. The lower figures result from the utilisation of an average value for altitude in the 25 km grid square. Eskdalemuir, however, has an elevation of 242 m, and model elevation of 241 m a.s.l.

The effect of the land-sea mask on windspeeds in PRECIS-Re may be significant. The “windspeed grid” is offset by half a grid point to the land-sea

mask, so a windspeed calculated for a land cell surrounded by sea cells will incorporate surface energy fluxes from the sea into the calculation. This will tend to artificially raise the windspeeds calculated for this cell. Hence, with an eastward shift of the "wind grid" relative to the land-sea mask, coastal cells on the east coast will incorporate sea cell fluxes, producing artificially higher windspeeds. Due to this eastward shift this effect is not seen on the west coast, where model to observation ratios are lower. Figure 3.30 shows the ratios for ERA40 data to observations do not follow those patterns for PRECIS-Re, indicating the impact of a different land-sea and orography mask. A fractional land-sea mask is utilised to produce ERA40 data, at a much coarser resolution than that used in PRECIS (1.125^{o} compared with 0.220^{0}). The coarser resolution partially explains the lower range of observation to model ratio values achieved with ERA40, compared to PRECIS-Re, for both daily mean windspeeds and DMGS.

Slightly greater differences are evident in seasonal ratios of DMGSs exceeding 98^{th} percentile, than for the entire record, with a ~6% difference between the winter (lowest ratio) and summer (highest) for both PRECIS-Re and ERA40 data. It is important that this intra-annual variation is relatively low since the simulation of damaging windspeeds directly impacts the quantification of historic and future windstorm loss estimates in Chapters 5 and 6 respectively. Windstorm loss is greatest in autumn and winter, so it is desirable that damaging windspeeds in these seasons are reliably simulated. Inter-annual variation in the ratio of observed damaging windspeeds to model values approaches 10%, suggesting that seasonal variations are insignificant compared to inter-annual variations.

Since the highest, and therefore most damaging, DMGSs occur in autumn and winter, the ability of PRECIS-Re and ERA40 data to capture these events is assessed here. Figure 3.31 shows the monthly frequency of damaging windspeeds.

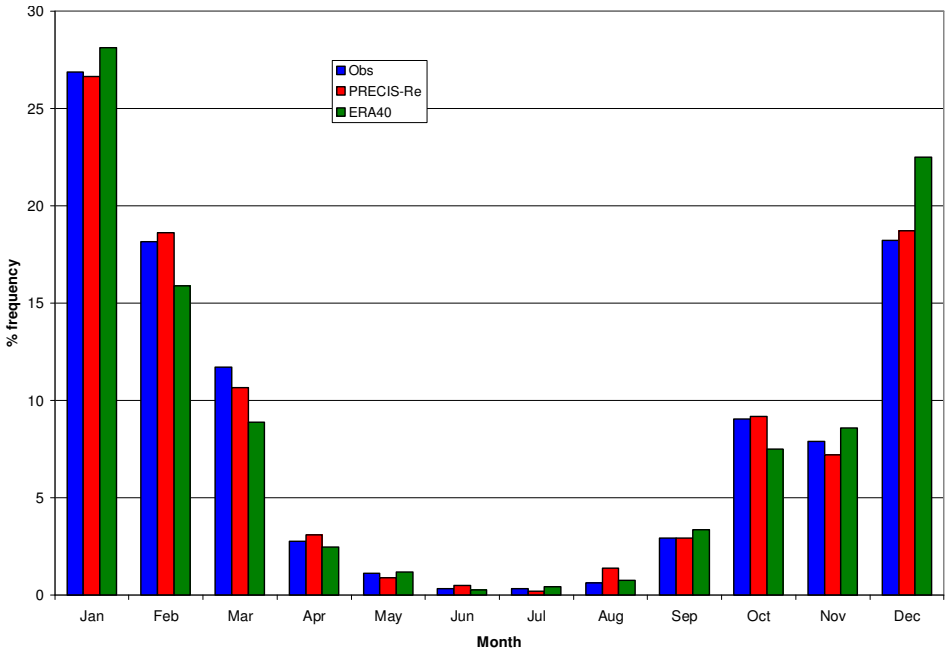

Figure 3.31 - Intra-annual variation of the occurrence of the top 2% of DMGS in observation (blue), PRECIS-Re (red) and ERA40 (green) data, at 43 stations across the UK, during the period 1980-2001.

PRECIS-Re data, compared with ERA40 data, manages to replicate the pattern shown in the observation dataset in Figure 3.31 more accurately. ERA40 data overestimate the occurrence of damaging winds in November, December and January, while underestimating them in October, February and March. It will be shown in Chapter 5 that annual windstorm losses are somewhat dependent on the time of the year damaging windspeeds occur. Therefore it is essential that the PRECIS-Re is able to accurately reflect the observed pattern, which it appears to do.

3.4 Summary and Conclusion

The first research aim of this project is to assess the historical and future UK wind regime. A 26-year (1980-2005) observational dataset containing information on daily mean windspeeds and daily maximum gustspeeds (DMGS) at 43 Met Office stations across the UK is established and analysed in section 3.1. Raw and dynamically downscaled reanalysis data, presented in section 3.2, provide information on the UK wind regime for a period before observations are available (1959-1979). Thus, an assessment of the historical UK wind regime during the period 1959-2005 is provided in this chapter,

fulfilling the first part of the first research aim. These datasets are subsequently utilised in Chapter 5 to achieve the first part of the third research aim; quantifying historical windstorm losses.

A unique observation dataset containing information on DMGS and daily mean windspeed in the UK has been generated in this project, with temporal and spatial variations identified in section 3.1. Observed values of daily mean windspeed and DMGS tend to be higher in coastal locations, with elevation and with increasing latitude, in accordance with previous studies (Wheeler and Mayes, 1997; Palutikof *et al.*, 1997). West coast stations tend to exhibit higher windspeeds (both DMGS and daily mean windspeeds) than those on the east coast, due to the increased fetch associated with the Atlantic Ocean. Damaging windspeeds (i.e. DMGSs exceeding the local 98th percentile value) also follow this spatial pattern.

The observed data suggest a downward trend in daily mean windspeeds over the course of the study (1980-2005). The Network Average of annual average daily mean windspeed shows a 0.5 ms^{-1} decrease. Significant (at the 95% confidence level) downward trends are seen in 14 stations in southern and northern England. The Network Average of annual mean DMGS decreases by a similar magnitude, with significant decreases recorded at 12 stations in southern and eastern regions of England and in Scotland. Reductions are seen in all seasons. Annual 98th percentile values of DMGS also exhibit a downward trend; the Network Average decreasing by 2 ms^{-1}, with a significant decrease of 2.5 ms^{-1} in autumn. These decreases are significant in stations in southern England, and northern England and southern Scotland, with those in southern England the greatest (up to 5.5 ms^{-1}). These results, suggesting a slight decline in annual mean values over the course of the study, are in agreement with Sinden (2007), whose results suggest a reduction in windspeeds recorded at 66 stations across the UK in 1970-2003. Despite the minimal reductions in the Network Average, statistically significant decreases in mean windspeeds and gustspeeds are recorded at stations in southern parts of England. Furthermore, these decreases appear to manifest in a decreasing frequency of damaging windspeeds over the period 1980-2005. Verification of the temporal trends identified here is difficult due to the sparse

literature surrounding the topic, especially with regard to gust speeds. The impact on windstorm losses of the features in the windspeed dataset identified here, are quantified in Chapter 5.

Previous analyses of the UK wind regime are mostly limited to mean windspeeds (e.g. Sinden, 2007; Palutikof *et al.*, 1997). Thus, the 26-year record of gust speed developed in this project is a potentially powerful resource. The observational dataset, whose features are briefly described above, can be utilised in a number of ways. Mean windspeed data are applicable for use in the wind power industry (e.g. Sinden, 2007; Pryor *et al.*, 2005a). Reliable, continuous observed windspeed data have been shown to be difficult to acquire for the UK in order to assess RCM performance (Hanson and Goodess, 2004) and also for statistical downscaling purposes (Pryor *et al.*, 2005b). The dataset established here has undergone strict quality control and is therefore suitable for these applications. Furthermore, the establishment of the long, continuous DMGS dataset can fill the void in the verification of gust parameterisation in RCMs (Leckebusch *et al.*, 2006). In this project the observation dataset is utilised to develop a windstorm loss model in Chapter 4 and also to produce loss estimates of historic windstorms in Chapter 5.

During the course of the investigation into observed DMGS in section 3.1.2 a rather surprising result emerged regarding the time of the day DMGSs occur. An afternoon (12:00-15:00) peak is found as expected, but also a nocturnal peak (23:00-01:00) is observed. The nocturnal peak is evident even when only high DMGS are considered (those exceeding high percentile and absolute thresholds). The afternoon peak can be explained by solar radiation driving thermal mixing, and the subsequent transport of energy to the surface in the form of gusts. The nocturnal peak is more prominent compared with the afternoon peak in coastal locations, where surface instability created by surface heating is subdued, therefore reducing the afternoon peak. The mechanisms producing this nocturnal peak are unclear. Results following an investigation into wind profiler data from Wattisham are inconclusive, due to the limited quantity and quality of the data.

The regular occurrence of DMGSs in the period 23:00-01:00 is likely due to surface cooling and the development of a temperature inversion, compressing and lowering the level containing maximum windspeeds. Another potential mechanism is the nocturnal jet, first described by Blackadar (1957). The exact processes involved in the development of an nocturnal jet are not fully established (Conangla and Cuxart, 2006), but centre on the formation of a friction free layer containing supergeostrophic flow. However, it is unknown whether this layer may descend low enough to enable gusts to make their way to the surface. The unique observation dataset established here provides a basis for further research regarding the manifestation of the nocturnal peak.

In addition to the relatively long record of observations (1980-2005), ERA40 and PRECIS-Re data were analysed in section 3.2 to provide information on the UK wind regime dating back to 1959. Results suggest slight (less than 0.5 ms^{-1}) upward trends in the Network Average of annual average values of daily mean windspeed and DMGS, as well as the upper 2% of DMGSs, over the course of the study (1959-2001). The 98^{th} percentile values of DMGS increase at all stations with 9, in Scotland and northern England, exhibiting significant increases of up to 1 ms^{-1}. Annual mean DMGS values of the Network Average in the ERA40 dataset indicate a significant upward trend of 0.4 ms^{-1}, with a significant increase of 1 ms^{-1} in winter values. Similarly, the Network Average shows an increase of 1.5 ms^{-1} in damaging windspeeds, with significant upward trends at 24 stations in central and northern England, and in Scotland. The upward trends seen in both model datasets are largely driven by increases in winter windspeed values. Predominantly, stations located in the northern part of the UK exhibit greater increases in windspeed than those located further south.

Although the model data suggest overall increases in both daily mean windspeed and DMGS, an analysis of data for the period 1980-2001 (corresponding with observations) reveals downward trends. These reductions are of similar magnitudes and in similar locations to those exhibited by observed data, suggesting some confidence can be placed in the reliability of model data. In order to fully assess the reliability of model data a comparison of ERA40 and PRECIS-Re data to observations was undertaken in section

3.3. It is important to establish the reliability of PRECIS output data as they are utilised in Chapter 6 to complete the second part of the first research aim; an assessment of the future UK wind regime. In addition, PRECIS output data are used in Chapters 5 and 6 to quantify the historic and future impact of the UK wind regime on insured losses (the third research aim).

Simulated windspeed data for the period 1980-2001 from PRECIS-Re and ERA40 were compared with observations. The degree to which variations seen in observed daily mean windspeeds and DMGSs is captured by model data are assessed through R^2 values. Daily mean windspeed is shown to be more reliably modelled by both PRECIS-Re and ERA40, than DMGS, in line with Hanson *et al.* (2004) and Leckebusch *et al.* (2006). This was an expected result given that model DMGS is actually the daily maximum 2.5-minute mean windspeed in PRECIS and the daily maximum of four mean windspeeds in ERA40, as discussed in section 2.1.2. The spatial variation in R^2 values is similar for both daily mean windspeed and DMGS, and in both PRECIS-Re and ERA40 data. PRECIS-Re data generally produce stronger correlations with observations than ERA40 data. There is perhaps a tendency for model data to be less reliable at stations in the south east of and north east coast of England and in Scotland. Analysis of model damaging windspeeds compared to observed values, reveals relatively low R^2 values, but again produces a similar spatial pattern. These R^2 values should, however, be treated with care due to the limited number of days considered (160 days out of over 8000).

Generally, model daily mean windspeeds are slightly higher (~15%) than observed values, while model DMGSs are markedly *lower* (~40%) than observed values. The ratio of model damaging windspeeds (DMGS exceeding the 98th percentile value) to observed values is 0.55 for PRECIS-Re and 0.57 for ERA40 (equivalent to underestimations of 45% and 43% respectively). In terms of quantifying the impact of damaging windspeeds on insured losses, these ratios importantly show little inter- and intra-annual variation (less than 10%). Markedly lower ratios are seen on the east coast of the UK compared with the west coast in PRECIS-Re data, particularly for damaging windspeeds. This may, in part, be an artefact of an offset “wind grid” relative to the land-sea mask. Additionally, stations at high elevations exhibit higher ratios, indicating

that the orography mask does not fully capture the variability of the UK terrain. This seems plausible given that the spatial resolution of the orography mask in PRECIS is approximately 25km.

It is interesting to compare the ratio of model data to observed daily mean windspeeds (an average of 1.13 for PRECIS-Re) with that produced by Hanson and Goodess (2004), who compared windspeeds at Ringway (*station 32*) and Yeovilton (*43*) recorded in 1983-1999 with those simulated by HadRM3H (driven by HadAM3H) for 1960-90. They found a ratio of observed to model data of 0.60, compared with figures reported here of 1.18 and 1.22 for Ringway and Yeovilton respectively. Although HadRM3H is a slightly earlier version of the RCM utilised in this project, very little difference exists between the models, and these results demonstrate the benefit of driving a RCM with reanalysis data. This enables the model performance to be assessed more reliably, without biases in the driving GCM data unduly affecting results.

It is already suggested in this discussion that PRECIS-Re outperforms ERA40 in reliably simulating windspeeds for the UK. The added value PRECIS provides is assessed through a comparison of the performance of PRECIS-Re and ERA40 in simulating windspeeds for the period 1980-2001. It is demonstrated that PRECIS-Re captures the variability of the UK wind regime more reliably than ERA40 data, and also produces lower absolute errors between observations and model data. There are a limited number of stations (3 and 5) where ERA40 data more accurately replicate daily mean windspeed and DMGS observations respectively. However, damaging windspeeds are simulated more reliably by PRECIS-Re than ERA40 at every station. This emphasises the importance of the spatial resolution of a model when considering meteorological variables which are affected by terrain (e.g. windspeeds). Despite some of the limitations, discussed in section 2.2.2 and highlighted within this chapter, PRECIS provides added value to ERA40, and is seen a viable tool with which to explore future changes in the UK wind regime and subsequent impacts on insured losses in Chapter 6. Furthermore, the PRECIS-Re dataset has been shown to be reliable and will be utilised to identify and quantify high impact historical storm events in Chapter 5.

Although it is shown that damaging windspeeds are markedly underestimated by PRECIS, similar studies have found that RCM data, and even GCM data, is still capable of producing realistic windstorm loss estimates (e.g. Leckebusch *et al.*, 2007; Pinto *et al.*, 2007).

Chapter 4: Development of a Windstorm Loss Model

As described in section 1.3.2 a number of studies have attempted to utilise insurance claims data and corresponding meteorological parameters from certain storm events in order to produce a predictive windstorm loss model. These studies are somewhat limited due to the lack of both meteorological and loss data. This chapter addresses the second research aim outlined in section 1.6; the development of an operational windstorm loss model. This project benefits from the availability of a continuous, long record of both claims data and windspeed information at a high spatial and temporal resolution. These datasets enable a deterministic relationship between windstorm losses and meteorological variables to be established, facilitating the development of a windstorm loss model. Unlike previous studies (Dorland *et al*., 2000; Hanson *et al*., 2004), which consider a limited number of storms, the model developed here utilises 10 years of daily windspeed and insurance claims data.

The three main components of a loss model, as described in section 1.3, are hazard, exposure and vulnerability. In order to incorporate aspects of vulnerability and exposure, socio-economic parameters, introduced in section 2.3.1 and described in detail in section 4.1.2, are utilised. The extensive windspeed dataset established in Chapter 3 provides high temporal and spatial resolution windspeed information, allowing the windstorm hazard to be quantified. The direct relationship between windspeeds and insured loss is explored in section 4.1.3, where the term “damaging windspeeds”, used frequently in this project, is quantitatively derived and defined.

Calibration of the windstorm loss model is carried out using Ecclesiastical Insurance Group (EIG) 16-year record (1990-2005) of wind-related insured domestic property losses, introduced in section 2.3.2. A further detailed description of these data occurs in section 4.1.1 in order for the reader to have full appreciation of its characteristics on the temporal and spatial scales utilised here. Claims data are only available from a single insurance company. Therefore it is important to establish whether it is representative of industry-wide losses, a task undertaken in section 4.1.1. Model development in section 4.2 includes a description of the regression analysis undertaken. Verification

of the model utilises data from 2000-2005 in section 4.3. Unlike previous studies (Dorland *et al.*, 2000; Hanson *et al.*, 2004; Klawa and Ulbrich, 2003), the fact that this project benefits from the availability of such an extensive claims database allows model verification using independent data from a period excluded from the calibration process. The chapter concludes with a summary and discussion of findings in section 4.4.

4.1 The Variables

During the process of developing the windstorm loss model a number of independent variables are investigated, including meteorological parameters and socio-economic factors. These variables include the observed windspeed data established in Chapter 3, along with domestic property information described in section 2.3.1. The model is developed using data for these variables from the period 1990-1999, with data from 2000-2005 used in the verification process. For consistency, exactly the same procedure is carried out on all data (1990-2005) in order for the variables to be at the correct spatial and temporal resolution. A thorough description of all the variables and how the data are processed is provided here.

4.1.1 Insured Loss Data

The dependent variable in the windstorm loss model is insured loss. Windstorm domestic property claims from EIG have previously been described in section 2.3.2. Quality control is carried out, and the claims are georeferenced and aggregated to postcode sectors as described in section 2.3.2. The data are at a daily temporal resolution.

Clearly EIG claims for a particular windstorm event, or time period, are not the sole losses recorded in Great Britain. Therefore it is desirable to establish that the EIG claims are at least representative of industry-wide losses. For that reason, a comparison is made between EIG claims and industry-wide (ABI) quarterly statistics.

Year	No. of postcode sectors filing claims	EIG Storm Loss (£m)	ABI Storm Loss (£m)	ABI Total Domestic Loss (£m)
1990	1008	6.82		2549.05
1991	1866	1.53		800.63
1992	3843	2.69		463.29
1993	5576	4.64		576.35
1994	3711	3.08		372.45
1995	3519	2.71		345.21
1996	3299	2.52		661.84
1997	4153	4.67		531.83
1998	4208	5.69	485.70	886.47
1999	2609	3.74	354.71	710.98
2000	4156	7.89	444.33	969.79
2001	1892	3.07	295.43	844.38
2002	3701	7.70	508.23	1078.29
2003	1042	1.49	148.12	542.02
2004	1797	3.52	225.75	324.31
2005	5075	7.26	303.00	490.33

Table 4.1 – EIG and ABI annual insured domestic property losses (£). Values are adjusted to 2005 values for inflation.

Table 4.1 shows the annual wind-related insured domestic property losses suffered by EIG, along with the number of different postcode sectors reporting losses. Industry-wide (ABI) wind-related and total domestic losses are included, although, for reasons previously cited, the length of record of storm related losses from the ABI are limited to 1998-2005. The ratio of EIG to industry-wide losses indicates that EIG claims represent between 1 and 1.8% of industry wide storm related claims between 1998 and 2004, with a 2.4% share in 2005. In terms of the percentage contribution of EIG storm claims to total industry-wide domestic property losses, values range from 0.2% to 1% between 1990 and 2004, with a figure of 1.5% in 2005. The inter-annual variation in these ratios is shown in Figure 4.1.

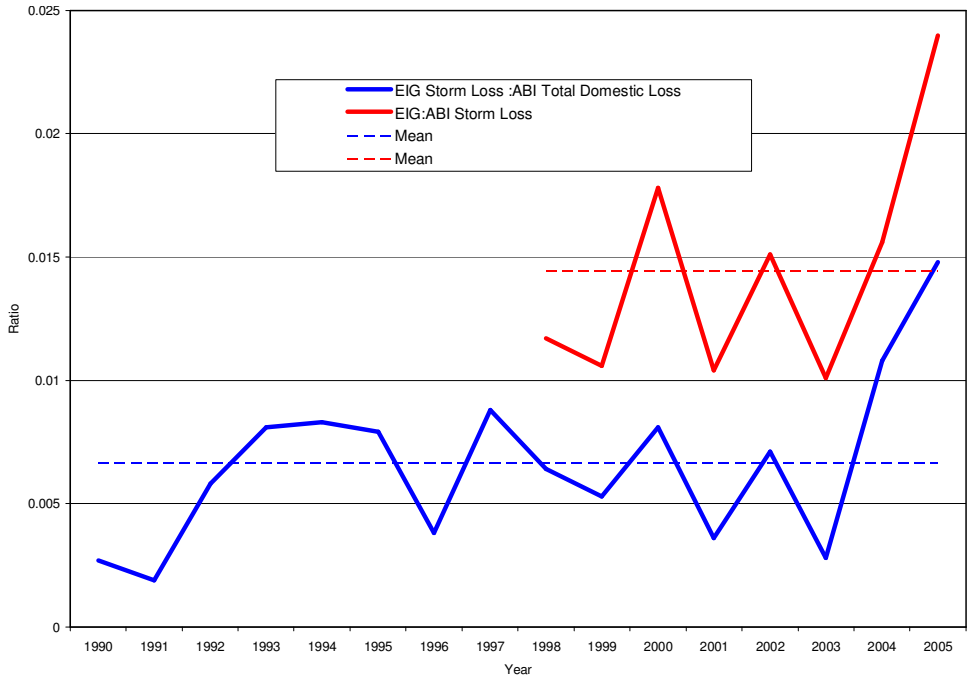

Figure 4.1 - Ratio of EIG Storm Losses: ABI Total Domestic Loss (Blue) and EIG: ABI Storm Losses (Red) and the respective means (dotted).

Unfortunately, the number of policies issued by EIG each year and the total sum insured are commercially sensitive and therefore unavailable. However, the comparison to ABI loss data can be used as a method of establishing whether changes in EIG's exposure, relative to the industry-wide average, are driving changes in losses. For the period 1990 to 2004 the ratio of EIG to ABI losses remains fairly constant. But in 2005 this ratio exhibits a sudden jump, shown in Figure 4.1, which may be a result of an increase in the EIG exposure, either through a higher number of policies being written, an increase in total sum insured, or a combination of the two.

Following an investigation of the ratios between EIG and industry-wide losses, the assumption is made that the exposure of the EIG domestic property portfolio to windstorm is unchanged relative to the industry-wide exposure, throughout the study period (1990-2005). However, the national exposure to wind-related losses may have altered during that period. Munich Re (2002b) suggest that between 1990 and 1999, due to an increase in insured density and average sum insured per policy, losses could have been amplified by 7-8% annually in western Europe. Therefore, with the assumption that this trend continued to 2005, EIG losses are adjusted by 7.5% annually, in order that storm losses in 1990 may be directly comparable to those in 2005.

A further issue of concern is that the regions in which EIG write polices must again be representative of the whole insurance industry. As previously stated information regarding the number and location of policies issued and sum insured is unknown, so a spatial analysis of the location of claims is made to ensure they are not subject to bias due to EIG exposure. The spatial analysis of losses over the entire period of interest (1990-2005) does not reveal any pattern, i.e. no areas exhibit an exceptional number of claims compared to another. However, certain areas do not report any losses in the study period, most notably in northern Scotland. These patterns are shown in Figure 4.4, in section 4.2, where this issue is readdressed in more depth. Following correspondence with EIG, their exposure can be considered to be "reasonably uniform" across Great Britain.

An overview of the EIG claims revealed that of the 5844 days in the period 1990-2005, nearly 75% recorded losses despite only 15% experiencing damaging windspeeds[1]. An underlying assumption is that in order for damage to occur, and subsequently insured loss, damaging windspeeds need to be recorded. Therefore, the exclusion of data on days without damaging windspeeds from the model development was considered. However, it was decided that this may unduly bias the model since part of the development process is to establish the threshold for damaging windspeeds. Other uncertainties are present in the claims dataset. Claims handling errors, discussed in section 2.3.2 may have resulted in losses being reported on incorrect dates. In addition, fraudulent claims may have been filed for wind-related damage on days without damaging windspeeds. It is impossible to establish where errors in claims data may lie, and therefore every day is included in the model development.

As with climate data, insurance data are not without their uncertainties. However, while the EIG loss information has its uncertainties, it may be considered a reliable dataset for the development and verification of the windstorm loss model.

[1] The term damaging windspeed is used throughout this project to described daily maximum gustspeeds exceeding the local 98th percentile. Justification for this terminology is presented in section 4.1.3.

4.1.2 Socio-economic data

The sources of socio-economic data utilised in the development of the windstorm loss model are introduced in section 2.3.1. Variables include resident numbers, household numbers and types extracted from census 1981, 1991 and 2001 data, and property value from Experian 2000 data. A domestic property vulnerability index based on Spence *et al.* (1998) is also included. All data are aggregated, where necessary, to a postcode sector resolution.

Resident Numbers (*Res*)

The number of people living in domestic properties is extracted from Census data for 1981, 1991 and 2001. Unfortunately, information on the interim years is unavailable since the census is only undertaken once every 10 years. Using ArcGIS, the data are aggregated to postcode sector level and linear extrapolation is carried out at that resolution to provide estimates of resident numbers for the years without a census. No extrapolation was carried out post 2002 as no data were available, and therefore the figure for 2001 was used in the years 2002-2005. Overall, the number of residents in Great Britain increased by approximately 10% between 1990 and 2001, from just over 51.5 million to just over 57 million in 2001.

Property Type

Census data from 1991 and 2001, described in section 2.3.1, provide information on the number of detached, semi-detached, terraced, residential, converted flatlet and converted flats. These are combined under the headings semi-detached, detached, terraced properties, and flats/maisonettes (which includes the residential classification). The number of each type of dwelling is established for each postcode sector. These headings act to clearly define the different, dominant types of domestic properties in Great Britain and fall in line with those used in the Total Property Value and Vulnerability Index variables described below. The breakdown of property types in 2001 is 37% terraced, 35% detached, 21% semi-detached and 6% flats. Again, figures for the interim years between censuses are derived through linear extrapolation on a postcode sector level. Unfortunately, this information is not contained within

the 1981 census data and therefore the value for 1991 is used for 1990. Similarly, 2001 figures are used for 2002-2005.

These variables are subsequently know as *detached, semi, terraced,* and *flats* respectively. The total number of properties in each postcode sector is summed, producing the *Household Number (HH)* variable.

Total Property Value (*TPV*)

Information on property sales between 1995 and 2000 is available in the Experian 2000 dataset. This dataset is described in section 2.3.1, and contains information regarding the average sales price of different property types in each postcode sector. It would seem logical to find the total value of the property in each postcode sector by simply multiplying the average sales price of each property type by the number of those properties and calculate the total. However, sale prices for different dwelling types vary geographically due to discrepancies in their demand. As a result, Experian produces a Standardised Average Sales price. This value accounts for the mix of properties being sold at that time, i.e. an average price for each property type in each postcode sector is established, based not only on sales in that area, but also accounting for the national demand for that type of property. Therefore, given that it is important to try to incorporate variables which are directly comparable across the whole of Great Britain, this figure is utilised here. The total property value is found by multiplying the number of households in a postcode sector (*HH*) by the standardised average sales price. A value is established in each sector, for each year in the period 1995-2000, with the values at the beginning and end of this period used for 1990-1994 and 2001-2005 respectively. This variable is subsequently termed *TPV*.

A map of the spatial variation shown in the Total Property Value in 2001 is shown in Figure 4.2.

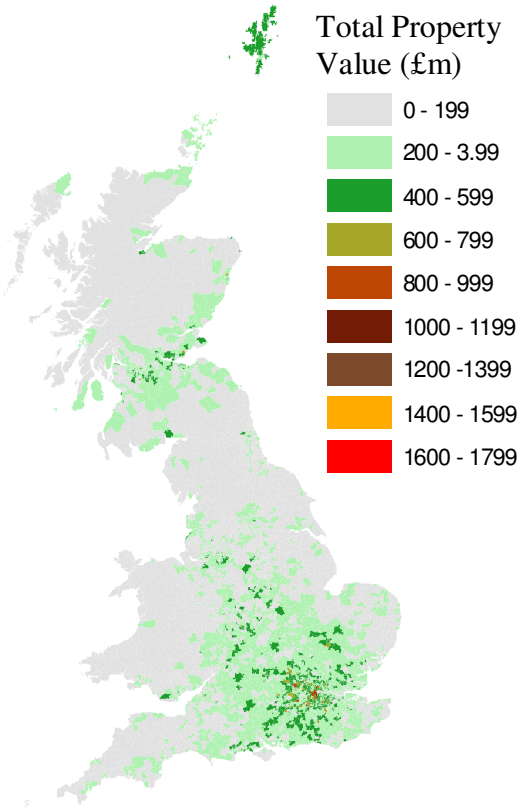

Figure 4.2 - Total Property Value in Great Britain postcode sectors (adjusted to 2005 £ million values) in 2001

Figure 4.2 unsurprisingly shows that the majority of the greatest *TPV*s are found in the south east of England, and more specifically around London. The large areas of some of the postcode sectors in Scotland result in high *TPV*s.

Vulnerability Index (*VI*)

The vulnerability index proposed by Spence *et al.* (1998), and introduced in section 2.3.1, was designed to help quantify the exposure of the UK housing stock to wind damage. A vulnerability score is assigned to different types of properties of different ages. Unfortunately, information regarding the age of properties is not available in either the Experian or Census data. Therefore, the vulnerability index presented by Spence *et al.* (1998) is adapted slightly in order that each postcode sector can be ascribed a vulnerability index which may be directly comparable with all other sectors.

Initially, the vulnerability index is adapted to remove the different age bands, and a mean value is found for each property type, based on a knowledge of the percentage of housing stock in each age band. Subsequently, vulnerability

indices are combined (where necessary) to fall under the property types described above. The final Vulnerability Index is as follows:

Property Type	Vulnerability Index
Terraced	0.875
Semi-detached	1.026
Detached	1.338
Flats	0.608

Table 4.2 - Vulnerability Index (adapted from Spence *et al.*, 1998).

Table 4.2 suggests that detached properties are most vulnerable to windstorm damage. This is logical given that roof damage accounts for a high proportion of wind-related damage (Baxter *et al.*, 2001; Spence *et al.*, 1998), and detached properties tend to have a greater roof surface area. Conversely, flats in a tower block will have little or no roof (aside from the very top floor), and subsequently have a low Vulnerability Index.

The overall Vulnerability Index for each postcode is derived from the numbers of different property types within it and their relative vulnerability indices. This variable is subsequently termed *VI*.

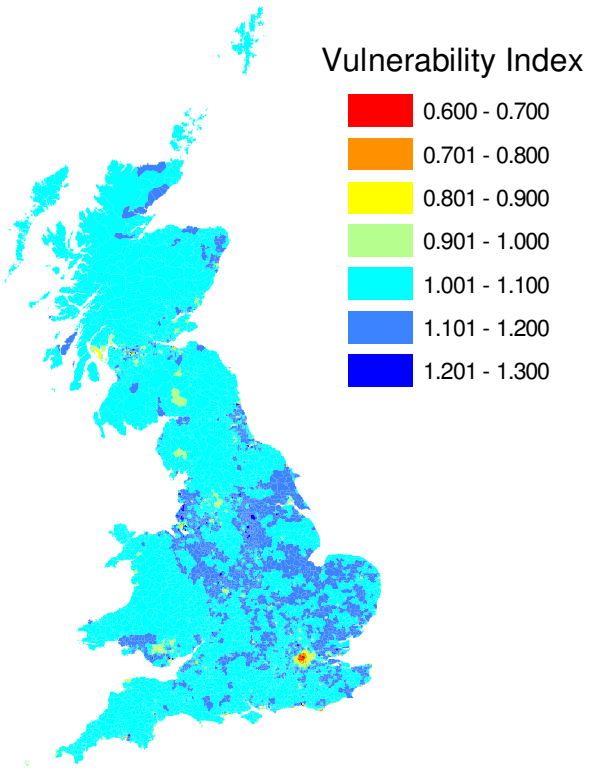

Figure 4.3 - Vulnerability Index of domestic properties in Great Britain postcode sectors in 2001.

The spatial variation of *VI* shown in Figure 4.3 reflects the spatial pattern of the various property types. The higher the ratio of semi-detached and detached properties to terraced houses and flats in a postcode sector, the greater *VI*. This results in the low *VI*s seen in sectors in London and Cardiff. Interestingly, sectors with high values of *TPV* (shown in Figure 4.2) tend to have slightly lower *VI* values (shown in Figure 4.3). The two maps suggest that in central England, areas with a *VI* greater than 1 have *TPV*s of under £200m. Conversely, areas in central England with a *VI* of less than 1 correspond with those with *TPV*s exceeding £200m.

4.1.3 Windspeed Data

The extensive mean windspeed and gust speed dataset established in Chapter 3 is utilised to provide windspeed variables in the windstorm loss model. Daily mean windspeeds and Daily Maximum Gust Speeds (DMGS) are available for the period 1990-2005, at 43 stations across the UK. A single value is obtained for each postcode sector though the ArcGIS interpolation methods described in section 2.3.3. A sensitivity study regarding these interpolation methods is presented in Appendix C. The interpolation process produces a maximum and mean interpolated value of DMGS and daily mean windspeed for each postcode sector.

Clearly, a direct relationship between wind-related insured loss and windspeed exists. It has been shown that a windspeed threshold for damage, and subsequently insured loss, also exists (e.g. Dorland *et al.*, 2000; Klawa and Ulbrich, 2003). Before any further socio-economic variables are considered, an initial investigation into this damage threshold is made. Using the GIS tools and methods described in section 2.3.3, a selection of threshold values are investigated including absolute and percentile values. The observed daily mean windspeed and DMGS is normalised to the local thresholds (i.e. windspeed minus threshold windspeed at each station) and interpolated using ArcGIS. A 'windspeed exceedance' value is thus found for each postcode sector in Great Britain, with the sum correlated to the daily total EIG losses. Due to the resource intensive nature of this process (as described

in section 2.3.3) it is only possible to analyse a limited period of windspeed data. The selected year was 1997, since the annual EIG loss in that year was roughly equivalent to the overall mean, and it occurs in the middle of the study period.

In addition to the variety of thresholds tested, a number of different relationships between losses and windspeed exceedance are tested. As discussed in section 1.3.2, various relationships between windspeed and insured loss have been found (Klawa and Ulbrich, 2003; Heneka and Ruck, 2004; Rootzen and Tajvidi, 1997). For this reason linear, square, cubic and exponential relationships are all explored. The windspeed value (both DMGS and daily mean windspeed) at each station is normalised to the local threshold value, and then raised to the appropriate power, before the interpolation process occurs. Again the windspeed exceedance in each postcode sector is summed for Great Britain as a whole and correlated to daily EIG losses. The results from these analyses are presented in Table 4.3 for mean interpolated DMGS value only.

Threshold	Relationship			
	Linear	Square	Cubic	Exponential
90th percentile	0.340	0.670	0.818	0.222
95th percentile	0.349	0.669	0.821	0.234
96th percentile	0.370	0.701	0.854	0.250
97th percentile	0.396	0.684	0.842	0.244
98th percentile	0.411	0.701	0.873	0.253
99th percentile	0.407	0.695	0.866	0.250
15 ms^{-1}	0.247	0.426	0.525	0.137
20 ms^{-1}	0.149	0.264	0.316	0.105
25 ms^{-1}	0.097	0.182	0.206	0.060

Table 4.3 – Strength of correlation (R^2 values) of interpolated gust speeds exceeding various thresholds with EIG daily wind-related insured domestic property losses for 1997.

Values of R^2 presented in Table 4.3 for DMGS figures are higher than those for mean windspeeds (not shown) at every threshold, and with every relationship, by values ranging from 5-25%. Furthermore, it was found that the correlation is marginally improved when the mean (rather than maximum) interpolated values are used. Table 4.3 shows that a local percentile threshold is more appropriate than an absolute threshold. The use of the 98th percentile as a threshold results in the strongest correlation with all relationships.

An additional analysis is carried out by finding the annual total of daily windspeed exceedance values in each postcode sector and correlating them with the annual (1997) EIG loss in that sector. Results are shown in Table 4.4.

Threshold	Mean interpolated value of DMGS	Max interpolated value of DMGS	Mean interpolated value of daily mean windspeed	Max interpolated value of daily mean windspeed
90th percentile	0.176	0.175	0.129	0.126
95th percentile	0.177	0.177	0.143	0.142
96th percentile	0.181	0.18	0.152	0.150
97th percentile	0.179	0.177	0.148	0.147
98th percentile	0.183	0.180	0.155	0.154
99th percentile	0.180	0.179	0.148	0.146
15 ms^{-1}	0.141	0.140	-	-
20 ms^{-1}	0.109	0.109	-	-
25 ms^{-1}	0.089	0.088	-	-

Table 4.4 - Strength of correlation (R^2 values) of the annual total of interpolated gust speeds exceeding various thresholds with EIG annual total wind-related insured domestic property losses on a postcode sector basis in 1997.

Values of R^2 in Table 4.4 are shown for the cubic relationship of windspeed exceedance, with the other relationships yielding weaker correlations (as shown in Table 4.3). The table illustrates once more that mean windspeeds and DMGSs normalised to the 98th percentile are more highly correlated to insured loss than when other thresholds are used. The results for mean daily windspeed are shown, demonstrating the inferior correlations produced using daily mean windspeed compared with DMGS. In addition, Table 4.4 shows the marginal increase found in R^2 values by considering the mean interpolated value in postcode sectors as opposed to the maximum value. It should be noted that these initial analyses are based on windspeeds and losses recorded in 1997, a sample of the overall 16-year record later used in the development of the full windstorm model in section 4.2.

The ratio of the 98th percentile value of DMGS to the 99th and 99.5th percentile values shows little variation (1.06 to 1.13 and 1.13 to 1.22 respectively) across the 43 UK Met Office stations comprising the observation network detailed in section 2.1.1. This suggests that values exceeding the 98th percentile threshold can be viewed as a measure of storm intensity independent of non-

meteorological factors such as altitude or exposure. Furthermore, building design incorporates return periods of meteorological parameters, and therefore a percentile threshold seems appropriate when considering the relationship between windspeed and damage (and subsequent insured loss). The spatial and temporal variation of the 98th percentile of DMGS is discussed in depth in section 3.1.2. Throughout the project "damaging windspeeds" are considered those DMGS exceeding the local 98th percentile value. Justification for this is presented here.

Table 4.3 and Table 4.4 also suggest that a cubic relationship produces the best correlation between windspeeds and insured losses. This is further explored in the development of the loss model. However, the cubic relationship appears logical given that the advection of kinetic energy is proportional to the cube of windspeed. It is also the relationship found in similar studies (Dorland *et al.* (2000); Klawa and Ulbrich (2003).

The wind variable utilised in the development of the windstorm loss model is the DMGS normalised to the local 98th percentile value. These values are interpolated using ArcGIS on a daily basis, with the mean interpolated value from each postcode sector utilised. The variable is subsequently known as *WSE* (WindSpeed Exceedance). *WSE (linear), WSE (square), WSE (cube),* and *WSE (exp)* refer to the variables which have had linear, square, cubic and exponential functions applied to the normalised DMGS before the interpolation process, as described above.

4.2 Model Development

The aim of this section is to produce an operational model that can reliably predict the magnitude and location of wind-related insured loss on a postcode sector basis, given a particular storm pattern. Similar attempts have been made in the published literature, based on limited windspeed and insured loss data (Dorland *et al.*, 2000; Hanson *et al.*, 2004). This project benefits from the extensive, continuous record of high spatial and temporal resolution wind and

insured loss data described in section 4.1, and is able to utilise multiple storm events rather than a select few as in previous studies.

An initial investigation into the correlation of damaging windspeeds (all *WSE* relationships were considered) and daily insured losses on a postcode sector level produces discouraging results. Almost no correlation is seen. When the top 150 (10) storms, in terms of losses, are considered the correlation improves, with the highest R^2 value of 0.002 (0.003) produced when *WSE (cube)* is used. This, however, is still extremely weak, suggesting that it is necessary to incorporate some aspect of exposure. This would provide a true assessment of the relative severity of the storm (compared to other storms), and not be reflective of the exposure of the EIG domestic property portfolio. For instance, where only one claim in a postcode sector is filed following a storm, it is not discernable from the claims dataset whether this is a result of only one policy being written in that area, or whether the storm caused minimal damage.

The assumption that the EIG exposure is unchanged throughout the course of the study means that the loss from one event relative to the total loss provides some measure of the relative severity of that event. For example, over the course of the 16 years of the study period the exposure in a postcode sector is not assumed to change, and therefore loss from a single event relative to the 16-year total can be seen as an indication of the severity of that event compared with others occurring in that period. For this reason the losses in each postcode sector from the top 150 storms are converted into a percentage of the total loss. These values are then correlated against the windspeed exceedance values, with *WSE (cube)* producing an R^2 value of 0.036, which is still extremely low.

EIG claims for windstorm losses do not emanate from all the postcode sectors in Great Britain, with just over 80% (7264) reporting claims in the 16-year study period. The locations of postcode sectors not reporting losses in the study period are shown in black in Figure 4.4.

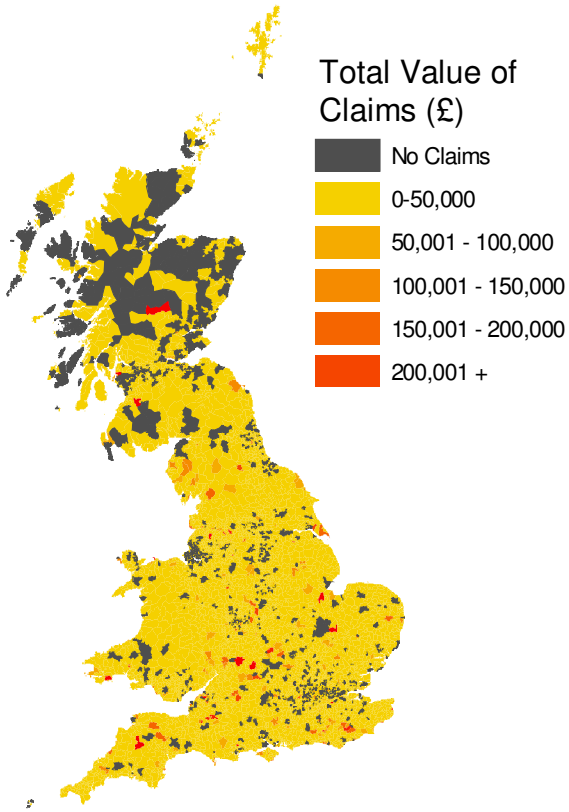

Figure 4.4 - Total EIG losses in Great Britain by postcode sector in the period 1990-2005. Values are adjusted to reflect inflation and changes in insured density and average value insured per policy following Munich Re (2002b).

Unfortunately, it is unknown whether the (nearly 2000) postcode sectors which report no losses between 1990 and 2005 have not been subjected to high enough windspeeds, or whether EIG does not write policies in these areas. The large number of sectors in northern Scotland suggests EIG's exposure is minimal in this area, although this cannot be proven. However, in order to try to establish some relationship between EIG losses and windspeed exceedance, the assumption is made that if no claims are filed in a postcode sector during the period 1990-2005, then no policies are written in these locations. This has the effect of removing nearly 20% of the postcode sectors from the analysis and results in the correlation between daily windspeed exceedance and EIG losses of the top 150 storms on a postcode sector level, improving once again (R^2 = 0.050 for *WSE (cube)*). This correlation is still extremely weak and unsuitable as a foundation for a windstorm loss model.

At this stage the EIG claims database is revisited and with aim of refining it to try to establish a robust relationship between losses and windspeed exceedance values. The fact that following a major windstorm claims are not

always recorded for the correct date has already been discussed in sections 2.3.2 and 4.1.1. For this reason, claims related to the top 150 storm events are analysed. Claims recorded on the seven days following a top 150 storm event are attributed to that event. If another top 150 storm event occurred in that period, only claims reported between the two are attributed to the initial event. A similar procedure is undertaken by Dorland *et al.* (2000) and Hanson *et al.* (2004), who attributed all losses in a whole month to individual storm events in those months (October 1987, January 1990 and February 1990). When events in the top 150 occur back to back (i.e. one day after another), they are considered as one event. On such occasions the maximum value of wind exceedance over the course of those days is found for each postcode sector, along with the total sum of the claims reported in the same period. As a result, the top 150 events considered at the outset shrinks to 129. The correlation between the wind exceedance of these 129 events and the EIG losses on a postcode sector basis is subsequently stronger than previous ones, but is still very weak ($R^2 = 0.09$ with *WSE (cube)*).

Following this initial analysis of daily wind exceedance and EIG losses on a postcode sector level it appears that a suitably strong correlation cannot be established, despite employing various data manipulation techniques. It is concluded that in order to be able to accurately model the spatial pattern of losses produced by a particular storm footprint, it is essential to have a knowledge of the exposure of, in this case, the EIG domestic property portfolio. Information regarding the total sum insured or the number of policies written would enable the loss ratio (insured loss divided by total insured value) or claims density (number of claims divided by number of policies written) to be established. These measures would allow a true assessment of the severity of a windstorm at a high spatial resolution, and hence facilitate the development of windstorm loss model with a spatial component.

At the outset of the model development process it was anticipated that insurance data containing information regarding the number of policies written in a particular region, and potentially the total sum insured, would be available. Indeed, one insurance company promised such data, but after several long delays and assurances that they would be made available, the data were not

obtainable. At this juncture the project was heavily advanced and it was decided that the modelling process should continue using the EIG claims dataset only. As a result, the model developed in this section includes no spatial component. Daily losses are aggregated for Great Britain as a whole. However, the methodology employed here, in theory, could be applied to data at a higher spatial resolution.

The loss model developed here, using the variables described in section 4.1, utilises the statistical software package SPSS (see SPSS Inc. (2005) for a description of the software and its capabilities). A multiple regression analysis, briefly described in section 2.3.4, is carried out to try to establish the relationship between insured loss and windspeed exceedance and the other socio-economic variables. The final model is subsequently verified against EIG losses recorded in a period outside of that used in model development (i.e. 2000-2005).

4.2.1 Regression Analysis

The independent variables, described in section 4.1, in each postcode sector recording damaging windspeeds, are totalled to produce one value for the whole of Great Britain for each day. For example, on a given day if damaging windspeeds occur in just five postcode sectors in Great Britain, the variable values are simply the sum of the number of various property types (*HH, semi, detached, terraced* and *flats* variables), the sum of the number of residents (*Res)*, and the sum of the total property value (*TPV*) in the five sectors. The Vulnerability Index (*VI*) is based on the total number of different types of properties impacted, and their respective vulnerability indices. The *WSE* is the total windspeed exceedance of the five postcode sectors. These values, along with the total EIG loss in Great Britain, are calculated for each day in the period 1990-1999.

Initially, the strength of the correlation between the dependent variable (daily EIG loss) and each independent variable is assessed, and presented in Table 4.5.

Variable	R	R^2	$\bar{R}^2$	t value	Significant (at 99%)
RES	0.855	0.731	0.731	99.579	Yes
HH	0.855	0.732	0.731	99.724	Yes
Semi	0.839	0.704	0.704	93.198	Yes
Detached	0.772	0.596	0.596	73.431	Yes
Terraced	0.796	0.634	0.634	79.547	Yes
Flats	0.904	0.818	0.818	128.008	Yes
TPV	0.890	0.792	0.792	117.981	Yes
WSE (linear)	0.550	0.303	0.302	39.799	Yes
WSE (square)	0.736	0.542	0.542	65.768	Yes
WSE (cube)	0.848	0.718	0.718	96.473	Yes
WSE (Exponential)	0.511	0.261	0.261	38.764	Yes
VI	0.111	0.012	0.012	6.761	Yes

Table 4.5 – Strength of correlation between dependent and independent variables.

The 't value' column provides the two-tailed p value used in testing the null hypothesis that the regression coefficient is zero, with the significance column indicating that all variables are statistically significant at the 99% confidence level. The t values are also all positive, indicating the coefficients (not shown) are positive, which means that as each variable increases, the insured loss increases. This is logical for all variables, except perhaps the Vulnerability Index (*VI*). As described in section 4.1.3, the strength of the relationship between *WSE (cube)* is greater than that of the linear, square and exponential *WSE* values. Of the socio-economic factors, the R^2 values suggest that the number of flats (*flats)* and the total value of the exposed properties (*TPV*) are the most important predictors. The Vulnerability Index (*VI*) has a very low R^2, indicating it explains little of the variance shown by the dependent variable, but is significant and so is retained. However, to avoid issues of collinearity all the *WSE* variables, aside from *WSE (cube)* are removed, and regression results from model (i), containing all the other variables, are presented in Table 4.6.

Variable	Unstandardised Coefficients	Standardised Coefficients	t value	Significant (at 99%)
Constant	8182.869		6.565	Yes
RES	-5.93410^{-4}	-10.017	-25.083	Yes
Semi	$3.595\text{x}10^{-3}$	4.521	23.233	Yes
Detached	$-3.475\text{x}10^{-3}$	-7.165	-14.120	Yes
Terraced	$3.345\text{x}10^{-3}$	7.634	13.580	Yes
Flats	$2.985\text{x}10^{-4}$	0.142	1.459	No
TPV	$4.399\text{x}10^{-9}$	2.731	8.954	Yes
WSE (cube)	1.178	2.991	12.133	Yes
VI	-10388.706	$-2.020\text{x}10^{-2}$	-3.367	Yes

Table 4.6 - Regression results form model (i)

A notable omission from model (i) is the household number variable (*HH*). At this stage SPSS output suggests that inclusion of *HH* does not significantly increase the performance of the model (i.e. does not contribute to the R^2 value when other variables are included). This can be attributed to the fact that the model already includes all the other property type variables. It should be noted that although household number is excluded from this model it is used in the simplified model in Chapters 5 and 6, since information regarding the numbers of different property types is limited to the period 1990-2005. The simplified model incorporates only *WSE (cube)* and *HH*, which, from Table 4.5, show high predictive capabilities (high R^2 values).

The overall performance of model (i) is assessed through $\check{R}^2$ (adjusted R^2); preferred to R^2 for reasons outlined in section 2.3.4. Model (i) produces a $\check{R}^2$ value of 0.869. All coefficients of all the variables, with the exception of *flats*, are statistically significant at the 99% confidence level. This suggests that the *flats* variable should be excluded from the model.

At this stage it is useful to consider the residuals produced by model (i) (i.e. observed value minus predicted value). Homoscedasticity is the assumption that the residuals are approximately equal for all predicted values. So the plot of residuals against predicted values should result in a rectangular pattern of random points. Figure 4.5 shows a plot of the standardised residuals against the standardised predicted values of model (i).

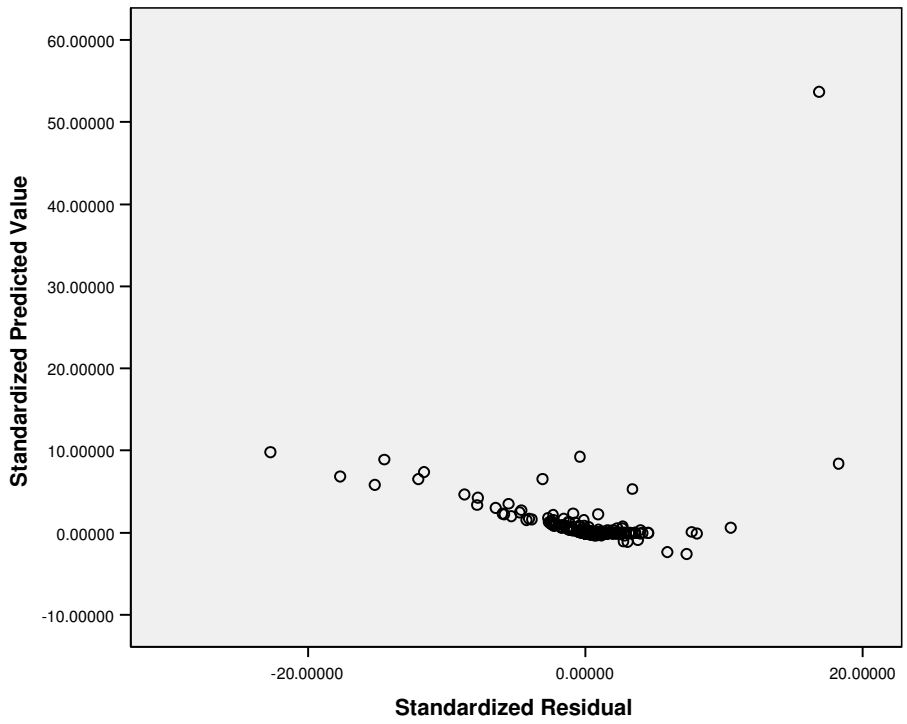

Figure 4.5 - Standardised residuals against standardised predicted values of model (i)

It is important to identify outliers in the data, as these can unduly influence the regression equation, causing it to become unrealistic. To prevent this Tabachnick and Fidell (2001) suggest cases with standardised residuals outside the range of -3 to 3 be rescored, transformed or removed. Figure 4.5 indicates a high proportion of standardised residual values are outside of this range. Furthermore, the distribution of the residuals is not equal for all predicted values, suggesting model (i) is in violation of the assumption of homoscedasticity. These factors suggest that the values of the independent variables should be transformed.

The skewness of the independent variables is assessed, since this can impact the pattern shown by the residuals in Figure 4.5. It is found that all independent variables possess a significant positive skewness in the range of 25-35, except *WSE* (1.2) and *VI* (2.7) and *TPV* (3.8). Tabachnick and Fidell (2001) suggest that the greater the skewness the more severe the transformation should be. For this reason a logarithmic transformation is chosen for *Res, semi, terraced* and *detached*, and a square root for *TPV* and *VI*. When the *WSE (cube)* variable is transformed it becomes negatively skewed, and therefore no transformation is performed. The transformations

had the effect of reducing the skewness to values below 3 for all variables. The transformed variables are termed *ln_Res, ln_semi, ln_terraced* and *ln_detached*, and *rt_TPV* and *rt_VI* respectively.

When the transformed variables are re-entered the correlation coefficients of *ln_Res* and *ln_terraced* are shown to be insignificant, and hence these variables are removed from the model (known as model (ii)). At this point the residuals are considered once more. The standardised residuals of model (ii) are plotted against the standardised predicted values in Figure 4.6.

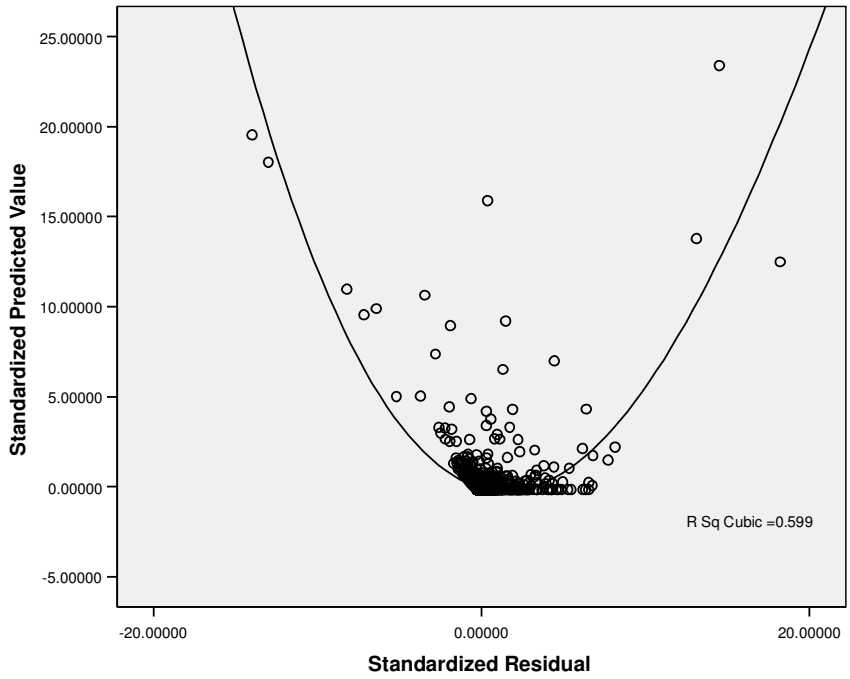

Figure 4.6 - Standardised residuals against standardised predicted values of model (ii)

Although Figure 4.6 indicates that the spread of standardised residuals is narrower in model (ii) than model (i) (Figure 4.5), a number of points are present with standardised residuals outside the range -3 to +3. These outliers, 35 cases in total, equivalent to 1% of the total data, are removed. A number of significant storm events are among these cases, notably 25th January 1990. Also, among these cases are several dates with high losses and no damaging windspeeds. Interestingly a number of these cases fall on the first of the month and it is speculated here that these are falsely reported losses. In these instances perhaps losses occurring at some point in that month, with an unknown date, were entered into the database as if they occurred on the first.

Following the removal of these outliers the plot of the standardised residuals follows a cubic pattern, as suggested in Figure 4.6. Hence the dependent variable (EIG claims) is transformed, using a cube root.

The transformed variables are re-entered in the regression analysis to form model (iii), with the regression results shown in Table 4.7.

Variable	Unstandardised Coefficients	Standardised Coefficients	t value	Significant (at 99%)
Constant	15.971		95.598	Yes
ln_detached	-0.900	-0.516	-2.107	Yes
WSE (cube)	2.484×10^{-6}	0.055	2.522	Yes
rt_TPV	0.295	0.305	1.534	Yes
ln_semi	0.587	0.332	0.650	No
rt_VI	7.279×10^{-2}	0.402	7.929	Yes

Table 4.7 - Regression results for model (iii)

The combination of the removal of some of the outliers, along with the variable transformations, has resulted in a reduction of $\check{R}^2$ value to just 0.368. Although it would appear that performance of the model has reduced, importantly the model no longer violates the assumptions of regression. As evident from Table 4.7 the correlation coefficient of *ln_semi* is no longer significant and therefore is removed from the model. Of concern is the negative coefficient for *ln_detached*. This suggests, somewhat illogically, that as the number of detached houses subject to damaging windspeeds increases, then the insured loss decreases. This raises uncertainty as to whether the *ln_detached* should be retained.

A further assumption of linear regression is that of linearity; that relationships between the independent variables and the dependent variables are linear. A method of establishing whether this is the case for *ln_detached*, is to run the model without *ln_detached* and subsequently plot the unstandardised predicted values against *ln_detached* values.

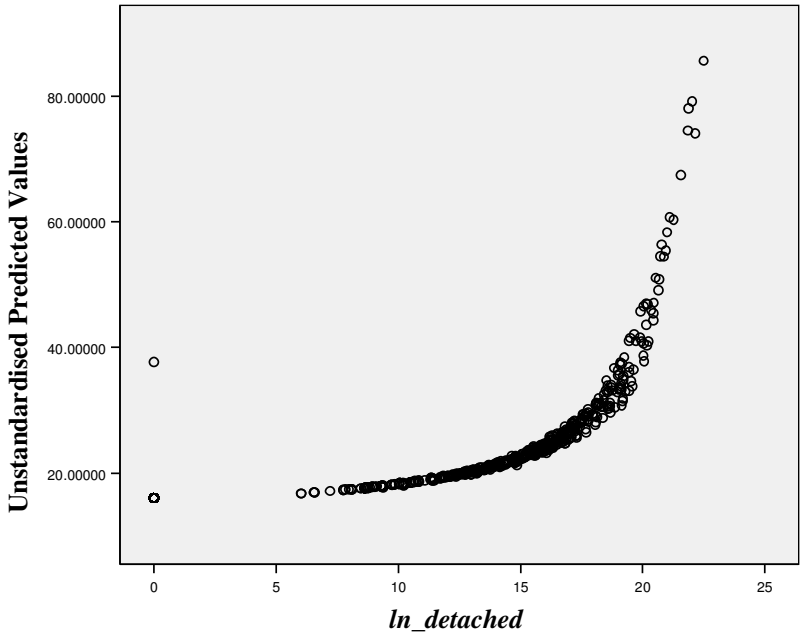

Figure 4.7 – Unstandardised predicted values from model (iii) (excluding *ln_detached*) against *ln_detached*.

Figure 4.7 shows the relationship between the predicted value and *ln_detached* approaches a quadratic one. Therefore, in order to avoid violating the assumption of linearity the square of *ln_detached* is incorporated in the regression analysis to produce model (iv).

A further assumption of regression is that there is no multicollinearity between the variables. Multicollinearity is the situation where two variables are highly correlated with each other, and as such may result in the incorrect or unnecessary inclusion of one in the model. SPSS co-linearity diagnostics of model (iv) are shown in Table 4.8.

Dimension	Eigenvalue	Condition Index	WSE (cube)	rt_VI	rt_TPV	$(ln\_detached)^2$
1	3.405	1	7.58×10^{-3}	2.841×10^{-4}	2.165×10^{-3}	1.209×10^{-2}
2	1.016	1.830	1.402×10^{-2}	1.827×10^{-4}	7.69×10^{-4}	1.500×10^{-2}
3	0.492	2.629	7.734×10^{-2}	1.218×10^{-3}	3.910×10^{-4}	0.204
4	0.070	6.977	0.584	0.151	0.043545	0.732
5	0.016	14.685	0.316	0.844	0.953	3.607×10^{-2}

Table 4.8 - Collinearity diagnostics of model (iv)

Eigenvalues approaching zero indicate the independent variables may be highly intercorrelated, and that small changes in the data could result in large changes in correlation coefficients. The Condition Index, in the second column, is computed as the square root of the ratios of the largest eigenvalue to each successive eigenvalue. The presence of multicollinearity is identified where the Condition Index exceeds 15 and there are two incidents of independent variables with correlations of 0.5 or greater (Tabachnick and Fidell, 2001). The collinearity diagnostics output from SPSS, in Table 4.8, indicate that *rt_VI* and *rt_TPV* are very close to meeting these criteria. The effect of removing each of these variables from the model in turn results in the overall $\check{R}^2$ changing from 0.270 to 0.268 on both occasions. Since the $\check{R}^2$ altered negligibly and in order to be certain that there is no multicollinearity it is decided one of the variables should be removed. The two sets of collinearity diagnostics produced when each variable is removed and the model is run did not indicate the presence of any multicollinearity, and the eigenvalues are fairly similar. The Condition Index values are slightly lower when *rt_TPV* is included. The plot of residuals against predicted value reveals slightly lower standardised values when *rt_TPV* is included. Given that the Vulnerability Index perhaps has more uncertainty surrounding it than *TPV* (as described in section 4.1.2), and the reliability of the model is perceived to be greater if one variable is removed, it is decided that *rt_TPV* be retained, and *rt_VI* discarded. It should be noted that when *ln_semi* was included in the model, collinearity diagnostics revealed high intercorrelation with *ln_detached*. This is logical when one considers that the combination of these property types account for over 50% of the overall household number. This suggests that as the number of one property type increases in a particularly postcode sector, the number of the other decreases. Hence the decision to remove *ln_semi* is reinforced.

With the removal of *rt_VI* the final model is established, which does not violate any of the assumptions of regression, and is left with three independent variables in the following form:

$$\text{EIG Claims} = (1.987\text{x}10^{-6}\ \textit{WSE (Cube)} + 1.360\text{x}10^{-6}(\textit{Total Value})^{0.5} + 2.40\text{x}10^{-2}\ (\textit{ln\_detached})^2 + 16.03)^3$$

The normal probability plot of the final model (Figure 4.8) shows only minor deviations from a normal distribution, suggesting the model does not violate the assumption of normality.

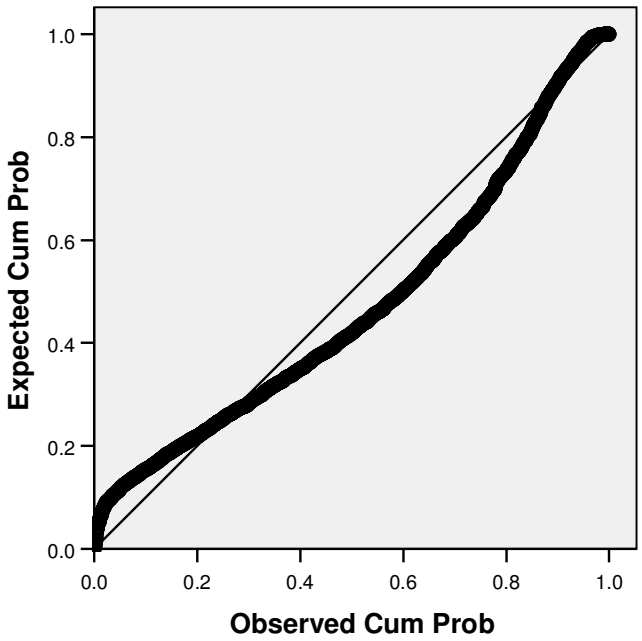

Figure 4.8 - Normal probability plot for final model

While high R^2 values were found at the beginning of the regression analysis (Table 4.5), inclusion of several of these variables violated a number of assumptions regarding linearity, multicollinearity and homoscedasticity. Through the regression analysis several independent variables were transformed, and a number still found to be unsuitable to be included in the model. The $\check{R}^2$ of the final model is subsequently much reduced, at only 0.268.

4.3 Model Verification

The regression model developed in section 4.2 is used to produce estimates of daily EIG insured loss for the period 1990-2005. Estimates are compared with actual EIG loss data and a R^2 value of 0.78 is found. However, this value may be misleading given that two thirds of the data used in the verification were utilised to develop the regression equation in the first place. For this reason, the model is verified against independent loss data from the period 2000-2005; a period from which data were not included in the calibration of

the model. Although this period represents only 6 years, it should be sufficient to provide a fair assessment of the model performance.

Overall, the model underestimates actual losses significantly, with the mean daily loss under-predicted by nearly £10,000 (or 60%). The R^2 value for the entire 6-year period is 0.37. Figure 4.9 shows the predicted loss values plotted against actual values, with the x=y line illustrating the substantial underestimation of losses, particularly for large loss events (certain events are noted on the graph). It should be noted that these figures are adjusted for inflation and also for changes in the insured density and average sum insured per policy as suggested by Munich Re (2002b). The underestimation of the model may be due to the removal of some high loss events during model development, which has the effect of raising the mean actual loss, while lowering the model loss mean.

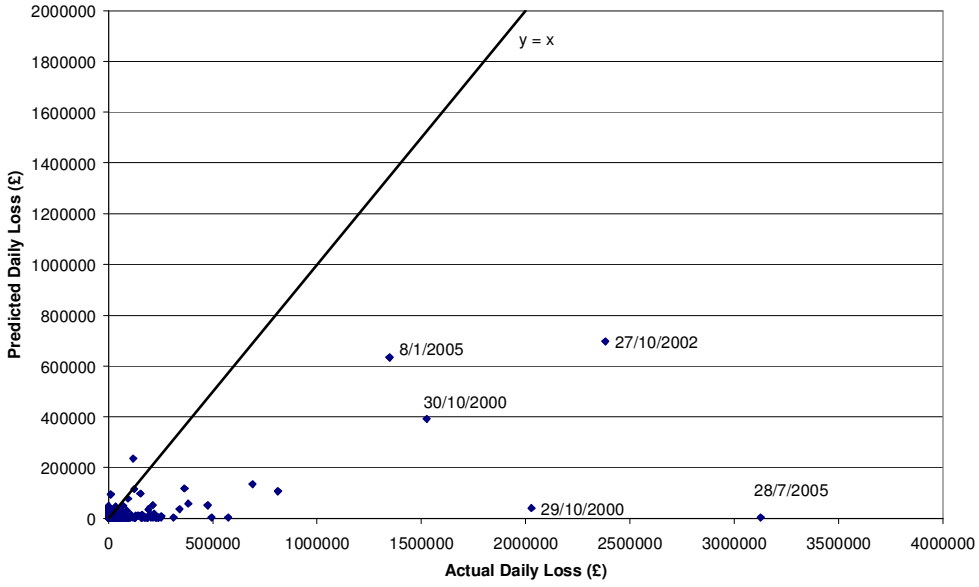

Figure 4.9 - Actual daily EIG losses plotted against model predicted values for the period 2000-2005 (Adjusted to 2005 £ values for inflation and changes in insured density and average value insured per policy following Munich Re (2002b)).

Table 4.9 suggests that the seasonal performance of the model is greatest in spring, with an R^2 value of 0.69 and the mean predicted value only 23% lower than the actual mean.

	R^2	Actual Mean Claim (£)	Predicted Mean Claim (£)	Actual Standard Deviation (£)	Predicted Standard Deviation (£)
DJF	0.66	17464	9215	78838	30978
MAM	0.69	6610	5078	32343	6761
JJA	0.00	17310	4198	138215	690
SON	0.65	23744	7002	152848	34130

Table 4.9 - Performance of the windstorm loss model on a seasonal basis for the period 2000-2005.

Despite R^2 values exceeding 0.65 in both winter and autumn, times that losses are at their highest, the model significantly underestimates daily losses by 47% and 71% respectively. This suggests that while the seasonal variance is reasonably well captured, the model is unable to predict the full extent of larger events. On a monthly basis the model performance is highest in March (R^2 = 0.77), followed by January (R^2 = 0.76), although the model still under-predicts the mean loss by 41% and 52% respectively. It should be noted that during the model development no transformation of windspeed data was undertaken, as with other variables, to remove the positive skew. This will likely result in skill inflation, with slightly elevated R^2 values reported here.

Figure 4.10 shows the quarterly losses predicted by the model, alongside the actual values.

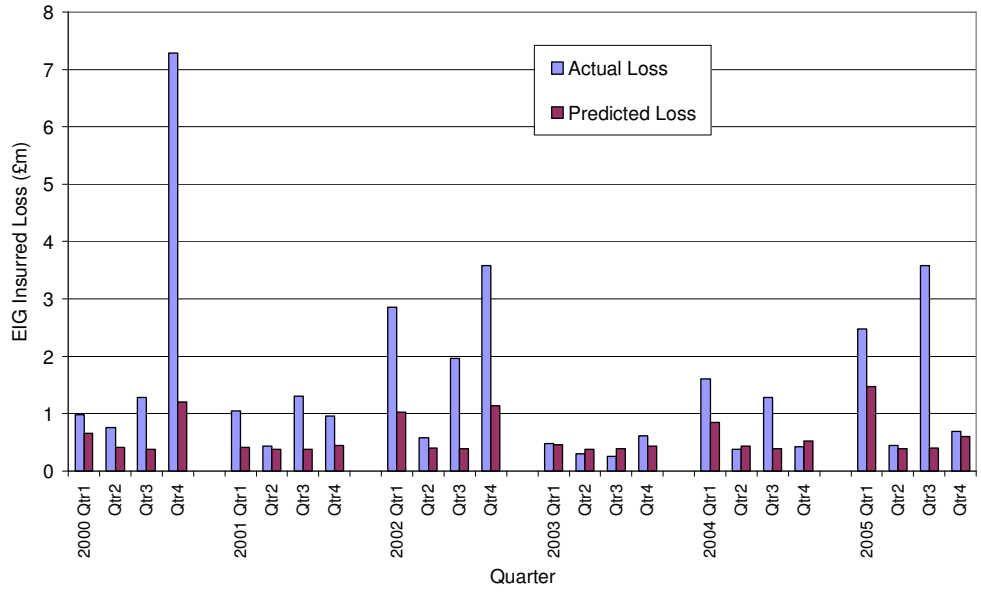

Figure 4.10 - Predicted quarterly losses (purple) and actual EIG losses (blue) for the period 2000-2005. Values are adjusted to reflect inflation and changes in insured density and average value insured per policy following Munich Re (2002b).

The large discrepancy between predicted and actual loss values in the third quarter of 2005 (shown in Figure 4.10) is a direct result of the tornado which touched down in Birmingham on 28th July in that year. Over 85% of EIG loss in that quarter is recorded on that date, despite the windspeed exceedance value for the whole of Great Britain calculated as zero. This illustrates the ineffectiveness of the model when considering small scale events. However, although the project is concerned with windstorms, of which tornadoes could be considered a class, the main focus is on synoptic scale winter features. The model will also be relatively ineffective when considering mesoscale features such as gusts associated with thunderstorms, which often occur in summer months. The performance of the model is greatest in winter and autumn periods, as described above, suggesting its suitability as a model for predicting losses relating to extratropical cyclones, rather than mesoscale events such as thunderstorms and tornadoes.

Figure 4.10 illustrates the underestimation of losses by the model, most notably in the fourth quarter of 2000. During this period losses are reported on every day in the EIG claims database, with an average daily loss of nearly £80,000 (values quoted here are adjusted to reflect inflation and changes in insured density and average sum insured per policy following Munich Re (2002b)). The largest loss event occurs on 29/30th October, with over £3.5m actual losses (£400,000 predicted loss for the corresponding period). Over the course of the next four days in excess of £1m losses are reported despite no measurements of damaging windspeeds in the 43-station network in that period.

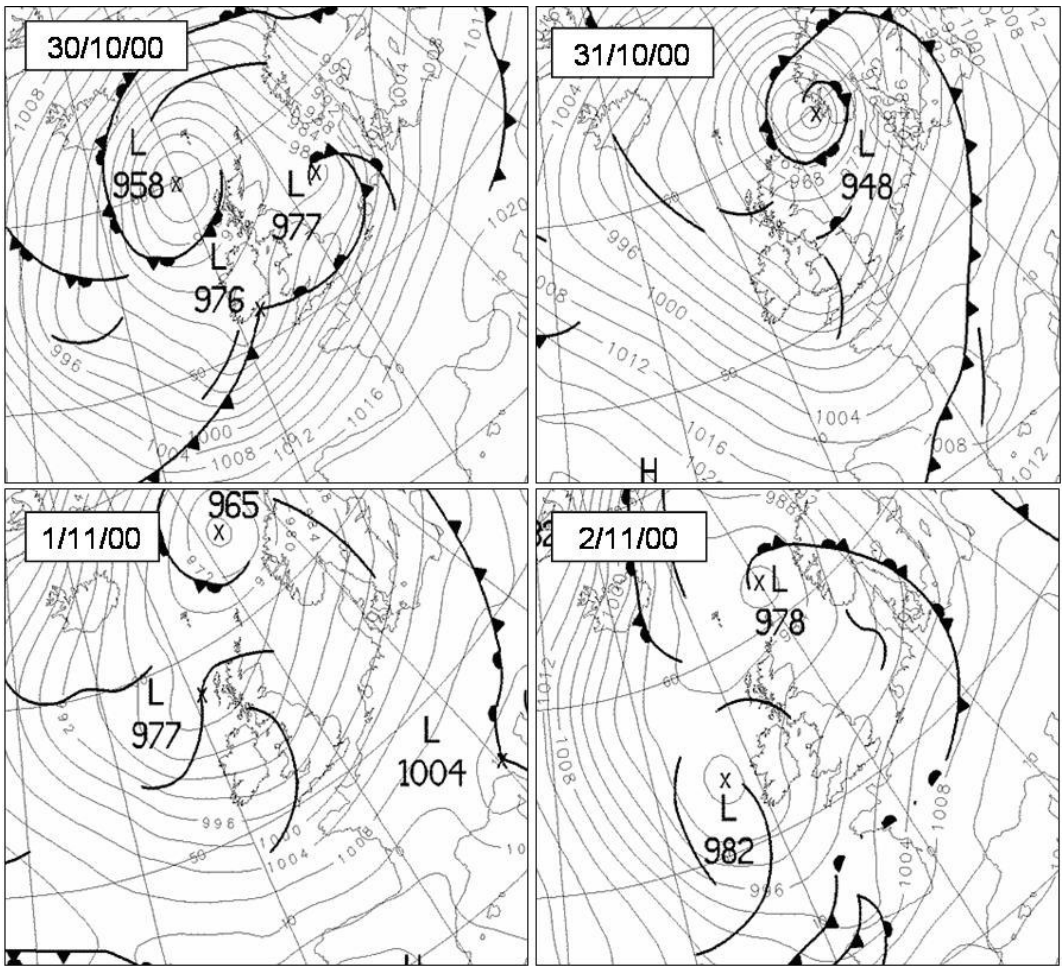

Figure 4.11 - Mean sea level pressure at 00:00 GMT on 30th October (top left), 31st October (top right), 1st November (bottom left) and 2nd November (bottom right) 2000. Source: www.wetterzentrale.de

Figure 4.11 shows the mean sea level pressure over North West Europe between 30th October – 2nd November 2000, with the low pressure systems producing damaging winds over much of the UK on 29th-30th October evident in the top left panel. Over the course of the next 3 days these systems move away, leaving a slack pressure gradient over the UK (indicated by the increasing spacing between isobars), suggesting calmer, more settled conditions. Windspeeds from the observational dataset suggest that during the period 31st October- 2nd November DMGSs are close to average for that time of year, with no stations recording damaging windspeeds. The fact that claims were reported during this period suggests errors in their assignment to the correct date. This is not an uncommon feature in the EIG claims database, with large number of claims assigned to days following large events on several occasions. Issues over the validity of these claims are discussed in

section 4.1.1 and 4.2, as well as in section 2.3.2, with the subsequent effect on model performance discussed below.

One of the assumptions made during the development of the windstorm loss model was that damage, and subsequent insured loss, only occurs when the windspeeds exceed a certain threshold. The final model includes a constant, which implies that even with no damaging windspeeds (*WSE (cube)* = 0) wind-related domestic property insured losses still occur. This reflects the data utilised in the development of the model; real insured loss data, accompanied by their own uncertainties. During the period drawn on for model development (1990-1999), there are several days when no postcode sector experienced windspeeds in excess of the local damage threshold. However, there are losses recorded on a high proportion of those days. Indeed on only just over 500 occasions (out of 3652) are no losses reported, despite there being nearly 3000 days when no damaging windspeeds were recorded anywhere in Great Britain. If the verification is carried out using data for days only recording damaging windspeeds (*WSE (cube)*>0) in the period 2000-2005, the overall model performance improves (R^2 = 0.63, with winter and autumn values improving to nearly 0.70). A consideration during the development of the loss model was to only include days on which damaging windspeeds accompanied insured losses. However, this was rejected due to the relatively low number of occasions that this occurred, and the potential for it to unduly bias the model. However, the verification process suggests that the model would perform more accurately were this the case. Further development of the model would therefore benefit a claims database with all losses correctly assigned to the correct date.

It must be noted that from an insurance company's perspective, an operational model would only likely be run in the event that damaging windspeeds are recorded. Hence from an operational standpoint, the model performance is reasonable (R^2 = 0.63), although the daily losses are still significantly underestimated (mean predicted loss is £21,000 compared with the actual value of £53,000).

As described in section 4.1.1 the ratio of EIG claims to industry-wide losses increased markedly in 2005. Since the information is not available regarding the total value insured and the number of policies issued by EIG, it is unclear whether their exposure increased in 2005. The assumption that EIG's exposure did not change above the national average had to be made in this study since no other information was available. This is not an unreasonable assumption following discussions with EIG. The 2005 annual EIG loss is only slightly above average for the period 2000-2005, but the relatively high ratio of EIG losses to industry-wide losses in 2005 may adversely affect the performance of the model. For this reason model performance for the period 2000-2004 was assessed, with a resultant R^2 value of 0.58. This suggests that the EIG exposure most likely changed in 2005, relative to any industry-wide shifts. This highlights the potential of the model, and indeed the improvement which could be made if information regarding exposure became available.

4.4 Conclusion

The second research aim of this project, outlined in section 1.6, is to develop a deterministic relationship between wind-related insured domestic property losses and meteorological variables. An operational windstorm loss model is developed in this chapter based on this relationship, which incorporates socio-economic aspects to quantify exposure and vulnerability of the domestic property stock to the windstorm hazard. The model provides estimates of wind-related insured domestic property losses on a daily basis for Great Britain, but, for reasons described in section 4.2, unfortunately has no spatial component.

In the published literature regarding loss models several are developed using a limited number of storm events (Dorland *et al.*, 2000; Hanson *et al.*, 2004). While Klawa and Ulbrich (2003) use a continuous record of wind data in the development of their windstorm loss model for Germany, calibration is carried out using annual loss values, and the model contains no spatial component. Unlike these three studies, this project benefits from the availability of daily loss data from EIG at very high spatial resolution (postcode sector). It was

hoped that the high temporal and spatial resolution of both the insurance and meteorological data would facilitate the development of a windstorm loss model capable of reproducing loss patterns of individual storms events. Unfortunately, the insurance information data carried with them no information regarding the exposure of EIG's domestic property portfolio, such as number of policies written or total value insured. As a result, an analysis undertaken in section 4.2 revealed no strong correlation between daily losses and damaging windspeeds on a postcode sector level (R^2 values less than 0.1). However, when claims are aggregated to Great Britain as whole, a very strong correlation is shown with damaging windspeeds (R^2 values in excess of 0.85). Subsequently, model development proceeded without including a spatial component; losses for the whole of Great Britain are considered only.

The unique windspeed dataset established in this project (Chapter 3), made it possible to establish a relationship between windspeed and wind-related insured loss. This strong correlation, for Great Britain as whole, is shown in Table 4.3. It is found that Daily Maximum Gust Speed (DMGS) and not daily mean windspeeds exhibit a stronger correlation to wind-related insured losses for Great Britain as a whole, and also at the postcode sector level. Furthermore, findings in section 4.1.3, suggest that a local threshold exists which gustspeeds must exceed in order for damage to occur. Percentile values of the local DMGS are shown to be more appropriate as a threshold than absolute values, with results suggesting the 98th percentile value is the most suitable. This finding is in line with Schwierz *et al.* (in submission), Klawa and Ulbrich (2003) and Pinto *et al.* (2007). The relationship between windspeed and losses (or damage) proved to be nonlinear, as with other studies (Rootzen and Tajvidi, 2001; Klawa and Ulbrich, 2003; Munich Re, 2002b), with a cubic relationship producing the strongest correlation. Thus, this section justifies the terminology of DMGSs in excess of the local 98th percentile values as "damaging windspeeds"; a term used repeatedly throughout the project.

The final windstorm loss model includes variables containing information on the number of detached properties, as well as the total value of all the properties, impacted by damaging windspeeds. However, it is shown in

section 4.2.1 that the correlation between the number of households and insured losses is a strong one. Given that information regarding the variables included in the final model is not available for periods outside of 1990-2005, while household number data are, this variable (*HH*) is included in the simplified loss model utilised in Chapters 5 and 6. It is worth noting that the correlation between household number and the number of detached properties, as well as total property value, is also strong. Through the inclusion of household number an appreciation of the exposure of the domestic property stock in Great Britain to the windstorm hazard is incorporated. In the loss model developed by Dorland *et al.* (2000) for the UK, based on October 1987 and January 1990, the number of properties was also used as a predictive variable. Although Klawa and Ulbrich (2003) used population numbers in their model, these are highly correlated to household numbers. These studies, along with results presented here, confirm that including household numbers in the simplified windstorm loss model is appropriate.

The development of the windstorm loss model (described in section 4.2) utilises data from the period 1990-1999, with the model subsequently verified (in section 4.3) against data from 2000-2005. Unlike previous studies (Dorland *et al.*, 2000; Hanson *et al.*, 2004; Klawa and Ulbrich, 2003) this model is evaluated using data not included in the calibration process. Furthermore, the model is verified against multiple storm events. This rather more stringent testing partially explains the relatively poor performance of the model (overall $R^2 = 0.37$). However, at the outset of the project the aim was to development an *operational* loss model, suitable for use by an insurance company. As such, the model would not be run on days without damaging windspeeds. If the model is verified against losses reported on days experiencing damaging windspeeds only, the performance improves markedly ($R^2 = 0.63$). Overall, the model significantly underestimates losses, by a figure approaching 60%. The performance of the model may be compared to the overestimation (underestimation) of relative residential property damage by 14% (43%) modelled by Dorland *et al.* (2000) for October 1987 (January 1990). Meanwhile Hanson *et al.* (2004) managed to produce predicted losses to within 3% for the same two periods. Although model performance here

appears inferior to these, it must be emphasised once more that a significantly higher number of storms are included in the verification (not to mention the development) stage. Klawa and Ulbrich (2003) found a strong correlation of predicted to observed annual German losses ($R^2 = 0.96$) over 28 years, which again appears favourable to the performance of the model represented here. However, it is important to appreciate that the calibration and verification periods here do not overlap, as in Klawa and Ulbrich (2003). In fact if the model performance is assessed for the period 1990-1999, a much stronger correlation is found between predicted and observed daily loss values ($R^2 = 0.87$).

During winter (a period with the greatest proportion of annual loss), the model performance is at its highest. An R^2 value of 0.66 is found for winter, although losses are still underestimated by 40%. With over 70% of EIG loss occurring in winter and autumn, the predicted losses correlate with actual losses with an R^2 value of 0.61, although again losses are significantly underestimated (by nearly 60%). This suggests that for periods suffering the greatest loss, the model performs reasonably well, which is highly desirable for an operational loss model.

One of the primary reasons that it was not possible to derive a more robust relationship between losses and meteorological variables at the postcode sector level was the lack of information regarding the exposure of the EIG domestic property portfolio. Section 4.2 describes the attempt to derive a relationship at this level, which ultimately results in the inability of the model to produce loss estimates with the spatial resolution originally desired. The three models developed by Dorland *et al.* (2000), Hanson *et al.* (2004) and Klawa and Ulbrich (2003) incorporate information on the total value insured, and in the case of the former two studies, information on the number of policies written. A knowledge of the exposure enables a true assessment of the severity of a storm event. It facilitates the identification of regions which are heavily impacted by a storm in terms of losses, rather than regions with above average insurance coverage (both in terms of insured sums and number of policies). All commercial catastrophe modelling companies incorporate these elements through an intimate understanding of their client's exposure. These

companies are privy to information regarding high resolution spatial variations and long-term temporal changes in exposure which, due to commercial sensitivity, are not made available to academia. That the windstorm loss model presented here performs reasonably well for Great Britain as whole, at such a high temporal resolution, highlights its potential for accurately predicting losses at a higher spatial resolution. If information regarding the EIG exposure could be incorporated, it is confidently anticipated that a spatial component could be added to the model.

An additional factor hampering model performance are the errors in assigning losses to the correct dates in the EIG database. A closer examination of the EIG claims database identified several occasions where it is likely that losses were attributed to the wrong date (e.g. days following the 29/30th October 2000 windstorm). Furthermore, it is postulated here that several cases where an exact date for the damage is unknown, it is entered into the database as occurring on the first of the month. Not only will these features hinder model development, but they will also affect the verification process. This study is not alone in finding inconsistencies such as these in a claims database, with Dorland *et al.* (2000) and Hanson *et al.* (2004) encountering similar problems.

The assumption is made in section 4.1.1 that the EIG exposure, over the course of the study period, does not change relative to industry-wide shifts (i.e. the total sum insured and number of policies written by EIG relative to the industry-wide values did not vary from year to year). Following correspondence with EIG, this is a reasonable assumption, and one which had to be made in order that the loss model could be developed. Subsequent comparisons with industry-wide loss data suggested this assumption is valid for the period 1990-2004, but the ratio of EIG losses to industry-wide losses increases significantly in 2005. Furthermore, during the verification process in section 4.3, it is shown that the correlation is much greater between predicted losses and observed losses in the period 2000-2004 compared with 2000-2005. Therefore, it is postulated here that changes in the EIG exposure do occur in 2005. This illustrates the importance of having an understanding of the exposure, once again highlighting potential model improvements which could be undertaken if exposure information became available. It is likely that

these improvements would increase performance as well as enabling the model to perform at a higher spatial resolution.

While the development of a windstorm loss model partially achieves the research aim, the fact that the model has no spatial component means it is not fully accomplished. However, the model performs well on an operational basis (i.e. on days experiencing damaging windspeeds), predicting daily losses for Great Britain as whole. This suggests that were a similar methodology employed, with the appropriate exposure data, a spatial component could be added. As with all "real world" data, insurance claims data have been shown to contain many uncertainties, which are incorporated into the loss model and subsequently impact upon its performance. As with all scientific endeavours, the model would benefit from improved raw input data, both in terms of quality and quantity, with the attribution of claims to the correct windstorm event highly desirable. It will not have escaped the reader's attention that the citations in this chapter largely refer to the same limited number of studies. This does not reflect academic interest in the topic of windstorm loss modelling; rather it underlines the fact that the availability of data to complete such a study is very limited due to its commercial sensitivity.

More positively, the application of the windspeed dataset, established earlier in this project, illustrates its potential as a powerful tool for use in applied arenas. This extensive dataset of windspeeds and gustspeeds is shown here to be a reliable foundation on which to develop a windstorm loss model. Future work refining the model, by adding a spatial component, would no doubt benefit from the existence of this dataset.

Chapter 5: Quantifying Historical Windstorm Losses in Great Britain

An analysis of the historical wind regime of the UK is presented in Chapter 3, along with a description of the temporal and spatial trends of damaging windspeeds. In this chapter the observed and PRECIS-Re windspeed datasets are utilised to identify periods of significant wind-related insured loss, and individual high impact windstorm events in Great Britain[1]. As highlighted in section 1.2.2 the trend in wind-related insured losses in the UK is difficult to establish due to limited data. Industry-wide data are only available for the period 1987-2005, while windstorm losses are only separated from all weather-related losses from the fourth quarter of 1997 onwards. These data are aggregated on a quarterly basis and contains no spatial information. This chapter presents a simplified windstorm loss model, which is used in conjunction with the comprehensive windspeed information to extend the record of windstorm related insured losses back to 1959. Due to the relatively high spatial resolution of the windspeed data collated in this project, it is also possible to compare the spatial distribution of model losses of historic windstorms occurring between 1959 and 2005; something not currently possible with freely available insured loss data.

It should be noted that a robust relationship between windspeeds and insured loss is developed in Chapter 4, during the development of the windstorm loss model. A simplified model is utilised in this chapter as sufficient socio-economic data (namely property sales prices and numbers of different property types) are not available dating back to 1959, and extrapolation of available data to that year is inappropriate. Additionally, the simplified model is utilised once more in Chapter 6, where insured losses associated with future UK wind regimes in 2021-2050 and 2071-2100 are quantified. Therefore, the socio-economic variables incorporated in the simplified model are kept to a minimum. This avoids the inclusion of projections of these variables for 2021-2050 and 2071-2100, which could further increase the uncertainty in the results.

[1] While the windspeed data presented in Chapter 3 concerns the whole of the UK (England, Scotland, Wales and Northern Ireland), claims data and census data used to develop the simplified loss model in this chapter concern Great Britain only (England, Scotland and Wales).

The simplified loss model used in this chapter is introduced in section 5.1. Observed and PRECIS-Re wind datasets, along with household numbers, are utilised in order to include elements of exposure and vulnerability of the Great Britain domestic building stock to the windstorm hazard. Insurance data used to calibrate and verify the model are described section 2.3.2, and includes industry-wide data (from the ABI) from the fourth quarter of 1997 to the end of 2005 on a quarterly basis. In addition this project benefits significantly from the provision of more than 40000 individual Ecclesiastical Insurance Group (EIG) wind-related claims from the period 1990-2005.

The observed wind dataset is used in section 5.2 in order to produce estimates of quarterly losses for the period 1980-2005. However, with the benefit of the extended windspeed dataset established in Chapter 3 (i.e. the PRECIS Re dataset) it becomes possible to produce similar quarterly loss estimates back to 1959. These results are presented in section 5.3. The ability of the PRECIS-Re dataset to capture the variability in observed damaging windspeeds is discussed in Chapter 3. A correction factor is established in section 5.3, in order that damaging windspeeds in the PRECIS-Re dataset accurately reflect those in the observational record.

Dating back to 1959, individual windstorm events are identified in section 5.4 which are likely to have produced large insured losses. An independent record of storms in the UK is utilised to establish whether large insured loss events necessarily correspond to meteorologically severe windstorms. Spatial patterns of model losses for different events are presented to demonstrate the regional variability in windstorm losses across Great Britain. The spatial variability of individual events is put into context with an analysis of the long term mean distribution of windstorm losses, identifying locations more prone to windstorm losses than others.

5.1 A simplified model to estimate windstorm losses

As discussed in the opening stages of the this chapter, the aim here is not to derive a robust relationship between windspeeds and insured losses; that aim

is achieved in the development of an operational windstorm loss model described in Chapter 4. Socio-economic data, used in the windstorm loss model, are not available for the entire time period considered here (1959 onwards), and hence a less sophisticated model is utilised.

During the development of the windstorm loss model it was shown that only the top 2% of local Daily Maximum Gust Speeds (DMGS) result in damage. Furthermore, it was shown that insured loss is proportional to the cube of the gust speed. In order to quantify the exposure of domestic properties to the windstorm hazard the number of households impacted by damaging windspeeds is included. This variable is shown to be very strongly correlated to losses in section 4.2.1. Information on household numbers is available from census data.

Hence for the period 1959-2005 the insured Loss Potential can be estimated by a knowledge of the wind regime and household number, and can be written thus:

$$\text{Loss Potential} = \sum_{PCS=1\ldots i} HH\ (PCS) \left(\frac{DMGS\ (PCS)}{98^{th}\ P\ DMGS\ (PCS)} - 1 \right)^3$$

Where HH = Household Number
PCS = Postcode Sector
DMGS = Daily Maximum Gust Speed

Positive Loss Potentials only are considered, i.e. it is assumed loss occurs only when the DMGS exceeds the local 98th percentile value. In order to produce estimated loss values the following regression equation is developed using the actual ABI and EIG loss data and the calculated Loss Potentials;

$$\text{Loss} = (\text{Loss Potential}) \times \beta + k$$

Where β = regression coefficient
k = constant

Loss Potentials are calculated for each 24-hour period and aggregated to quarterly[2] periods from 1980 to 2005. The quarterly values of Loss Potential

[2] Quarterly periods refer to financial quarters (January to March, April to June, July to September and October to December), since losses are published on this basis.

are regressed against EIG loss data (1990-2005), and ABI loss data (1997-2005). This provides the regression coefficient (β) and constant (*k*).

Despite being a fairly simple relationship, Klawa and Ulbrich (2003) showed that a similar one (population numbers were used instead of household numbers) could reliably estimate annual wind-related insured losses in Germany.

The EIG and ABI data are already adjusted to 2005 values to allow for inflation as described in section 2.3.2. However Munich Re (2002b) estimate that insured value in western Europe increased by a factor in the range of 1.8-2.0 between 1990 and 1999. This increase is based on increases in insurance density and average sum insured per policy, which Munich Re (2002b) suggest could amplify losses by 7-8% annually (which includes inflation). For this reason the EIG and ABI data are adjusted from original values to 2005 values using an annual figure of 7.5%, before being used in the calibration and verification of the model. It should be noted therefore, that all loss estimates presented are in 2005 values. These factors should be considered when comparing loss estimates with absolute losses reported at the time of historic windstorm events.

Household number information incorporated into the simplified model is taken from the 1971, 1981, 1991 and 2001 censuses. Although household numbers are not available for the interim years, values are estimated using a simple linear extrapolation on a postcode sector basis. The greatest increase in overall household numbers in Great Britain occurred between 1991 and 2001 (from just over 22 million to nearly 24.75 million). This represents an annual increase of 1.2% during this period. A similar increase is seen in the household number between 1971 and 1981 (annual increase of 1.1%). For comparison an annual increase of 0.4% was seen between 1981 and 1991.

The impact of varying household number on Loss Potential is not a straightforward relationship, since household numbers in different postcode sectors do not follow a uniform fluctuation rate. For this reason household numbers are estimated for each postcode sector in the interim years between

censuses using linear extrapolation. No extrapolation is attempted for the period 1959-1970 and 2002-2005, since information is unavailable for these periods. During these periods, the household numbers and distribution are considered to be identical to those for 1971 and 2001 respectively. For this reason, loss potential and loss estimates for 1959-1970 may be somewhat over inflated, while those for 2002-2005 may be underestimated.

The degree to which estimates of losses may be over (under) estimated in the 1959-1970 (2001-2005) period is assessed by analysing loss estimates with and without incorporating changing household numbers. Quarterly estimates for the period 1971-2001 with a stationary household number (the 2001 value was used) were compared with estimates with a dynamic household number. Unsurprisingly, loss estimates tended to be higher with a stationary household number, by an average of 2.2%. This figure exceeded 10% on two occasions (16.4% in the first quarter of 1974 and 13.9% in the fourth quarter of 1979), while remaining below 5% for the most part (109 quarters of the 120 considered). The increase in overall household number in the period 1971-2001 is 30% (from just under 19 million to just under 24.75 million). Therefore, the over (under) estimation of losses for the period 1959-1970 (2002-2005) is likely to be minimal, given that the change in household number is likely to be significantly lower than the 30% increase seen between 1971 and 2001.

5.2 Estimating historic windstorm losses with observed wind data

Using the equation described in section 5.1 modelled industry-wide (ABI) and EIG quarterly wind-related losses are calculated and shown alongside actual losses in Figure 5.1 and Figure 5.2 respectively. It should be noted that these model loss estimates, and indeed all that follow, can be considered relative to one another with no correction necessary (e.g. inflation or changes in average sum insured per policy). All loss estimates are in 2005 pound values as a result of the methodology utilised for their calculation. For the same reasons, loss estimates should not be taken as absolute losses suffered in a certain period (i.e. are not directly comparable to values published elsewhere).

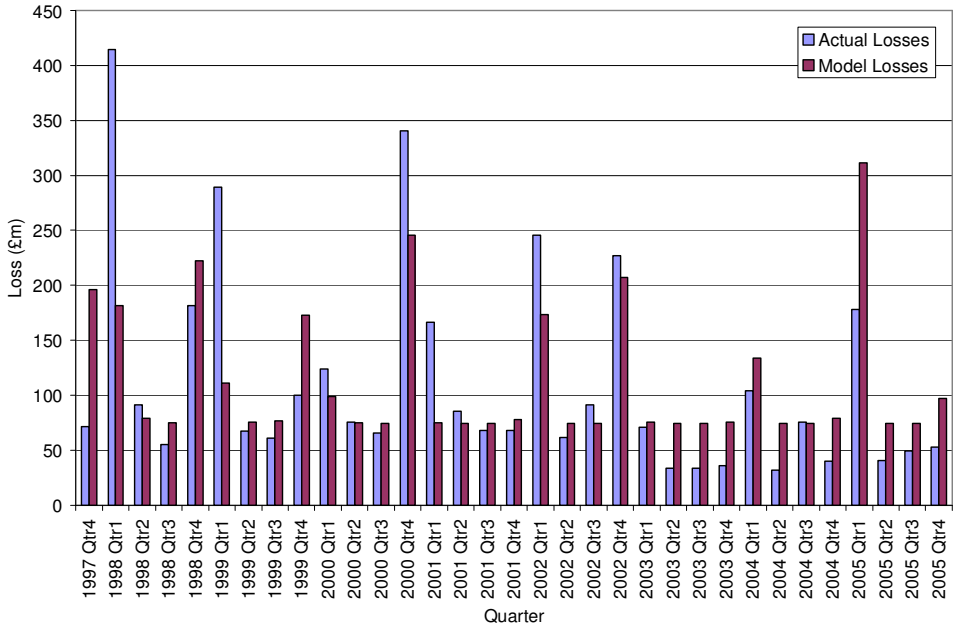

Figure 5.1 - Actual (blue) and modelled (purple) industry-wide quarterly wind-related insured domestic property losses (1997-2005).

Modelled industry wide loss estimates, shown in Figure 5.1, suggest the model tends to underestimate the larger loss quarters, while overestimating quarters with lower loss totals. Overall, the timeseries of modelled losses and actual losses are reasonably well correlated (*r* value of 0.66).

Model quarterly losses suffered by EIG due to wind-related damage to domestic properties for the period 1990-2005 are compared to actual losses in Figure 5.2.

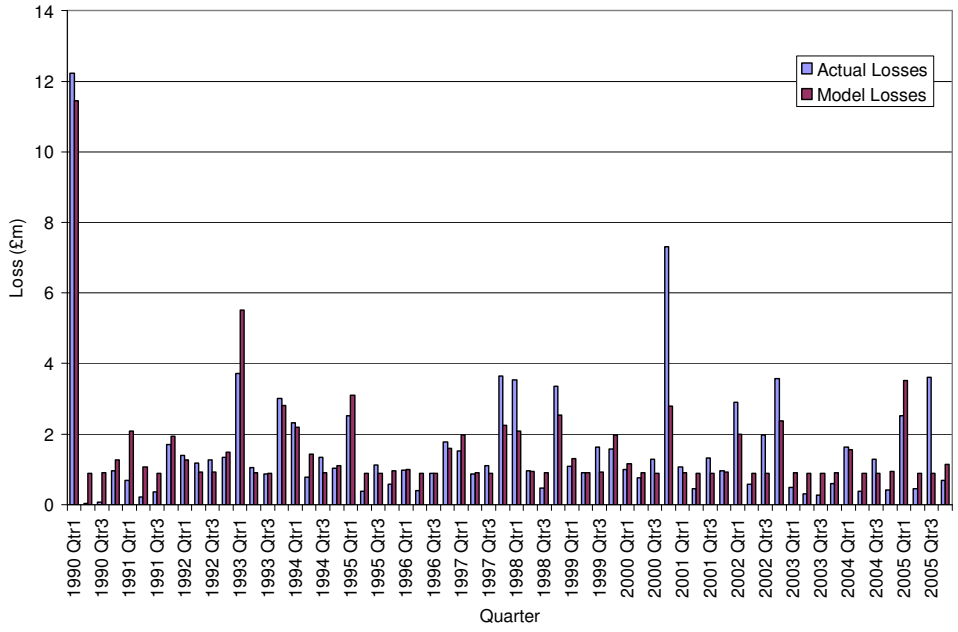

Figure 5.2 - Actual (blue) and modelled (purple) EIG quarterly wind-related insured domestic property losses (1990-2005).

The model producing EIG loss estimates outperforms that for industry–wide loss estimates, with model losses producing an *r* value of 0.87 (compared with 0.66) when compared to actual losses. In the first part of the time series (1990-1997) the model losses are more strongly correlated with actual losses (r = 0.96), than in the second half (1998-2005) (r = 0.66). The *r* value for this later period mirrors the value the industry-wide model produces over a similar period (quarter 4, 1997 to 2005). The high *r* value for the earlier period is likely a direct result of the very large loss in the first quarter 1990. The model tends to underestimate losses towards the end of the time series (1998 onwards) and overestimate losses in the earlier part of it (1990-1997). For this reason a separate regression coefficient and constant was found for the period 1990-1997 and 1998-2005. However, this had a negligible effect on the overall correlation between the timeseries of model estimates and actual losses, and is therefore discarded. This discrepancy seen between the first and second half of the timeseries may be the result of a change in the exposure of EIG's domestic property portfolio. Unfortunately, details regarding the number of policies written and value of insured property are not available. However, as described in Chapter 4, shifts in the EIG portfolio can be considered minimal. This suggests that other aspects may be playing a role in producing higher than expected losses in the later half of the timeseries. A likely source of error

could lie in the adjustment of losses carried out prior to the construction of the model. Annual adjustments of 7.5% of original claims values were made for the entire period, based on data from Munich Re (2002b) from the period 1990-99. It may be possible that this figure may have dropped after 1999, subsequently resulting in artificially high loss estimates past that point.

It is noticeable from Figure 5.1 and Figure 5.2 that variation in the second and third quarters (i.e. periods of minimal losses) is not captured particularly well. Figure 5.3 shows the quarterly EIG losses plotted against the corresponding Loss Potentials for Quarter 1 (red), Quarter 2 (green), Quarter 3 (purple) and Quarter 4 (blue) for the period 1990-2005. The correlation between actual losses and calculated Loss Potentials are indicated by R^2 values.

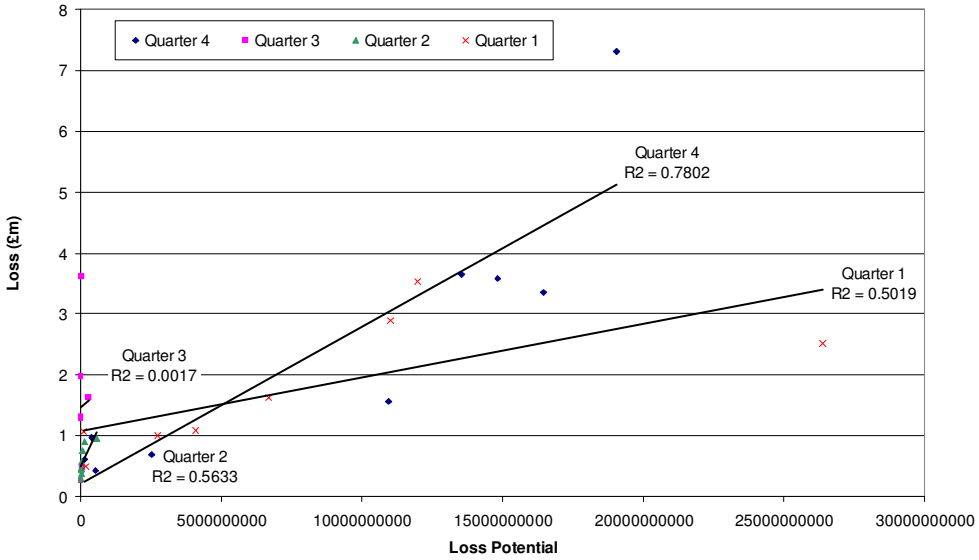

Figure 5.3 – EIG quarterly wind-related insured domestic property losses against Loss Potential (1990-2005)

A similar pattern is seen when industry-wide losses are plotted against Loss Potentials (for the period 1997-2005), although Quarter 3 losses displays a downward trend with increasing Loss Potential. The R^2 values for the industry-wide data are 0.088, 0.329, 0.013 and 0.685 for Quarters 1-4 respectively. The slopes of the linear trend lines in Figure 5.3 for Quarters 1 and 4 (during which the greatest losses are suffered) imply that domestic properties are more vulnerable to high windspeeds in the fourth quarter (steeper slope) than the first (shallower slope). This feature may reflect the commonly held belief that storms earlier in the winter cause greater damage. As described in

Chapter 1, the October storm of 1987 resulted in particularly high losses partially due to the fact that the trees were still in leaf. Additionally, damage sustained by a structure during a storm can be higher if, in the preceding few months, the structure has not been subjected to particularly high windspeeds. These factors may play a role in generating the steeper trend line exhibited by Quarter 4 than Quarter 1 in Figure 5.3.

It is beyond the scope of this project to fully explore the determining factors governing the intra-annual variability in the susceptibility of the Great Britain housing stock to windstorm damage. However, as illustrated in Figure 5.3, in order to produce accurate loss estimates for each quarter it is logical to develop separate regression coefficients and constants for each quarter. This is achieved by regressing quarterly loss data against accumulated loss potentials for each quarter separately. From this juncture this method is termed as Model (2), while the model described above (using the same regression coefficient and constant for each quarter) is termed Model (1). The correlation between modelled and actual industry-wide losses becomes stronger using Model (2) (with the *r* value increasing from 0.66 to 0.77). The comparison between loss estimates derived from Model (1) and Model (2) are shown in Figure 5.4 and Figure 5.5, along with actual losses for industry-wide and EIG data respectively.

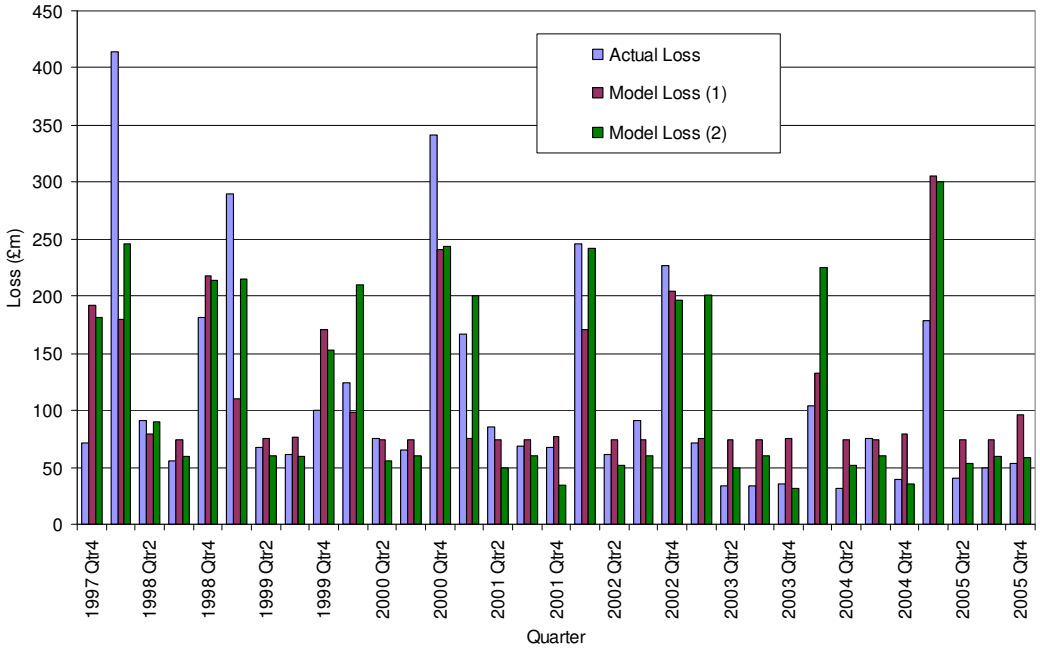

Figure 5.4 – Actual (blue), Model (1) (purple) and Model (2) (green) industry-wide quarterly wind-related insured domestic property losses (1990-2005).

Utilising Model (2) has the effect of strengthening the overall correlation between modelled and actual EIG losses (from an *r* value of 0.87 to 0.91), compared with Model (1).

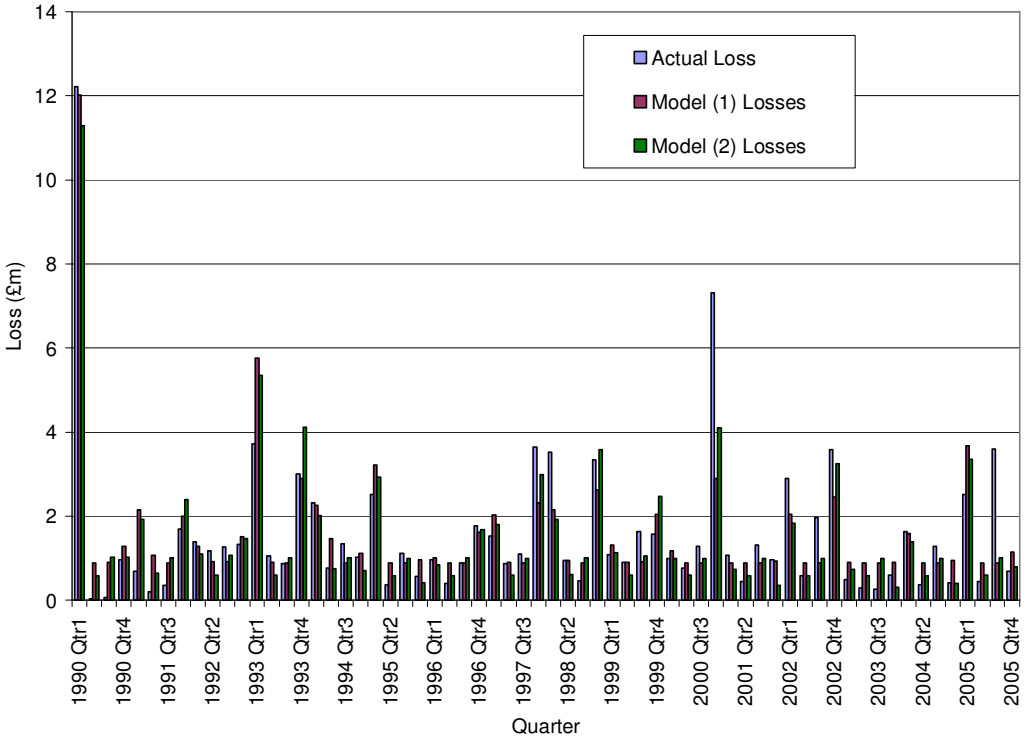

Figure 5.5 - Actual (blue), Model (1) (purple) and Model (2) (green) EIG quarterly wind-related insured domestic property losses (1990-2005).

Along with the increase in the correlation between actual losses and model losses achieved by using Model (2), compared with Model (1), the mean absolute error decreases (by 13% and 19% for ABI and EIG loss estimates respectively). For this reason Model (2) is retained while Model (1) is rejected.

Model (2) has been shown to reliably estimate both EIG and industry-wide quarterly wind-related domestic property losses. The model is applied to monthly aggregated Loss Potentials, with model EIG losses showing a strong correlation with actual losses (*r* value of 0.78), indicating that the model developed from quarterly data can be applied to shorter time periods. Model losses for individual storm events (i.e. 24-hour periods) are explored in section 5.4. Given that the observed windspeed dataset extends back to 1980, prior to both ABI and EIG loss records, it is possible to utilise the model to estimate losses in the period where no loss data are available. Figure 5.6 presents quarterly industry-wide loss estimates for the period 1980-2005, based on the

observed windspeed dataset. Section 5.3 describes how the PRECIS-Re dataset can be utilised to extend this record further still, back to 1959.

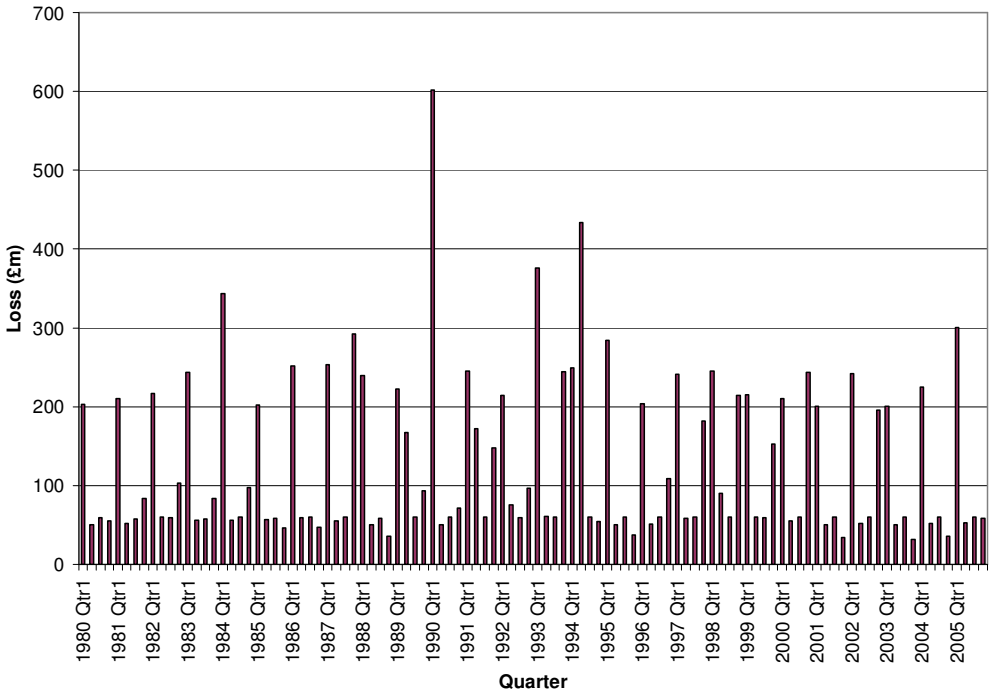

Figure 5.6 - Modelled industry-wide quarterly wind-related insured domestic property losses (1980-2005).

Figure 5.6 suggests that the first quarter of 1990 saw the highest wind-related losses, followed by quarter 2 in 1994 and the first quarter of 1993. The windstorm events driving these large loss quarters are further explored in section 5.4. The largest losses tend to occur in the first and fourth quarters; in line with findings in Section 3.3.3 that indicate more than 90% of the top 2% of DMGS occur in these periods. There appears to be a very slight, statistically insignificant, increasing trend in losses over the period 1980-2005 (less than 0.01%). This is somewhat contradictory to the decreasing trend in DMGS found in section 3.1.2. However, its magnitude is substantially smaller than the uncertainty surrounding even the simplified model.

5.3 Extending the wind-related insured loss record using reanalysis data

In the previous section the model estimates of quarterly EIG and ABI wind-related insured domestic property losses have been shown to be reasonably

reliable. The observed wind dataset has been utilised to extend the record of losses back to 1980. The aim of this section is to use the simplified model (Model (2)) in conjunction with the PRECIS-Re dataset to further extend estimates of losses back to 1959.

Chapter 3 has established that damaging windspeeds (DMGSs exceeding the local 98th percentile value) are reasonably reliably simulated in the PRECIS-Re dataset. However, as highlighted in section 3.3 there is a systematic underestimation of the DMGS values both overall and for those exceeding the 98th percentile value. Correction factors are therefore applied to the DMGS values in the PRECIS-Re dataset before their input into Model (2).

DMGS Correction Factor

DMGS in the PRECIS-Re dataset are adjusted here using a correction factor developed using a similar methodology utilised by Hanson and Goodess (2004). The 5th, 10th, 25th, 50th, 75th, 90th, 95th, 98th, 99th and 99.5th percentile values of DMGS are calculated for each year (1980-2001) for observed and PRECIS-Re data, and plotted against each other. Emphasis is placed on the upper percentiles (with the inclusion of 3 values in the upper 2 percentile) as these are the windspeeds which result in damage. Examples of these plots are shown in Figure 5.7 for two (random) stations; Aberporth (*1*) and Leuchars (*24*).

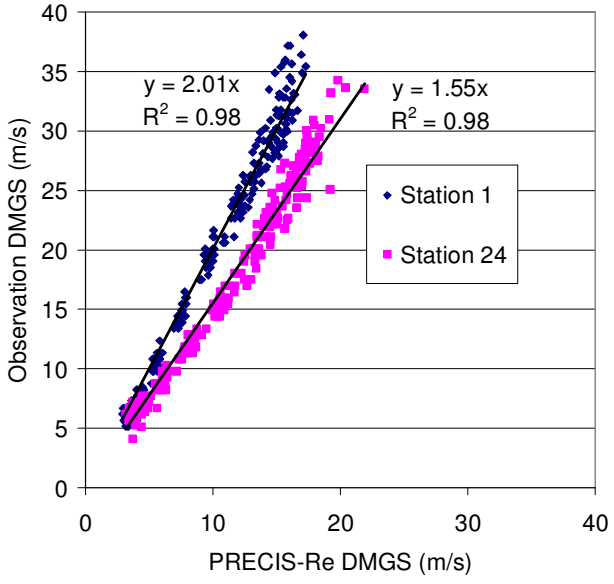

Figure 5.7 - Plot of the annual 5th, 10th, 25th, 50th, 75th, 90th, 95th, 98th, 99th and 99.5th percentile values of DMGS from the Observation and PRECIS-Re datasets for period 1980-2001, for Aberporth (S*tation 1*) and Leuchars (*Station 24*).

A strong correlation exists between the PRECIS-Re and observed values, with no station exhibiting an R^2 value under 0.95. A linear trend line is established for each station with the correction factor derived from the gradient. In the example in Figure 5.7, Aberporth (Leuchars) PRECIS-Re DMGS values are adjusted by a correction factor of 2.01 (1.55). The correction factors for the remaining stations range from 1.37 to 2.23, and are presented in Table 5.1.

Station	Name	CF	Station	Name	CF
1	Aberporth	2.01	*23*	Lerwick	1.61
2	Aldergrove	1.67	*24*	Leuchars	1.55
3	Bala	1.96	*25*	Lossiemouth	1.78
4	Bedford	1.61	*26*	Lyneham	1.75
5	Bingley	1.85	*27*	Machrihanish	2.14
6	Blackpool Squires Gate	1.49	*28*	Manston	1.48
7	Camborne	1.84	*29*	Middle Wallop	1.70
8	Chivenor	1.94	*30*	Nottingham Watnall	1.62
9	Church Fenton	1.59	*31*	Plymouth Mountbatten	1.93
10	Coltishall	1.56	*32*	Ringway	1.71
11	Coningsby	1.55	*33*	Ronaldsway	1.72
12	Cranwell	1.66	*34*	Salsburgh	2.23
13	Culdrose	1.80	*35*	Shawbury	1.78
14	Dunstaffnage	1.90	*36*	St Mawgan	1.84
15	Durham	1.60	*37*	Stornoway Airport	1.67
16	East Malling	1.51	*38*	Valley	1.88
17	Eskdalemuir	2.13	*39*	Waddington	1.62
18	Heathrow	1.54	*40*	Wattisham	1.56
19	Hurn	1.64	*41*	West Freugh	1.37
20	Kinloss	1.68	*42*	Wittering	1.66
21	Kirkwall	1.63	*43*	Yeovilton	1.74
22	Leeming	1.78			

Table 5.1 – Correction factors (CF) applied to PRECIS-Re DMGS values.

Loss Estimates 1959-2001

The adjusted PRECIS-Re DMGS values are employed in Model (2) to produce Loss Potentials which are then aggregated on a quarterly basis. Individual windstorm events (i.e. 24-hour periods) are considered separately in section 5.4. Since a correction factor is used to adjust the PRECIS-Re data, the same regression coefficient and constant developed using the observed dataset is again used to transform Loss Potentials into loss estimates. Industry-wide and EIG loss estimates, dating back to 1959, are generated.

Figure 5.8 shows industry-wide quarterly loss estimates for wind-related domestic property losses using both the observed and PRECIS-Re datasets, alongside actual losses for the period 1997-2001.

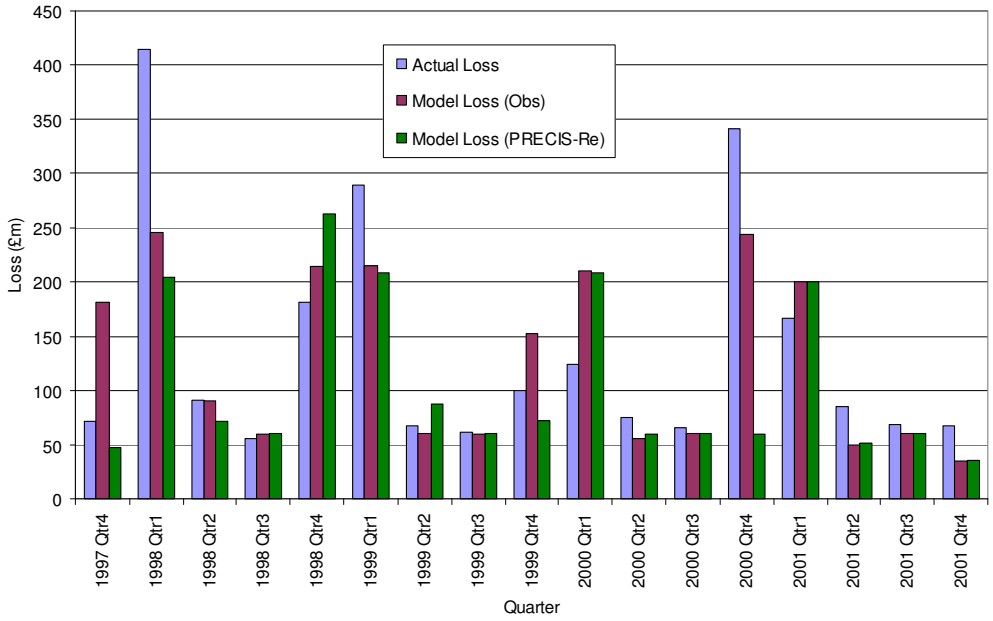

Figure 5.8 - Actual (blue) and modelled industry-wide quarterly wind-related insured domestic property losses (1997-2001). Model loss (Obs) refers to model losses calculated using observed wind data, while Model losses (PRECIS-Re) are calculated using PRECIS-Re wind data.

The correlation of the model losses based on observed wind data (model losses (Obs)) to actual losses has already been explored above. The correlation of the actual losses and those estimated by the model based on PRECIS-Re data (model losses (PRECIS-Re) is slightly weaker (*r* value of 0.56). However, this may be partially the result of the limited time series considered; only 4.25 years are taken into account, including the four highest quarterly losses in the full ABI record (1997-2005). The verification period is, however, longer for EIG data, at 12 years (1990-2001). EIG model losses (PRECIS-Re) exhibit a significantly weaker correlation to actual losses (*r* value of 0.42) compared with model losses (Obs) (*r* value of 0.91). Pinto *et al.* (2007) use a similar simplified model to estimate loss ratios (ratio of insured claims to insured value) using ERA40 data for Germany. For annual loss ratios between 1970 and 1997 the authors found an *r* value of 0.87 when correlated to actual insurance data. Although loss ratios for the UK are estimated in the Pinto *et al.* (2007) study, the model used to produced them is calibrated with German insurance data, and no verification is carried out

against actual losses suffered in the UK. Therefore, although the model presented here does not perform as well as the one present by Pinto *et al.* (2007), it does benefit from being calibrated and verified against actual UK loss data. In addition, unlike the Pinto *et al.* (2007) model, the model here is developed using observed wind data rather than reanalysis data.

The reliability of PRECIS-Re data to accurately estimate industry-wide losses is somewhat debatable given the limited time period over which assessment can be made (4.25 years). However, an *r* value of 0.56 indicates that some confidence may be placed in the industry-wide loss estimates shown in Figure 5.9. Although these estimates must be considered with caution, they do highlight known periods of high impact windstorms described in section 5.4 and identified by Tsokri and Blackmore (2003) (discussed later in this section).

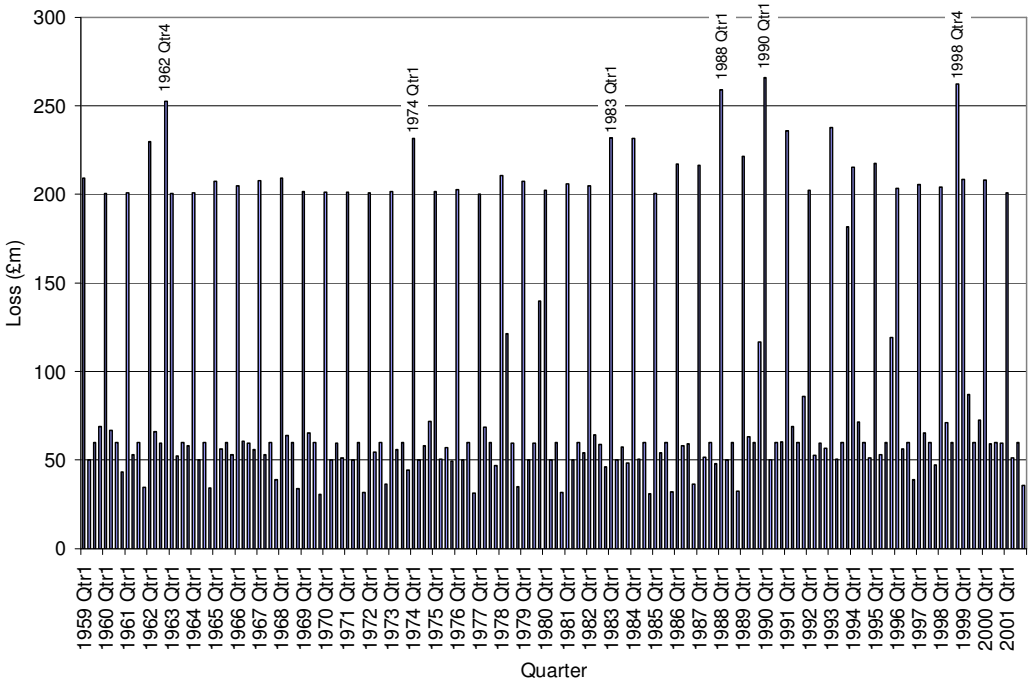

Figure 5.9 – Modelled industry-wide quarterly wind-related insured domestic property losses (1959-2001)

Little variance exists between the modelled seasonal losses year by year, particularly in spring and summer, when losses are at a minimum. Model losses in these seasons are therefore dominated by the constant (*k*) employed, with variations in Loss Potentials masked. Peaks exhibited by the industry-wide model losses in Figure 5.9 generally correspond with those in the EIG model losses, shown in Figure 5.10.

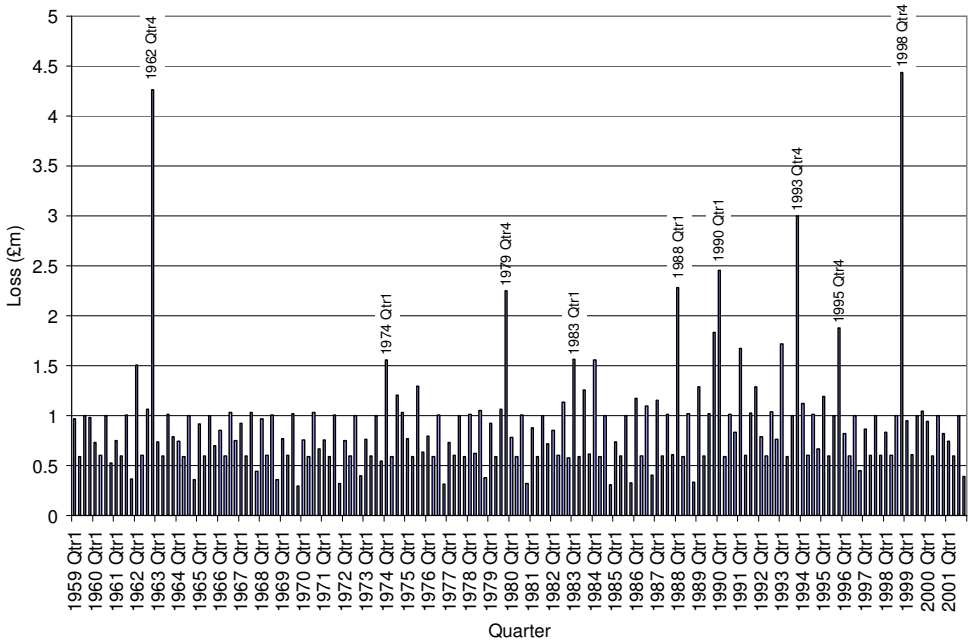

Figure 5.10 – Modelled EIG quarterly wind-related insured domestic property losses (1959-2001).

Annual industry-wide loss estimates are presented in Figure 5.11.

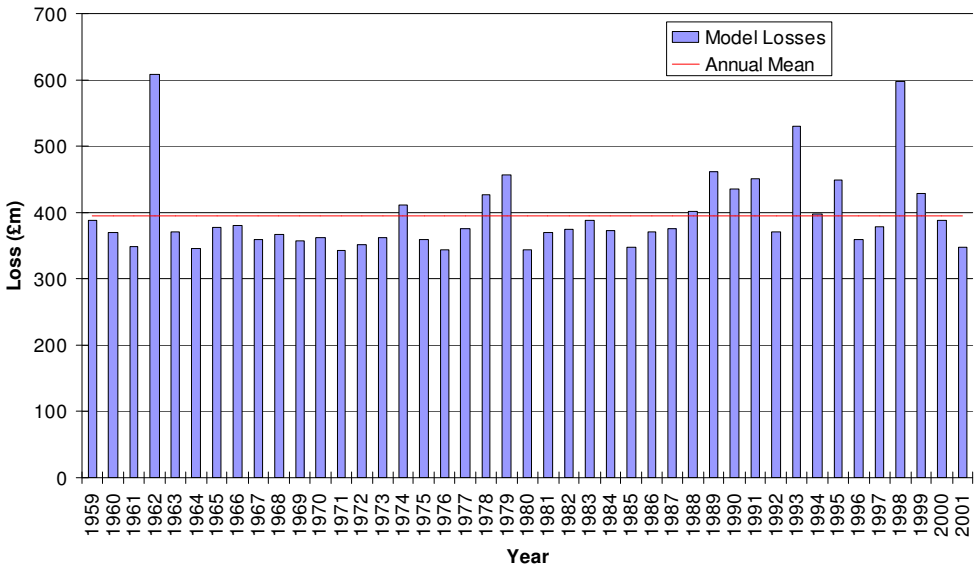

Figure 5.11 – Modelled industry-wide annual wind-related insured domestic property losses (blue bars) and long term mean (red line) for the period 1959-2001.

Industry-wide loss estimates, in both Figure 5.9 and Figure 5.11, do not fully capture the variability in actual losses. Indeed, even the short comparison period (1997-2001 in Figure 5.8) shows that the three quarters suffering the greatest losses are greatly underestimated. However, the mean annual estimated loss for the period 1959-2001 (just under £400m) (red line in Figure 5.11) is comparable to the actual mean annual loss value for the period 1997-

2005 (£480m). If the corresponding periods are considered (i.e. 1997-2001) similar values are also seen (£425m and £520m for model and actual mean annual losses respectively).

Caution should be taken when interpreting these results; the peaks in these graphs should be considered indicative of periods of large losses. Quarters encompassing large events (such as the 16th October 1987 storm, in Quarter 4, 1987 and Windstorm Daria (25th January 1990) in Quarter 1, 1990), when multi-billion-pound actual losses were recorded, are not captured. It may, therefore, be more informative to consider the Loss Potentials, rather than absolute loss estimates. Loss Potentials lie at the core of the model, and allow comparisons to be made between different years without the assumptions surrounding the relationship between insured loss and Loss Potentials. In addition, any uncertainty surrounding the adjustment of claims values, following Munich Re (2002b), is removed. Figure 5.12 shows the annual Loss Potentials calculated form PRECIS-Re data for the period 1959-2001.

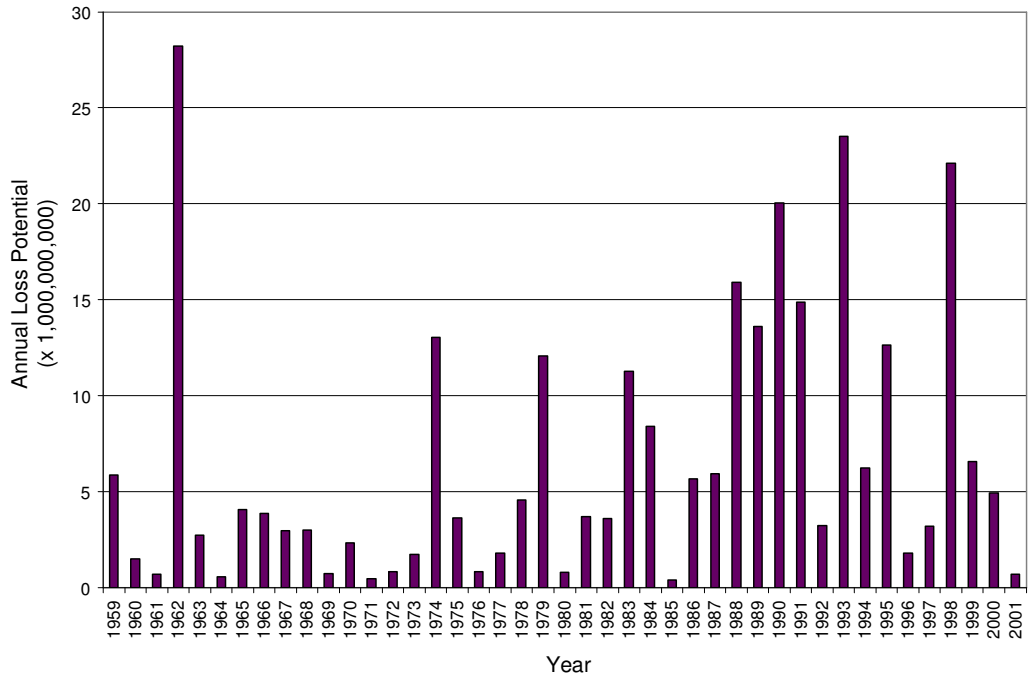

Figure 5.12 - Annual Loss Potentials calculated from PRECIS-Re windspeed data

The Loss Potentials shown in Figure 5.12 can be considered as indicative of insured losses in the period 1959-2001. It has been established above that loss estimates based on these Loss Potentials do not reliably replicate the

large loss years (e.g. 1990 and 1987). However, these years are depicted by large Loss Potentials in Figure 5.12. Several years preceding the loss record also display high Loss Potentials (e.g. 1962, 1974 and 1979). Both the annual Loss Potentials and annual loss estimates suggest an increasing trend during the period 1959-2001, in accordance with findings in section 3.2.2, which suggested PRECIS-Re DMGSs also increased during that period. However, the increases of 6% and 7% for loss estimates and Loss Potential respectively are not statistically significant.

Unfortunately, it is not possible to compare the Loss Potentials in Figure 5.12 to any industry-wide actual loss data prior to 1997. However, it is possible to consider alternative indicators of the destructiveness of wind, such as the damage incident data presented in section 1.2.2, taken from work by Tsokri and Blackmore (2003). These data, shown in Figure 5.13, are based on media reports of wind-related property damage collated by the Buildings Research Establishment.

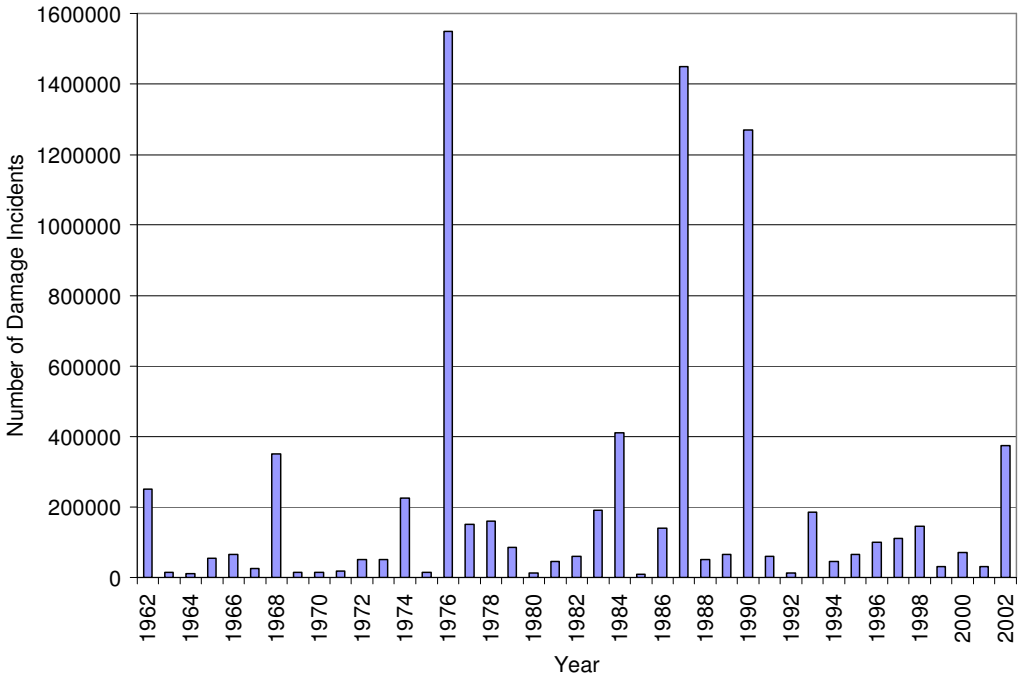

Figure 5.13 - Number of wind-related damage incidents reported in the media in the period 1962-2003, collated by the Building Research Establishment. Source: Tsokri and Blackmore (2003)

The peaks in the Tsokri and Blackmore (2003) incident data in 1962, 1974 and 1990 are replicated in annual Loss Potential data in Figure 5.12. However, certain other years exhibiting peaks in the incident data (most

notably 1976, 1987, 1994 and 2002) do not exhibit prominent peaks in the Loss Potential data. In addition to the reliability issues surrounding the collation of incident data from newspaper clippings, discussed in section 1.2.2, additional factors prevent a quantitative comparison between incident numbers and Loss Potential data; no information regarding the geographic location of damage incidents is available, and the relationship between the number of damage incidents and total insured loss is not temporally or spatially consistent. The individual events creating the peaks in the incident data and annual Loss Potentials values are further investigated in section 5.4. Additionally, the discrepancies between peaks in incident numbers and annual Loss Potential are further examined.

5.4 Identifying historic windstorm events

Annual and quarterly loss estimates based on observed and PRECIS-Re wind datasets are presented above. This section identifies historical windstorm events which drive these losses. A single "event" (i.e. windstorm) is considered here as one 24-hour period (based on the DMGS measurement period, in the windspeed datasets, of 00:00-23:59).

Initially industry-wide loss estimates for individual events are generated using both observed and PRECIS-Re windspeed data. Subsequently EIG loss estimates are produced and verified against actual loss data. Finally, since it is not possible to thoroughly verify industry-wide loss estimates, given the lack of data, the Loss Potentials of individual events are examined. Loss Potentials provide a mechanism for comparing the potential impact of windstorms directly, and allow large events to be identified dating back to 1959. A "Storm Catalogue" (from Palutikof *et al.*, 1997) is utilised in order to compare findings here to an independent source. Analysis of Loss Potentials of individual events also facilitates the spatial variation of wind-related insured domestic property losses to be assessed.

5.4.1 Industry-wide loss estimates

Industry-wide loss estimates are produced for individual windstorm events using the simplified model, with observed and PRECIS-Re wind data for the periods 1980-2005 and 1959-2001 respectively. The top 25 events, in order of industry-wide estimated losses, based on observed windspeed data, are presented in Table 5.2, alongside the loss estimates based on PRECIS-Re data and actual losses (where available).

Date	Estimated Loss (Observations) (£m)	Estimated Loss (PRECIS-Re) (£m)	Actual Loss (£m)
01 April 1994	390	71	
25 January 1990	287	48	6027 [1]
16 October 1987	254	0	7392 [2]
08 January 2005	214	-	250 [3]
27 March 1987	208	143	
27 October 2002	195	-	
26 December 1998	158	104	208 [1]
11 April 1989	149	56	
24 December 1997	148	35	304 [1]
04 January 1998	146	11	306 [1]
26 February 1990	145	65	
06 February 2001	143	125	
13 January 1984	143	41	
17 March 1995	138	6	
20 March 2004	132	-	
30 October 2000	124	26	
10 February 1985	118	10	
13 February 1989	117	10	
28 January 2003	117	-	
24 March 1986	117	101	
19 February 1997	114	39	
09 December 1993	111	129	
09 February 1988	106	175	
27 January 1994	101	59	

Table 5.2 – Top 25 industry-wide wind-related domestic property loss estimates based on observed wind data (1980-2005), and the corresponding estimated losses based on PRECIS-Re data (1980-2001). Actual loss values for these events are taken from [1] Munich Re (2002b), [2] Munich Re (1999) and [3] Guy Carpenter (2005b), and adjusted to be directly comparable to loss estimates, following Munich Re (2002b).

As noted in section 5.1, the loss estimates are produced using a model which is calibrated on loss data adjusted to 2005 values, for both inflation and changes in insurance density and insured value (following Munich Re, 2002b). Even when similar adjustments are made to published losses for storm

events, the estimates are shown to be significantly lower than actual losses, exemplified by 6 recent storm events in Table 5.2.

The two biggest loss events since 1980 (the beginning of the observed wind dataset) are the 16th October 1987 storm and windstorm Daria (25th January) in 1990. When these losses are adjusted to make them directly comparable with the loss estimates, they become an order of magnitude greater than the loss estimates. The model loss for Daria based on PRECIS-Re data is two orders of magnitude less than actual losses, while no loss is estimated for the October 1987 storm. Loss estimates based on observations for the smaller recent events are somewhat lower than the actual losses, with the PRECIS-Re based loss estimates even lower. While these results suggest caution should be taken when interpreting the estimates of industry-wide loss estimates, particularly those based on PRECIS-RE wind data, it is important to realise that there are very few data to verify the estimates with. As already stated industry-wide data are only available on a quarterly basis for a limited temporal extent, with the figures in Table 5.2 coming from a variety of different sources.

5.4.2 EIG Loss Estimates

The model is used to produce EIG loss estimates, and unlike industry-wide estimates, it is possible to verify these estimates against actual losses. The top 10 events, in terms of actual losses in the period 1990-2001, are shown in Table 5.3, alongside the corresponding loss estimates and the ranking of those estimates in the 1990-2001 timeseries.

Event	Actual Loss (£m)	Estimated Loss (Observations) (£m)	Rank	Estimated Loss (PRECIS-Re) (£m)	Rank
25 January 1990	10.80	5.39	1	0.44	32
24 December 1997	2.83	2.44	4	0.44	31
29 October 2000*	2.13	0.11	103	0.04	135
4 January 1998	1.67	1.15	13	0.04	122
30 October 2000*	1.54	2.09	5	0.35	39
26 December 1998	1.31	2.64	3	1.76	2
8 December 1993	0.99	1.36	11	0.76	13
23 January 1993	0.89	1.04	14	0.18	68
26 February 1990	0.61	2.72	2	0.60	17
1 November 2000*	0.58	-	-	-	-

Table 5.3 - Top 10 EIG wind-related insured domestic property loss events (1990-2001), and corresponding loss estimates based on observed and PRECIS-Re windspeed data, along with their respective ranking.
*** Uncertainty of the actual date/s damage occurred is discussed in section 4.3. It is likely that losses on these dates all refer to one event.**

Again, loss estimates based on PRECIS-Re wind data are lower than those generated using observed wind data. However, unlike industry-wide loss estimates, EIG loss estimates based on observations more accurately reflect actual losses. The top 20% of actual EIG loss events in the period 1990-2001 are compared to the model loss estimates based on observed and PRECIS-Re windspeed data, producing *r* values of 0.77 and 0.16 respectively. This suggests that EIG loss estimates for individual events are reliably simulated by the simplified model using observed, but not PRECIS-Re, windspeed data. Figure 5.14 shows EIG loss estimates based on observations (top) for the period 1980-2005, with the timeseries of actual losses (1990-2005) (bottom) provided for comparison. While there is evidence for underestimation of very large events (e.g. windstorm Daria on 25th January 1990), the model is able to accurately replicate losses for individual events very well. Additional high impact events may be identified from the top timeseries, e.g. 16th October 1987 and 13th January 1984; both known to be dates on which severe storms took place.

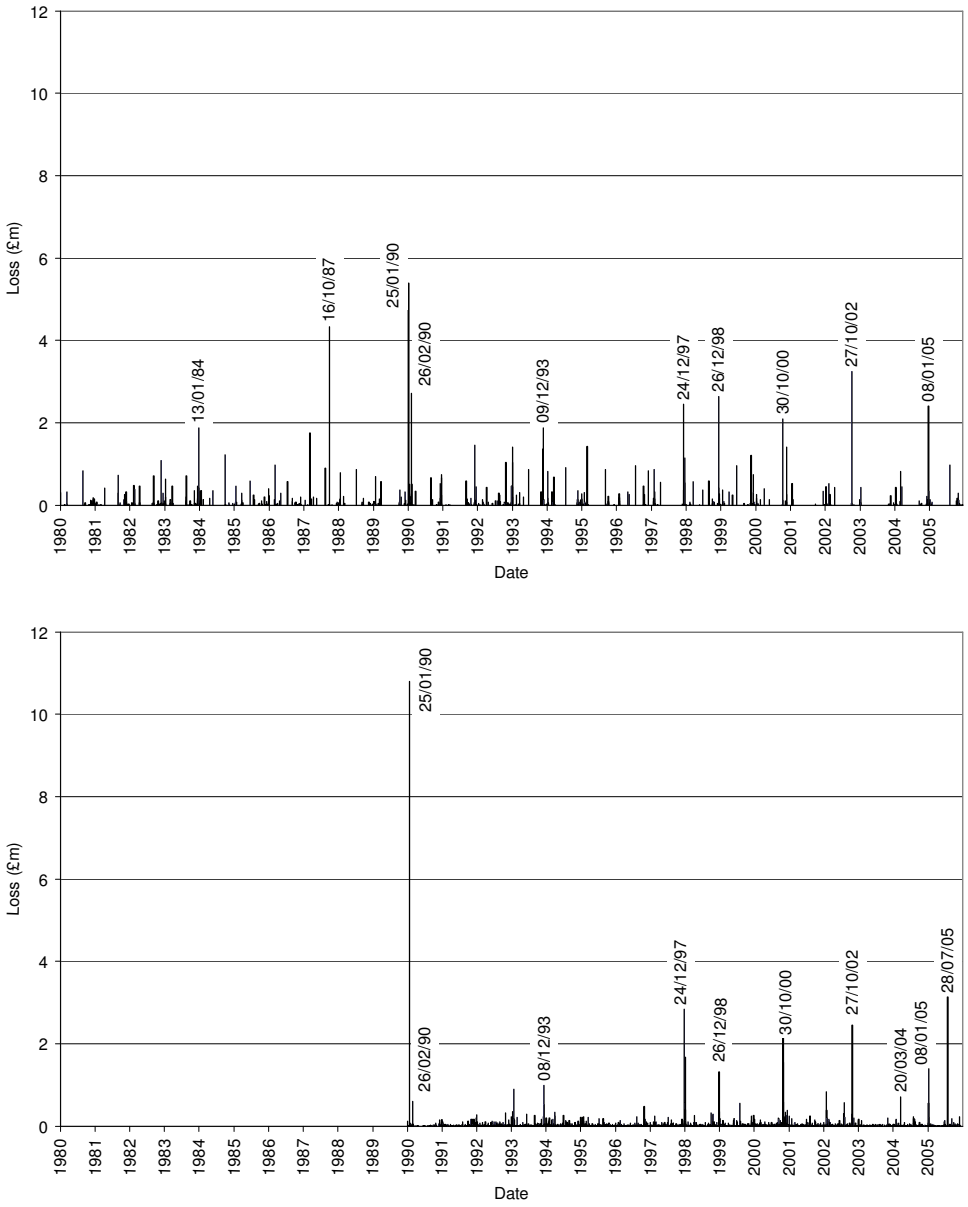

Figure 5.14 - Top 20% of EIG wind-related insured domestic property loss estimates based on observed windspeed data (top) (1980-2005) and actual losses (bottom) (1990-2005).

The highest industry-wide estimated loss based on observations is on 1st April 1994 (in Table 5.2). Information regarding industry-wide losses on this date is unavailable. EIG losses are reasonably high on both 31st March and 1st April 1994 (totalling in excess of £330000). An analysis of the DMGS dataset reveals that damaging windspeeds were recorded in the late hours of 31st March and early on April 1st, suggesting that this can be considered a single windstorm event. Estimated EIG losses (based on observations) rank this March 31st/April 1st event at 20th. Therefore, although the position of 1st April

1994 at the top of Table 5.2 is misleading, it is not unreasonable to assume that this event caused significantly high actual industry-wide losses.

It is not possible to assess the model's ability to reliable produce industry-wide loss estimates due to the lack of high resolution temporal data. However, given that EIG losses can be viewed as representative of industry-wide losses, this provides some confidence in the industry-wide loss estimates based on observed data. However, as described above, care should be taken when considering the very high loss events.

5.4.3 Loss Potentials

One of the aims of this chapter was to quantify large loss events dating back to 1959. Model estimates of industry-wide losses for single events, particularly very large loss events, have been shown to be somewhat unreliable. For this reason the remainder of this section will consider Loss Potential as an indicator of the impact of the storm on insured losses. It is therefore possible to compare storm events directly and postulate why certain storms generate more loss than others. Relative Loss Potentials (RLPs) are calculated by comparing the Loss Potential associated with each windstorm relative to the highest value. Hence, the Relative Loss Potential calculated using the observed and PRECIS-Re windspeed data is 100 for windstorm Daria (25th January 1990), and 100 for the 16th February 1962 storm respectively. In this manner RLPs provide a mechanism for comparing storms throughout the study period (1959-2005) without the uncertainty associated with producing loss estimates.

Figure 5.15 shows the top 50 RLPs based on observed windspeed data (subsequently know as RLP (observations)) and PRECIS-Re windspeed data (RLP (PRECIS-Re)) for the periods 1980-2005 and 1959-2001 respectively.

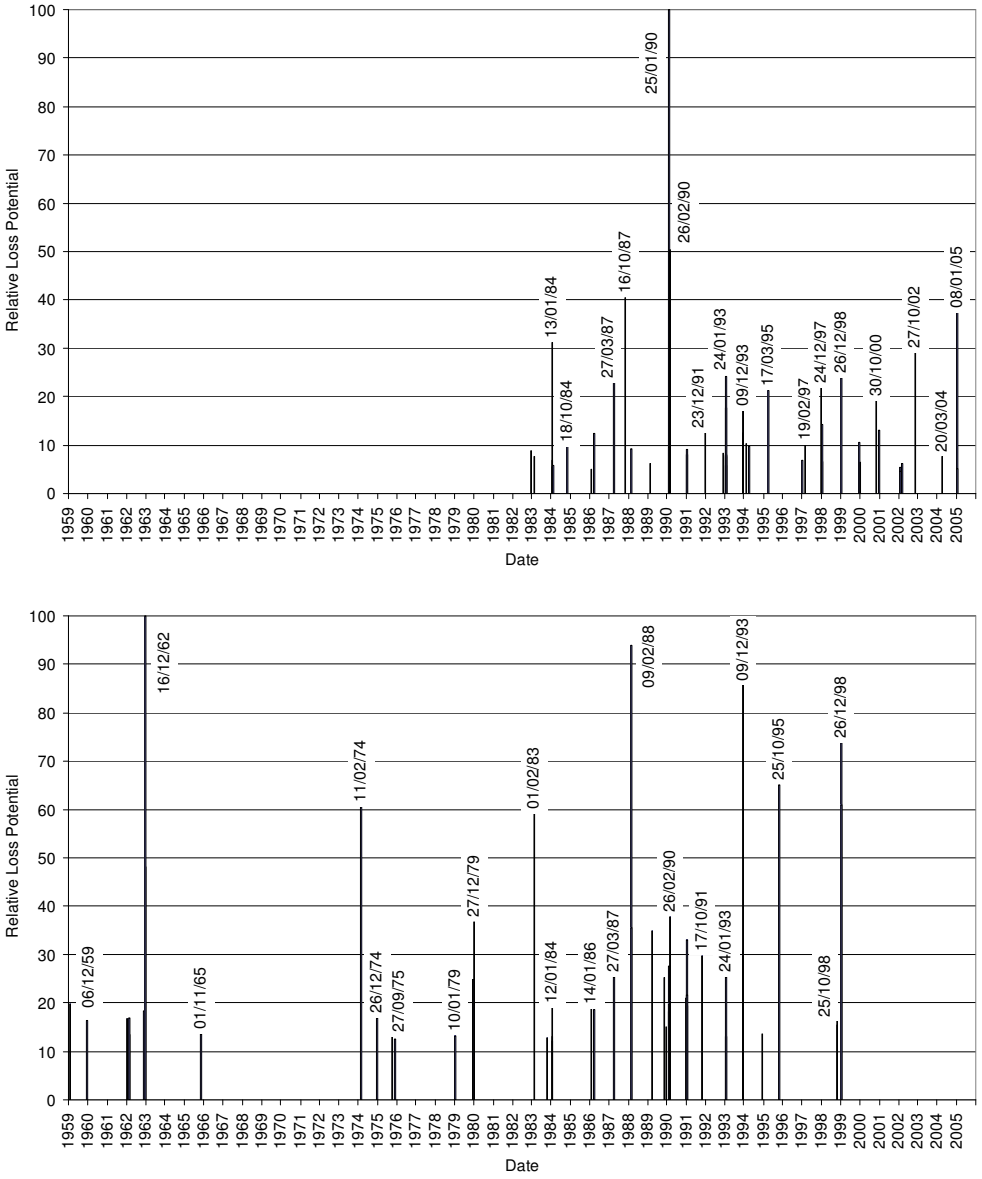

Figure 5.15 - Top 50 Relative Loss Potentials for single events calculated using observed wind data (top) (1980-2005) and PRECIS-Re wind data (bottom)(1959-2001).

As discussed in section 3.3.1 the damaging winds in the observation dataset are reasonably well captured by those in the PRECIS-Re dataset. Therefore, it is expected that the RLPs calculated from PRECIS-Re windspeed data reasonably replicate those calculated from observed windspeed data. Figure 5.15 indicates that windstorm Daria has almost twice the RLP (observations) than any other event in the period 1980-2005. RLP (PRECIS-Re) is highest for the 16th December 1962, with two other events exceeding a RLP value of 85 (9th February 1988 and 9th December 1993).

Given the lack of insured loss data it is difficult to assess the accuracy of these RLPs. Part of the benefit of using reanalysis data in this project is that RLPs can be generated for periods without wind observation records (i.e. 1959-1979). However, the accuracy of the PRECIS-Re DMGS (from which Loss Potentials are calculated) compared with observations is not perfect (discussed in section 3.3). Therefore, additional data are sought to try to establish whether the RLP (PRECIS-Re) can be considered reliable. One such source of data is Palutikof *et al.* (1997) who present a "Storm Catalogue" for the period 1920-1990 based on Palutikof and Skellern (1991)[1].

Palutikof *et al.* (1997) present a Storm Catalogue of 47 "severe" storms in Britain between 1920 and 1990, obtained from the literature. The authors assess the relative severity of each storm based on the maximum recorded windspeed (weighted by the one–in-fifty year gust speed), duration and area affected. The events occurring in the period 1959-1990 are presented in Table 5.4, alongside the rank of the RLP (PRECIS-Re) for the same period.

[1] This report, commissioned by Commercial Union, could not be accessed due to commercial sensitivities.

"Storm Catalogue" Overall Rank	Date	RLP (PRECIS-Re) Rank
1	25 January 1990	10
2	02 January 1976	227
4	16 October 1987	-
5	16-17 February 1962	25
6	12 January 1974	245
10	26 February 1990	6
11	9-10 February1988	2
13	01 February 1983	4
16	24 March 1986	21
17	13 January 1984	33
19	11 January 1962	26
21	13 February 1989	123
24	2-3 April 1973	435
28	14-15 January 1968	42
32	16-17 September 1961	505
33	11-12 January 1978	84
34	12-13 November 1972	167
37	16-17 December 1989	28
40	06 March 1967	353
43	16 May 1962	-
44	27-28 January 1974	255
45	4-5 December 1979	-
46	23-25 November 1981	434

Table 5.4 – Storms appearing in the Storm Catalogue (Palutikof *et al.*, 1997) in the period 1959-1990[2], and their overall ranking for the period 1920-1990. The corresponding RLP (PRECIS-Re) ranks for the period 1959-1990 appear in the right hand column.

A similar table is presented below for RLP (observations), for the period 1980-1990.

Overall Rank	Date	RLP (observations) Rank
1	25 January 1990	1
4	16 October 1987	3
10	26 February 1990	2
11	9-10 February1988	10
13	01 February 1983	12
16	24 March 1986	6
17	13 January 1984	4
21	13 February 1989	14
37	16-17 December 1989	31
46	23-25 November 1981	39

Table 5.5 - Storms appearing in the Storm Catalogue (Palutikof *et al.*, 1997) in the period 1980-1990[2], and their overall ranking for the period 1920-1990. The corresponding RLP (observations) ranks for the period 1980-1990 appear in the right hand column.

The dates with high ranking in the Palutikof *et al.* (1997) Storm Catalogue correspond well with the RLP (PRECIS-Re) and RLP (observations) in Table

[2] The full Storm Catalogue (1920-1990) can be found in Appendix D.

5.4 and Table 5.5 respectively. Although the Palutikof *et al.* (1997) Storm Catalogue does consider the area affected, it does not take into account the number of properties exposed to the damaging windspeeds. This may partially explain the subtle differences seen in the rankings in the tables above. However, there is general agreement, which suggests some confidence may be placed in the use of RLPs to identify historic high impact windstorms.

In section 5.3 a graph of the annual Loss Potential (Figure 5.12) is compared to the annual number of wind-related damage incidents (Figure 5.13). Some discrepancies exist between the graphs; some years with high incident numbers do not correspond to years with high Loss Potentials (e.g. 1976). Windstorm Capella (2nd-4th January 1976) is largely responsible for the spike in incident numbers seen in 1976 in Figure 5.13, and ranks second in the Palutikof *et al.* (1997) Storm Catalogue behind windstorm Daria (25th January 1990). The relative Storm Score, developed by Palutikof *et al.* (1997), for Daria is approximately 5750, with Capella scoring 4250. Values of RLP (PRECIS-Re) are 27% and 2% for Daria and Capella respectively, while the RLP (observations) for Capella is unavailable due to a lack of windspeed data. Part of the reason Capella is ranked so highly in the storm catalogue, but has a low RLP is that the highest windspeeds were recorded in northern England and Scotland; areas with relatively low household density. In comparison the wide area impacted by Daria included south east England; an area of very high household density. Actual insured losses for Capella were less than a fifth of those associated with Daria, suggesting that both the Storm Catalogue and incident numbers overestimate the storms impact, while the RLP (PRECIS-Re) values suggest the impact is somewhat underestimated.

The Loss Potentials (and RLP) generated here benefit from having a spatial component. Data presented in the Storm Catalogue (Palutikof *et al.*, 1997) and incident numbers (Tsokri and Blackmore, 2003) do not include spatial information. Aggregated insured losses are increasingly regularly published (e.g. by the ABI or major reinsurers) for major windstorm events, but usually carry little, or no, spatial information. It is possible for different windstorms to produce similar losses despite impacting different locations with different windspeeds. These subtleties are not reflected in the aggregated loss data

published. In contrast, Loss Potentials enable the impact of different storm paths and intensities to be identified. For instance three storm events with similar RLP (PRECIS-Re) are 11th February 1974 (RLP of 61%), 1st February 1983 (61%) and 27th December 1998 (59%). Although the RLPs are similar for all three events, the geographic distribution of Loss Potential differs significantly, as shown in Figure 5.16. The Loss Potential for 11th February 1974 and 1st February 1983 are more evenly distributed over a wider area compared to the highly concentrated Loss Potentials for 27th December 1998. However, Loss Potentials up to 35 times higher than those calculated for 11th February 1979 and 1st February 1983 are calculated for some postcode sectors of mainland Scotland on 27th December 1998.

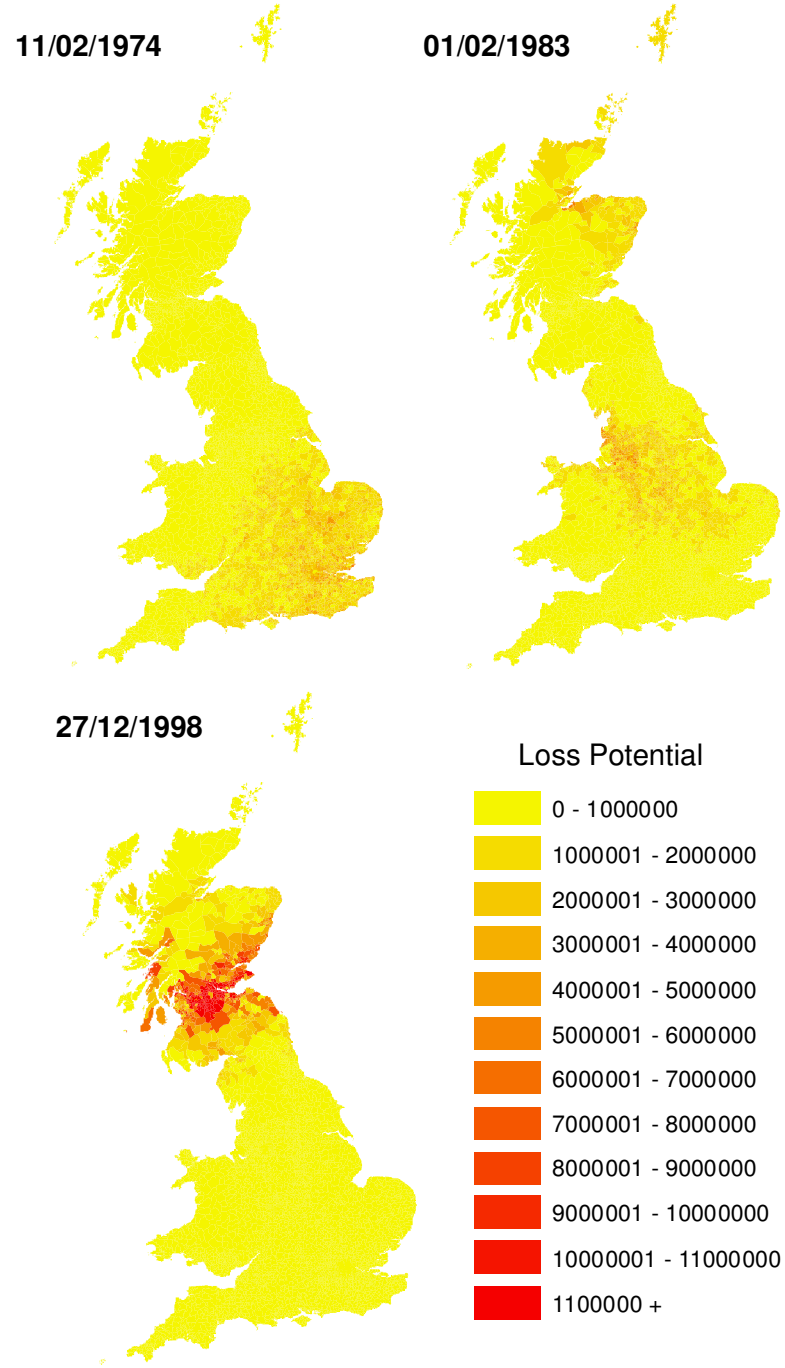

Figure 5.16 – Postcode sector Loss Potential calculated from PRECIS-Re windspeed data for 11th February 1974 (top left), 1st February 1983 (top right) and 27th December 1998 (bottom left).

It is interesting to note that during the sensitivity study described in section 5.1, regarding the shifting household density, it was found that losses in the first quarter of 1974 were 16.4% greater if the 2001 household distribution was used. The increase in household density was greatest in south east England between 1974 and 2001, with increases in household number up to 360% seen in some London postcode sectors. The fact that windstorm activity in the

first quarter of 1974, including 11th February, was largely over this area results in the relatively high increase in loss estimates under a static household number (16.4%).

The patterns of Loss Potentials shown in Figure 5.16 illustrate the fact that the entire building stock of the Great Britain is subject to windstorm damage. Actual industry-wide loss data are not freely available in this format, so it is difficult to make an assessment of the areas most at risk to the windstorm hazard. However, through work carried out in this project maps of Loss Potential, like those shown in Figure 5.16, can be produced, allowing individual loss events to be analysed. These maps form the basis from which regional variations in the risk of windstorm loss can be visualised. The mean annual RLP (observations) and RLP (PRECIS-Re) are presented in Figure 5.17.

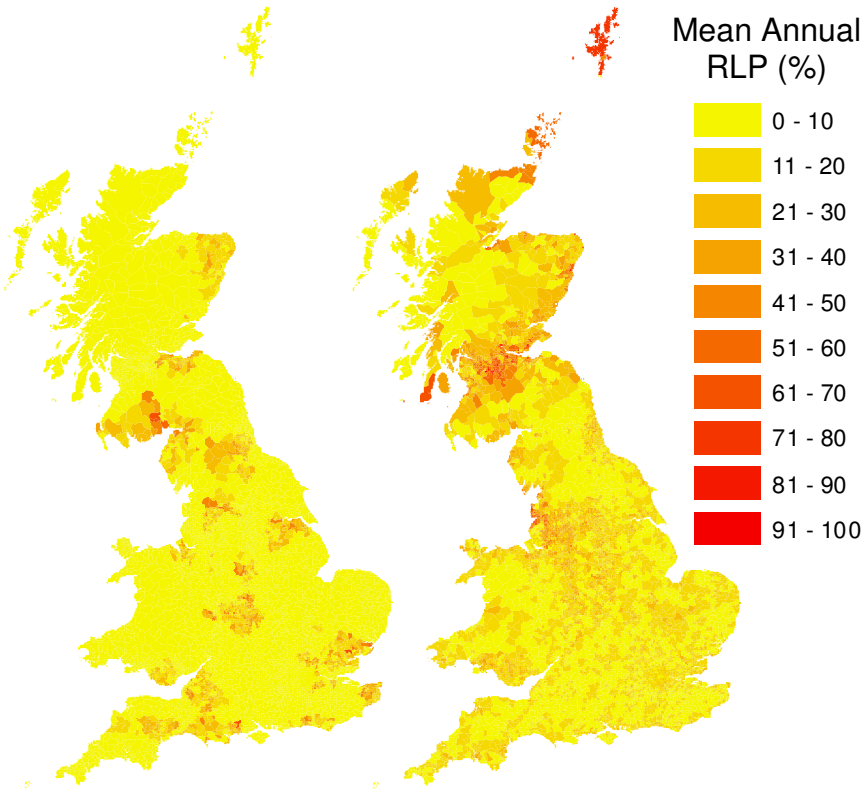

Figure 5.17 - Mean annual Relative Loss Potential based on observed (left) (1980-2005) and PRECIS-Re (right) (1959-2001) windspeed datasets.

The difference between absolute values of annual Loss Potential calculated using observed wind data compared to PRECIS-Re data, discussed in sections 4.3 and 4.4, means that direct comparisons between mean annual

values of Loss Potential are uninformative. However, mean annual RLP patterns are directly comparable. Slightly different spatial patterns are shown by the mean annual RLP (observations) and RLP (PRECIS-Re) maps in Figure 5.17, although the main areas of high RLP value are similar in both maps. These maps identify regions, based on 26 and 43 years of observed and PRECIS-Re windspeed data respectively. No industry-wide data are available regarding absolute losses during these periods on this spatial level. As a result it is not possible to compare these maps to actual losses.

The left panel of Figure 5.17 suggests high RLP (observations) in parts of south Wales and the Midlands. The establishment of a network of observing stations, undertaken in section 2.1.1, identified these areas as being barren of reliable windspeed data. Therefore, mean annual RLPs for these urban locations, may not be truly representative due to uncertainties involved in windspeed interpolation (as described in a sensitive study of the windspeed interpolation methods in Appendix C). In addition, the uncertainties may be amplified due to the high household density in these locations.

5.5 Conclusions

A simplified windstorm loss model is presented in section 5.1, based on household numbers and DMGSs from the observed and PRECIS-Re datasets described in Chapter 3. The role of exposure and vulnerability in windstorm damage is discussed throughout Chapter 1, with the simplified model produced here incorporating aspects of both (the 98^{th} percentile of DMGS is used as a threshold to incorporate aspects of vulnerability, while the number of properties impacted is incorporated to reflect exposure). Initially a Loss Potential is established for each 24-hour period, and then aggregated into quarterly values. Quarterly industry-wide (ABI) and EIG loss data are adjusted for inflation and changes to insured value resulting from changes in insured density and average sum insured (following Munich Re, 2002b). Regression is then used to establish an equation to calculate quarterly industry-wide and EIG loss estimates from Loss Potentials.

Intra-annual variation is found to exist in relationship between Loss Potential and insured loss, shown in Figure 5.3. Actual losses are shown to be higher for a given Loss Potential in the fourth quarter than the first (losses during these two quarters combined comprise over 90% of annual losses). A second model is therefore proposed, comprising of four different equations, one for each quarter. Industry-wide and EIG loss estimates are presented in section 5.2, using observed wind data in the simplified loss model for the period 1997-2005. Verification against actual claims data reveals *r* values of 0.66 and 0.87 for industry-wide and EIG loss estimates respectively, which are improved to 0.77 and 0.91, when the second loss model is utilised. These values indicate that even using a simplified model, wind-related losses can be estimated at an industry-wide level, as well as for an individual insurance company for aggregated time periods.

Annual and quarterly model loss estimates presented in section 5.2 for the entire period observed wind data are available (1980-2005). Some caution should be exercised when interpreting the industry-wide results due to the minimal data used for verification (records of industry-wide quarterly windstorm losses only begin in the fourth quarter of 1997). Known periods of significant actual losses (e.g. the first quarter of 1990) are recognised in the timeseries of estimated EIG and industry-wide losses. However, there is a slight tendency for model losses to underestimate quarters with high actual losses and overestimate for those which saw low losses. A very slight (less than 0.01%) statistically insignificant upward trend is suggested by annual losses. However, the inability of the model to fully capture high loss quarters suggests little confidence can be placed in this trend.

The simplified model facilitates the extension of the wind-related insured loss record back to 1980. The length of this record is limited by the availability of windspeed observations, detailed in Section 2.1.1. However, this project benefits from dynamically downscaled reanalysis data; the PRECIS-Re dataset, which provides continuous, high temporal and spatial resolution windspeed information for the period 1959-2001. This dataset provides a means to extending the loss record back to 1959, in conjunction with a DMGS correction factor applied in section 5.3 following Hanson and Goodess (2004).

The corrected PRECIS-Re DMGS are used in the model to produce quarterly industry-wide and EIG loss estimates, initially for the periods 1997-2001 and 1990-2001 respectively. Verification of these estimates are made against actual losses with *r* values of 0.56 and 0.42 for industry-wide and EIG loss estimates respectively. These are lower than *r* values reported for loss estimates calculated using observed wind data. Model losses for high loss quarters are significantly lower than actual losses (e.g. the highest quarterly industry-wide loss estimate is £260m in the first quarter of 1990, during which actual losses from Daria alone were 10 times that amount). For this reason a timeseries of annual Loss Potentials is presented and is seen as a viable indicator of insured losses. Using the Loss Potentials calculated using PRECIS-Re windspeed data, facilitate the identification of periods suffering high wind-related insured losses between 1959 and 1979. In this period years of high Loss Potential were identified as 1962, 1974 and 1979. Relatively high annual wind-related damage incident numbers, reported by Tsokri and Blackmore (2003), are also recorded in those years. An increasing trend (7%) is seen in the annual Loss Potentials in the period 1959-2001, in line with the increasing DMGSs found in PRECIS-Re in section 3.2.2. Although this trend is markedly stronger than that shown by loss estimates derived from observed wind data in section 5.2, it is still statistically insignificant, and therefore should be considered with care.

Section 5.4 explores individual loss events, using loss estimates and Loss Potential calculated using observational and PRECIS-Re windspeed data. It is shown that industry-wide loss estimates based on PRECIS-Re windspeed data are significantly lower than those based on observations, while even those tend to underestimate the very high losses (e.g. 16th October 1987 and 25th January 1990) by an order of magnitude. Unfortunately, verification of industry-wide loss estimates is difficult due to the limited availability of actual loss data. Model estimates of EIG losses for individual events, calculated from both observed and PRECIS-Re windspeed data, are made for the top 20% of actual EIG losses in the period 1990-2001. Loss estimates calculated using observations are far more accurate (r = 0.77) compared to those based on PRECIS-Re data (r = 0.16). In a similar fashion to industry-wide loss estimates, EIG loss estimates also do not fully capture the largest loss events

(e.g. model estimates for the £10.8m actual loss on 25th January 1990 are £5.4 and £0.4m based on observations and PRECIS-Re data respectively).

While the accuracy of industry-wide loss estimates is difficult to assess, the results from the EIG losses provide some confidence in individual loss estimates calculated using observations. However, loss estimates based on PRECIS-Re data seem to be significantly lower than actual losses. It is therefore only possible to extend the record of individual loss events back to 1980 (when the wind observation record starts) with some confidence. However, through the use of Relative Loss Potentials (RLP), rather than absolute loss estimates, a gauge of the impact of historic windstorms can be achieved back to 1959 (the start of the PRECIS-Re dataset). This method identifies a number of potentially high loss events (e.g. 15-16th December 1962, 11th February 1974 and 20th January 1959). Although no loss data extends back to 1959, an attempt at verification is made by comparing the RLP of events with known historic severe storms identified by Palutikof *et al.* (1997). Several events with high RLP (PRECIS-Re) in the period 1959-1979 correspond to those identified by Palutikof *et al.* (1997), such as 11th January 1962, 28th January 1974 and 4th December 1979.

Historic records of incident numbers (Tsokri and Blackmor, 2003) and storm severity ranking (Palutikof *et al.*, 1997) are unable to fully capture the impact of windstorm events on insured loss. While attempts at quantifying individual event losses in the period 1959-1979, using the simplified model are shown to be unreliable, utilising Loss Potentials provides a measure of the impact historic storms. An added benefit of considering Loss Potentials over published loss data is the spatial detail proffered. Three different windstorms, with similar RLPs, are shown to produce three completely different spatial patterns of Loss Potential. The regional variations in Loss Potentials shown by different windstorms form the basis on which to make an assessment of the long term impact of the windstorm hazard on insured losses in Great Britain. Maps are presented depicting the mean annual RLP in each postcode sector of Great Britain, based on observed and PRECIS-Re wind data. Areas displaying high mean RLPs are liable to experience greater insured losses,

although the maps are intended to be indicative, rather than provide absolute loss values.

The fact that model loss estimates and actual insured losses, on a quarterly and individual event basis, do not exhibit a perfect correlation suggest other factors play a role in dictating the location and extent of wind-related insured domestic property loss. These factors are further explored in Chapter 4, where a more supplicated windstorm loss model is developed using additional socio-economic information. However, it is established here that even a simplified model, using observed windspeed data, is able to provide reasonably accurate estimates for historic events. While observational data can extend the record back to 1980, reanalysis data enables loss estimates to be made back until 1959. While absolute estimates based on the PRECIS-Re dataset are not reliable, the Relative Loss Potential measure allows comparisons to be made between historic storms. The simplified model presented in this chapter enables an assessment of the long term impact of windstorms on insured domestic property losses in Great Britain. Chapter 6 utilises the same model to assess whether or not that impact is altered under future wind regimes in 2021-2050 and 2071-2100. The fact that the simplified model operates at a postcode sector level will enable any future spatial variations to be identified.

Chapter 6: The Future UK Wind Regime and its Impact on Windstorm Losses

In order to achieve the research aims outlined in section 1.6, so far an assessment of the historical UK wind regime has been made in Chapter 3 and a windstorm model developed in Chapter 4. The impact of the historical UK wind regime on wind-related insured domestic property loss is assessed in Chapter 5. This chapter completes the final part of the first research aim; an assessment of the future UK wind regime. Results from the PRECIS future climate simulations are presented here. The third and final research aim is to estimate potential losses under a future wind regime. Windspeed information from the PRECIS experiments is incorporated into the simplified loss model, presented in Chapter 5. This enables the impact of the future UK wind regim on wind-related insured domestic property losses to be quantified.

Section 6.1 focuses on the PRECIS experiments, detailing results regarding windspeeds from the future climate simulations for 2021-2050 and 2071-2100. An assessment of the changes in the UK wind regime is made, with a focus on damaging windspeeds. Subsequently, the windspeed information is utilised in section 6.2, with the simplified loss model, to produce Loss Potentials for future climates.

6.1 The future UK wind regime

The PRECIS system, described in section 2.2.2, is utilised to provide high temporal and spatial resolution future climate simulations for the UK domain. Windspeed data are extracted from these simulations and analysed in this chapter. Chapter 3 describes the historical wind regime simulated by PRECIS, with boundary conditions provided by reanalysis data (the PRECIS-Re dataset). Results presented in this section are from experiments with boundary conditions derived from two GCMs; ECHAM4 and HadAM3P. A full description of these experiments can be found in section 2.2.3, with the main details shown in Table 6.1.

Experiment Name	Time Period	SRES Emissions Scenario	Source of Lateral Boundary Conditions
PRECIS-Re*	1959-2001	-	ERA40
PRECIS-EA	1961-1990	A2	ECHAM4
PRECIS-EA-Mid	2021-2050	A2	ECHAM4
PRECIS-EA-Late	2071-2100	A2	ECHAM4
PRECIS-H	1961-1990	-	HadAM3P
PRECIS-HA	2071-2100	A2	HadAM3P
PRECIS-HB	2071-2100	B2	HadAM3P

Table 6.1 - Summary of PRECIS climate simulations generated in this study. *Data from PRECIS-Re are kindly provided by the Hadley Centre

Initially, output from the baseline experiments, PRECIS-H and ECHAM-EA, are examined in section 6.1.1, to ensure the "current" climate is simulated realistically. Once this is established, section 6.1.2 considers the windspeed output from future simulations (PRECIS-EA-Mid, PRECIS-EA-Late, PRECIS-HA and PRECIS-HB) in relation to the baseline values.

6.1.1 Baseline experiments

Before an assessment of the future wind regime can be made, it is important to establish whether the climates simulated for the baseline 1961-90 period (i.e. PRECIS-H and PRECIS-EA) are realistic. Chapter 3 describes the PRECIS-Re dataset and compares it to observed values. Section 3.3 demonstrates that, while there is a tendency to underestimate damaging windspeeds, PRECIS-Re captures the variability of the observed UK wind regime reasonably well. For this reason, PRECIS-Re is considered "current" climate, against which the reliability of the baseline experiments to simulate realistic windspeeds is assessed. The comparison of baseline simulations to reanalysis data is a common technique (e.g. Leckebusch *et al.* (2007) use ERA40 and Pinto *et al.* (2007) use NCEP reanalysis data). However, often the reanalysis data are at a course spatial and temporal resolution, increasing the uncertainty in the process. This project benefits from the availability of dynamically downscaled reanalysis data (PRECIS-Re), which are at the same temporal and spatial resolution as the baseline experiments.

The windspeed data utilised in the simplified model in Chapter 5 and in section 6.2 are extracted from PRECIS data at the 43 grid points corresponding to the locations of the stations in the observation network established in section 2.1.1. A similar methodology is employed in the analysis of model windspeeds in Chapter 3. Therefore, it is important to establish that the windspeed characteristics at these locations in baseline simulations are comparable to those in PRECIS-Re. Hence the annual average daily mean windspeed, and the annual mean value and 98th percentile value of the DMGS are found in each of the two baseline experiments, at each grid cell corresponding to the 43 stations. These values are compared to the values obtained from PRECIS-Re, as are seasonal values. The bias (the difference between the values from the baseline experiments and PRECIS-Re) is found for each station, with the mean of all stations (the Network Average) shown in Figure 6.1 for the DMGS biases.

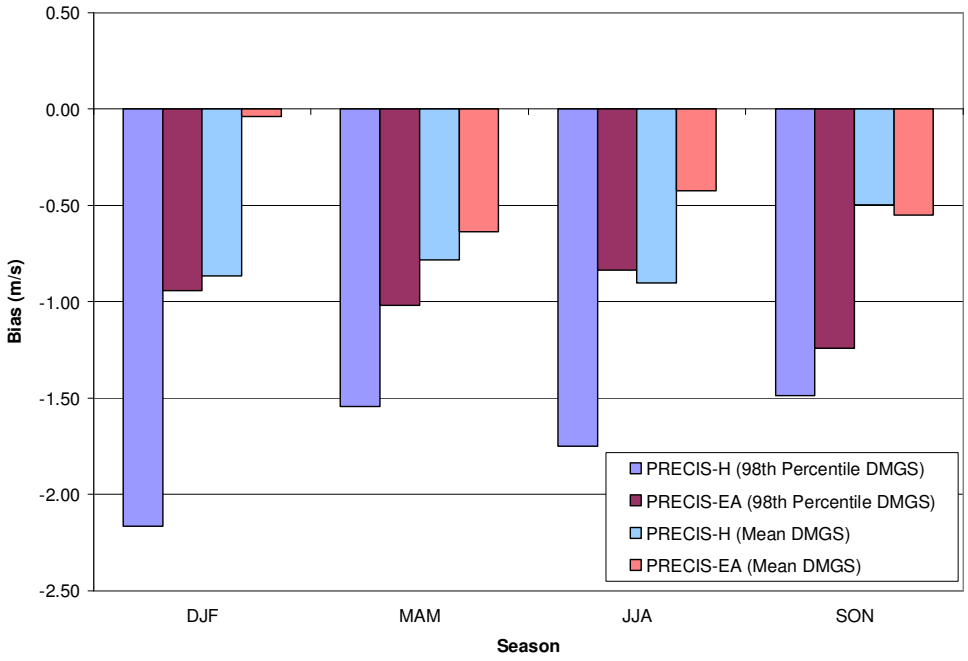

Figure 6.1 – Network Average seasonal bias between baseline experiments and PRECIS-Re, for the annual 98th percentile value of DMGS (dark blue and purple bars for PRECIS-H and PRECIS-EA respectively) and annual mean value of DMGS (light blue and red bars for PRECIS-H and PRECIS-EA respectively).

The Network Average bias for the annual average daily mean windspeed is -0.45 ms^{-1} (-8.2%) and -0.19 ms^{-1} (-3.5%) in PRECIS-H and PRECIS-EA simulations respectively. Bias values shown by PRECIS-H are -1.72 ms^{-1} and -0.76 ms^{-1} for the annual 98th percentile value and annual mean value of

DMGS respectively (equivalent to -11.5% and -10.0%). The corresponding figures for PRECIS-EA are -0.91 ms^{-1} (-6.1%) and -0.41 ms^{-1} (-5.4%) respectively. Along with the values shown in Figure 6.1, these figures indicate that the baseline experiments systematically underestimate DMGS, with PRECIS-H exhibiting a greater negative bias then PRECIS-EA.

The discussion now focuses on the 98th percentile values of DMGS since the simplified model utilised in section 6.2 incorporates these data (i.e. damaging windspeeds). Although the greatest absolute bias in PRECIS-H 98th percentile values of DMGS is seen in winter, the summer bias is greater as a proportion of the PRECIS-Re value (-13.2% compared to -14.8%). PRECIS-EA exhibits a slightly lower intra-annual variation in the bias of the 98th percentile value of DMGS, with the greatest bias in autumn (-1.24 ms^{-1} or -8.3%). Very slight regional variations also exist, with a tendency for the greatest biases to occur at coastal stations. This pattern is shown by both PRECIS-H (Figure 6.2) and PRECIS-EA, and also exists if the percentage bias values are considered. While there are intra-annual variations in bias values, the spatial pattern shown in Figure 6.2 shows no temporal variation.

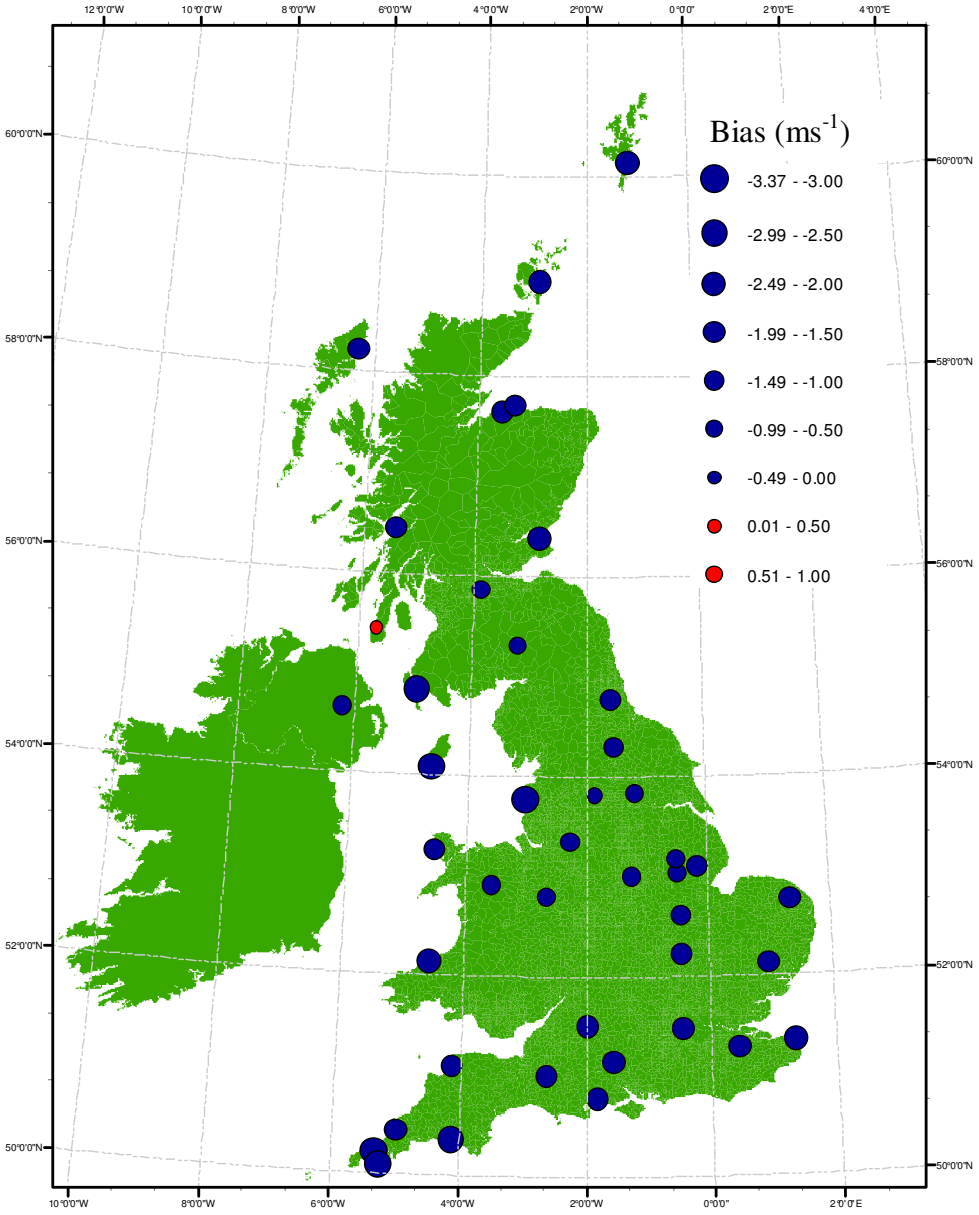

Figure 6.2 - Bias (ms^{-1}) of the 98th percentile values of DMGS simulated in PRECIS-H compared to PRECIS-Re.

Spatial variations in the DMGS and daily mean windspeed biases are similar to those shown in Figure 6.2, albeit with lower magnitudes.

In addition to windspeed values, the time of the year damaging windspeeds occur has been shown to be important in terms of the insured loss they produce (see section 5.2). Figure 6.3 shows the time of the year that damaging windspeeds occur in the baseline experiments compared with PRECIS-Re data.

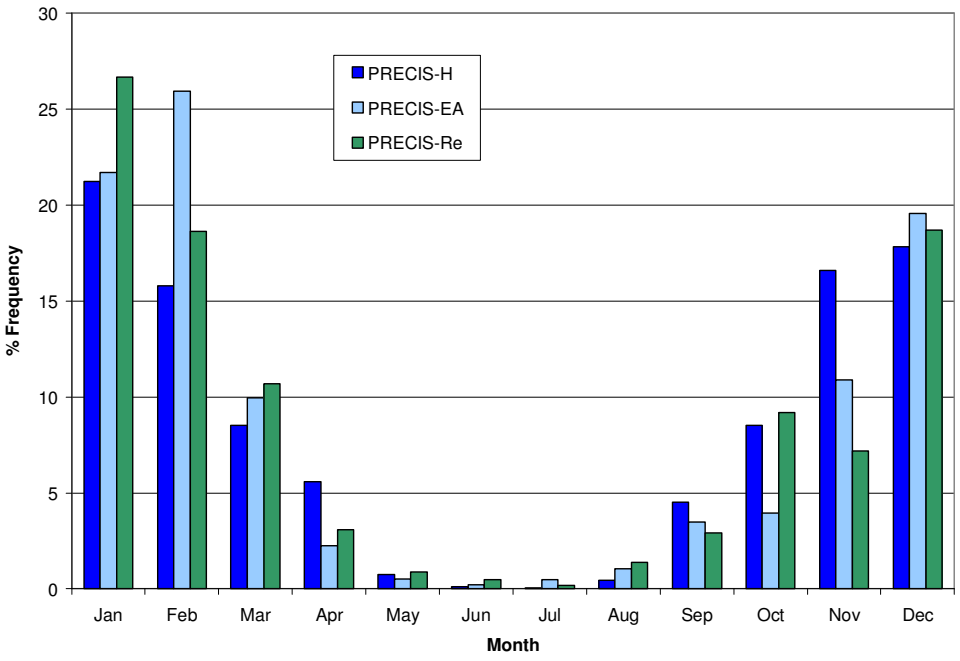

Figure 6.3 - Intra-annual variation of the occurrence of damaging windspeeds in the PRECIS-H (dark blue), PRECIS-EA (light blue) and PRECIS-Re (green) simulations.

EIG claims data in Chapter 5 revealed that more than 70% of annual wind-related insured loss occurs in autumn and winter. Therefore it is important that damaging windspeeds are accurately simulated in these periods. Figure 6.3 demonstrates that both baseline experiments underestimate the occurrence of damaging winds in January, while overestimating their occurrence in November. PRECIS-H underestimates the occurrence of damaging windspeeds in winter by approximately 10%, while overestimating by a similar magnitude in autumn. The reverse is true for PRECIS-EA, although the magnitude of the difference is significantly lower at just 2-3%.

Summary

The bias between baseline experiments and PRECIS-Re shows that PRECIS-EA more accurately reflects "current" climate than PRECIS-H. Both baseline experiments underestimate mean windspeeds, as well as DMGSs and damaging windspeeds. The an overall bias for damaging windspeeds in PRECIS-EA is -0.91 ms^{-1} (or -6.1%) compared to a figure of -1.72 ms^{-1} (-11.5%) for PRECIS-H. There appears to be some intra-annual variation in the bias, with the greatest percentage biases occurring in summer and autumn for PRECIS-H and PRECIS-EA respectively. The time of the year damaging windspeeds occur is shown to be accurately simulated in PRECIS-EA.

However, there is a 10% underestimation of occurrences in PRECIS-H for winter, with a corresponding overestimation in autumn.

Following the comparison of PRECIS-Re DMGS data to observations in section 3.3.1, no attempt is made to compare baseline experiments with observations. It was shown that PRECIS-Re significantly underestimates gust speeds, largely arising from the difference in measurement times (model data DMGS are a 2.5-minute windspeed average, whereas observations are taken over just 3 seconds). However, it was demonstrated that PRECIS-Re reliably captures the spatial and temporal variations of observed DMGS, and can therefore be considered as a good proxy for "current climate". As described above the baseline experiments accurately capture windspeeds in the PRECIS-Re dataset, although possessing a slight negative bias. Hence all future changes in the wind regime are considered relative to the baseline experiments, with the percentage change indicative of the change compared to the current observed climate. However, future simulations of absolute windspeed values should be considered with caution.

6.1.2 Future climate simulations

The future simulations of climate for two periods (2021-2050 and 2071-2100), using two different emissions scenarios (A2 and B2) and two different driving GCMs (HadAM3P and ECHAM4) are described in section 2.2.3. Windspeed data from these simulations are compared to the baseline experiments, and changes in the wind regime are quantified in this section. Although the project focus surrounds damaging windspeeds (i.e. the upper 2% of DMGSs), changes in mean windspeeds and DMGS are considered to give perspective to shifts in damaging windspeeds.

In order to assess the statistical significance of the simulated changes a Student's t test (at the 95% confidence level) is applied to the complete set of data, and also to seasonal and monthly subsets. The t test is applied to data extracted at grid point corresponding to each observation station, as previously described. The number of 'stations' demonstrating significant

changes is included in the right side of Table 6.2, Table 6.3 and Table 6.4. The relative changes in future simulations are assessed at each station, with the Network Average quoted in the results, unless otherwise specified. Although the network distribution may be slightly uneven, the Network Average may be considered representative of the study area. Furthermore, windspeed data from grid cells corresponding to the stations are used to generate future Loss Potentials, and therefore it is informative to identify any changes at these locations, rather than across the whole of the UK. Maps are presented showing the relative changes in windspeeds at individual stations, enabling spatial variations to be identified.

Daily mean windspeeds

Figure 6.4 shows the relative changes in the overall, seasonal and monthly averages of daily mean windspeeds in the future simulations.

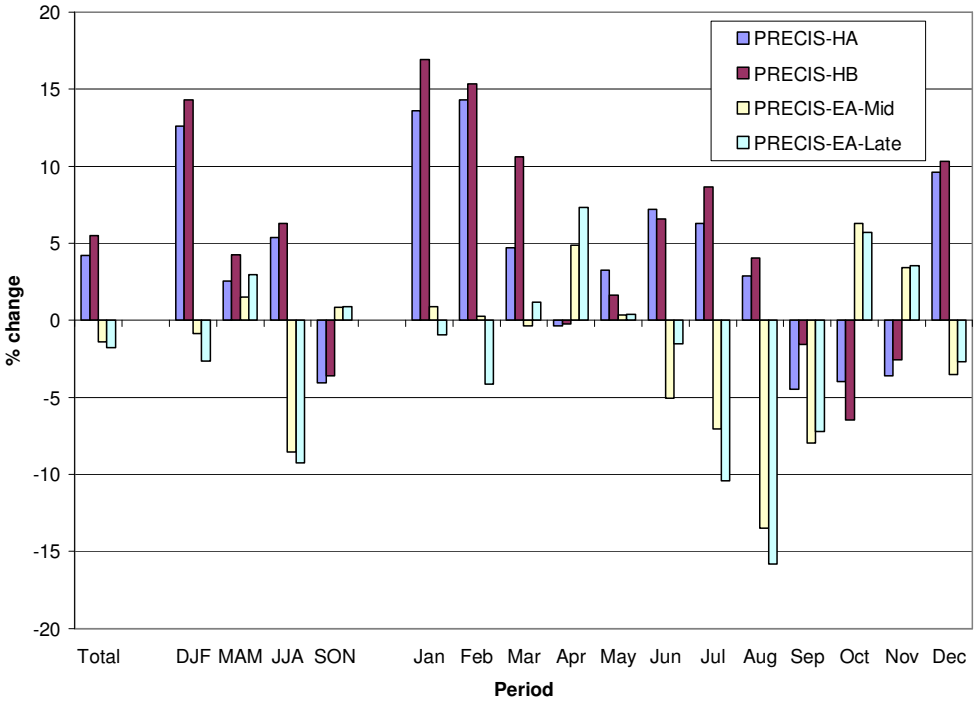

Figure 6.4 - Relative changes in the overall, seasonal and monthly averages of daily mean windspeed in future climate simulations compared with baseline experiments.

The absolute values of the changes illustrated above are shown in Table 6.2, along with the number of stations exhibiting a statistically significant shift in mean windspeeds.

	Absolute change (ms^{-1})					No. of stations with significant changes			
	PRECIS-HA	**PRECIS-HB**	**PRECIS-EA-Mid**	**PRECIS-EA-Late**		**PRECIS-HA**	**PRECIS-HB**	**PRECIS-EA-Mid**	**PRECIS-EA-Late**
Total	0.2	0.3	-0.1	-0.1		39	43	22	25
DJF	0.7	0.8	-0.1	-0.2		43	43	30	21
MAM	0.1	0.2	0.1	0.2		25	32	20	26
JJA	0.2	0.3	-0.4	-0.4		39	41	41	42
SON	-0.2	-0.2	0.0	0.0		35	35	28	29
Jan	0.8	1.0	0.1	-0.1		42	43	25	18
Feb	0.8	0.9	0.0	-0.3		41	43	21	19
Mar	0.3	0.6	0.0	0.1		24	38	14	23
Apr	0.0	0.0	0.2	0.4		2	3	25	30
May	0.1	0.1	0.0	0.0		24	18	6	11
Jun	0.3	0.3	-0.2	-0.1		38	39	35	13
Jul	0.2	0.3	-0.3	-0.4		36	37	34	40
Aug	0.1	0.2	-0.6	-0.7		25	28	43	43
Sep	-0.2	-0.1	-0.4	-0.4		30	13	37	36
Oct	-0.2	-0.3	0.3	0.3		30	32	34	33
Nov	-0.2	-0.1	0.2	0.2		27	24	26	27
Dec	0.6	0.6	-0.2	-0.2		37	39	21	19

Table 6.2 – Absolute change in the overall, seasonal and monthly averages of daily mean windspeeds in future climate simulations compared with baseline period, and the number of stations exhibiting significant changes.

The magnitude of change in the overall and seasonal means shown in Figure 6.4, are slightly greater in PRECIS-HB than PRECIS-HA. In addition, in all but five months, the magnitude of changes simulated under the B2 emissions scenario (PRECIS-HB) are greater than those simulated under the A2 (PRECIS-HA). Results for DMGS values also exhibit this feature. This is inconsistent with previous studies (e.g. Pryor *et al.* (2006) and Räisänen *et al.* (2004)). Indeed, Christensen and Christensen (2007) state that simulations under the B2 scenario generally produce similar patterns in future windspeed changes to simulations under the A2 scenario, but with a lesser magnitude. These discrepancies are addressed in the summary in this section and in section 6.3.

Changes in the monthly average of daily mean windspeeds in PRECIS-EA-Late are rather contrary to those in PRECIS-HA or PRECIS-HB. While the greatest changes in daily mean windspeeds are seen in the summer months

in PRECIS-EA-Mid and PRECIS-EA-Late, they occur in the winter months in PRECIS-HA and PRECIS-HB. This manifests in opposite changes in seasonal means in all but spring. Along with the fact that the lowest windspeeds tend to be recorded in the summer months, these features result in the minimal change in overall daily mean windspeeds simulated by PRECIS-EA-Mid and PRECIS-EA-Late.

The regional variation shown by changes in winter and summer daily mean windspeeds in PRECIS-HB and PRECIS-EA-Late are shown in Figure 6.5. Similar variations are exhibited by PRECIS-HA and PRECIS-EA-Mid simulations respectively, but with slightly lower magnitudes of changes.

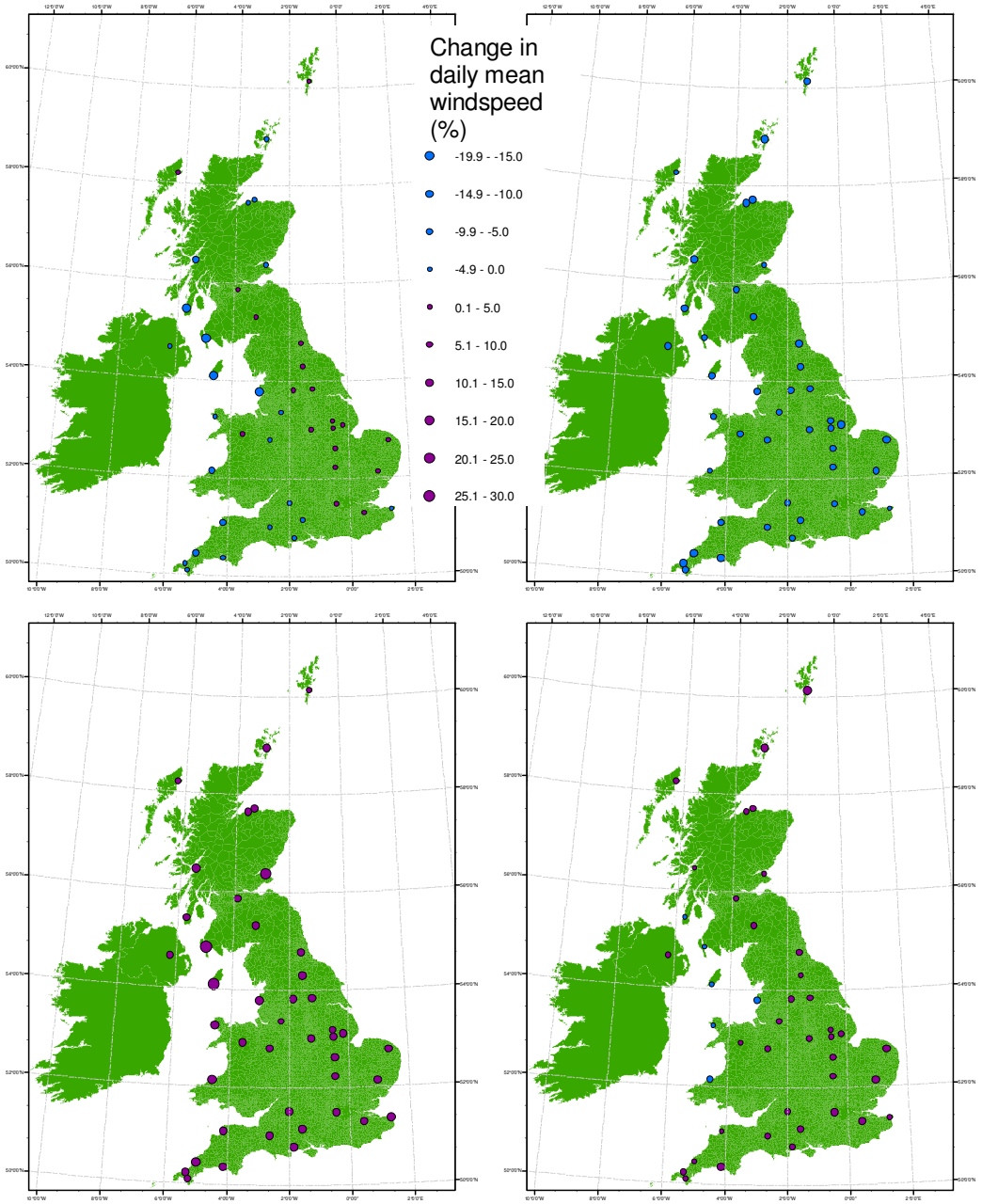

Figure 6.5 - Relative changes in winter (left) and summer (right) daily mean windspeeds in PRECIS-EA-Late (top) and PRECIS-HB (bottom) simulations.

The spatial variation of changes in the daily mean windspeeds simulated by PRECIS-EA-Late largely follows that for winter (top left panel in Figure 6.5), except Coltishall (*10*), Heathrow (*18*) and Leuchars (*24*) exhibit decreases rather than increases. Also, the magnitudes of increases in winter seen in the eastern parts of the UK are diminished slightly. Changes in daily mean windspeeds in the PRECIS-HB simulation are positive at every station, as in winter (bottom left panel of Figure 6.5). The greatest increases occur to the south of a line from the Severn estuary to the Wash, and north of the Scottish

border. Relative increases vary from nearly 9% at Manston (*28*) on the English south coast, to values less than 1% in northern England and up to 10% as you progress north into Scotland. The increases also tend to be larger in coastal locations.

DMGS

Figure 6.6 shows changes in the overall, seasonal and monthly mean values of DMGS in the future PRECIS simulations, relative to the baseline simulation.

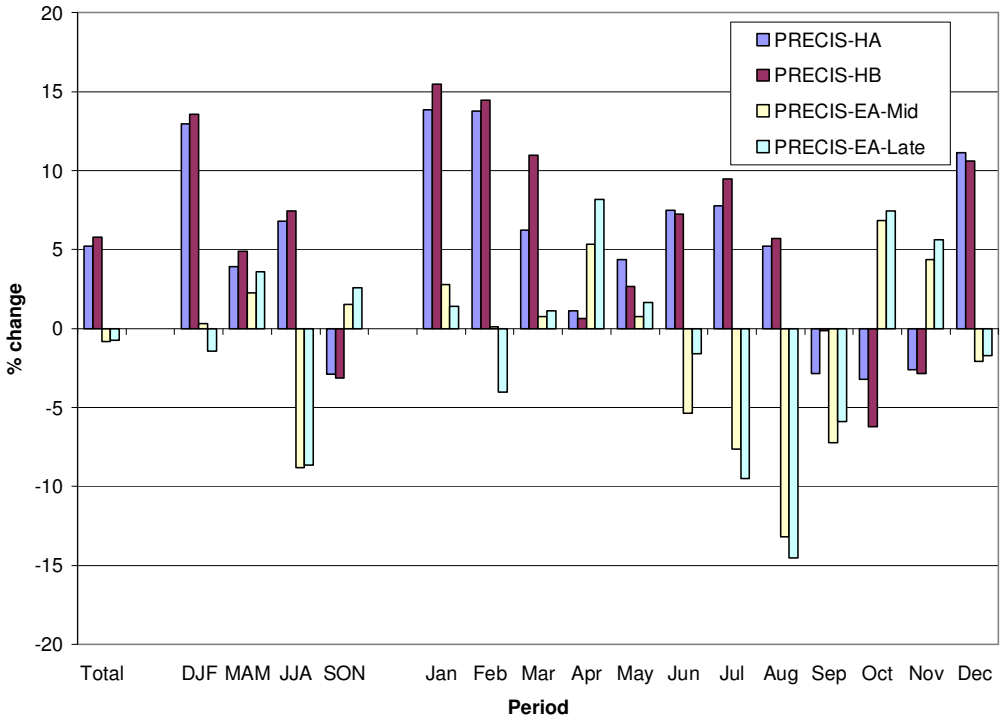

Figure 6.6 - Relative changes in the overall, seasonal and monthly mean values of DMGS in future climate simulations compared with baseline experiments.

Absolute values of the changes depicted in Figure 6.6 are shown in Table 6.3, along with the number of stations exhibiting significant changes.

	Absolute change (ms^{-1})					No. of stations with significant changes			
	PRECIS-HA	**PRECIS-HB**	**PRECIS-EA-Mid**	**PRECIS-EA-Late**		**PRECIS-HA**	**PRECIS-HB**	**PRECIS-EA-Mid**	**PRECIS-EA-Late**
Total	0.4	0.4	-0.1	-0.1		42	42	20	28
DJF	1.0	1.0	0.0	-0.1		43	43	29	26
MAM	0.3	0.3	0.2	0.2		39	39	26	30
JJA	0.4	0.4	-0.5	-0.5		42	40	43	43
SON	-0.2	-0.2	0.1	0.2		35	34	27	34
Jan	1.1	1.2	0.2	0.1		43	43	29	22
Feb	1.1	1.1	0.0	-0.3		43	43	20	19
Mar	0.4	0.8	0.1	0.1		32	42	29	22
Apr	0.1	0.0	0.4	0.6		6	3	29	36
May	0.3	0.2	0.0	0.1		33	23	8	14
Jun	0.4	0.4	-0.3	-0.1		38	38	38	14
Jul	0.4	0.5	-0.5	-0.6		39	39	38	42
Aug	0.3	0.3	-0.8	-0.9		35	36	43	43
Sep	-0.2	0.0	-0.5	-0.4		18	12	38	34
Oct	-0.2	-0.5	0.5	0.5		30	34	38	35
Nov	-0.2	-0.2	0.3	0.4		26	28	33	36
Dec	0.8	0.8	-0.2	-0.1		41	42	17	15

Table 6.3 – Absolute change in the overall, seasonal and monthly mean values of DMGS in future climate simulations compared with baseline period, and the number of stations exhibiting significant changes.

The greatest changes in DMGSs are exhibited by the HadAM3P-driven simulations (PRECIS-HA and PRECIS-HB) (5-6% increases overall), compared to ECHAM4-driven runs (PRECIS-EA-Mid and PRECIS-EA-Late) (less than 1% overall decreases). Once again, the results indicate that simulations under the B2 emissions scenario produce greater changes in windspeed than those under the A2 scenario, with all but 5 months exhibiting a greater magnitude of change in PRECIS-HB compared to PRECIS-HA.

It is important to note that results from PRECIS-EA-Late, and not PRECIS-EA-Mid, are comparable with those from PRECIS-HA and PRECIS-HB. However, it is interesting to observe that on several occasions (including changes in the mean values and 98th percentile values of DMGS) the magnitude of change in PRECIS-EA-Mid is greater than that seen in PRECIS-EA-Late. This feature is discussed further in section 6.3.

All seasonal means of DMGS show an increase in PRECIS-HA and PRECIS-HB simulations except autumn, with the greatest increases in winter (12.9% and 13.6% respectively). These values, along with the fact that the highest DMGS are seen in winter, result in the increase exhibited by the overall mean of DMGS.

Results from ECHAM4-driven simulations show little agreement with those from PRECIS-HA or PRECIS-HB, exemplified by an overall decrease in DMGS values in both PRECIS-EA-Mid and PRECIS-EA-Late (-0.83% and -0.75%). Similarly contrasting results are seen in the seasonal mean values, with PRECIS-EA-Late exhibiting changes of the opposite sign to the PRECIS-HA and PRECIS-HB in all seasons but spring. The season al mean exhibiting the greatest change in DMGS in ECHAM4-driven simulations, and also the lowest windspeeds, is summer, while minimal changes, and highest DMGSs, occur in winter. These results, combined with the increase in autumn (also a season with high DMGS), act to offset each other, resulting in the very low decrease seen in overall mean of DMGS in both PRECIS-EA-mid and PRECIS-EA-Late.

The change in the DMGS simulated by PRECIS-HA and PRECIS-HB was statistically significant at every station except Blackpool Squires Gate (*6*). This station was the only station in the HadAM3P-driven simulations to exhibit a reduction in the values (-0.47% and -0.11% in PRECIS-HA and PRECIS-HB respectively), and was also the station exhibiting the greatest reduction in ECHAM4-driven experiments (-11.11% and -11.20% in PRECIS-EA-Mid and PRECIS-EA-Late respectively). Further regional variations in relative changes in mean values of DMGSs are similar to those for the 98th percentile values of DMGS, presented in Figure 6.8. One slight difference is that for the PRECIS-EA-Late winter values, stations along the west coast exhibit greater relative decreases in the mean value than 98th percentile value of DMGS. In addition 4 stations in south England (Hurn (*19*) Lyneham (*26*), Middle Wallop (*29*) and Yeovilton (*43*)) show a relative increase in 98th percentile winter DMGS values, but a decrease in overall values, simulated in PRECIS-EA-Late.

98th percentile value of DMGS

Figure 6.7 displays changes the overall, seasonal and monthly 98th percentile values of DMGS relative to the corresponding values in the baseline experiments.

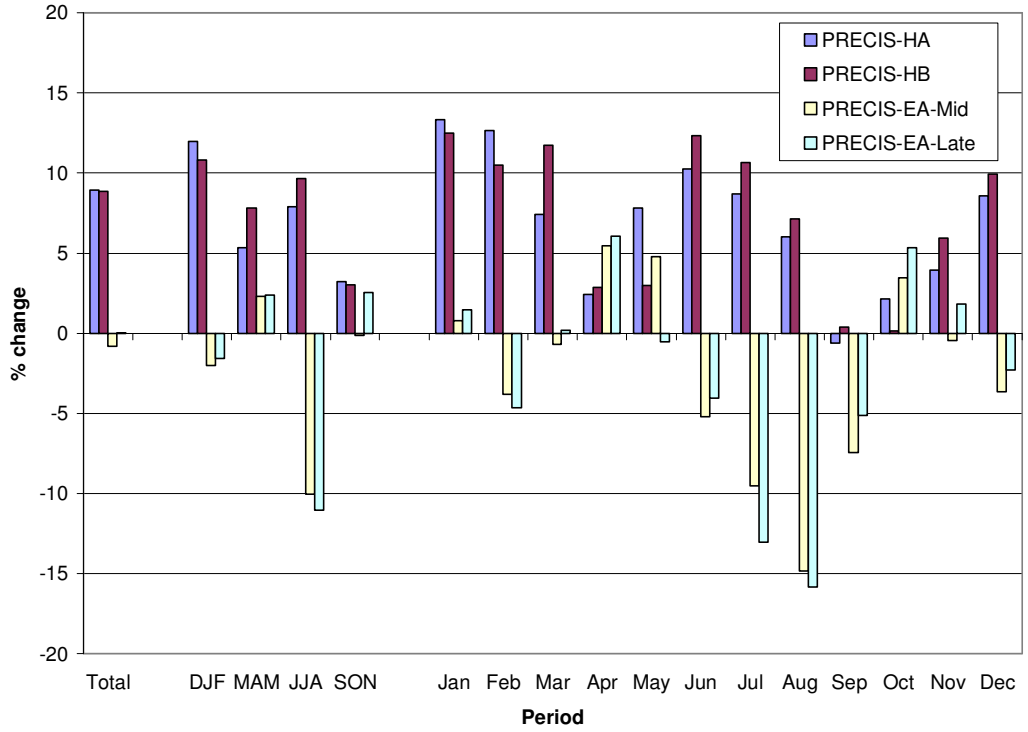

Figure 6.7 - Relative changes in the overall, seasonal and monthly 98th percentile values of DMGS in future climate simulations compared with baseline experiments.

HadAM3P-driven simulations produce 9% increases in the overall 98th percentile value, while a minimal change is seen in the ECHAM4-driven simulations (-0.8% and +0.01% changes in PRECIS-EA-Mid and PRECIS-EA-Late respectively). Absolute values of the changes in the 98th percentile value are shown in Table 6.4. Significance tests are run on the upper 2% of DMGS (i.e. damaging windspeeds) with the number of stations with significant shifts recorded in the right-hand column.

	Absolute change (ms^{-1})					No. of stations with significant changes			
	PRECIS-HA	**PRECIS-HB**	**PRECIS-EA-Mid**	**PRECIS-EA-Late**		**PRECIS-HA**	**PRECIS-HB**	**PRECIS-EA-Mid**	**PRECIS-EA-Late**
Total	1.2	1.2	-0.1	0.0		31	21	3	0
DJF	1.7	1.5	-0.3	-0.2		19	5	8	0
MAM	0.7	1.0	0.3	0.3		10	7	1	1
JJA	0.8	1.0	-1.1	-1.2		0	2	0	3
SON	0.4	0.4	0.0	0.3		2	0	2	1
Jan	1.9	1.8	0.1	0.2		7	2	0	4
Feb	1.8	1.5	-0.6	-0.7		11	0	4	3
Mar	1.0	1.5	-0.1	0.0		6	4	1	1
Apr	0.3	0.4	0.7	0.7		3	1	1	1
May	0.8	0.3	0.5	-0.1		0	0	0	0
Jun	1.0	1.2	-0.5	-0.4		0	0	0	0
Jul	0.8	1.0	-1.0	-1.4		0	0	0	0
Aug	0.6	0.7	-1.7	-1.8		0	0	0	2
Sep	-0.1	0.1	-1.0	-0.7		0	2	1	0
Oct	0.3	0.0	0.5	0.7		0	1	1	3
Nov	0.6	0.8	-0.1	0.3		0	2	1	0
Dec	1.2	1.4	-0.6	-0.4		1	7	9	0

Table 6.4 – Absolute change in the overall, seasonal and monthly 98th percentile values of DMGS in future climate simulations compared with baseline period, and the number of stations exhibiting significant changes.

Interestingly, the pattern seen in the average daily mean windspeeds and mean values of DMGS for HadAM3P-driven simulations is somewhat reversed here, with a greater increases in damaging windspeeds suggested by the PRECIS-HA simulations than PRECIS-HB; a result more in line with the studies cited previously. Although this feature is only seen in 4 months (one *less* than in mean windspeeds and DMGS values), significantly it is seen in winter and autumn. As already stated, relative changes in these seasons have a greater bearing on the overall change since the highest DMGSs occur in these periods.

It should be noted that the number of stations with statistically significant changes in damaging windspeeds are far fewer than when all DMGS data are considered. As with overall mean values of DMGS, the HadAM3P-driven simulations produce more significant changes at stations than ECHAM4-

driven simulations. In fact no stations display any significant changes in PRECIS-EA-Late, while only 3 (Eskdalemuir (*17*), Salsburgh (*34*) and St Mawgan (*36*)) exhibiting significant changes in PRECIS-EA-Mid. The relative change at each station in the 98th percentile value of DMGS in PRECIS-HA and PRECIS-EA-Late is shown in Figure 6.8, with similar patterns (although slightly lower magnitudes of changes) seen in PRECIS-HB and PRECIS-EA-Mid respectively (not shown).

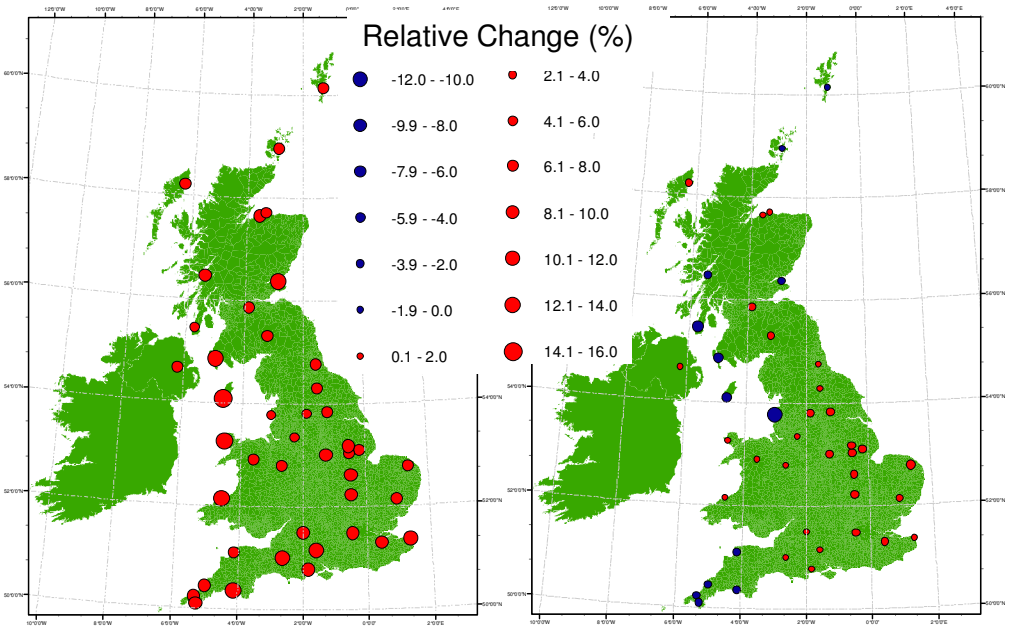

Figure 6.8 - Relative changes in the 98th percentile value of DMGS simulated by PRECIS-HA (left) and PRECIS-EA-Late (right).

An east-west divide is suggested the right panel of Figure 6.8, with stations in the west tend to exhibit decreases, and stations to the east exhibiting increases, in damaging windspeeds simulated by PRECIS-EA-Late. However, as noted previously none of these changes are statistically significant. Generally, greater relative increases in damaging windspeeds simulated by PRECIS-HA occur at coastal stations, most notably those on the west coast.

The 98th percentile value of DMGS is used as a threshold for damaging windspeeds in the simplified model in the section 6.2. Hence, the standard deviation of the upper 2% provides information on the variance of damaging windspeeds. An increase in standard deviation in the future simulations, compared with baseline simulations, indicates the increase of extreme damaging windspeeds. All stations in the PRECIS-HA simulation, except West

Freugh (*41*), exhibit increased standard deviations in damaging windspeeds, with a Network Average increase of 30%. A slightly lower value is seen in PRECIS-HB (23% increase) with 3 stations showing decreases of less than 10%. PRECIS-EA-Mid simulations suggest the standard deviation decreases by 7%, while a 4% increase is exhibited by the Network Average in the PRECIS-EA-Late simulation.

While it useful to have an appreciation for the spatial variation shown in the change in the overall 98th percentile value of DMGS, assessing the intra-annual variations is also important when considering wind-related damage. As noted previously changes in damaging windspeeds in winter drive changes in the overall value. Figure 6.9 shows the spatial variation in relative changes in summer and winter 98th percentile values of DMGS in PRECIS-HA and PRECIS-EA-Late. Summer figures are included to put winter changes into context.

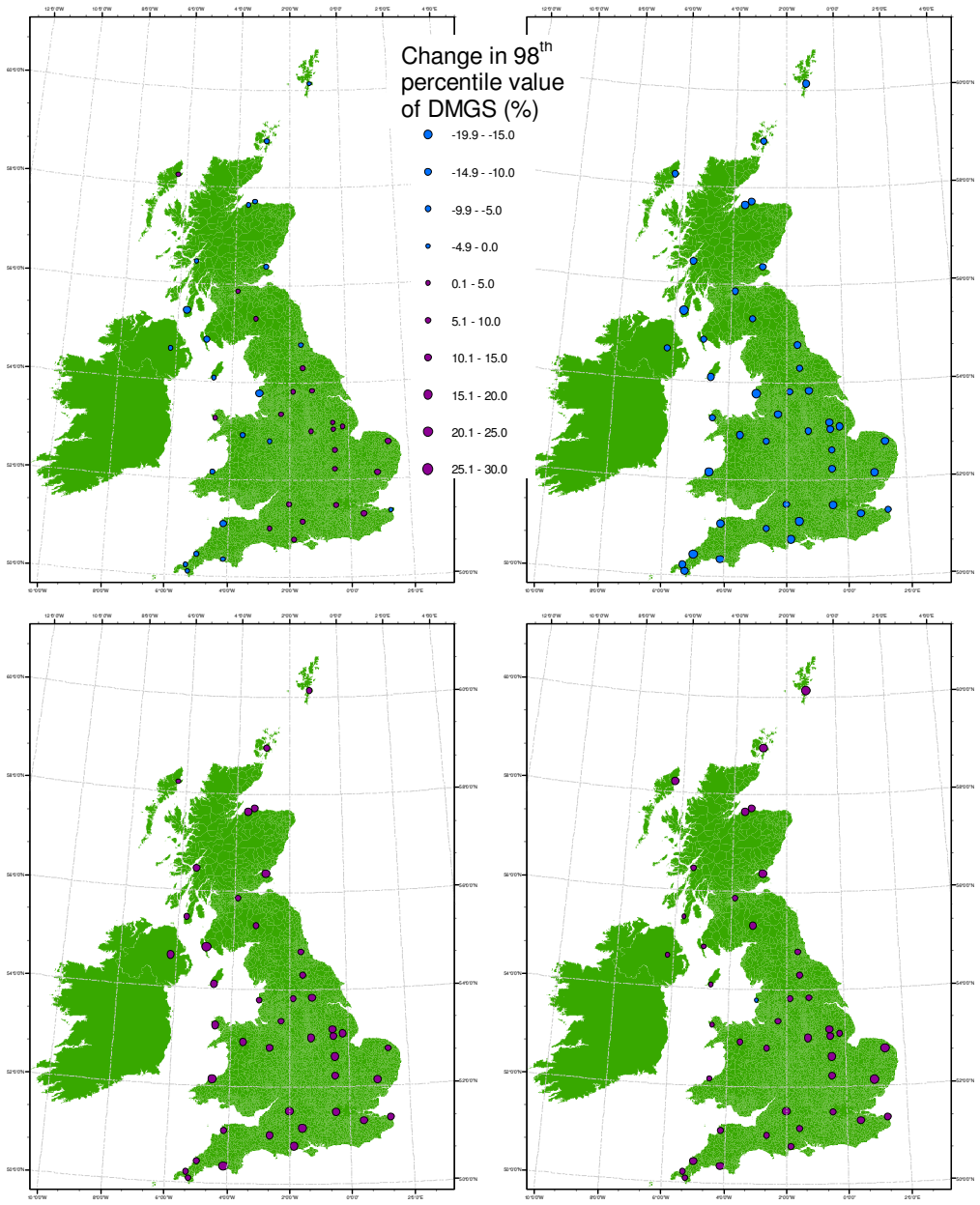

Figure 6.9 - Relative changes in winter (left) and summer (right) 98th percentile values of DMGS in PRECIS-EA-Late (top) and PRECIS-HA (bottom) simulations.

Relative changes in PRECIS-EA-Late winter value of the 98th percentile of DMGS suggest decreases in the west, and increases in the east (top left panel in Figure 6.9). This follows the pattern exhibited by the overall 98th percentile value, shown Figure 6.8. The station seeing the greatest reduction is Blackpool Squires Gate (*6*) (-13.1%) while the greatest increase is seen at Wattisham (*40*) (+5.7%). Summer values (top right) are negative at all stations ranging from -16.1% at Blackpool Squires Gate (*6*) to -3.9% at West Freugh (*41*). Stations in the south and south east of England which exhibited some of the greatest increases in winter values, also show some of the highest

decreases in summer values. This illustrates the dominance of winter changes over summer changes in influencing the overall change.

With the exception of Blackpool Squire gate (*6*) all stations in both winter and summer exhibit an increase in damaging windspeeds in HadAM3P-driven simulations, with the greatest seen in winter. Stations on the west coast tend to display some of the greatest increases in winter values in conjunction with some of the lowest in summer. This effect is not evident on the east coast, where several stations exhibit greater increases in summer than winter.

The importance of the time of the year damaging windspeeds occurs has been highlighted in section 5.2. Figure 6.10 and Figure 6.11 show the intra-annual variation in the occurrence of damaging windspeeds in the HadAM3P-driven and ECHAM4-driven future simulations respectively.

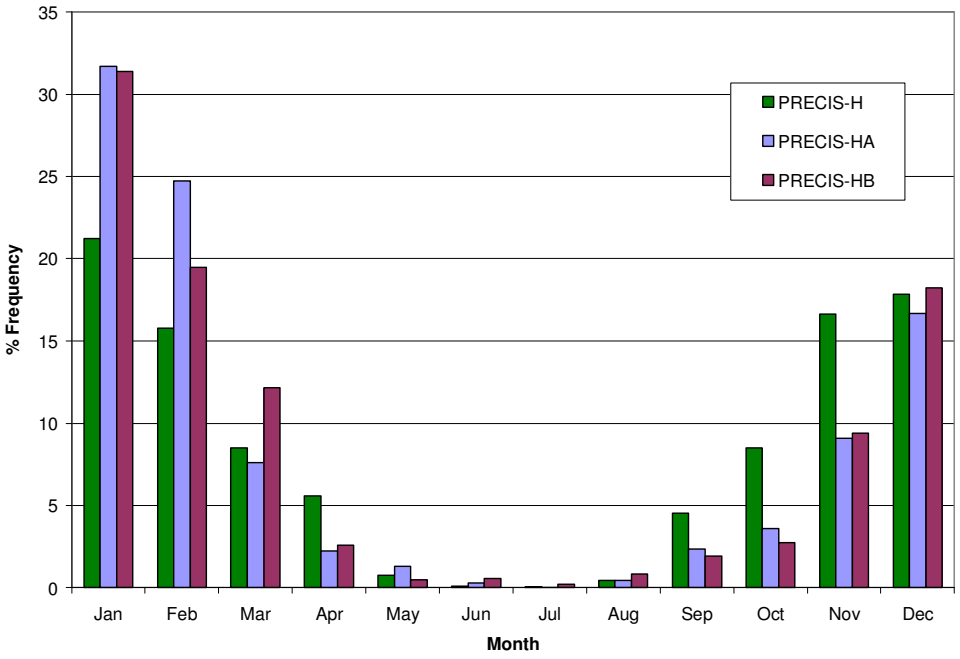

Figure 6.10 - Intra-annual variation of the occurrence of damaging windspeeds in the PRECIS-HA (light blue) and PRECIS-HB (purple) simulations, compared to the PRECIS-H baseline (green).

The intra-annual variation in the occurrence of damaging windspeeds simulated by PRECIS-HA and PRECIS-HB are fairly similar, except for the 5% discrepancies in February and March. Although PRECIS-H exhibiting a -10% bias in winter, the increases shown by future HadAM3P-driven simulations far outweigh that figure. The shift towards a greater percentage of damaging

windspeeds occurring in winter corresponds with a decrease in autumn. Where the distribution of damaging windspeeds was reasonably even in the months from November to February in the baseline simulation, prominent peaks exist in January and February in the future simulations. This is significant when considering the insured loss associated with damaging winds and will be further explored in section 6.2.

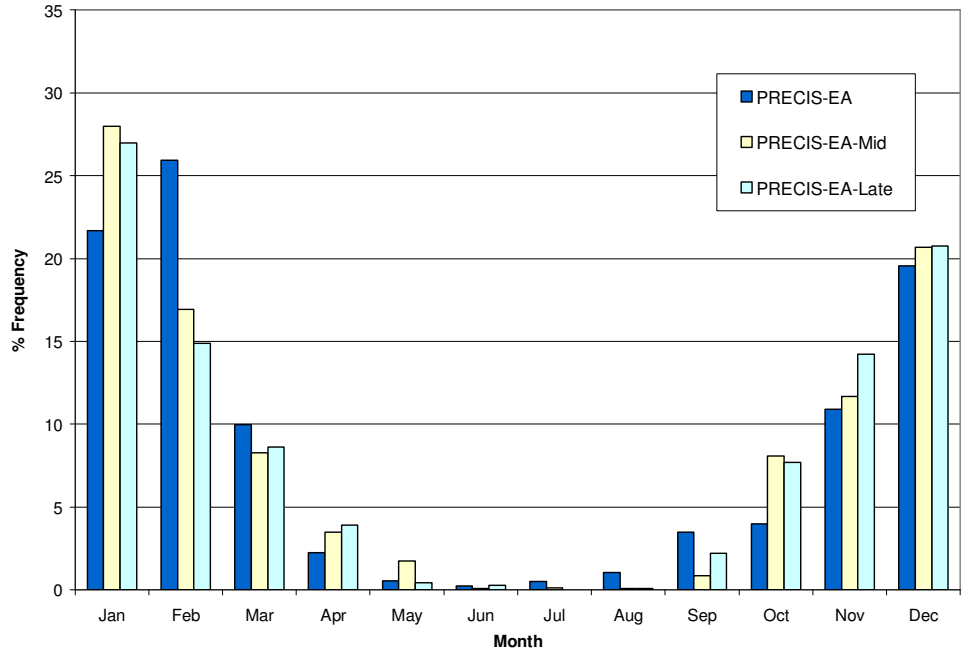

Figure 6.11 - Intra-annual variation of the occurrence of damaging windspeeds in the PRECIS-EA-Mid (yellow) and PRECIS-EA-Late (light blue) simulations, compared to the PRECIS-EA baseline (dark blue).

PRECIS-EA-Mid and PRECIS-EA-late simulations of damaging winds also display a shift compared to the baseline simulations, with a greater percentage occurring in the period October to January, and a decrease in September and February. Both future simulations suggest the period in which damaging windspeeds are most prominent is likely to shrink to December and January from December to February.

6.1.3 Summary

Daily mean windspeeds simulation by PRECIS-EA-Mid and PRECIS-EA-Late show a decrease of just under 2%, relative to the baseline simulation (PRECIS-EA). PRECIS-EA-Late suggests a marginally larger decrease than

PRECIS-EA-Mid overall, and in all seasons. Winter and summer values in PRECIS-EA-Late are 3% and 9% lower than in the baseline simulations respectively. These changes exceed the bias shown between PRECIS-EA and PRECIS-Re (considered “current” climate).

Mean daily windspeeds simulated in HadAM3P-driven experiments show a greater deviation from the baseline simulation than those driven by ECHAM4. Results indicate increases of 5.5% (4.2%) in PRECIS-HB (PRECIS-HA), with all seasonal means increasing except autumn, relative to the baseline simulation. Winter exhibits the greatest increase (14% in PRECIS-HB and 12.6% in PRECIS-HA), while autumn was the only other season with a changing mean greater than the bias (-3.6% in PRECIS-HB and -4.1% in PRECIS-HA). The overall increase in daily mean windspeeds occurs at every station, driven by the winter increases. Greatest increases occur in the south of England, and in Scotland.

Relative changes in the overall, seasonal and monthly mean values of DMGS in HadAM3P- and ECHAM4-driven simulations reveal a similar pattern to changes in daily mean windspeeds. Decreases of less than 1% are seen in overall DMGS values in PRECIS-EA-Late and PRECIS-EA-Mid simulations. These are markedly lower values than the bias seen between PRECIS-EA and PRECIS-Re indicating the result should be viewed with caution. The 9% decrease in summer DMGS values is the only change which exceeds the bias value in both PRECIS-EA-Mid and PRECIS-EA-Late.

An increase in DMGS values simulated by PRECIS-HA (PRECIS-HB) of 5% (6%) is less than the bias (-10%) found between the PRECIS-H and PRECIS-Re datasets. However, in both simulations 42 of 43 stations exhibit significant increases in DMGS values. As with daily mean windspeeds, seasonal mean values of DMGS are shown to increase with the exception of autumn. The 13% (14%) increase in the winter mean value and 3% (3%) decrease in the autumn mean value in PRECIS-HA (PRECIS-HB) simulations exceed the bias in those seasons.

Significant changes in damaging windspeeds are only seen at 3 (0) stations in PRECIS-EA-Mid (PRECIS-EA-Late) simulations. A decrease of 0.8% is seen in PRECIS-EA-Mid values, while a minimal (0.01%) increase is seen in PRECIS-EA-Late. These compare to a -6.1% bias exhibited by PRECIS-EA. Winter and summer damaging windspeeds decrease by 2% (2%) and 10% (11%) respectively in PRECIS-EA-Mid (PRECIS-EA-Late) simulations. Increases are seen in spring and autumn, but are less than the bias.

Similar to the relative changes in daily mean windspeeds and DMGSs, HadAM3P-driven simulations of damaging windspeeds show a greater shift than ECHAM4-driven values. A 9% increase occurs in PRECIS-HA and PRECIS-HB simulations, along with increases in every season. Winter values exhibit the greatest increase (12% and 11% in PRECIS-HA and PRECIS-HB respectively). However, no changes are greater than the bias between PRECIS-H and PRECIS-Re, suggesting any changes when compared to current climate, cannot be confidently presented. Pryor *et al.* (2006) found similar results, with the variability manifest in the statistical downscaling of the 10-GCM ensemble greater than the change in mean and 90th percentile windspeeds. The authors assessed future changes over Scandinavia in the periods 2046-2065 and 2081-2100, under an A2 emissions scenario. While not directly comparable to results present here, increases of up to 20% (35%) were seen at stations for 2046-2065 (2081-2100) for the mean and 90th percentile. Results from the Leckebusch *et al.* (2006) study are directly comparable since they used HadRM3P at the 0.44^0 resolution, under the A2 emissions scenarios, driven by HadAM3P to simulate 10-metre windspeeds over the UK. Changes in the 99th percentile of windspeeds over the UK for the period were found in the range of +8-16% over northern England and +4-8% over East Anglia, with minimal changes over the remaining area. Findings from these two studies suggest results presented here are certainly reasonable.

The standard deviation of damaging windspeeds in the PRECIS-HA simulation increases by 30%, with a slightly lower value for PRECIS-HB (23% increase). The PRECIS-EA-Mid simulation suggests a decrease of 7%, while a 4% increase is seen in PRECIS-EA-Late. Hanson *et al.* (2004), using

HadRM3H driven by HadCM3 at 0.44^0 resolution for the period 2070-2099, found the standard deviation of the number of days when the gust speed exceeded the 95^{th} percentile diminished by up to 3 days over East Anglia. This result is slightly contrary those reported here. However, under the B2 scenario, Hanson *et al.* (2004) found an in increase in the standard deviation over south and central England, in accordance with results here.

Figure 6.10 and Figure 6.11 imply that the period with the highest frequency of damaging windspeeds narrows. PRECIS-HA and PRECIS-HB simulations suggest more than 50% of damaging windspeeds will occur in January and February (an increase of 15-20%), with the percentage in December remaining unchanged. This is coupled an increase in winter damaging windspeeds of up to 10%, suggesting that winters in the future (2071-2100) could produce more frequent and higher damaging windspeeds. PRECIS-EA-Mid and PRECIS-EA-Late simulations suggest that there may be a shift toward more damaging windspeeds later in the year, with increases in October to January, and a 10% decrease in February. These are coupled with relative increases in damaging windspeeds in January and October of roughly 2% and 4% respectively. The potential impact of these changes on wind-related insured losses is explored in section 6.2.

Results presented here demonstrate that model uncertainty (different driving GCMs) outweighs radiative forcing uncertainty (different scenarios), verifying previous work by Déqué *et al.* (2007).

6.2 Implications for insured windstorm losses

6.2.1 Introduction

The characteristics of the future UK wind regime are described above, including an assessment of the changing frequency and intensity of damaging windspeeds in the periods 2021-2050 and 2071-2100. The aim of this section is to incorporate this information into the simplified loss model developed in Chapter 5, in order to quantify future wind-related insured losses.

In Chapter 5 the PRECIS-Re windspeed data in the simplified loss model were adjusted before input. The correction factor was determined through the direct comparison of PRECIS-Re data to observed windspeed data. However, this relationship cannot be assumed to be temporally stable, and hence no adjustment is made to PRECIS data in this section. Therefore, no actual loss estimates are produced based on future simulations, as absolute values will not be comparable to estimates made in Chapter 5. Instead, Loss Potentials are once again utilised and can be viewed as indicative absolute losses.

As stated previously no information regarding UK household numbers in the future periods 2021-2050 and 2071-2100 is available. The simplified model incorporates the household number and distribution from 2001, and so all changes in Loss Potential are therefore considered relative to the current distribution of domestic properties. Part of the benefit of using the simplified loss model over the more sophisticated one developed in Chapter 4 is that projections of the independent variables (property type and property prices) are not available for the future time periods considered. Incorporation of all these variables would result in estimates of Loss Potentials with unacceptable levels of uncertainty. Restricting the model to just household number reduces the uncertainty in future projections.

In future climates, if the assumption is made that the vulnerability of domestic properties is unchanged (i.e. the same top percentage of windspeeds is causing damage) then the building stock could be said to have undergone "adaptation" to the new wind regime. However, in future climates where properties possess the same vulnerability as they do in the current climate, i.e. without adaptation, the threshold for damage remains constant. In other words, without adaptation, the absolute value of the damage threshold from the current climate is used as the threshold in the future. Using these two methods (from here on known as "with adaptation" and "without adaptation"), changes in Loss Potentials are quantified for two situations; one in a world where the risk of damage to buildings is identical to current levels (with adaptation), and one in a world where the risk of damage is altered based purely on a shift in the wind climate (without adaptation). A similar methodology is employed by Leckebusch *et al.* (2007) and Pinto *et al.* (2007).

6.2.2 Results

It has been shown that PRECIS-Re wind data capture variations shown in the observed wind dataset with some confidence, in section 3.3. In addition, Loss Potentials calculated from PRECIS-Re data reflect those calculated from observed windspeed data reasonably well. It is shown in section 6.2.1 that while there is some difference between PRECIS-Re and the baseline experiments (PRECIS-H and PRECIS-EA), they may be viewed as representative of the "current" climate. As such, Loss Potentials calculated on a postcode sector basis, using data from future PRECIS simulations, are presented relative to those calculated using data from the baseline simulations.

The Loss Potential for each postcode sector in Great Britain is calculated using the formula developed in section 5.1 with windspeed data from the baseline experiments (PRECIS-H and PRECIS-EA), as well as the future PRECIS simulations. The future mean annual Loss Potentials for Great Britain as a whole are presented relative to those calculated for baseline simulations. Initially a temporal analysis, with a quantification of inter- and intra-annual variations, is presented. Subsequently, an assessment of the spatial variation in future Loss Potentials concludes this section.

Annual Loss Potential

The mean annual total Loss Potential for Great Britain is calculated using windspeed data from future simulations, summing the individual Loss Potentials in each postcode sector. The relative change in both HadAM3P- and ECHAM4-driven simulations are shown in Figure 6.12. Values "with adaptation" and "without adaptation" are depicted in blue and purple respectively.

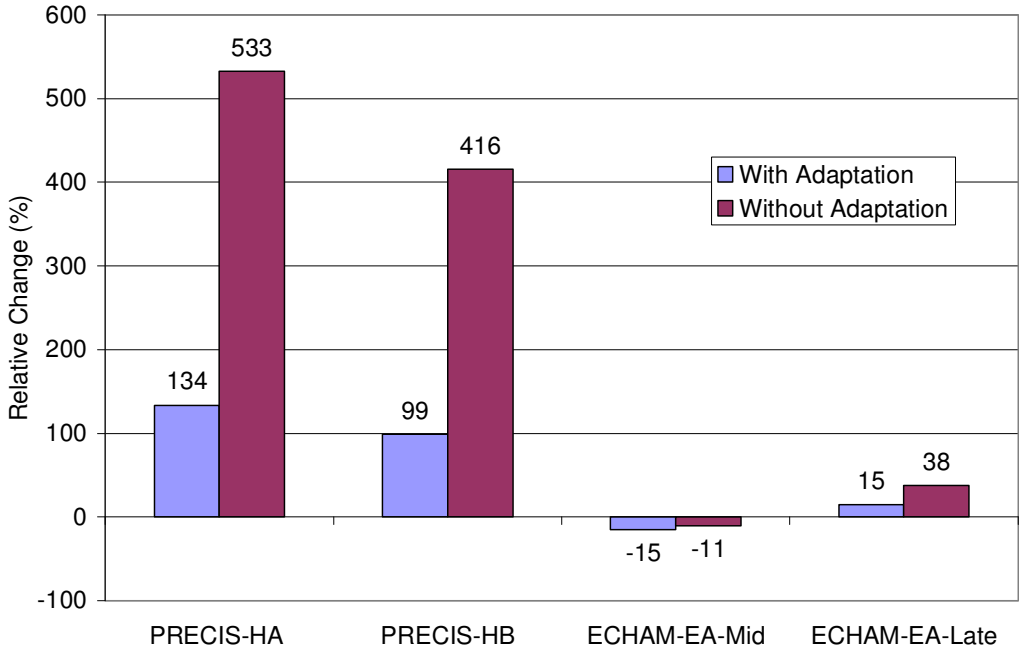

Figure 6.12 – Relative change (%) in mean annual Great Britain Loss Potential calculated from future simulations, compared to those calculated from baseline simulations.

The relative change in the mean annual Loss Potential shown above are found to be significant (at the 95% confidence level) for future simulations driven by HadAM3P, but not those driven by ECHAM4. Following the increases in 98th percentile values of DMGS values described above in HadAM3P-driven simulations and minimal increases (or decreases) in ECHAM4-driven simulations, it follows that changes in Loss Potentials (without adaptation) should exhibit a similar pattern. Variation in Loss Potentials calculated with and without adaptation outweighs the variations between the two scenarios and two driving GCMs utilised in this study. Loss potentials, with adaptation, appear to be related to changes in the standard deviation of damaging windspeeds. Simulations with a greater increase in standard deviation correspond those exhibiting the greater increases in mean annual Loss Potential with adaptation (increases in standard deviation in the upper 2% of DMGS are 30%, 23% and 4% for PRECIS-HA, PRECIS-HB and PRECIS-EA-Late respectively).

Inter-annual variation in Loss Potentials

The standard deviation of annual Loss Potential reflects the inter-annual variability of the impact of windstorms on insured losses. Relative changes in the standard deviation of future annual Loss Potentials, compared to baseline

values, are shown in Table 6.5. Increases are shown by PRECIS-HA and PRECIS-HB, indicating that in these simulations higher annual Loss Potentials than experienced in the baseline period will be experienced.

	PRECIS-HA	PRECIS-HB	ECHAM-EA-Mid	ECHAM-EA-Late
With Adaptation	+259%	+109%	-17%	-5%
Without Adaptation	+683%	+342%	-16%	+11%

Table 6.5 - Relative change in the standard deviation of future annual Loss Potentials.

Intra-annual variation in Loss Potentials

As described in section 5.2 the time of the year damaging windspeeds occur will have an impact on losses. The proportion of mean annual Loss Potential occurring in each season in the future and baseline simulations are shown in Figure 6.13.

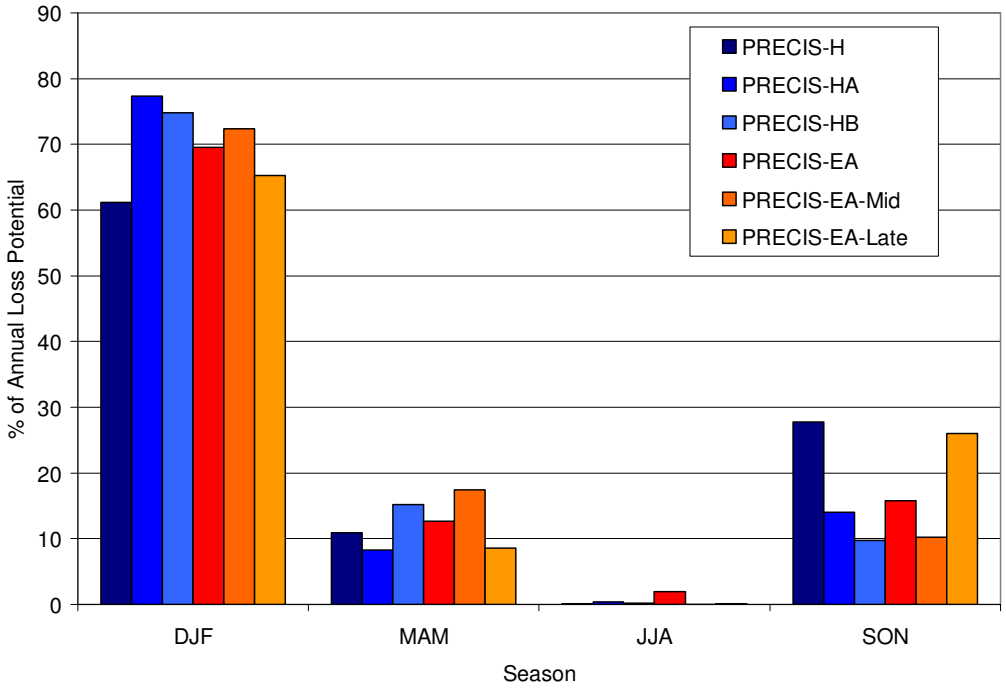

Figure 6.13 - Intra-annual distribution of annual Loss Potential in future and baseline and baseline.

PRECIS-HA and PRECIS-HB simulations suggest the percentage of total annual Loss Potential occurring in winter will increase, with a corresponding decrease in autumn. PRECIS-EA-Mid exhibits a similar pattern, while

PRECIS-EA-Late suggests the reverse, with a decrease in winter and an increase in autumn. These changes correspond to those in the intra-annual variation of occurrence of the top 2% of DMGS presented in Figure 6.10 and Figure 6.11.

Spatial variations in future Loss Potentials

Relative changes in mean annual and seasonal Loss Potentials in future simulations, described above, are not uniform across the whole of Great Britain. Before the regional variations in mean annual Loss Potentials are explored, future simulations of winter Loss Potential, which have been shown to account for up to nearly 80% of the annual value are presented. Figure 6.14 shows the relative change in Loss Potentials in each postcode sector for HadAM3P-driven simulations without adaptation, while Figure 6.15 shows similar values for ECHAM4-driven simulations. Different scales are used to emphasis regional variations.

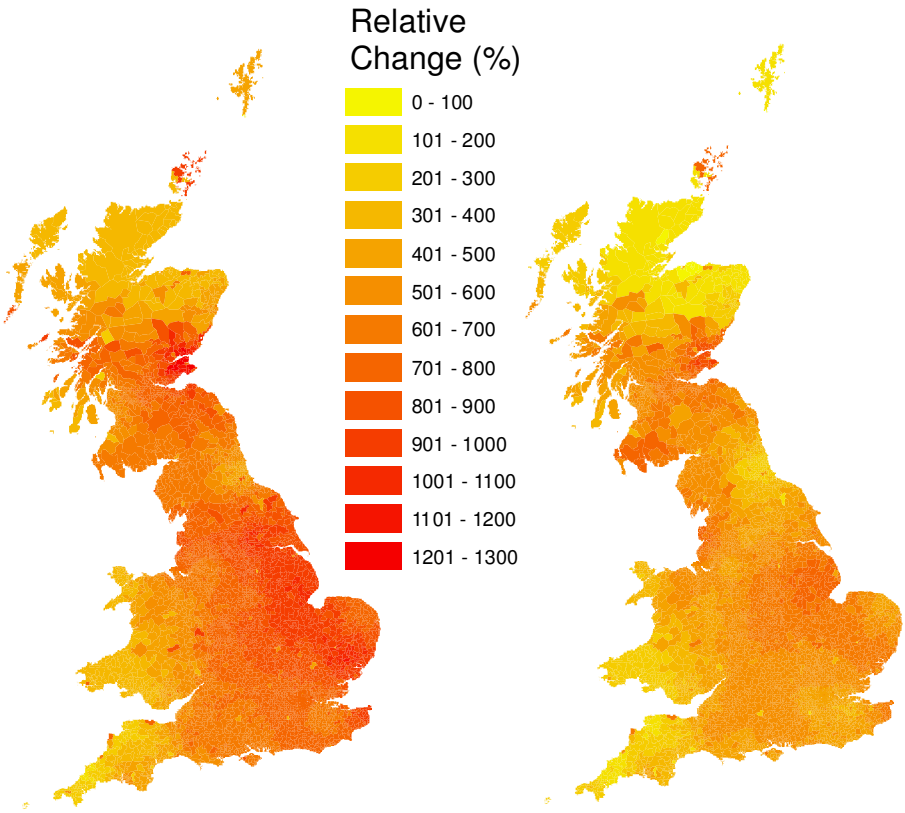

Figure 6.14 - Relative change in winter Loss Potential in each postcode sector, simulated by PRECIS-HA (left) and PRECIS-HB (right) without adaptation.

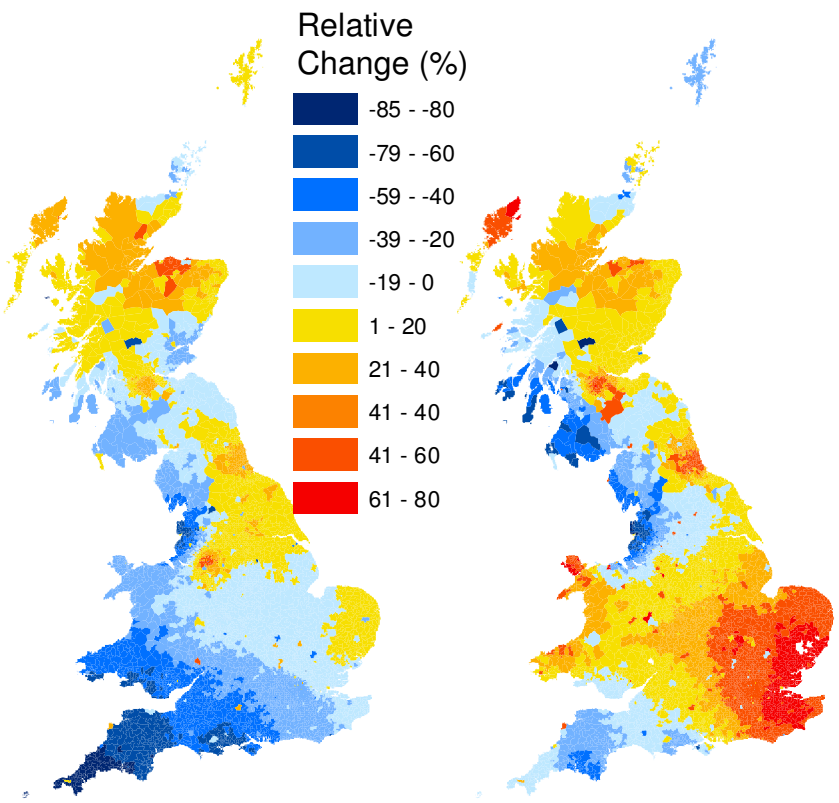

Figure 6.15 - Relative change in winter Loss Potential in each postcode sector, simulated by PRECIS-EA-Mid (left) and PRECIS-EA-Late (right) without adaptation.

Figure 6.14 and Figure 6.15 show relative changes without adaptation; values with adaptation are not shown since the intention here is to show that winter changes drive changes in mean annual Loss Potentials shown in Figure 6.16 and Figure 6.17. With adaptation, relative changes in the winter Loss Potential of -50% to 500% are seen in HadAM3P-driven simulations, and -80% to 60% for ECHAM4-driven simulations. Relative changes in winter Loss Potential in PRECIS-HA and PRECIS-HB shown in Figure 6.14 follow a similar pattern, although the magnitudes are slightly lower in the later. Hence the relative change in annual mean Loss Potential is only shown for PRECIS-HA in Figure 6.16.

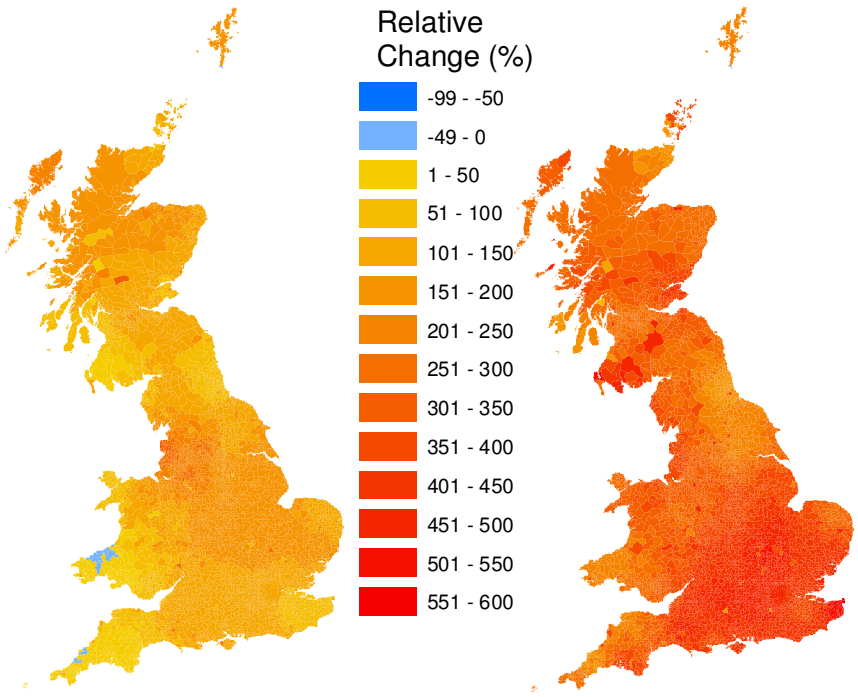

Figure 6.16 - Relative change in mean annual Loss Potential in each postcode sector simulated by PRECIS-HA with adaptation (left) and without adaptation (right).

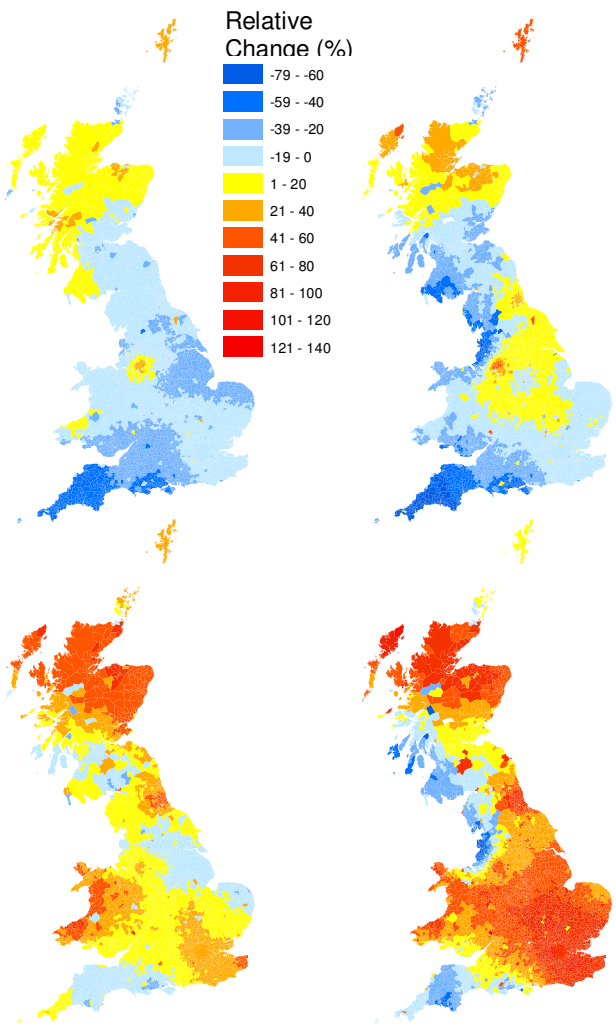

Figure 6.17 - Relative change in mean annual Loss Potential in each postcode sector simulated by PRECIS-EA-Mid (top) and PRECIS-EA-Late (bottom with (left) and without (right) adaptation.

Some spatial variations, shown in Figure 6.16 and Figure 6.17, exist between changes in mean annual Loss Potential with and without adaptation. The postcode sectors with the greatest increase in mean annual Loss Potential in PRECIS-HA (and PRECIS-HB) with adaptation lie in the north west of England, around Manchester and Liverpool. Values without adaptation are highest in south east of England. Although there is a significant difference between the spatial pattern exhibited by PRECIS-HA and PRECIS-EA-Late, a similar feature is shown; south east England exhibits some of the highest values without adaptation, but not with adaptation. Areas exhibiting negative changes in Loss Potentials in PRECIS-EA-Late with adaptation tend to exhibit even greater reductions without adaptation. However, this is not the case for north east England and northern parts of East Anglian, which show a reduction with adaptation and an increase without adaptation.

The spatial variation exhibited by changes in the mean annual Loss Potential without adaptation in PRECIS-EA-Late, in Figure 6.15, is very similar to that shown by changes in the 98th percentile values of DMGS, in Figure 6.8. Similarities also exist for HadAM3P-driven simulations, despite being more difficult to distinguish. This reinforces the earlier finding that changes in the 98th percentile value of DMGS are driving changes in Loss Potential without adaptation.

Loss Potentials simulated by PRECIS-EA-Mid suggest a large proportion of Great Britain will experience a decline in the period 2021-2050. However, while some areas may also experience a decrease in 2071-2100 (PRECIS-EA-Late), others actually may see a marked increase (e.g. Wales and the south east of England). These changes mirror those in the wind regime in ECHAM4-driven simulations outlined in section 6.1. This indicates the varying nature of the wind regime, and subsequently Loss Potentials, over the course of the twenty first century.

6.2.3 Summary

Mean annual Loss Potentials simulated by PRECIS-HA and PRECIS-HB, relative to the baseline simulation (PRECIS-H), suggest increases of 134% (533%) and 99% (416%) with (without) adaptation respectively. Leckebusch *et al.* (2007) report changes in loss ratios for the UK of +22% (+80%) and -2% (+8%) simulated by HadCM3 and HadAM3P with (without) adaptation respectively, for the period 2070-2099, under A2 emissions scenario. Changes in the standard deviation of annual Loss Potential reflects changes in the inter-annual variability. Increases are shown by PRECIS-HA and PRECIS-HB with adaptation (without adaptation) of 259% (683%) and 109% (342%) respectively. These figures are higher than those published by Leckebusch *et al.* (2007), who saw changes in the standard deviation of loss ratio for the UK of +113% (+233%) and -4.8% (+8.9%) with (without) adaptation for HadCM3 and HadAM3P simulations respectively. Differences between the mean annual figures and standard deviation values presented here and those found by Leckebusch *et al.* (2007) may, in part, be explained

by the higher spatial resolution climate simulations utilised here. Additionally, the loss model utilised by Leckebusch *et al.* (2007) was developed with German insurance data.

The change in mean annual Loss Potential simulated in PRECIS-EA-Mid and PRECIS-EA-Late are markedly lower than those by PRECIS-HA and PRECIS-HB. In fact the value decreases by 15% (11%) in PRECIS-EA-Mid, but increases by 15% (38%) in PRECIS-EA-Late with (without) adaptation. For comparison, Leckebusch *et al.* (2007) found a similar changes in loss ratio for the UK, of -9% (+21%) with (without) adaptation, using ECHAM4/OPYC3 under an A2 emissions scenario, for the period 2070-2099. Pinto *et al.* (2007) also found changes in loss ratio of a similar amount for the UK, of -4% (+24%) with (without) adaptation using a 3-member ECHAM5/MPI-OM1 ensemble under an A2 emissions scenario.

Compared with HadAM3P-driven simulations minimal changes in the standard deviation of annual Loss Potentials are calculated from ECHAM4-driven simulations, with PRECIS-EA-Mid actually showing a decrease of 17% (16%) with (without) adaptation. PRECIS-EA-Late shows a decrease of 5% with adaptation, but an increase of 11% without adaptation. Similarly Leckebusch *et al.* (2007) report a decrease of 5% with adaptation and an increase of 42% without, in the standard deviation of loss ratio for the UK in an ECHAM4/OPYC3 simulation. Although the baseline period used by Leckebusch *et al.* (2007) for ECHAM4/OPYC3 was 1890-1990, their results are comparable to those presented here. Again, differences may have evolved due to the course resolution (2.8^{o} spatial grid) of the ECHAM4/OPYC3 simulation. In a similar study Pinto *et al.* (2007) found increases in the standard deviation of loss ratio over the UK of 19% (85%) with (without) adaptation. These figures were produced by ensemble of ECHAM5/MPI-OM1 simulations for the period 2060-2100 (with a baseline period of 1960-2000), under the A2 emissions scenario. These values, along with those from Leckebusch *et al.* (2007), demonstrate that those presented here for Great Britain are within current model estimates and may be considered plausible.

It is shown that the change in mean annual Loss Potential is predominantly driven by changes in winter Loss Potential. Increases of 10-15% in the proportion of annual Loss Potential occurring winter are simulated by PRECIS-HA and PRECIS-HB. Corresponding increases and decreases in the proportion of annual Loss Potential occurring in winter are found in autumn in all simulations. A 2% increase is seen in winter in PRECIS-EA-Mid, while a 5% decrease occurs in PRECIS-EA-Late. This suggests that while the mean annual Loss Potential decreases in PRECIS-EA-Mid, a greater proportion occurs in winter.

Given the high proportion of annual Loss Potential occurring in winter it is no surprise that the spatial variations of changes in annual Loss Potential largely follow those in winter. Figure 6.16 and Figure 6.17 suggest that, while certain regions may experience a decrease in annual Loss Potential with adaptation, an increase may occur without adaptation. Such a situation is suggested in the north east of England in PRECIS-EA-Mid and PRECIS-EA-Late simulations. This emphasises the importance of considering the change in standard deviation as well as the increase in absolute damaging windspeeds. All simulations for the period 2071-2100 suggest that without adaptation south east England will see the greatest increase in Loss Potentials. However, with adaptation the greatest increase is seen in the north east of England in HadAM3P-driven simulations, while this area exhibits a decrease in PRECIS-EA-Late.

6.3 Conclusions

An analysis of the future wind regime simulated over the UK is presented in section 6.1, completing the first research aim of this project; an assessment of the historic and future UK wind regime. With the windspeed information provided by PRECIS simulations the impact of the future wind regime on wind-related insured domestic property losses in Great Britain is quantified, accomplishing the final research aim.

The mean daily windspeeds, DMGSs and damaging windspeeds in future PRECIS simulations are assessed in section 6.1, relative to the baseline simulations. Increases of 5-10% in all three values were found in HadAM3P-driven simulations, while ECHAM4-driven simulations generally suggested a slight decrease (less than 3%). However, consistent negative biases of similar magnitudes to these results exist in the baseline simulations compared with PRECIS-Re (considered "current" climate). Therefore, changes in windspeed values in future climates should be considered with caution. Increases of 4-5% are shown by mean daily windspeeds in HadAM3P-driven simulations, while 2-3% decreases are exhibited by ECHAM4-driven simulations. These must be interpreted with bias values of -8% and -3% for PRECIS-H and PRECIS-EA respectively, in mind. Similarly, increases in the mean (98^{th} percentile) value of DMGS in HadAM3P-driven experiments of 5-6% (9-10%) must be considered against a bias value of -10% (-12%). Corresponding changes in ECHAM4-driven simulations of -1-2% (-1-0%) compare to a bias value of -5% (-6%). While the magnitude in the baseline bias appears to be greater than the overall changes in windspeed values, it must be noted that this is not the case for some seasonal values (for instance, mean winter DMGS value bias for PRECIS-H is -7%, while increases in HadAM3P-driven simulations are 13-14%).

An interesting feature of the ECHAM4-driven simulations lies in the changes in DMGSs and damaging windspeeds. Results suggest that decreases in these values are greater in 2021-2050 than in 2071-2100, compared with the baseline period of 1961-1990. Although the differences are small, this emphasises the variable nature of the climate system. Future climate simulations have traditionally been made for the 2020-50 and 2070-2100 periods. However, the increasing volume of work in this area, and increasing resource availability, has led to more varied time periods being assessed. For instance, the ENSEMBLES project, outlined by Christensen and Christensen (2007), includes several simulations running continuously from the present day to 2100. ECHAM4 data are available to drive PRECIS continuously until 2100; however, resource and time restrictions did not permit this in this project. It would be very informative to analyse how the wind regime over the

UK evolved over the twenty-first century to produce the results seen in PRECIS-EA-Mid and PRECIS-EA-Late.

Also somewhat surprising are the results generated by HadAM3P-driven experiments under the A2 scenario and B2 scenario (i.e. PRECIS-HA and PRECIS-HB). Christensen and Christensen (2007), among others, suggest that climate change signals tend to be stronger in simulations run under the A2, rather than B2, emissions scenario. Results presented here for daily mean windspeeds and DMGSs suggests the opposite, albeit by just a few percent in most cases. However, when damaging windspeeds are considered, the PRECIS-HA signal is slightly stronger. In this regard these results correspond with those for high percentile mean windspeeds in Hanson *et al.* (2004), Leckebusch *et al.* (2006) and Pryor *et al.* (2005a). The difference in the results between the A2 and B2 scenario may be within the model uncertainty, and would require further simulations to be generated in order to have confidence in this pattern. Unfortunately, no ECHAM4-driven simulations were carried out under the B2 emissions scenario. In the design of the project the ECHAM4-driven experiments were limited to one emissions scenario due to time and resource limitations. The A2 scenario was chosen over the B2, as it is more commonly utilised and was perceived to produce a greater climate change signal when driven by HadAM3P and ECHAM4 (Räisänen *et al.*, 2004). It would be informative to carry out further PRECIS simulations with ECHAM4, under the B2 scenario, to see if a similar pattern of results are shown to those produced by PRECIS-HA and PRECIS-HB.

The changes in the UK wind regime described in section 6.1 are utilised to assess changes in wind-related insured domestic property loss. Changes in Loss Potentials are produced, relative to baseline experiments, for future PRECIS simulations, with the spatial and temporal variations analysed. Two values are produced; the first considers properties have adapted to the future wind regime (with adaptation), while a second assumes the same absolute damage threshold as in the baseline simulation (without adaptation).

Mean annual Loss Potentials increase in all three 2071-2100 simulations, while the only simulation for 2021-2050 suggests a decrease. The

combinations of higher damaging windspeeds, and the increase in their standard deviation, drive increases in Loss Potentials. Changes in standard deviation are largely responsible for changes in Loss Potentials with adaptation, since damaging windspeeds in the calculation are normalised to the new 98th percentile of DMGS. Without adaptation the threshold for damage does not alter, therefore changes in the magnitude of damaging windspeeds, indicated by 98th percentile values of DMGS, drive changes in the Loss Potential. Changes in mean annual Loss Potentials are greater in HadAM3P-driven simulations than in PRECIS-EA-Late, with values of +533% (+134%), +416% (+99%) and 15% (+38%) for PRECIS-HA, PRECIS-HB and PRECIS-EA-Late with (without) adaptation respectively. An earlier period, 2021-2050, is simulated by PRECIS-EA-Mid to experience a decrease in mean annual Loss Potential of 15% (11%) with (without) adaptation. These values are comparable with those presented by Leckebusch *et al.* (2007) and Pinto *et al.* (2007) despite different methods of loss modelling and their use of GCM data, rather than the RCM data utilised here.

As discussed earlier in this section, the climate change signal under the A2 emissions scenario is generally stronger than that simulated under B2. While this is not necessarily true for windspeeds simulated in this project, it is certainly the case for Loss Potentials. In addition, results indicate that the changes in windspeeds, and subsequently Loss Potential, are markedly greater in HadAM3P-driven simulations than those driven by ECHAM4. Räisänen *et al.* (2004) found that the climate change signal was greater when the Rossby Centre coupled regional climate model (RCAO) was driven by ECHAM4/OPYC3, than HadAM3H. While some differences exist between HadAM3H and HadAM3P, used in this project, their impact on the climate change signal is negligible. In HadAM3H-driven simulations Räisänen *et al.* (2004) found a decrease in annual mean 10-metre windspeeds up to 4% across much of the UK, but also increases up to 4% south east England. Using ECHAM4/OPYC3 decreases of up 4% were seen across England and Wales, with increases up to 8% seen in northern Scotland. While these are mean windspeeds, it is not unreasonable to assume damaging windspeeds may follow a similar pattern (as they do somewhat in this project). Due to the greater density of households in south east England than Scotland, this would

likely result in overall Loss Potential increasing significantly when calculated from windspeeds simulated by HadAM3H than by ECHAM4/OPYC3.

The inter-annual variability in the severity of windstorms and their related losses also impacts the insurance industry. Unexpected high loss years, or events, influence equity management, as well as underwriting strategies (Hawker, 2007). The standard deviation of damaging windspeeds increases up to 30%, in future simulations, in conjunction with increases in the magnitude of damaging windspeeds of up to 9%. This suggests unprecedented DMGSs may occur in the future, with what are currently considered extreme gust speeds in the todays climate, occurring more often. The standard deviation of annual Loss Potentials in 2071-2100 simulations also indicates relative increases, of 259% (683%) and 109% (342%) in PRECIS-HA and PRECIS-HB with (without adaptation) respectively. An increase is also seen in PRECIS-EA-Late without adaptation (11%), although a decrease is seen with adaptation (5%). Although two different driving GCMs and two different emissions scenarios are utilised, all three PRECIS future simulations suggest that without adaptation to the 2071-2100 wind regime the inter-annual variation in losses will increase.

One of the benefits of using RCM simulations to investigate changes in Loss Potentials is that regional variations within the study area may be identified. Changes in mean annual Loss Potential in individual postcode sectors within Great Britain are presented. Similar studies using GCMs (Leckebusch *et al.*, 2007; Pinto *et al.*, 2007) are unable to achieve such a high resolution analysis as this. Mean annual Loss Potentials in all simulations of the period 2071-2100 suggest south east England will see the greatest increases without adaptation (up to 562% in some postcode sectors). With adaptation, the location with the greatest increases is in north west regions of England (up to 358%) in HadAM3P-driven simulations and in the north east of Scotland and West Wales (up to 128%) in PRECIS-EA-Late simulations.

Changes in the mean annual Loss Potentials are driven by changes in winter Loss Potential values. The proportion of annual Loss Potential occurring in winter increases in all future simulations except PRECIS-EA-Late, with

corresponding decreases in autumn. This factor, coupled with the increase in the inter-annual variability of Loss Potentials, amplifies the potential for a very high impact event, or string of events. This can result in added stress on the insurance industry, not just through increased losses, but large numbers of claims in a short period of time can strain resources. Periods such as January 1990, which saw over 3 million claims in a four-week period, could be experienced more regularly, and even more severely.

While changes in future Loss Potentials are presented for two different situations (with and without adaptation), it is important to realise that many other factors will play a role in dictating future wind-related insured domestic property losses. Although not quantifiable, changes in the nature of insurance density and insured value will also contribute to the extent of future losses. Alterations in the exposure of the building stock, brought about by new housing developments will also affect windstorm risk. As with the flood risk to the proposed development in the Thames Gateway, insurers may play an increased role in the siting of large new housing developments. Part of their considerations may be the increase in windstorm risk properties may experience in certain regions of Great Britain, as identified in this project.

Chapter 7: Conclusions

At the beginning of the project three research aims were outlined in section 1.6: (1) an assessment of the historical and future UK wind regime; (2) construction of a windstorm loss model; (3) quantification of the historic and future impact of the UK wind regime on insured windstorm losses. The major research findings are outlined in section 7.1, including a comparison with the conclusions of other relevant studies in the recent literature. The current status of research in the multiple areas considered in this project is discussed in section 7.2, with potential future research stemming from this project considered in section 7.3.

7.1 Achieving the Research Aims

7.1.1 Assessment of the historical and future UK wind regime

During the literature review undertaken in Chapter 1, it was found that the UK wind regime is fairly poorly documented, with almost no information regarding gust speeds. In order to fill this gap, extensive data mining was carried out on the BADC archives, resulting in a continuous 26-year (1980-2005) dataset of daily mean windspeeds and daily maximum gustspeeds (DMGS) recorded at 43 Met Office stations across the UK. Dynamically downscaled (PRECIS-Re) and raw (ERA40) reanalysis data for the period 1959-2001 supplemented the observational dataset; thereby facilitating an assessment of the historic UK wind regime for the period 1959-2005. The windspeed data are subsequently utilised in Chapter 4 to develop a windstorm loss model, and in Chapter 5 to estimate historic windstorm losses.

Temporal and spatial variations in the observed data are described in section 3.1. Windspeeds are found to be higher in coastal locations, increasing with elevation and latitude, in agreement with Wheeler and Mayes (1997) and Palutikof *et al.* (1997). The Network Average exhibits a decrease in daily mean windspeeds and DMGS of 0.5 ms^{-1} over the course of the study (1980-2005), while damaging windspeeds (i.e. those DMGS exceeding the local 98th

percentile value) decrease by 2 ms^{-1}. Although these changes are not statistically significant (at the 95% confidence level), several stations, mainly in the south and east of England, show significant decreases. The mean windspeed results are similar to those published by Sinden (2007). No verification of the trends identified in DMGS could be made due to a lack of similar studies.

Temporal trends in the PRECIS-Re dataset for the period 1980-2001 are analogous to those identified in the observational data, but with lower magnitudes. However, the Network Average 98^{th} percentile value of DMGS shows a very slight increase (less than 0.1 ms^{-1}). For the longer 1959-2001 period, data suggest damaging windspeeds increased slightly, with 9 stations in northern England and in Scotland exhibiting significant increases. These results, in conjunction with the observed data, suggest that over the course of the period 1959-2005 damaging windspeeds have tended to increase in northern parts of the UK by up to 8%, with recent (1980-2005) decreases in southern England (up to 20%).

In section 3.3, dynamical downscaling of reanalysis data is demonstrated to more reliably reproduce the UK wind regime than raw reanalysis data, thus illustrating the added value provided by PRECIS. The higher resolution land-sea mask and orography mask utilised by PRECIS enables windspeeds to be modelled with greater reliability. Accurate representation of these features has been show to be important in modelling terrain dependent variables such as windspeed (Rockel and Woth, 2007). While a full evaluation of PRECIS is beyond the scope of this project, it was desirable to assess the reliability of the model to simulate windspeed variables over the UK. PRECIS-Re data were compared to observations, with results suggesting the variability shown in observed daily mean windspeeds is more accurately simulated than that exhibited by observed DMGSs (although both produce R^2 values greater than 0.6). Simulated daily mean windspeeds tend to be overestimated by 15%, while DMGSs are underestimated by 40%. The inability of RCMs to fully capture the magnitude of gust speeds has been previously documented (Rockel and Woth, 2007; Leckebusch *et al.*, 2006), but unfortunately no alternative method to calculate gust speeds at the desired spatial and

temporal resolution was available (e.g. a RCM with gust parameterisation, which carries its own uncertainties). As a result, in Chapter 4, in order to produce windstorm loss estimates, correction factors based on observations are applied to PRECIS-Re DMGS values.

An assessment of the future UK wind regime was achieved through an analysis of the windspeed data produced by the PRECIS future climate simulations. Two driving GCMs and two emissions scenarios were utilised, thus considering two major sources of uncertainty in future climate modelling (Déqué *et al.*, 2007). Consideration of the third, sampling uncertainty, was limited due to processor and time constraints.

Daily mean windspeeds and DMGSs simulated in the baseline (1961-1990) experiments show slight negative biases compared to PRECIS-Re. Any changes not exceeding this bias should therefore be treated with care when interpreting changes relative to current climate.

A marginal decrease is seen in daily mean windspeeds in ECHAM4-driven experiments (about 3%). Increases are shown by PRECIS-HA (4.2%) and PRECIS-HB (5.5%) simulations, but these do not exceed the bias between the baseline experiment and PRECIS-Re. These increases are driven by changes in winter mean daily windspeeds, with southern England and Scotland showing the greatest increases.

The overall increase in DMGSs seen in HadAM3P-driven simulations is less than the bias between the baseline experiment and PRECIS-Re, despite 42 of 43 stations exhibiting significant increases (relative to the baseline). However, the 13% (14%) increase in winter DMGS in PRECIS-HA (PRECIS-HB) is greater than the bias. A slight decrease (less than 1%) is seen in ECHAM4-driven DMGSs.

Changes in damaging windspeeds in future simulations, relative to the baseline experiments, are shown in Figure 7.1.

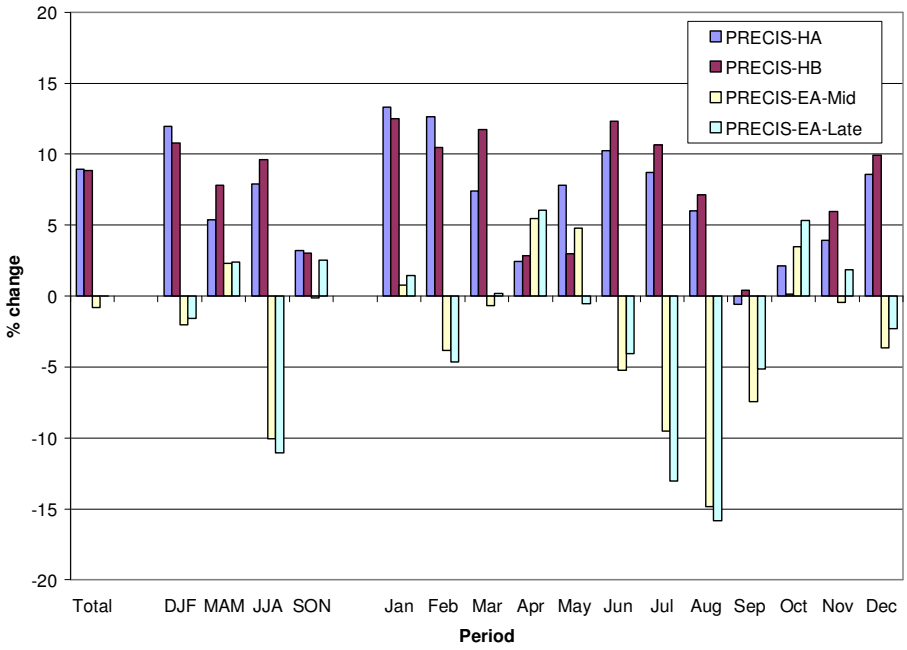

Figure 7.1 - Relative changes in the 98th percentile value of DMGS (i.e. damaging windspeeds) in future climate simulations compared with baseline experiments.

Figure 7.1 suggests minimal overall changes in damaging windspeeds in ECHAM4-driven simulations. However, a 9% increase is seen in HadAM3P-driven simulations, with the greatest increase in winter (increases of 12% and 11% in PRECIS-HA and PRECIS-HB respectively). It must be noted, however, no changes are greater than the bias seen between PRECIS-H and PRECIS-Re. Results suggest that the period with the highest frequency of damaging windspeeds narrows in all simulations. PRECIS-HA and PRECIS-HB simulations suggest that more than 50% of damaging windspeeds will occur in January and February (an increase of 15-20%), while PRECIS-EA-Mid and PRECIS-EA-Late simulations show a shift towards more damaging windspeeds in October to January, and a 10% decrease in February. The importance of intra-annual variations in damaging windspeeds is demonstrated in section 5.2, with properties more vulnerable to windspeeds in the fourth quarter of the year (October – December) than the first (January – March).

7.1.2 Construction of a windstorm loss model

Utilising the unique windspeed dataset generated by this project, a deterministic relationship between wind-related insured domestic property

losses and meteorological variables was derived in Chapter 5. Subsequently, an operational windstorm loss model was developed, incorporating socio-economic aspects to quantify exposure and vulnerability of the domestic property stock to the windstorm hazard. The model was calibrated and verified with a continuous daily record of EIG claims from 1990-1999 and 2000-2005 respectively, making it unique compared with previous studies (Hanson *et al.*, 2004; Dorland *et al.*, 1999; Klawa and Ulbrich, 2003). The original research aim was to develop a loss model capable of predicting losses with a spatial reference. Unfortunately this was not possible due to inadequate information regarding the exposure of EIG's domestic property portfolio.

Daily maximum gust speeds, and not daily mean windspeeds, are shown to be more highly correlated with insured losses, in agreement with Klawa and Ulbrich (2003), Schwierz *et al.* (in submission) and Dorland *et al.* (2000). A threshold for damage, and subsequent loss, is shown to be the local 98th percentile value in accordance with Klawa and Ulbrich (2003). Thus "damaging windspeeds", a termed used frequently in this study, are considered to be those DMGS exceeding this threshold. A cubic relationship between damaging windspeeds and losses is also shown to be the most appropriated for predicting insured losses.

The final windstorm loss model is developed through a regression analysis, incorporating the number of detached properties, and the total value of all the domestic properties, impacted by damaging windspeeds. Detached properties are most vulnerable to wind-related damage (Spence *et al.*, 1998) due to the relatively large surface area of the roof, suggesting the inclusion of the detached property variable is a logical one.

Verification of the loss model against six years of independent data (i.e. data not incorporated in the calibration period), results in a relatively poor R^2 value of 0.37. However, this value increases to 0.61 in winter and autumn; periods suffering the majority of losses. On an operational basis (days recording damaging windspeeds), model performance is significantly improved (R^2 = 0.63), although predicted losses are still underestimated by nearly 60%. If

predicted losses are verified against actual losses from the calibration period (as with other studies) model performance is very good (R^2 = 0.87).

Information regarding the exposure of the EIG domestic property portfolio was unavailable in this project due to its commercial sensitivity. In order to accurately assess the impact of a storm it is important to establish whether areas filing a large number and value of claims are those experiencing high windspeeds, as opposed to those areas with a high exposure (i.e. large number of policies written and sum insured). Although the windstorm loss model performs reasonably well by assuming that the EIG exposure was stationary over the course of the study, relative to industry-wide changes, performance could be enhanced, and a spatial component added, if full details of the EIG exposure could be incorporated. Furthermore, if the appropriate industry-wide claims data were available the model could be adapted to produce industry-wide loss estimates.

7.1.3 Quantifying the impact of the historical and future UK wind regime on insured windstorm losses

Using the windspeed data established for the historic and future UK wind regime, historic and future wind-related insured domestic property losses are quantified. The windstorm loss model, presented in Chapter 4, is simplified since all the variables are not available for the time periods considered (1959-2005, 2021-2050 and 2071-2100). The simplified model, presented in section 5.1, incorporates household numbers and DMGSs exceeding the local 98th percentile value, thus incorporating exposure and vulnerability of the domestic property stock, and a measure of the windstorm hazard. The loss data used in calibration are adjusted to account for inflation and changes in insured density and the total sum insured per policy (following Munich Re, 2002). The impact of the future UK wind regime on losses does not include projected changes in household numbers since that information is unavailable. As such, changes in future losses directly reflect changes in the wind regime, rather than socio-economic shifts or changes in the nature of insurance over the next 90 years, which are beyond the scope of this project.

Observed and PRECIS-Re data were utilised in Chapter 5 to assess the impact of the historic UK wind regime on losses in the period 1959-2005. The simplified model combines household numbers and windspeed data to form a Loss Potential. Subsequently, an equation to calculate quarterly industry-wide and EIG loss estimates from Loss Potentials is developed. Results from sections 5.3 and 5.4 indicate that even a simplified model can produce reasonably reliable aggregated wind-related loss estimates at an industry-wide level, as well as for an individual insurance company. However, it must be noted that loss estimates for periods suffering high actual losses (e.g. winter 1990) are markedly underestimated. Annual loss estimates, based on observed windspeeds, suggest no temporal trends during the period 1980-2005.

PRECIS-Re DMGS data are used to extend the record of insured losses back to 1959, allowing not only the impact of individual storms pre-dating the observation dataset to be assessed but also identifying high loss periods. Quarterly loss estimates are verified against actual quarterly losses, revealing the relatively poor performance of the simplified model (compared to when observed data are utilised). Furthermore, loss estimates for high loss periods are up to an order of magnitude lower. For this reason, Loss Potentials are analysed instead of loss estimates, but may be considered indicative of monetary loss values. Annual Loss Potentials were produced for each year in the period 1959-2001 (presented in Figure 7.2), capturing known periods of high losses (e.g. 1990 and 1998), and identifying others (1962 and 1974). The dearth of insured loss records prior to 1987 has been highlighted in the project repeatedly, therefore alternate indicators of insured loss were sought to verify the annual Loss Potentials. The high annual Loss Potentials generally coincide with high annual numbers of wind-related property damage incidents reported by Tsokri and Blackmore (2003).

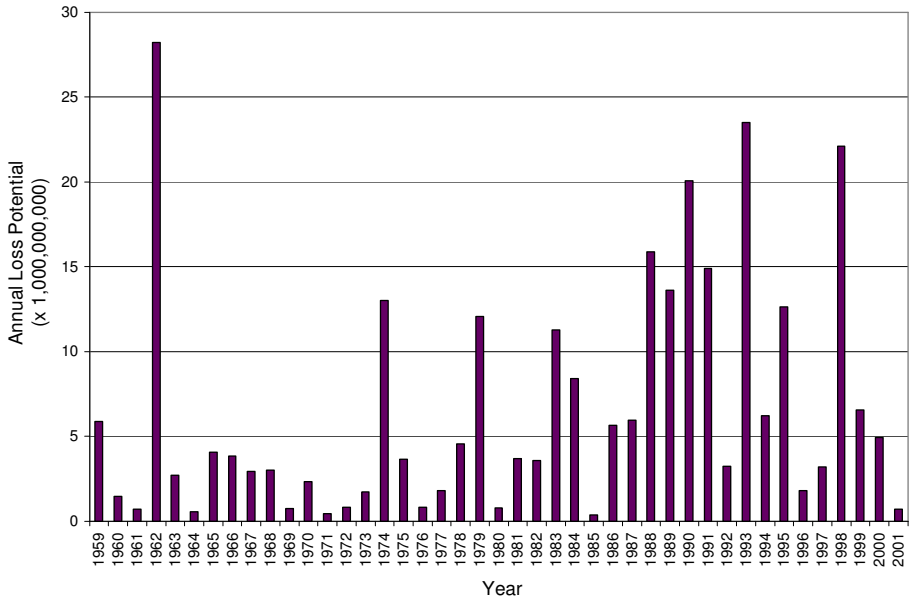

Figure 7.2 - Annual Loss Potentials calculated from PRECIS-Re wind data.

While no statistically significant temporal trend in these annual Loss Potentials is found, the results suggest an increase of 7% during the period 1959-2001. This is in accordance with the increasing windspeeds exhibited by PRECIS-Re data during that period, presented in section 3.2.2.

The impact of individual storm events was quantified using both observed and PRECIS-Re windspeed data. The simplified model performs markedly better with observed data than PRECIS-Re data, but still underestimates the losses of very severe events (e.g. 16th October 1987 and 25th January 1990). In order that events dating back to 1959 may be identified and their impacts quantified, their Relative Loss Potential (RLP) was calculated. This enables the impacts of storms throughout the period of study to be directly comparable. This method identifies a number of potential high loss events (e.g. 15-16th December 1962, 11th February 1974 and 20th January 1959). Although no loss data extend back to 1959, in an attempt at verification the RLP of events are compared with known historic severe windstorms identified by Palutikof *et al.* (1997). Several windstorm events with high RLP correspond to high ranking storms in Palutikof *et al.* (1997) “Storm Catalogue”. This provides a level of confidence in this methodology, and the results.

Since the simplified loss model operates at a postcode sector level, spatial variations in Loss Potentials for individual storms can also be quantified. This

high spatial resolution is not present in published literature regarding insured losses, for individual storms or aggregated periods. However, results presented in section 5.4.3 provide information on the spatial variation of the long term (1980-2005 and 1959-2001) annual average RLP in each postcode sector in Great Britain, calculated using observed and PRECIS-Re windspeed data respectively. These variations are depicted in Figure 7.3.

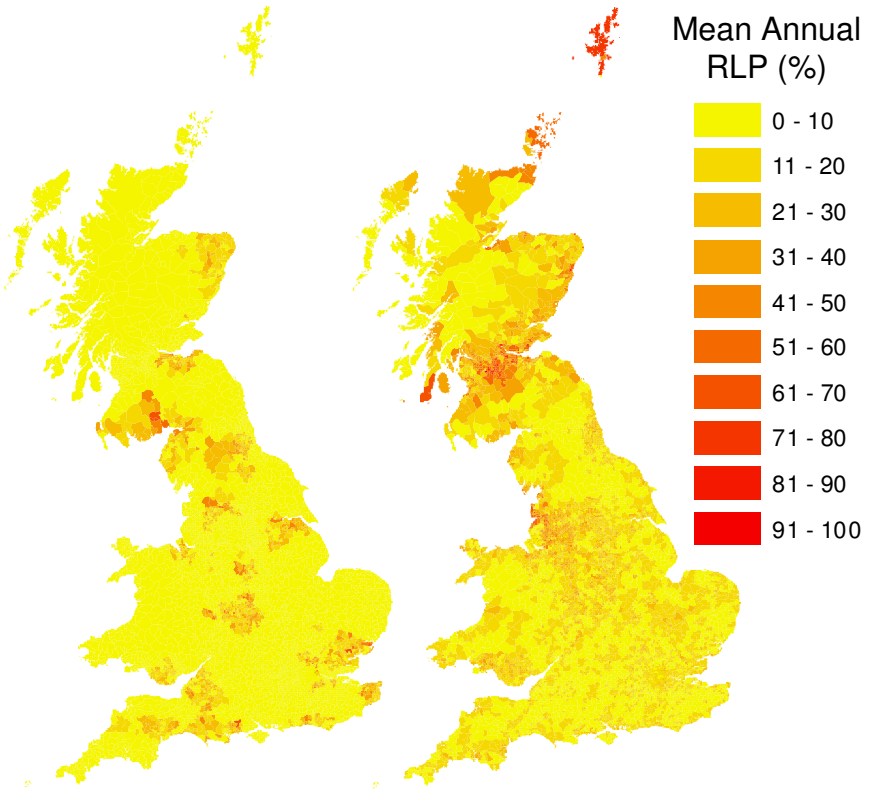

Figure 7.3 - Mean annual Relative Loss Potential in Great Briatin postcode sectors based on observed (left) (1980-2005) and PRECIS-Re (right) (1959-2001) windspeed datasets.

Figure 7.3 identifies regions in north west England and southern Scotland as those exhibiting the greatest RLP, suggesting that during the period 1959-2005 these areas have been subject to the greatest Loss Potential, and therefore likely the greatest insured losses.

Verification for the loss estimates and Loss Potentials presented in Chapter 5, for the period prior to ABI insured loss data (i.e. 1959-1986), is very difficult, despite other indicators of damage being utilised. Hence while results

presented here go some way to filling the gap in the literature, they should be seen as encouragement for further novel research to assess their validity.

Future Loss Potentials were calculated using RCM windspeed data for the periods 2021-2050 and 2071-2100, with spatial and temporal variations in Loss Potentials, relative to baseline experiments, analysed in section 6.2. Two Loss Potential values are produced; one which considers an adaptation of domestic properties to the future wind regime (with adaptation), while the second assumes the same absolute damage threshold as in the baseline simulation (without adaptation). Results regarding changes in the UK wind regime, coupled with those regarding changes in future Loss Potentials, suggest that without adaptation changes in Loss Potential reflect changes in the 98th percentile value of DMGS, but with adaptation reflect changes in the standard deviation of damaging windspeeds. Changes in future mean annual Loss Potential, relative to the baseline experiments, are shown in Figure 7.4.

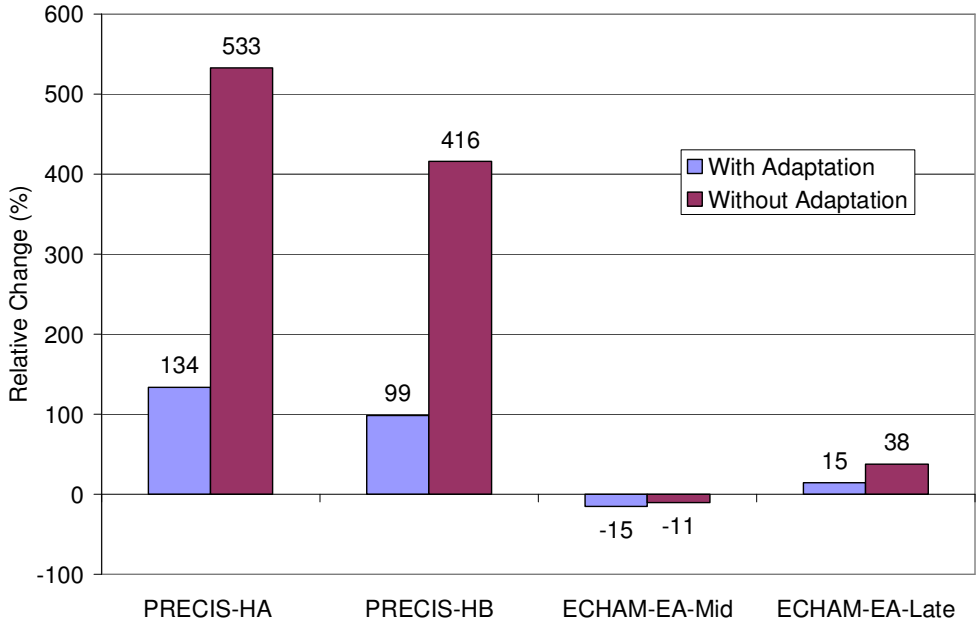

Figure 7.4 – Relative change (%) in Loss Potentials calculated from future simulations, compared to those calculated from baseline simulations.

Changes in Loss Potentials calculated from ECHAM4-driven experiments are of similar magnitudes to changes in the insured loss ratio calculated by Leckebusch *et al.* (2007) and Pinto *et al.* (2007) (using ECHAM4/OPYC3 and ECHAM5/MPI-OM1 data respectively). Significantly greater changes are shown by Loss Potentials calculated from HadAM3P-driven experiments. This

finding is in line with Leckebusch *et al.* (2007) (who used HadAM3P data directly), although relative changes here are approximately 6 times higher.

The changes shown in Figure 7.4 are predominantly driven by changes in winter Loss Potential. Increases of 10-15% in the proportion of annual Loss Potential occurring in winter are simulated by PRECIS-HA and PRECIS-HB, with corresponding decreases in autumn. The proportion of the annual Loss Potential occurring in winter exceeds 65% in all future simulations, with increases in this value seen in all simulations except PRECIS-EA-Late. Changes in the intra-annual variation in Loss Potential may have a relatively limited impact on the insurance industry, compared to changes in the inter-annual variation. While a concentration of annual loss in winter may not affect overall company profits, it may place added strain on company resources (e.g. claims handling). However, an increased inter-annual variability in the future, resulting in unexpected high losses, will affect equity management and underwriting strategies. The standard deviation of annual Loss Potential reflects the inter-annual variability, with future changes shown in Table 7.1.

	PRECIS-HA	PRECIS-HB	ECHAM-EA-Mid	ECHAM-EA-Late
With Adaptation	+259%	+109%	-17%	-5%
Without Adaptation	+683%	+342%	-16%	+11%

Table 7.1 - Relative change in the standard deviation of annual Loss Potentials calculated from future PRECIS simulations.

All climate simulations for the period 2071-2100 suggest that without adaptation regions in south east England will see the greatest increase in Loss Potentials. However, with adaptation, the regions seeing the greatest increase are projected to be in the north west of England by HadAM3P-driven simulations, and in north east England, west Wales and north east Scotland by PRECIS-EA-Late. These changes are illustrated in Figure 7.5.

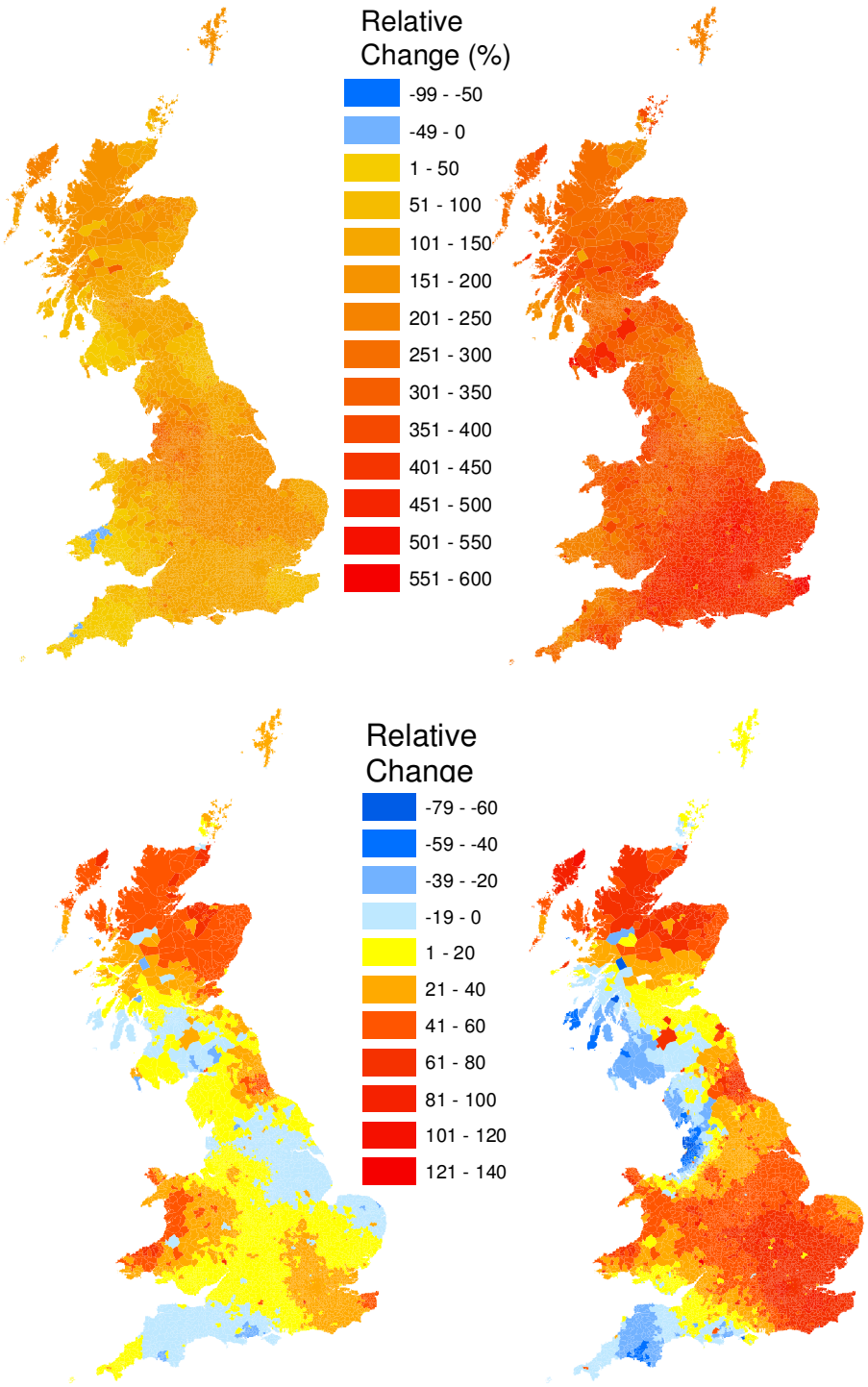

Figure 7.5 - Relative change in mean annual Loss Potentials in postcodes sectors simulated by PRECIS-HA (top) and PRECIS-EA-Late (bottom) with adaptation (left) and without adaptation (right). Scales are different to emphasise spatial variations.

7.2 Conclusion

This study is one of the first to utilise RCM windspeed data to estimate the impact of future UK wind regime on windstorm losses. Although Leckebusch *et al.* (2007) and Pinto *et al.* (2007) published work midway through this project which utilised GCM data to estimate the change in loss ratios, their loss models are calibrated with German insurance data. This study is the first to utilise UK insurance data. As yet unpublished work by Schwierz *et al.* (in submission) does utilise RCM data (including RCMs with gust parameterisation), but uses a Swiss Re loss model, of which little information is available due to commercial sensitivity. Therefore, this project remains the sole study which presents a transparent methodology to quantify windstorm losses in the future based on RCM data. In theory, this methodology can be used in conjunction with an ensemble of RCMs to quantify uncertainty, and given the appropriate insurance data, could be applied to any region in Europe.

There is much scientific, and indeed political, interest in establishing whether upward trends in global weather-related insured losses in the last few decades are as a result of socio-economic changes or shifts in climate (IPCC, 2007; Pielke Jr. *et al.*, 2008; Changnon, 2007; ABI, 2005). Both the windstorm loss model developed in Chapter 4 and the simplified model utilised in Chapters 5 and 6 are calibrated against insured loss data. These data are adjusted to account for inflation and changes in insured density and the total sum insured per policy (following Munich Re, 2002), and is considered normalised to 2005 values and exposure. No statistically significant temporal trend in insured loss (or Loss Potential) in the period 1959-2005 could be found. Although some elements of the socio-economic changes which occurred during that period have been taken into account here, a full examination of these shifts and their effects was not within the project scope. However, the methodology developed, and data produced, could be utilised in further studies to quantify the impact of societal and economic shifts on windstorm losses in the UK.

The limited number of studies regarding windstorm loss modelling generally focus on individual events (e.g. Dorland *et al.*, 2000; Hanson *et al.*, 2004) or

aggregated periods (Klawa and Ulbrich, 2003), whereas the model developed in this project utilised daily losses for a continuous period of 16 years. It is the only model to operate at such a high temporal resolution for a continuous period. It proved exceeding difficult (as expected) to extract loss information from an insurance company, and although EIG were unable to provide exposure data, they are gratefully acknowledged for their collaboration. Further work refining the windstorm loss model presented here, with additional and higher quality insurance claims (and exposure) data will only improve its reliability. Issues regarding the reliability of insurance claims, particularly with regard to attributing losses to the correct event, have been previously highlighted (Dorland *et al.*, 2000; Hanson *et al.*, 2004; Heneka and Ruck, 2004). Data quality is a bane of all research, and this project illustrates the potential of, and is not alone in calling for (Dlugolecki, 2004; Hoppe and Pielke Jr., 2006; Lloyd's, 2007), more high quality insurance claims data.

Throughout the course of this study the sparse information regarding insured losses available in the literature has been highlighted, as has the reluctance of the insurance industry to collaborate with academic researchers. The commercial sensitivity of insurance data and catastrophe models mean re/insurance companies and catastrophe modelling companies are somewhat reluctant to partner with academia. However, potential impacts posed by climate change are increasingly publicised within the industry (e.g. Lloyd's, 2007), and the re/insurance industry may be more open to collaborations (e.g. Swiss Re's work with Schwierz *et al.* (in submission), the Tropical Storm Risk project, the Lighthill Risk Network and the Willis Research Network). Currently, in-house assessments of the impact of climate change on the industry are carried out by such companies as Munich Re, Swiss Re and RMS. Coupling of the extensive climate change research in academia with the expertise in risk assessment and management of the (re)insurance industry will enable the uncertainty surrounding potential future climate-related losses to be reduced.

7.3 Future Work

The unique windspeed dataset established in this project has a number of applications; in the wind power industry, structural design and recreational activities. The long, continuous DMGS record is a powerful resource, which may be applied in the verification of RCMs with gust parameterisation; a task as yet overlooked due to a lack of data (Rockel and Woth, 2007). With increasing RCM simulations being produced for the UK (e.g. under PRUDENCE, ENSEMBLES and UKCIP08 projects), the entire windspeed dataset can facilitate the verification of windspeed variables. In addition, the DMGS dataset has the potential to be utilised in developing empirical gust parameterisation in RCMs, as well as in statistical downscaling applications (Pryor *et al.*, 2005). The performance of catastrophe models can be greatly improved if a temporally and spatially stable link can be established between gust speeds and other meteorological variables in model output; facilitating a more accurate assessment of the European wind storm risk.

A target for renewable electricity generation has been set at 15% of demand in the UK (Office of Gas and Electricity Markets, 2006). It is likely that the majority of this will come from wind power, including on- and off-shore wind farms and wave energy systems. Managing the performance risk for renewable energy systems can increase confidence in likely revenues and therefore facilitate projects attracting financial investment; wind power derivatives are a relatively new tool for enabling this. If revenue falls below a pre-determined level payments are paid to the producer and, conversely, if revenue exceeds a certain level payments are made to the derivative provider. Simulations of the future wind regime for 2021-2050 (a typical lifespan of a wind turbine) undertaken in this project, coupled with the observational windspeed dataset will allow an assessment of the potential of wind power derivatives. The potential utility of seasonal forecasts can also be explored and the combined reliability of offshore wind and wave energy systems for meeting electricity demand may also be assessed.

The diurnal cycle of DMGS discovered in section 3.1.2 was a most surprising result, with no comparable study documented in the literature. The secondary

midnight peak merits further investigation and, while this is primarily of meteorological interest, the timing of maximum wind gusts does have some bearing on the vulnerability of people to building damage. The atmospheric processes involved in producing the nocturnal peak were briefly investigated, but could not be confirmed. Further research involving sodar data, which provide a continuous record of windspeeds in the lowest few hundred metres of the atmosphere, could help identify the mechanisms involved. The timing of damaging windspeeds is of interest to the insurance industry, as windstorms occurring during daylight hours result in more personal injury and liability claims.

Annual mean windspeeds (daily mean windspeeds and DMGSs) recorded during the period 1980-2005 were all at their lowest in 1987, with damaging windspeeds 15% below average. The 16th October 1987 windstorm was considered to be particularly damaging and costly as southern parts of the UK had not experienced a severe storm for a number of years. The fact that it occurred during a year with well below average windspeeds may have been a contributing factor also. Results from Chapter 5 imply domestic properties are more vulnerable to damaging windspeeds in the fourth quarter (October – December) than the first (January – March). This suggests that after a number of months of relatively calm conditions (spring and summer), autumnal damaging windspeeds result in greater damage than those in the later part of winter. Little work has been done to quantify the impacts of antecedent conditions on losses relating to windstorms (e.g. soil moisture and time since last storm), and therefore an opportunity for further research lies in this area.

References.

ABI (2005a). Financial Risks of Climate Change, Climate Risk Management in association with Metroecomica for the ABI**:** 125.

ABI (2005b). Making Communities Sustainable - Managing Flood Risks in the Government's Growth Areas. London, Association of British Insurers**:** 40.

ABI (2005c). Stern Review into the Economics of Climate Change: Evidence from the Association of British Insurers. London, ABI**:** 29.

ABI (2007a). ABI Statistics. www.abi.org.uk. Last accessed 9/1/2008.

ABI (2007b). Flooding and Insurance. http://www.abi.org.uk. Last accessed 29/10/2007.

ABI (2007c). Latest Flood Costs. http://www.abi.org.uk. Last accessed 29/10/2007.

Ahrens, C. D. (2002). Meteorology Today: An Introduction to Weather, Climate, and the Environment. Brooks Cole: 624.

Alovisi, J., C. Souch and J. Toothill (2007). Windstorm Kyrill: A Glimpse into the Future? *Catastrophe Risk Management*. **April 2007:** 26-28.

Alexandersson, H., H. Tuomenvirta, T. Schmith and K. Iden (2000). Trends of storms in NW Europe derived from an updated pressure data set. *Climate Research* **14**: 71-73.

Barrow, E. and M. Hulme (1997). Describing the Surface Climate of the British Isles. In M. Hulme and E. Barrow (Ed), Climates of the British Isles Past, Present and Future. London and New York, Routledge**:** 33-61.

Barry, R. G. and R. Chorley (1998). Atmosphere, Weather and Climate. London, Routledge: 409.

Baxter, P. J., B. E. Lee, T. A. Wyatt and R. J. Spence (2001). Windstorms and Climate Change. In Department of Health (Ed), Health Effects of Climate Change in the UK - Expert Group on Climate Change and Health in the UK. 238.

BBC (2007). Michael Fish and the 1987 Storm. http://www.bbc.co.uk/weather/bbcweather/forecasters/michael_fish_1987storm.shtml. Last accessed 27/11/2007

Beersma, J. J., K. M. Rider, G. J. Komen, E. Kaas and V. V. Kharin (1997). An analysis of extra-tropical storms in the North Atlantic region as simulated in a control and 2xCO_2 time-slice experiment with a high-resolution Atmospheric Model. *Tellus* **49A**(3): 347-361.

Bengtsson, L., S. Hagemann and K. I. Hodges (2004). Can climate trends

be calculated from reanalysis data? *Journal of Geophysical Research* **109**: D11111.

Benfield (2005). Hazard and Risk Science Review 2005. London, Benfield Hazard Research Centre**:** 38.

Benfield (2007). European Windstorm Kyrill. London, Benfield Limited: 4.

Beniston, M. and D. Stephenson (2004). Extreme climatic events and their evolution under changing climatic conditions. *Global and Planetary Change* **44**: 1-9.

Berz, G. (2005). Windstorm and Storm Surges in Europe: Loss Trends and possible counter-actions from the viewpoint of an International Reinsurer. *Philosophical Transactions of the Royal Society a-Mathematical Physical and Engineering Sciences* **363**(1831): 1431-1440.

Blackadar, A. K. (1957). Boundary layer wind maxima and their significance for the growth of nocturnal inversions. *Bulletin of the American Meteorological Society* **38**: 282-290.

Blackmore, P. (1994a). The History of Wind Damage in the UK. *HSE Conference on wind loading on temporary structures*. Buxton, UK, Building Research Establishment.

Blackmore, P. (1994b). A Windstorm Damage Index, Building Research Establishment**:** 6.

Blackmore, P. and P. Delpech (2002). A comparison of wind damage to structures in France and the UK. *Impact of Wind and Strom on City and Built Environment***:** 39-47.

Blackmore, P. and E. Tsokri (2004). Windstorm damage to buildings and structures in the UK during 2002. *Weather* **59**(12): 336-339.

Bouwer, L. and P. Vellinga (2002). Changing Climate and Increasing Costs - Implications for Liability and Insurance. In M. Beniston (Ed), Climatic Change: Implications for the Hydrological Cycle and for Water Management. Kluwer Academic Publishers: 429-444.

Brauner, C. (1994). Global Warming: Element of Risk. Zurich, Swiss Reinsurance Company**:** 49.

Brauner, C. (2002). Opportunities and Risks of Climate Change. Zurich, Swiss Reinsurance Company**:** 27.

Bresch, D., M. Bisping and G. Lemcke (2000). Storm over Europe - an underestimated risk. Zurich, Swiss Re**:** 27.

Browning, K. A. (2004). The sting at the end of the tail: Damaging winds associated with extratropical cyclones. *Quarterly Journal of the Royal Meteorological Society* **130**(597): 375-399.

Burt, S. D. and D. A. Mansfield (1988). The Great Storm of 15-16 October 1987. *Weather* **43**: 90-108.

Carnell, R. E. and C. A. Senior (1998). Changes in mid latitude variability due to increasing greenhouse gases and sulphate aerosols. *Climate Dynamics* **14**(5): 369-383.

Changnon, S. (2003). Shifting Economic Impacts from Weather Extremes in the United States: A Result of Societal Changes, Not Global Warming. *Natural Hazards* **29**(2): 273-290.

Changnon, S. (2007). Catastrophic winter storms: An escalating problem. *Climatic Change* **84**: 131-139.

Changnon, S. and D. Changnon (1998). Record-High Losses for Weather Disasters in the United States During the 1990s: How Excessive and why? *Natural Hazards* **18**(3): 287-300.

Changnon, S. A., R. A. J. Pielke, D. Changnon, R. T. Sylves and R. Pulwarty (2000). Human Factors Explain the Increased Losses from Weather and Climate Extremes. *Bulletin of the American Meteorological Society* **81**(3): 437-442.

Christensen, J. and O. Christensen (2007). A summary of the PRUDENCE model projections of changes in European climate by the end of this century. *Climatic Change* **81**: 7-30.

Christensen, O. B., J. H. Christensen, B. Machenhauer and M. Botzet (1998). Very high resolution regional climate simulations over Scandinavia-present climate. *Journal of Climate* **11**: 3204–3229

Coleman, T. (2002). The Impact of Climate Change on Insurance against Catastrophes. *Living with Climate Change Conference*. Canberra, Insurance Australia Group**:** 12.

Conangla, L. and J. Cuxart (2006). On the turbulence in the upper part of the low-level jet: An experimental and numerical study. *Boundary-Layer Meteorology* **118**(2): 379-400.

Dailey, P. and J. Keller (2006). Modeling of Extreme Wind Events Using MM5: Approach and Verification, AIR**:** 4.

Danard, M. B., S. K. Dube, G. Gonnert, A. Munroe, T. S. Murty, P. Chittibabu, A. D. Rao and P. C. Sinha (2004). Storm Surges from Extra-Tropical Cyclones. *Natural Hazards* **32**: 177-190.

Déqué, M., D. Rowell, D. Lüthi, F. Giorgi, J. Christensen, B. Rockel, D. Jacob, E. Kjellström, M. de Castro and B. van den Hurk (2007). An

intercomparison of regional climate simulations for Europe: assessing uncertainties in model projections. *Climatic Change* **81**: 53-70.

Dlugolecki, A. (2004). A Changing Climate for Insurance - A summary report for Chief Executives and Policymakers. London, Association of British Insurers: 24.

Dlugolecki, A., M. Agnew, D. Crichton, N. Kelly, T. Loster, R. Radevsky, J. Salt, D. Viner, J. Walden and T. Walker (2001). Climate Change and Insurance, Chartered Insurance Institute**:** 98.

Dorland, C., R. S. J. Tol and J. P. Palutikof (1999). Vulnerability of the Netherlands and Northwest Europe to Storm Damage under Climate Change. *Climatic Change* **43**: 513-535.

Dorland, K., J. Palutikof and R. Tol (2000). Modelling Storm Damage in the Netherlands and the UK. In R. S. J. Tol (Ed), Weather Impacts on Natural, Social and Economic Systems in the Netherlands. Institute for Environmental Studies, Vrije Universiteit, Amsterdam**:** 57-81.

Drost, F., J. Renwick, B. Bhaskaran, H. Oliver and J. McGregor (2007). Simulation of New Zealand's climate using a high-resolution nested regional climate model. *International Journal of Climatology* **27**: 1153-1169.

Eden, P. (2005). Weatherlog January 2005. *Weather* **60**: supplement.

Emanuel, K. (2005). Increasing Destructiveness of Tropical Cyclones over the past 30 years. *Nature* **436**: 686-688.

Environmental Systems Research Institute (2005). ArcGIS 9 : what is ArcGIS 9.1? Redlands, California, ESRI: 114.

Gemmer, M., S. Becker and T. Jiang (2004). Observed monthly precipitation trends in China 1951–2002. *Theoretical and Applied Climatology* **77**: 39-45.

George, S. E. (2006). United Kingdom Windspeed: Measurement, Climatology, Predictability and Link to Tropical Atlantic Variability. University of London, London. PhD Thesis: 161

Gordon, C., C. Cooper, C.A. Senior, H. Banks,, T. C. J. J.M. Gregory, J.F.B. Mitchell and a. R. A. Wood (2000). The simulation of SST, sea ice extents and ocean heat transports in a version of the Hadley Centre coupled model without flux adjustments. *Climate Dynamics* **16**: 147-168.

Goyette, S., O. Brasseur and M. Beniston (2003). Application of a new wind gust parameterization: Multiscale case studies performed with the Canadian regional climate model. *Journal of Geophysical Research* **108**(D13): 4374.

Grønås, S. (1995). The seclusion intensification of the New Year's day storm 1992. *Tellus* **47A**(5): 733-746.

Grossi, P. and H. Kunreuther (2006). New Catastrophe Models for Hard Times. *Contingencies*, RMS. **Mar**/**Apr 06:** 33-36.

Grossi, P., H. Kunreuther and D. Windeler (2005). An Introduction to Catastrophe Models and Insurance. In P. Grossi and H. Kunreuther (Ed), Catastrophe Modelling: A New Approach to Managing Risk. Springer**:** 23-42.

Guy Carpenter (2005a). Windstorm Erwin. *Cat-i Catastrophe Information*, Guy Carpenter: 5.

Guy Carpenter (2005b). Windstorm Erwin/Gudrun - January 2005. *Speciality Practice Briefing - An update from the Property Speciality*, Guy Carpenter & Company Ltd**:** 14.

Guy Carpenter (2007). Windstorm Kyrill, *Cat-i Catastrophe Information* , Guy Carpenter**:** 3.

Hanson, C., T. Holt and J. Palutikof (2004). An Integrated Assessment of the potential for Change in Storm Activity over Europe: Implications for Insurance and Forestry in the UK. Norwich, Tyndall Centre**:** 98.

Hanson, C. and C. M. Goodess (2004). Predicting Future Changes in Wind. *BETWIXT Technical Briefing Note 5***:** 27.

Hanson, C. E. (2001). A Cyclone Climatology of the North Atlantic and its Implications for the Insurance Market. University of East Anglia, Norwich. PhD Thesis: 312.

Hawker, M. (2007). Climate Change and the Global Insurance Industry. *The Geneva Papers on Risk and Insurance* **32**: 22-28.

Heneka, P. and B. Ruck (2004). Development of a storm damage risk map of Germany - A review of storm damage functions. In D. Malzahn and T. Plapp (Ed), Proceedings of the International Conference for Disasters and Society. Karlsruhe, Germany, Logos Verlag: 129-136.

Hoppe, P. and R. Pielke Jr. (2006). Report of the Workshop on “Climate Change and Disaster Losses: Understanding and Attributing Trends and Projections”**:** 2.

IPCC (2007). Climate Change 2007: Impacts, Adaptation and Vulnerability. Contribution of Working Group II to the Fourth Assessment Report of the Intergovernmental Panel on Climate Change. M.L. Parry, O.F. Canziani, J.P. Palutikof, P.J. van der Linden and C.E. Hanson (Eds). Cambridge, UK: 976.

Johns, T. C., R. E. Carnell, J. F. Crossley, J. M. Gregory, J. F. B. Mitchell, C. A. Senior, S. F. B. Tett and R. A. Wood (1997). The second Hadley

Centre coupled ocean-atmosphere GCM: model description, spinup and validation. *Climate Dynamics* **13**: 103-134.

Jones, P. D., T. Jonsson and D. Wheeler (1997). Extension to the North Atlantic oscillation using early instrumental pressure observations from Gibraltar and south-west Iceland. *International Journal of Climatology* **17**(13): 1433-1450.

Jones, R. G., J. M. Murphy and M. Noguer (1995). Simulation of climate change over Europe using a nested regional climate model. I: Assessment of control climate, including sensitivity to location of lateral boundaries. *Quarterly Journal of the Royal Meteorological Society* **121**: 1413-1449.

Jones, R. G., M. Noguer, D. C. Hassell, D. Hudson, S. S. Wilson, G. J. Jenkins and J. F. B. Mitchell (2004). Generating high resolution climate change scenarios using PRECIS. Exeter, Hadley Centre, UK Meteorological Office**:** 35.

Jungo, P., S. Goyette and M. Beniston (2002). Daily wind gust speed probabilities over Switzerland according to three types of synoptic circulation. *International Journal of Climatology* **22**(4): 485-499.

Kennedy, M. (2006). Introducing Geographic Information Systems with ArcGIS. Hoboken, New Jersey, John Wiley: 624.

Kestens, E. and J. L. Teugels (2002). Challenges in modelling stochasticity in wind. *Environmetrics* **13**: 821-830.

Klawa, M. and U. Ulbrich (2003). A model for the estimation of storm losses and the identification of severe winter storms in Germany. *Natural Hazards and Earth Systems Sciences* **3**: 725-732.

Knippertz, P., U. Ulbrich and P. Speth (2000). Changing cyclones and surface wind speeds over the North Atlantic and Europe in a transient GHG experiment. *Climate Research* **15**(2): 109-122.

Kruger, A. C. and S. Shongwe (2004). Temperature trends in South Africa: 1960-2003. *International Journal of Climatology* **24**: 1929-1945.

Kunkel, K. E., R. A. Pielke Jr. and S. A. Changnon (1999). Temporal Fluctuations in Weather and Climate Extremes That Cause Economic and Human Health Impacts: A Review. *Bulletin of the American Meteorological Society* **80**(6): 1077-1098.

Kurtzman, D. and R. Kadmon (1999). Mapping of temperature variables in Israel: a comparison of different interpolation methods. *Climate Research* **13**: 33-43.

Lambert, S. J. (1995). The Effect of Enhanced Greenhouse Warming on Winter Cyclone Frequencies and Strengths. *Journal of Climate*: 1447-1452.

Leckebusch, G. and U. Ulbrich (2004). On the relationship between cyclones and extreme windstorm events over Europe under climate change. *Global and Planetary Change* **44**: 181-193.

Leckebusch, G., U. Ulbrich, L. Fröhlich and J. G. Pinto (2007). Property Loss Potentials for European midlatitude storms in a changing climate. *Geophysical Research Letters* **34**: L05703.

Leckebusch, G. C., B. Koffi, U. Ulbrich, J. G. Pinto, T. Spangehl and S. Zacharias (2006). Analysis of frequency and intensity of European winter storm events from a multi-model perspective, at synoptic and regional scales. *Climate Research* **31**: 59-84.

Lloyd's (2006). 360 Risk Project - Climate Change - Adapt or Bust. London, Lloyd's**:** 24.

Lloyd's (2007). 360 Risk Project - Catastrophic Trends and Rapid Climate Change. London, Lloyd's: 31.

Lozano, I., R. J. N. Devoy, W. May and U. Anderen (2004). Storminess and vulnerability along the Atlantic coastlines of Europe: analysis of storm records and of a greenhouse gases induced climate scenario. *Marine geology* **210**: 205-225.

Marsland, S. J., H. Haak, J. H. Jungclaus, M. Latif and F. Roske (2003). The Max-Planck-Institute global ocean/sea ice model with orthogonal curvilinear coordinates. *Ocean modelling* **5**: 91-127.

Matulla, C., W. Schoner, H. Alexandersson, H. von Storch and X. L. Wang (2007). European storminess: late nineteenth century to present. *Climate Dynamics* DOI 10.1007/s00382-007-0333-y.

McCallum, E. (1990). The Burns' Day Storm, 25 January 1990. *Weather* **45**: 166-173.

McGhee, C., R. Clarke and J. Collura (2007). The Catastrophe Bond Market at Year-End 2006, MMC Securities**:** 42.

McIlveen, R. (1992). Fundamentals of Weather and Climate. London, Chapman and Hall: 497.

Menzinger, I. and C. Brauner (2002). Swiss Re Focus Report - Floods are Insurable. Zurich, Swiss Re**:** 8.

Miller, K. F., C. P. Quine and J. Hunt (1987). The Assessment of Wind Exposure for Forestry in Upland Britain. *Forestry* **60**(2): 179-192.

Mills, E. (2005). Insurance in a Climate of Change. *Science* **309**: 1040-1044.

Mills, E. and E. Lecomte (2006). From Risk to Opportunity: How Insurers Can Proactively and Profitably Manage Climate Change, CERES**:** 42.

Mills, E., E. Lecomte and A. Peara (2002). Insurers in the Greenhouse. *Journal of Insurance Regulation* **21**(1): 43-80.

Moberg, A. and P. D. Jones (2004). Regional climate model simulations of daily maximum and minimum near-surface temperatures across Europe compared with observed station data 1961-1990. *Climate Dynamics* **23**(7-8): 695-715.

Munich Re (1999). Topics 2000: Natural Catastrophes – the current position. Munich, Munich Reinsurance Company**:** 126.

Munich Re (2002a). Topics - Annual Review: Natural Catastrophes 2001. Munich, Munich Reinsurance Company**:** 49.

Munich Re (2002b). Winter Storms in Europe (II) - Analysis of 1999 Losses and Loss Potentials. Munich, Munich Reinsurance Company**:** 76.

Munich Re (2005). Annual Review: Natural Catastrophes 2004. Munich, Munich Reinsurance Company**:** 60.

Munich Re (2006). Annual Review: Natural Catastrophes 2005. Munich, Munich Reinsurance Company**:** 52.

Munich Re (2007). Annual Review: Natural Catastrophes 2006. Munich, Munich Reinsurance Company**:** 50.

Nakicenovic, N., J. Alcamo, G. Davis, B. D. Vries, J. Fenhann, S. Gaffin, K. Gregory, A. Grübler, T. Y. Jung, T. Kram, E. L. L. Rovere, L. Michaelis, S. Mori, T. Morita, W. Pepper, H. Pitcher, L. Price, K. Riahi, A. Roehrl, H.-H. Rogner, A. Sankovski, M. Schlesinger, P. Shukla, S. Smith, R. Swart, S. V. Rooijen, N. Victor and Z. Dadi (2000). IPCC Special Report on Emissions Scenarios. Cambridge, Cambridge University Press: 599.

New, M., M. Hulme and P. Jones (1999). Representing Twentieth-Century Space-Time Climate Variability. Part I: Development of a 1961-90 Mean Monthly Terrestrial Climatology. *Journal of Climate* **12**(3): 829-856.

Oberhuber, J. M. (1993). Simulation of the Atlantic circulation with a coupled sea ice-mixed layer-isopycnal general circulation model. Part I: Model description. *Journal of Physical Oceanography* **22**: 808–829.

Office of Gas and Electricity Markets (2006). Renewables Obligation: Third annual report. London**: 35**.

Osborn, T. J. and M. Hulme (1997). Development of a Relationship between Station and Grid-Box Rainday Frequencies for Climate Model Evaluation. *Journal of Climate* **10**(8): 1885-1908.

Osborn, T. (2006). Recent variations in the winter North Atlantic Oscillation. *Weather* **61**(12): 353-355.

Office of National Statistics (2007). All items Retail Prices Index excluding Mortgage Interest Payments (RPIX) Table 2. http://www.statistics.gov.uk/statbase/Product.asp?vlnk=9414. Last Accessed 17/10/2007.

ONS Geography (2007). National Statistics Postcode Directory February 2007 Version Notes. Office for National Statistics**:** 13.

Palmer, T. N. (2005). Development of a European Multi-Model Ensemble System for Seasonal to Inter-Annual Prediction (DEMETER). *Tellus* **57A**: 217-218.

Palutikof, J., T. Holt and A. Skellern (1997). Wind: Resource and Hazard. In M. Hulme and E. Barrow (Eds), Climates of the British Isles: present, past and future. London, Routledge**:** 221-242.

Palutikof, J. P. and A. P. Skellern (1991). Storm Severity over Britain. *Report to Commercial Union*. Norwich, Climatic Research Unit, University of East Anglia**:** 102.

Pielke Jr., R., J. Gratz, C. Landsea, D. Collins, M. A. Saunders and R. Musulin (2008). Normalized Hurricane Damages in the United States: 1900-2005. *Natural Hazards Review* **9**: 29-42.

Pielke Jr., R. and C. W. Landsea (1998). Normalized Hurricane Damage in the United States: 1925-95. *Weather and Forecasting* **13**: 621-631.

Pinto, J. G., E. L. Fröhlich, G. C. Leckebusch and U. Ulbrich (2007). Changing European storm loss potentials under modified climate conditions according to ensemble simulations of the ECHAM5/MPI-OM1 GCM. *Natural Hazards and Earth Systems Science* **7**: 165-175.

Pope, V. D., M. Gallani, P. R. Rowntree and R. A. Stratton (2000). The impact of new physical parameterisations in the Hadley Centre climate model - HadAM3. *Climate Dynamics* **16**: 123-146.

Pryor, S. C., R. J. Barthelmie and E. Kjellstrom (2005a). Potential climate change impact on wind energy resources in northern Europe: analyses using a regional climate model. *Climate Dynamics* **25**(7-8): 815-835.

Pryor, S. C., J. T. Schoof and R. J. Barthelmie (2005b). Climate change impacts on wind speeds and wind energy density in northern Europe: empirical downscaling of multiple AOGCMs. *Climate Research* **29**(3): 183-198.

Pryor, S. C., J. T. Schoof and R. J. Barthelmie (2005c). Empirical downscaling of wind speed probability distributions. *Journal of Geophysical Research-Atmospheres* **110**(D19).

Pryor, S. C., R. J. Barthelmie and J. T. Schoof (2006a). Inter-annual variability of wind indices across Europe. *Wind Energy* **9**(1-2): 27-38.

Pryor, S. C., J. T. Schoof and R. J. Barthelmie (2006b). Winds of change?: Projections of near-surface winds under climate change scenarios. *Geophysical Research Letters* **33**(11).L11702.

Räisänen, J., U. Hansson, A. Ullerstig, R. Doscher, L. P. Graham, C. Jones, H. E. M. Meier, P. Samuelsson and U. Willen (2004). European climate in the late twenty-first century: regional simulations with two driving global models and two forcing scenarios. *Climate Dynamics* **22**(1): 13-31.

RMS (2006a). RMS Releases Comprehensive Europe Windstorm Model for Underwriting and Portfolio Risk Management. http://www.rms.com/NewsPress/PR_052606_EUWS.asp.

RMS (2006b). U.S. and Caribbean Hurricane Activity Rates - The New RMS Medium-term Perspective and Implications for Industry Loss. Newark, California, Risk Management Solutions**:** 9.

RMS (2007). The Great Storm of 1987: 20-year Retrospective. London, Risk Management Solutions**:** 18.

Rockel, B. and K. Woth (2007). Extremes of near-surface wind speed over Europe and their future changes as estimated from an ensemble of RCM simulations. *Climatic Change* **81**: 267-280.

Roeckner, E., K. Arpe, L. Bengtsson, M. Christoph, M. Claussen, L. Du¨menil, M. Esch, M. Giorgetta, U. Schlese and U. Schulzweida (1996). The Atmospheric General Circulation Model ECHAM-4: Model Description and Simulation of Present Day. *MPI-Report No. 218*, Max Plank Institute**:** 90.

Roeckner, E., G. Bäuml, L. Bonaventura, R. Brokopf, M. Esch, M. Giorgetta, S. Hagemann, I. Kirchner, L. Kornblueh, E. Manzini, A. Rhodin, U. Schlese, U. Schulzweida and A. Tompkins (2003). The atmospheric general circulation model ECHAM5. Part I: Model description. *Max Planck Institute for Meteorology Report 349*, Max Planck Institute for Meteorology**:** 127.

Rootzen, H. and N. Tajvidi (1997). Extreme Value Statistics and Wind Storm Losses: A Case Study. *Scandinavian Actuarial Journal* **1997; 1**: 70-94.

Rootzen, H. and N. Tajvidi (2001). Can Losses Caused by Wind Storms be Predicted from Meteorological Observations? *Scandinavian Actuarial Journal* **2001:2**(2): 162-175.

Rowell, D. (2004). An initial estimate of the uncertainty in UK predicted Climate Change Resulting from RCM formation, Hadley Centre: 7.

Sacre, C. (2002). Extreme wind speed in France: the '99 storms and their consequences. *Journal of Wind Engineering and Industrial Aerodynamics* **90**: 1163-1171.

Salt, J. (2000). Climate Change and the Insurance Industry. *Corporate Environmental Strategy* **7**: 146-155.

Sanders, C. H. and M. C. Phillipson (2003). UK adaptation strategy and technical measures: the impacts of climate change on buildings. *Building Research and Information* **31**(3-4): 210-221.

Santer, B. D., *et al.* (2004). Identification of anthropogenic climate change using a second-generation reanalysis. *Journal of Geophysical Research* **109**: D21104.

Schwierz, C., P. Heck, E. Zenklusen, D. N. Bresch, P.-L. Vidale, M. Wild and C. Schar (in submission). *Climatic Change.* Modelling European Winter Wind Storm Losses in Current and Future Climate: 40.

Simmons, A. J., P. D. Jones, V. da Costa Bechtold, A. C. M. Beljaars, P. W. Kållberg, S. Saarinen, S. M. Uppala, P. Viterbo, and N. Wedi (2004), Comparison of trends and low-frequency variability in CRU, ERA-40, and NCEP/NCAR analyses of surface air temperature, Journal of Geophysical Research **109**: D24115.

Sinden, G. (2007). Characteristics of the UK wind resource: Long term patterns and relationship to electricity demand. *Energy Policy* **35**(1): 112-127.

Smits, A., A. M. G. K. Tank and G. P. Konnen (2005). Trends in Storminess over the Netherlands, 1962-2002. *International Journal of Climatology* **25**: 1331-1344.

Spark, E. and G. Connor (2004). Wind forecasting for the sailing events at the Sydney 2000 Olympic and Paralympic Games. *Weather Forecast* **19**(2): 181-199.

Spence, R., W. Fawcett, A. Brown and A. Coburn (1998). The Windstorm Vulnerability of the UK building stock. *4th UK conference on Wind Engineering*: 3

SPSS Inc. (2005). SPSS 14.0: Brief guide. Chicago, Prentice Hall: 245.

Stephenson, J. (2007). Financial Risks to Federal and Private Insurers in Coming Decades are Potentially Significant. *Testimony Before the Committee on Homeland Security and Governmental Affairs, U.S. Senate*, United States Government Accountability Office**:** 22

Steppeler, J., G. Doms, U. Schättler, H. W. Bitzer, A. Gassmann, U. Damrath and G. Gregoric (2003). Meso-gamma scale forecasts using the nonhydrostatic model LM. *Meteorology and Atmospheric Physics* **82**: 75-96.

Strefford, S. (2002). Weather and Sailing. *Weather* **57**(6): 224-225.

Swiss Re (2002). An Introduction to Reinsurance. Zurich, Swiss Reinsurance Company**:** 34.

Tabachnick, B. G. and L. S. Fidell (2001). Using Multivariate Statistics. Needle Heights, Allyn & Bacon: 966.

Tsokri, E. and P. Blackmore (2003). Windstorm damage to buildings and structures in the UK during 2003. Watford, Building Research Establishment: 7.

UKMO (1988). The Meteorological Office report on the storm of 15/16 October 1987. *Meteorological Magazine* **117**: 97-140.

UKMO (2006a). Land Surface Stations data (1900-2000). http://badc.nerc.ac.uk/data/surface/. Last accessed 2/4/2007.

UKMO (2006b). MIDAS Land Surface Stations data. http://badc.nerc.ac.uk/data/ukmo-midas. Last accessed 9/1/2008.

UKMO (2007a). The Great Storm of 1987. http://www.metoffice.gov.uk/education/secondary/students/1987.html. Last accessed 9/11/2007.

UKMO (2007b). Great Weather Events - The Burns Day Storm of 1990. http://www.metoffice.gov.uk/corporate/pressoffice/anniversary/storm1990.html. Last accessed 9/11/2007.

UKMO (2007c). UK Climate and Weather Statistics. http://www.metoffice.gov.uk/climate/uk/. Last accessed 6/11/2007.

UK Met Office (2007d). Met Office Surface Data Users Guide. http://badc.nerc.ac.uk/data/ukmo-midas/ukmo_guide.html#5.5. Last accessed 3/12/2007.

Ulbrich, U., A. H. Fink, M. Klawa and J. G. Pinto (2001). Three Extreme Storms Over Europe in December 1999. *Weather* **56**: 70-80.

Uppala, S. M., P. W. Kållberg, A. J. Simmons, U. Andrae, V. da Costa Bechtold, M. Fiorino, J. K. Gibson, J. Haseler, A. Hernandez, G. A. Kelly, X. Li, K. Onogi, S. Saarinen, N. Sokka, R. P. Allan, E. Andersson, K. Arpe, M. A. Balmaseda, A. C. M. Beljaars, L. van de Berg, J. Bidlot, N. Bormann, S. Caires, F. Chevallier, A. Dethof, M. Dragosavac, M. Fisher, M. Fuentes, S. Hagemann, E. Hólm, B. J. Hoskins, L. Isaksen, P. A. E. M. Janssen, R. Jenne, McNally, A.P., , J.-F. Mahfouf, J.-J.

Morcrette, N. A. Rayner, R. W. Saunders, P. Simon, A. Sterl, K. E. Trenberth, A. Untch, D. Vasiljevic, P. Viterbo and J. Woollen (2005). The ERA-40 re-analysis. *Quarterly Journal of the Royal Meteorological Society* **131**: 2961-3012.

Valverde Jr., L. J. and M. W. Andrews (2006). Global Climate Change and Extreme Weather: An Exploration of the Scientific Uncertainty and the Economics of Insurance. *Insurance Information Institute Working paper Series*, III**:** 51.

Vidale, P. L., D. Lüthi, C. Frei, S. Seneviratne and C. Schär (2003). Predictability and uncertainty in a regional climate model. *Journal of Geophysical Research* **108**(D18): 45-86.

Wang, C.C., and J.C. Rogers (2001). A Composite Study of Explosive Cyclogenesis in Different Sectors of the North Atlantic. Part I: Cyclone Structure and Evolution. *Monthly Weather Review* **129**: 1481–1499.

West, C. and M. Gawith (2005). Measuring progress: preparing for climate change through UKCIP, UKCIP**:** 72.

Wheeler, D. and J. Mayes, Eds. (1997). Regional Climates of the British Isles. Regional Climate of the British Isles. London and New York, Routledge: 368.

Wieringa, J. (1980). Representativeness of Wind Observations at Airports. *Bulletin of American Meteorological Society* **61**(9): 962-971.

Woth, K., R. Weisse and H. von Storch (2006). Climate change and North Sea storm surge extremes: an ensemble study of storm surge extremes expected in a changed climate projected by four different regional climate models. *Ocean Dynamics* **56**(1): 3-15.

Yin, J. H. (2005). A Consistent Poleward Shift of the Storm Tracks in Simulations of 21st Century Climate. *Geophysical Research Letters* **32**: L18701.

Zanetti, A. (2006). Natural Catastrophes and man-made disasters 2005. *Sigma*. Zurich, Swiss Re**:** 40.

Zanetti, A. (2007). Natural Catastrophes and man-made disasters 2006. *Sigma*. Zurich, Swiss Re**:** 40.

Zanetti, A. (2008). Natural Catastrophes and man-made disasters 2007. *Sigma*. Zurich, Swiss Re**:** 46.

Zanetti, A., S. Schwartz and R. Enz (2005). Natural Catastrophes and man-made disasters in 2004. Zurich, Swiss Re**:** 40.

Appendix A – Map of the network of UK Met Office observing stations utilised in this study

Data from these stations are used to develop the daily mean windspeed and DMGS dataset described in Chapter 3.

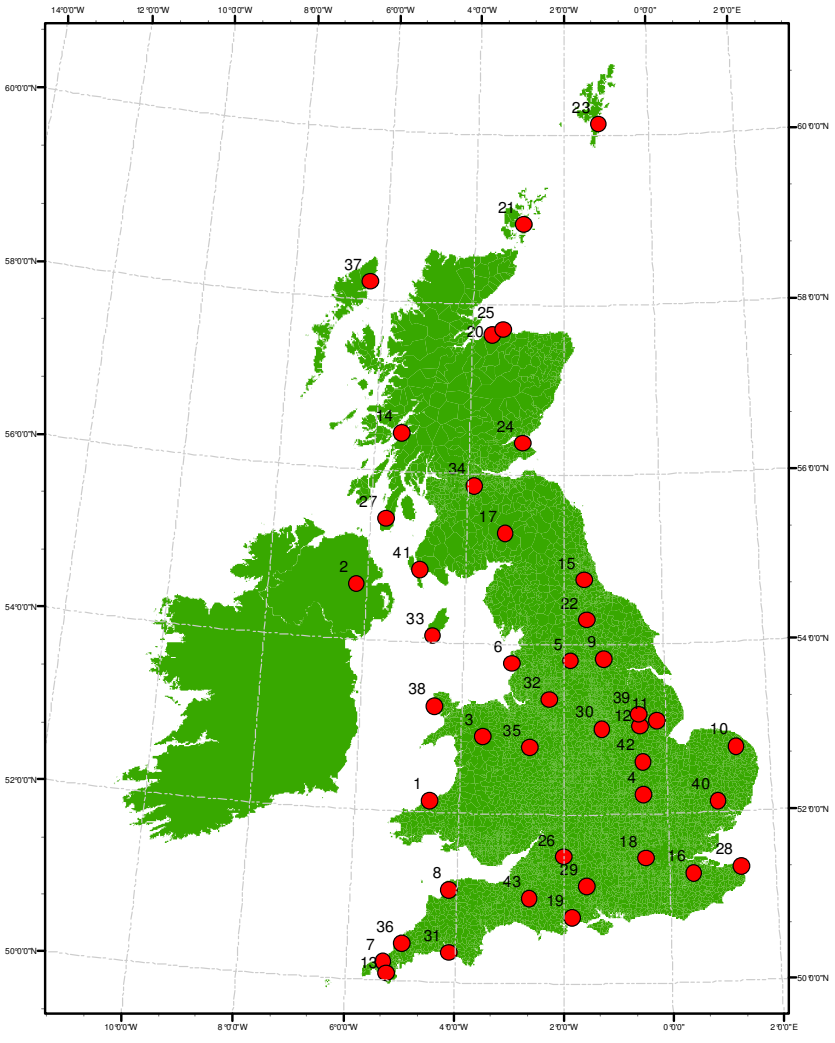

No.	Station
1	Aberporth
2	Aldergrove
3	Bala
4	Bedford
5	Bingley
6	Blackpool Squires Gate
7	Camborne
8	Chivenor
9	Church Fenton
10	Coltishall
11	Coningsby
12	Cranwell
13	Culdrose
14	Dunstaffnage
15	Durham
16	East Malling
17	Eskdalemuir
18	Heathrow
19	Hurn
20	Kinloss
21	Kirkwall
22	Leeming
23	Lerwick
24	Leuchars
25	Lossiemouth
26	Lyneham
27	Machrihanish
28	Manston
29	Middle Wallop
30	Nottingham Watnall
31	Plymouth Mountbatten
32	Ringway
33	Ronaldsway
34	Salsburgh
35	Shawbury
36	St Mawgan
37	Stornoway Airport
38	Valley
39	Waddington
40	Wattisham
41	West Freugh
42	Wittering
43	Yeovilton

Appendix B - RPIX table

RP07 RPI all items excluding Mortgage Interest Payments (RPIX)
percentage change over 12 months (CDKQ)

per cent

	Annual change	Jan	Feb	Mar	Apr	May	Jun	Jul	Aug	Sep	Oct	Nov	Dec
1978	8.6	10.5	10.3	9.9	8.7	8.3	7.9	8.1	8.0	7.9	7.7	7.9	8.0
1979	12.6	8.7	8.7	8.8	9.1	9.3	10.2	14.7	15.1	15.7	16.4	16.7	16.8
1980	16.9	17.3	17.8	18.6	20.7	20.8	20.1	15.9	15.2	14.8	14.3	14.2	14.0
1981	12.2	13.0	12.6	12.8	12.4	12.2	11.8	11.4	12.0	11.9	12.2	12.1	11.9
1982	8.5	11.7	10.6	9.9	9.1	9.1	8.8	8.4	7.6	7.3	6.9	6.7	6.6
1983	5.2	6.2	6.7	5.9	4.9	4.5	4.5	4.7	5.1	5.2	5.0	4.8	4.8
1984	4.5	4.5	4.5	4.6	4.9	4.9	4.9	4.5	4.3	3.9	4.2	4.1	4.1
1985	5.2	4.6	4.6	5.2	5.3	5.3	5.3	5.2	5.3	5.6	5.2	5.3	5.1
1986	3.6	4.9	4.8	4.0	3.4	3.2	3.3	3.2	3.3	3.4	3.3	3.3	3.4
1987	3.7	3.6	3.7	3.8	3.6	3.8	3.5	3.7	3.7	3.5	3.9	4.0	3.9
1988	4.6	3.7	3.6	3.8	4.2	4.4	4.7	5.0	5.0	5.2	5.1	5.1	5.1
1989	5.9	5.5	5.7	5.7	5.9	6.0	5.9	5.8	5.7	5.8	6.1	6.1	6.1
1990	8.1	6.1	6.2	6.3	7.9	8.1	8.2	8.3	9.1	9.5	9.5	9.2	9.0
1991	6.7	8.5	8.6	8.4	6.8	6.6	6.9	6.8	6.2	5.7	5.5	5.7	5.8
1992	4.7	5.6	5.6	5.7	5.7	5.3	4.8	4.4	4.2	4.0	3.8	3.6	3.7
1993	3.0	3.2	3.4	3.5	2.9	2.8	2.8	2.9	3.1	3.3	2.8	2.5	2.7
1994	2.3	2.8	2.8	2.4	2.3	2.5	2.4	2.2	2.3	2.0	2.0	2.3	2.5
1995	2.9	2.8	2.7	2.8	2.6	2.7	2.8	2.8	2.9	3.1	2.9	2.9	3.0
1996	3.0	2.8	2.9	2.9	2.9	2.8	2.8	2.8	2.8	2.9	3.3	3.3	3.1
1997	2.8	3.1	2.9	2.7	2.5	2.5	2.7	3.0	2.8	2.7	2.8	2.8	2.7
1998	2.6	2.5	2.6	2.6	3.0	3.2	2.8	2.6	2.5	2.5	2.5	2.5	2.6
1999	2.3	2.6	2.4	2.7	2.4	2.1	2.2	2.2	2.1	2.1	2.2	2.2	2.2
2000	2.1	2.1	2.2	2.0	1.9	2.0	2.2	2.2	1.9	2.2	2.0	2.2	2.0
2001	2.1	1.8	1.9	1.9	2.0	2.4	2.4	2.2	2.6	2.3	2.3	1.8	1.9
2002	2.2	2.6	2.2	2.3	2.3	1.8	1.5	2.0	1.9	2.1	2.3	2.8	2.7
2003	2.8	2.7	3.0	3.0	3.0	2.9	2.8	2.9	2.9	2.8	2.7	2.5	2.6
2004	2.2	2.4	2.3	2.1	2.0	2.3	2.3	2.2	2.2	1.9	2.1	2.2	2.5
2005	2.3	2.1	2.1	2.4	2.3	2.1	2.2	2.4	2.3	2.5	2.4	2.3	2.0
2006	2.9	2.3	2.3	2.1	2.4	2.9	3.1	3.1	3.3	3.2	3.2	3.4	3.8
2007	..	3.5	3.7	3.9	3.6	3.3	3.3	2.7	2.7	2.8	..	..	..

The Retail Prices Index excluding Mortgage Interest Payments (RPIX) table is used to convert insured losses values from previous years into a constant value, adjusted for inflation. This table is publicly available online through the Office of National Statistics (2007).

Traditionally RPI (**R**etail **P**rices **I**ndex) was used as a measure of inflation, however, from 1992 a target interest rate was set out by the government based on RPIX. Since the interest rate was set to curb inflation, including a consideration of mortgage payments in setting inflation would have been deceptive. In 1997 the new government, handed the Bank of England the task of setting interest rates to meet an inflation rate of 2.5% on the RPIX measure. Since 2003, the Consumer Price Index (CPI) is now used as a target measure.

Appendix C - Sensitivity Analysis of Windspeed Interpolation Techniques

The network of observing stations established for this study was heavily dependent on the availability of wind gust data, described in section 2.1.1. The dearth of long, continuous gust records resulted in areas of the UK with large conurbations being under-represented, e.g. South Wales. Certain other regions saw an abundance of stations meeting selection criteria, such as the area extending from Nottingham to the east coast of England. Part of the study utilises interpolation methods to estimate windspeeds across the UK. A sensitivity test is carried out here to assess the dependency of this surface on the information used to produce it.

Initially the effect of varying the search radius used in the ArcGIS Inverse Distance Weighting (IDW) interpolation tool is assessed. The search radius refers to the number of input points used to calculate the interpolated value of a particular cell. The fewer points included, the more efficient, in terms of processing time, the interpolation becomes. However, with too few input points the interpolation may be less reliable. ArcGIS provides the option of utilising a *variable* or *fixed radius*, within which all input points are included in the interpolation calculation. The *variable radius* option allows the same number of points to be included in the interpolation for each cell regardless of their distance from that cell. The *fixed radius* option used an absolute distance to determine which points should be included in the interpolation. Since the density of input points (i.e. the station coverage) in this study is not even (as shown in Figure 2.2 in section 2.1.1), the variable radius method is used. The variable radius parameter in the IDW interpolation is investigated using a cross-validation method.

A cross-validation analysis produces error statistics for the interpolated surface. A bootstrapping technique is used to estimate the effect of each station in the network on the interpolated surface. The cubed sum of the daily maximum gust speeds, normalised to the local 98^{th} percentile value, is calculated for each station over the entire period of study (1980-2005). The cubed value of 98^{th} percentile threshold exceedance is utilised since this is the

value used in the windstorm loss model in Chapter 5. By removing one station at a time, the squared difference between the omitted point and the interpolated surface generated from all other points is found. This process is carried out at a variety of radius values, used in the IDW tool, as results expressed as Root Mean Square Error (RMSE) (Figure C.1).

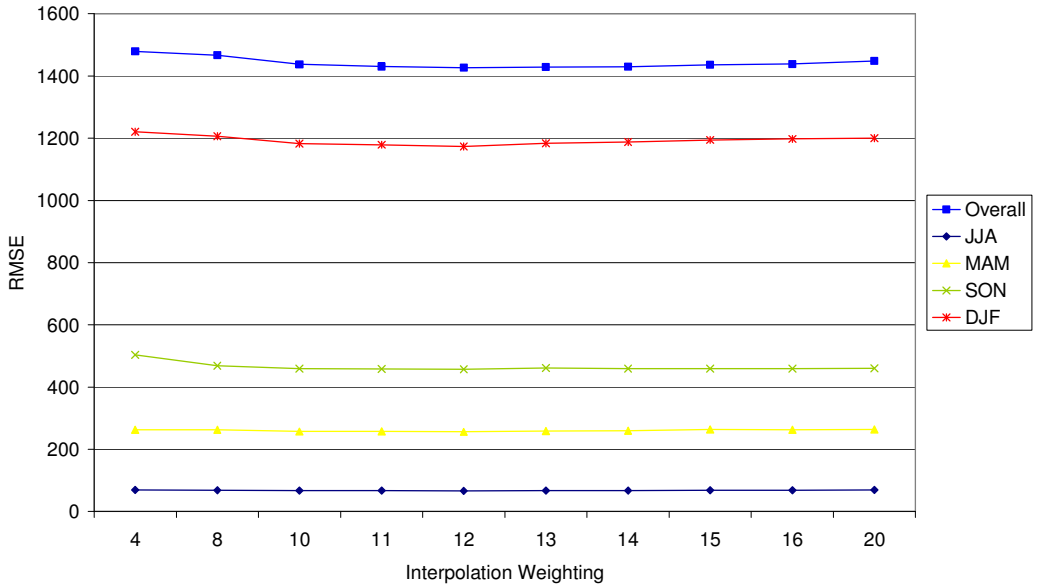

Figure C.1 - Root Mean Squared Error (RMSE) of the interpolated surface using different weighting in the IDW interpolation. Results are plotted for overall values (royal blue) and winter (red), spring (yellow), summer (navy blue) and autumn (green).

Ideally the cross-validation analysis would be carried out using the daily data from the entire period, but given the computer intensive nature of the interpolation process, this was not possible. Since this study is focussed on damaging windspeeds, which are most common during winter and autumn months, it is clearly important to ensure the choice of weighting minimises the RMSE in those periods also. Subsequently a seasonal analysis was carried out as well. These results are presented in Figure C.1. The search radius with the minimal Root Mean Squared Error (RMSE) overall, and for the winter months, was found to be 12, and hence is the value used in all subsequent interpolation. It should be noted, however, that the effect of varying the number of stations included in the interpolation was minor. The difference between the RMSE for interpolations with a variable radius of 4 to 20 is less than 10% in all seasons, and overall. Variable radii of 20 stations and greater (not shown in Figure C.1) produced significantly higher RMSEs than those with values below 20.

The cross-validation analysis also provides an indication of the importance of each station in producing the interpolated surface. The greater the absolute difference between the omitted point and the interpolated surface, the more significant that station becomes. This information is important when considering the impact of missing data. The rank of stations, in terms of their absolute errors, and their locations are presented in Table C.1.

No.	Station	Absolute Error
21	Kirkwall	25713
17	Eskdalemuir	22797
34	Salsburgh	17890
1	Aberporth	17391
23	Lerwick	15430
38	Valley	14840
43	Yeovilton	14689
31	Plymouth Mountbatten	13185
4	Bedford	12018
12	Cranwell	11425
39	Waddington	11100
26	Lyneham	10798
22	Leeming	9033
33	Ronaldsway	8657
42	Wittering	8363
30	Nottingham Watnall	8281
37	Stornoway Airport	8141
6	Blackpool Squires Gate	6512
5	Bingley	6262
35	Shawbury	6061
15	Durham	5502
27	Machrihanish	4870
9	Church Fenton	4809
11	Coningsby	4639
18	Heathrow	4636
36	St Mawgan	4335
10	Coltishall	4257
19	Hurn	4099
13	Culdrose	3561
14	Dunstaffnage	3462
2	Aldergrove	3349
25	Lossiemouth	3245
3	Bala	3033
7	Camborne	2873
32	Ringway	2695
41	West Freugh	2586
24	Leuchars	1737
16	East Malling	1644
20	Kinloss	1234
8	Chivenor	1199
29	Middle Wallop	866
28	Manston	746
40	Wattisham	485

Table C.1 - Rank of importance of stations when interpolating windspeeds. The absolute error refers to the absolute difference between an interpolated surface at a station and its actual observed value, when that station is omitted from the interpolation. The interpolation is carried out with the sum of the cubed normalised DMGSs over the entire period of study (1980-2005).

The relative importance of individual stations in the interpolation process, shown in Table C.1, is compared with Table 1.3 in section 2.1.1 detailing the number of days with missing observations for each station. It reveals that the most important stations, those near the top of Table C.1, have some of the lowest values of percentage of missing data (e.g. Kirkwall, Eskdalemuir, Aberporth, Lerwick and Valley all have less than 0.7% missing data). This quells any fears regarding the reliability of the interpolated surface resulting from heavy reliance of the procedure on stations with unreliable observations.

Similarly, an analysis of the *power parameter* used in the IDW tool was carried out. The *power parameter* controls the influence of observation points on the interpolated surface. By prescribing a higher *power parameter* a greater emphasis is placed on the nearest observation points. A similar methodology to that employed above was utilised, with the results (not shown) indicating a *power parameter* of 4 provided the most accurate interpolated surface (least RMSE values). In essence there is a trade off between the number of input points included in the interpolation (i.e. the *variable radius* value) and the weighting ascribed to each point (the *power parameter*). Although every combination was not explored due to computational restrictions many combinations were tested. The choices of power parameter of 4 and variable search radius of 12 were selected as these tended to produce the lowest RMSEs. However, the difference between various combinations was relatively low (~5-10%).

A drawback of the IDW method is that the interpolated surface is affected by an uneven distribution of observation points, resulting from an equal weighting being assigned to each observation point, regardless of whether it is in a cluster or not. Furthermore, the maximum and minimum values on the interpolated surface can only occur at observation points. Hence, the highest values of absolute error in Table C.1 tend to occur at stations exhibiting the highest observed windspeed exceedance values, e.g. Kirkwall (*station 21*) has the highest RMSE and also the highest exceedance value. However, this is not always the case, as illustrated by Eskdalemuir (*17*) which has the second highest absolute error, but the lowest exceedance value. Similarly, Yeovilton

(*43*) and Valley (*38*) have high (ranks 7 and 6 respectively) absolute errors but have the second and third lowest exceedance values, respectively.

Although the benefits of using IDW interpolation, such calculation speed and its simplicity in its underlying principal, are clear, it is not the sole interpolation technique available. Alternative interpolation methods are available in ArcGIS, including spline interpolation and kriging. Spline interpolation produces a surface that minimises overall surface curvature, while exactly passing through the observation points. Kriging, unlike spline and IDW interpolation, is a not a deterministic method of interpolation. A comparison of different techniques showed that IDW interpolation produced the lowest RMSEs, although the differences were marginal. Similarly, a negligible difference was found in the performance of various interpolation techniques utilised by Gemmer *et al.* (2004), while Kurtzman and Kadmon (1999) found IDW outperformed spline interpolation for winter temperatures, while the reverse was true in summer. The choices of interpolation technique, and the parameters used in the ArcGIS tool, are made based on minimising the RMSE in the cross-validation analysis.

Appendix D – Storm Catalogue 1920-1990 (from Palutikof *et al.*, 1997)

Ranking of storms in the Storm Catalogue, 1920 to 1990, by relative severity, from Palutikof *et al.*, 1997). Synoptic charts and meteorological observations were used to assign a storm an absolute severity. These are then considered relative to the one-in-fifty-year gust for the affected area, to produce the table below.

Rank	Date	Rank	Date
1	25 January 1990	25	18 January 1945
2	02 January 1976	26	04 November 1957
3	16 March 1947	27	26-30 November 1954
4	16 October 1987	28	14-15 January 1968
5	16-17 February 1962	29	26-27 November 1936
6	12 January 1974	30	28-29 October 1927
7	23-24 November 1938	31	6-7 January 1928
8	23-25 November 1928	32	16-17 September 1961
9	17 December 1952	33	11-12 January 1978
10	26 February 1990	34	12-13 November 1972
11	9-10 February1988	35	30 December 1951
12	07 April 1943	36	28 January 2027
13	01 February 1983	37	16-17 December 1989
14	31 January - 1 February 1953	38	04 November 1938
15	16-17 September 1935	39	21-23 December 1954
16	24 March 1986	40	06 March 1967
17	13 January 1984	41	26-27 January 1920
18	5-7 December 1929	42	9-10 February 1949
19	11 January 1962	43	16 May 1962
20	16-17 November 28	44	27/28 January 1974
21	13 February 1989	45	4-5 December 1979
22	29 July 1956	46	23-25 November 1981
23	18-19 October 1935	47	16-22 January 1937
24	2-3 April 1973		
25	18 January 1945		